UNCLASSIFIED

AD 402 379

Reproduced by the

DEFENSE DOCUMENTATION CENTER
FOR
SCIENTIFIC AND TECHNICAL INFORMATION
CAMERON STATION, ALEXANDRIA, VIRGINIA

UNCLASSIFIED

NOTICE: When government or other drawings, specifications or other data are used for any purpose other than in connection with a definitely related government procurement operation, the U. S. Government thereby incurs no responsibility, nor any obligation whatsoever; and the fact that the Government may have formulated, furnished, or in any way supplied the said drawings, specifications, or other data is not to be regarded by implication or otherwise as in any manner licensing the holder or any other person or corporation, or conveying any rights or permission to manufacture, use or sell any patented invention that may in any way be related thereto.

63-3-7

402 379

402379

CATALOGED BY ASTIA
AS AD No.

DESIGN AND DEVELOPMENT OF A FLIGHT PATH CONTROL SYSTEM FOR HELICOPTERS/VTOL AIRCRAFT

APRIL 11, 1963

PREPARED UNDER NAVY, BUREAU OF NAVAL WEAPONS

CONTRACT NOW62-0873-D

FINAL REPORT

JUNE 15, 1962 TO APRIL 8, 1963

Hamilton Standard DIVISION OF UNITED AIRCRAFT CORPORATION
ELECTRONICS DEPARTMENT BROAD BROOK, CONN.

ASTIA
APR 30 1963
TISIA D

Best
Available
Copy

HSER 2653

DESIGN AND DEVELOPMENT OF A FLIGHT PATH CONTROL SYSTEM FOR HELICOPTERS/VTOL AIRCRAFT

April 11, 1963

PREPARED UNDER NAVY, BUREAU OF NAVAL WEAPONS

CONTRACT NOW 62-0873-D

FINAL REPORT

June 15, 1962 to April 8, 1963

Written by ______ Senior Experimental Engineer
A. J. Ostheimer

______ Assistant Project Engineer
R. G. Giguere

Approved by ______ Project Engineer
T. E. O'Brien

______ Senior Project Engineer
W. C. Peck

______ Chief Development Engineer
F. A. Glassow

______ Chief Engineer
C. B. Brahm

ABSTRACT

The typical ASW helicopter mission is usually divided into two distinct phases, navigation and controlled flight. The navigation mode provides the pilot with his precise location and the flight profile to be flown. The autopilot implements the steering commands and provides a dynamically stable vehicle. This report provides a design which combines both phases to provide a flight path control system. This system enables the pilot to complete the ASW mission with minimum amount of navigation effort and manual control. The design provides the basis for a new concept in automatic flight control.

TABLE OF CONTENTS

Section	Title	Page
	TITLE PAGE	i
	ABSTRACT	ii
	TABLE OF CONTENTS	iii
	LIST OF ILLUSTRATIONS	v
	LIST OF TABLE	x
	LIST OF ABBREVIATIONS AND GLOSSARY	xi
1.0	INTRODUCTION	1-1
1.1	General	1-1
1.2	Selection of Aircraft	1-1
1.3	Flight Path Concept	1-1
1.4	FPC Operational Description	1-3
2.0	SUMMARY	2-1
2.1	Scope of Report	2-1
2.2	Design Conclusions	2-1
2.2.1	Navigation System	2-2
2.2.2	Inertial Measurement Systems	2-2
2.2.3	Flight Path Control	2-3
2.2.4	Digital Equipment Design	2-5
2.2.5	General Systems Design	2-5
2.3	Statement of Task Completion	2-6
3.0	DETAIL DESIGN	3-1
3.1	Navigation System	3-1
3.1.1	Introduction	3-1
3.1.2	Design Conclusions	3-2
3.1.3	Selection of Computational Frame of Reference	3-2
3.1.4	Description of Basic Navigation System	3-3
3.1.5	Erection and Alignment	3-6
3.2	Inertial Measurement System	3-44
3.2.1	Introduction	3-44
3.2.2	Design Conclusions	3-46
3.2.3	Gyros	3-46
3.2.4	Accelerometers	3-49
3.2.5	Instrument Calibration and Alignment	3-53
3.2.6	Pulse Torque Amplifier	3-76
3.2.7	Inertial Instrument Package	3-80
3.3	Flight Path Control Design	3-88
3.3.1	Introduction	3-88
3.3.2	Design Conclusions	3-88
3.3.3	Design Considerations	3-89
3.3.4	Basic Flight Path Concept	3-91
3.3.5	Flight Path Calculations	3-98
3.3.6	Flight Path Implementation	3-105
3.3.7	Flight Path Control Electronics	3-120

Section	Title	Page
3.4	Digital System Design	3-145
3.4.1	Introduction	3-145
3.4.2	Design Conclusions	3-145
3.4.3	Digital Coupler Trade-Off and Centralized vs. Channelized Study	3-147
3.4.4	Digital Simulation	3-151
3.4.5	Digital Computer Specification	3-162
3.4.6	Computer Input-Output Design	3-165
3.4.7	Computer Program	3-179
3.5	General Systems Design	3-196
3.5.1	Introduction	3-196
3.5.2	Design Conclusions	3-196
3.5.3	System Error Analysis	3-197
3.5.4	GFE Utilization	3-210
3.5.5	System Power Supply	3-212
3.5.6	Sensor Cost Reduction Trade Off Study	3-216
3.5.7	System Package Design	3-220
4.0	SUMMARY OF CONFERENCES AND VISITS	4-1
5.0	APPENDIX	5-1
5.1	Flight Path	5-1
5.1.1	Derivation of Flight Path Equations	5-1
5.1.2	Flight Path Error Analysis	5-3
5.2	List of References	5-7

ILLUSTRATIONS

Figure or Drawing No.	Title	Page No.
SK52217	FPC System Block Diagram	1 - 5
Fig. 1	Pictoral Representation of Coordinate Systems Related to the Earth Model - Isometric Projection	3 - 2 A
Fig. 2	Pictoral Representation of the Coordinate Systems Related to the Earth Model - Orthographic Projections	3 - 2 B
Fig. 3	Basic Block Diagram, Navigation Loop	3 - 4
Fig. 4	Definition of Relationships Between Sensor Package Location and Centers of Rotation of Aircraft Carrier	3 - 9
Fig. 5	Neumann Spectrum for Sea State 3	3 - 12
Fig. 6	Expanded Neumann Spectrum for Following Sea State 3	3 - 14
Fig. 7	Carrier Energy Spectra Distrubed Sea	3 - 15
Fig. 8	Carrier Motion Spectra Disturbed Sea	3 - 16
Fig. 9	Yaw-Axis Spectra Distrubed Sea	3 - 17
Fig. 10	Basic Gyrocompassing Loop Block Diagram	3 - 19
Fig. 11	Gyrocompassing Block Diagram & Freq. Response	3 - 21
Fig. 12	Gyrocompassing Block Diagram & Freq. Response	3 - 22

Fig. 13 Single Axis Representation of Position Tracking Loop 3 - 24

Fig. 14 Derivation of G/R Feedback 3 - 24

Fig. 15 Position Tracking Loop with External Velocity Input 3 - 25

Fig. 16 Ratio of Acceleration Error and Doppler Error Versus Doppler Error Frequency 3 - 27

Fig. 17 Ratio of Inertial Velocity Error and Doppler Error Versus Doppler Error Frequency 3 - 28

Fig. 18 Signal Flow Diagram Coarse Erection and Alignment (Moving Base) 3 - 31

Fig. 19 Coarse Erection and Alignment Direction Cosine Flow 3 - 33

Fig. 20 Pictoral Relationship Between E,N,U, e,n,u and X,Y,Z Coordinate Reference Frames 3 - 33

Fig. 21 Simplified Signal Flow Diagram Doppler-Inertial Fine Erection Process 3 - 35

Fig. 22 Time Response of Tuned Position Tracking Loop to Step Input of Acceleration 3 - 36

SK52200 Block Diagram of FPC Navigation Loop 3 - 38

Fig. 23 Ratio of Inertial Velocity Error Versus Doppler Error Frequency for Schuler Tuning with $\zeta = .09$ 3 - 40

Fig. 24 Gyro Sketches for Mass Unbalance Definition 3 - 54

Fig. 25 Definition of Package Orientation 3 - 57

Fig. 26 Calibration Program of Sane System 3 - 58

Fig. 27 Sane Calibration Program Data Reduction 3 - 68

Fig. 28 Alignment of the Inertial Package with the Doppler Axes 3 - 69

Fig. 29 Doppler Alignment Procedure 3 - 70

18X590809 SDIMU FPC Liquid Connection 3 - 82

18X509805 Strap-Down Inertial Measuring Unit, FPC 3 - 84

SK52216 SDIMU Wiring Schematic 3 - 85

Fig. 30 Possible Dunk Point to Dunk Point Flight Paths 3 - 92

Fig. 31 Base to First Dunk Point Flight Path 3 - 94

Fig. 32 Wind Computation Vector Diagram 3 - 96

Fig. 33 Flight Test Dunk Pattern 3 - 97

Fig. 34 Detail Diagram Dunk Point to Dunk Point Flight Path 3 - 98

Fig. 35 Detail Diagram Base to First Dunk Point Flight Path 3 - 103

Fig. 36 Flight Path Errors 3 - 110

Fig. 37 Transition Profile 3 - 111

Fig. 38 Altitude Channel Response to Transition Command 3 - 111

Fig. 39 Coordinated Turn Force Diagram 3 - 116

Fig. 40 Heading Command Vector Diagram 3 - 119

SK52213 Standard ASE Block Diagram 3 - 121
SK52214 FPC-1 Modified ASE Block Diagram 3 - 130
SK52202 Pulse Torque Amplifier - Electronic Output Filter 3 - 134
SK52210 8 Bit D/A Converter 3 - 136
SK52209 A/D Encoder - 7 - Bit 3 - 137
SK52208 Velocity Command Advisory Light System 3 - 138
SK52201 Altitude Command Loop 3 - 140
SK52204 Yaw Channel - Heading Command Loop 3 - 141
SK52203 Roll Command Generator 3 - 142
SK52205 Crossfeed Lockout Circuitry 3 - 144
Fig. 41 Actual and Predicted Values of Position Errors in Vertical Versus Time 3 - 156
Fig. 42 Runs 1, 2, 3, and 4: Longitude Versus Elapsed Time 3 - 158
Fig. 43 Latitude Versus Elapsed Time 3 - 159
Fig. 44 Runs 1, 2, 3, and 4 Radius Error Versus Elapsed Time 3 - 161
SK52212 (B) Pulse Torque Amplifier Interface Logic Diagram 3 - 167
SK52212 (E) Computer Input Register Logic Diagram 3 - 169
SK52212 (C) Doppler Interface Logic Diagram 3 - 170

SK52212 (D) Manual Inputs Interface Logic Diagram 3 - 172
SK52212 (A) Computer Input Control Logic Diagram 3 - 175
SK52212 (F) Computer Output Interface Logic Diagram 3-- 178
Fig. 45 Flight Path Controller Block Diagram Computer Program 3 - 181
Fig. 46 Flight Path Phases 3 - 184
Fig. 47 Flight Path Controller Generalized Flow Diagram - Computer Program 3 - 188
SK52223 Flow Diagram Computer Program 3 - 192
Fig. 48 Power Supply Block Diagram 3 - 215
SK52199 Sane/FPC Power Supply 3 - 218
18X590802 Input Output Console "A" 3 - 221
18X590810 Input Output Console "B" 3 - 222
18X590815 Frame Assy. Logic Module 3 - 223
18X590801 Preliminary Pilot Control Panel 3 - 225

LIST OF TABLES

Table No.		Page No.
1	Effective Constant Drift (W_{CE}) "X" and "Y" gyros	3-48
2	Effective Constant Drift "Z" Gyro (accel. 1g)	3-48
3	Effective Time Varying Drift "X" and "Y" Gryros	3-50
4	Effective Time Varying Drift "Z" Gyro (accel. 1g)	3-50
5	Gyro Important Characteristics "X" and "Y" Gryro	3-51
6	Accelerometer Requirements	3-52
7	Proposed Alignment Methods	3-75
8	Dunk Pattern Points	3-99
9	Cross Feed Lockout Circuit Cross Reference	3-143
10	Program Control Variables	3-193
11	Individual Power Requirements	3-213
12	Total Power Required	3-214
13	Power Supply AC-DC	3-217

Glossary of Abbreviations and Symbols

A -	Total acceleration vector as sensed during alignment.
A^{γ}_{i} -	The component of sensed acceleration as measured in the γ reference frame, along the i coordinate axis.
$[A(W)]^2$ -	The energy content of a distrubed sea (Neumann notation)
A/D -	Analog-to-Digital Converter
ALT -	Altitude
ASE -	Automatic Stabilization Equipment
ASW -	Anti-Submarine Warfare
a -	Transition-to-cruse distance
a_E, a_N, a_U	Gravitational mass attraction compensation components along the E, N, and U axes, respectively
$\bar{a}_i$, a_i -	Total acceleration and instantaneous acceleration, respectively, along the i axis during E and A, where i = Xo, Yo, Zo, for moving base E & A.
$\ddot{a}$ -	Total sensed acceleration
a_o, a_{comm} -	Transition acceleration command along x axis
a_x, a_y, a_z	- Inertially derived accelerations along helicopter x,y,z axes (used in flight path calculations).
b	- Transition-to-hover distance
BAR.ALT.	- Barometric Altimeter
BCD	- Binary Coded Decimal
BDHI	- Bearing Distance Heading Indicator
BMI	- Bearing Distance Heading Indicator

c - Constant coefficent

CE&A - Coarse Erection and Alignment

CEP - Circular Error Probability

CPLR - Coupler

CYC - Cyclic pitch of helicopter

D - Turn center-to-turn center distance

d - Arbitrary tracking distance

D/A - Digital to Analog Converter

D-I - Doppler - Inertial

Dopp - Doppler

E_o, N_o, U_o - an earth fixed, rectangular (EFR), orthogonal, right handed triad with the U_o axis lying along the earth's spin axis with the positive direction being from the earth's center towards the north pole, E_o lies along the intersection of the equatorial and Greenwich meridian planes directed along the outward normal at zero longitude, and N_o completes the triad.

Eorig - Longitude of origin of e,n grid.

E&A - Erection and Alignment

E - W - East - West

EF - Earth Fixed

EFR - Earth Fixed Rectangular Coordinate System

EFS - Earth Fixed Spherical Coordinate System

e, n, u - local east, north, and up, respectively; an orthogonal, rectangular, right handed triad whose origin travels with the craft; u lies along the local vertical, and e,n are in the horizontal plane with e perpendicular to the earth's polar axis, and pointing in an easterly direction, n points towards the north pole.

e - Acceleration error quantity

e - eccentricity of the ellipse associated with the earth model

e_a, n_a - Coordinates of end of transition to cruise

e_D, n_D - Coordinates of next dunk point

e_{DK}, n_{DK} - Coordinates of k^{th} dunk point

e_h, n_h - Coordinates of present position at the start of the dunk point-to-dunk point calculations

e_i, n_i - Coordinates of present position on line $\overline{AB}$ at the start of base-to-first dunk point calculations

e_j, n_j - Arbitrary point in tracking computation

e_o, n_o - Datum point coordinates

e_p, n_p - Coordinates of present position

e_s, n_s - Coordinates of first programmed turn; base-to-first dunk point.

e_T, n_T - Coordinates of start of turn toward next dunk point

e_γ - Doppler-Inertial error quantity

FE&A - Fine Erection and Alignment

F/F - Flip-Flop

FPC - Flight Path Controller

G - Gravitational field force

g - Acceleration of gravity

GFE - Government Furnished Equipment

GSDA - Ground Speed & Drift Angle Indicator

H_1, H_2 - Components of heading command

HPA - High power amplifier

HR - Helicopter Reference Coordinate System

HS - Hamilton Standard

h - Altitude command

hc - Cruise altitude

h_{hov} - Hover Altitude

I - General inertial variable

IA - Input Axis, Gyro

IC - Initial Condition Mode, Computer

$\overline{IC}$ - All other computer modes

ID - Identifiers, Computer Output

IR - Inertial Rectangular Coordinate System

IS - Inertial Spherical Coordinate System

MSD - Most Significant Digit

MTBF - Mean Time Between Failure

NM - No More

N-S - North-South

n - See e,n

n_a - See e_a

n_D - See e_D

n_{Dk} - See e_{Dk}

n_h - See e_h

n_i - See e_i

n_j - See e_j

n_o - See e_o

n_p - See e_p

n_s - See e_s

n_t - See e_t

nm - nautical miles

OA - Output Axis, gyro

PPM - Parts Per Million

PPR - Present Position Rectangular Coordinate System

PTA - Pulse Torque Amplifier

PTL - Position Tracking Loop

PTSA - Pulse Torque Servo Amplifier

Q_e - The error quantity between the actual east (e) vector and the platform e

Q_n - The error quantity between the actual north (n) vector and the platform n.

Q_z - The error quantity between the actual vertical and the platform vertical.

R - Earth's Radius

R - Range between successive dunk points

R_p - Horizontal distance between the carrier roll axis and the origin of the instrument axes.

R_{r1} - Horizontal distance between carrier pitch axis and the origin of the instrument axes.

R_{r2} - Horizontal distance between carrier yaw axis and the origin of the instrument axes.

R_y - Vertical distance between carrier roll axis and the deck.

r - Flight path turn radius

r_o - Radius of programmed coordinated turn

$S^{I}_{E,N,U}$ - The component of displacement, as measured in the Inertial reference frame, along the E, N, or U axis.

$S^{EF}_{\rho,\lambda_D,\gamma}$ - The component of displacement, as measured in the Earth Fixed reference frame, along the ρ, λ_D, or γ axis.

SA - Spin Axis, Gyro

SANE - Stabilization And Navigation Equipment

SDIMU - Strapped Down Inertial Measurement Unit

S-D - Strapped-Down

SRA - Spin Axis, Gyro

SI-A thru N - Switch one, wafer A through N

T - Helicopter lift vector (used in flight path calculations)

T - Tracking Computation (used in flight path calculations)

T - Time of one period of oscillation (used in navigation calculations)

TCDR - True Course and Distance Repeater indicator

t_D - Flight transition time

u - Local vertical unit vector; see e.

$\bar{u}$ - Apparent average vertical unit vector

u_p - polar semi-diameter of earth model

V - Inertial velocity

$\underline{v}_i^j$ - the component of velocity, as measured in the j reference frame, along the i coordinate axis as indicated by the Doppler system

V_c - Cruise velocity command

V^{EF}, Ve^{EF}, Vn^{EF} - Inertially derived velocities having Earth Fixed coordinates

V_E - Velocity error

V_{Eo} - Velocity error breakpoint; proportional - fixed acceleration command.

V_{hor} - Hover velocity command

V_{TAS} - True airspeed

V_x, V_y, V_z - Inertially derived airframe velocities

VGI - Vertical Gyro Indicator

$\underset{\sim}{V_i^j}$ - the component of velocity, as measured in the j reference frame, along the i coordinate axis as indicated by the navigation system

w.r.t. - with respect to

X,Y,Z - this coordinate system is fixed with respect to the helicopter, it is a rectangular, orthogonal, right handed triad with the X,Y,Z axes lying along the roll, pitch, and yaw axes of the craft, respectively.

X_o, Y_o, Z_o - an inertial, rectangular, orthogonal right handed triad that coincides with the X,Y,Z frame at the instant that coarse erection begins.

X',Y', Z' - this coordinate system represents the nonorthogonal triads formed by the instrument input axes and are in approximately the same orientation as the X,Y,Z system, note that although the notation is the same, these represent 2 sets of input axes, 1 for the gyros & 1 for accel.

X", Y", Z" - Triad representing the Doppler axes

X"' - Ship (carrier) longitudinal axis

XMTNG - Transmitting

X, Y - Wind based coordinate system

$\ddot{X}$ - Carrier surge acceleration

Y - See X

Y_o - See X_o

$\ddot{Y}$ - Carrier sway acceleration

Y' - See $\bar{\underline{X}}'$

Y'' - See $\bar{\underline{X}}''$

Z - See X

Z_o - See X_o

$\ddot{Z}$ - Carrier heave acceleration

Z' - See X'

Z" - See X"

β - Flight path turning angle

γ - Arbitrarily small angle for tracking err (used in flight path calculations)

γ, λ_c, ρ - an earth fixed, spherical set of coordinates, where ρ is the distance from the origin of the E_0, N_0, U_0 system to the origin of the X,Y,Z system, γ is longitude measured positive in an easterly direction from E_0, and λ_c is the geocentric latitude.

γ_I - inertial longitude; equal to $\gamma + \omega_{ie} t$

Δ - A differential quantity

γ - Arbitrarily small range for distance tracking (used in flight path calculations)

E_x, E_y, E_z - Arbitrary phase angles

E_ϕ, E_θ, E_χ - Arbitrary phase angles

η_H - The angle between n and X_H, measured positive in clockwise direction from n, where X_H is the horizontal projection of the X axis.

η_S - The angle between n and X''', measured positive in clockwise direction from n.

θ, χ, ϕ - a set of Eulerian angles relating X,Y,Z to e,n,u with the rotations taken about Y,Z,X in the order θ, χ, ϕ respectively.

θ - Pitch angle of helicopter when used in flight path calculations.

θ - Ship (carrier) roll angle (used in navigation calculations)

λ_c - Geocentric latitude; see γ .

λ_D - an earth fixed spherical coordinate; it is the geodetic latitude, used with ρ and γ .

γ - Frequency of wave encounter.

ξ - Bearing to next target point of flight path

ρ - Varying earth radius

ρ_e - initial earth radius as calculated from earth model

$\bar{\Phi}_w$ - Wind vector, average

Φ_w - Wind direction, average

$|\Phi|$ - Wind magnitude, instantaneous

$\Phi_e, \bar{\Phi}_e$ - Instantaneous and average wind magnitude in e direction respectively.

$\Phi_n, \bar{\Phi}$ - Instantaneous and average wind magnitude in n direction respectively.

$|\overrightarrow{\Phi}|$ - Average wind magnitude

$\Delta \Phi$ - Deviation from wind direction at dunk point

$\Delta \bar{\Phi}$ - Bounding value of $\Delta \Phi$.

ϕ - Helicopter roll angle (used in flight path calculations)

ϕ - Ship (carrier) pitch angle when used in navigation calculations

ψ - Yaw or heading angle of helicopter when used in flight path calculations.

ψ_{comm} - Heading command

ψ_{err} - Heading error

ψ - Ship (carrier) yaw angle when used in navigation calculations

Ω - The inertial angular rate of the earth

ie - the inertial angular rate of the earth

W_d - Damped resonant frequency

W_n - Natural resonant frequency

W_i^I - the sensed angular rate, as measured in the inertial reference frame, along the i axis

W_{ic}^I - W_i^I after dynamic compensation

ΔW_i - angular rate error signal for i axis for dynamic compensations

1.0 INTRODUCTION

1.1 General

This design study, in response to Bureau of Naval Weapons Contract No. NOW62-0873-D, has proceeded on the assumption that continued energetic development and production of Antisubmarine Weapon Systems are required to counter the potential threat of submarine attack on merchant convoys, naval task groups, amphibious forces, and on the continental United States. Also, this design study provides the ground work for development and production of weapons systems in related applications such as; assault systems, logistical support, interdiction, observation, and other applications related to the helicopter/VSTOL Aircraft.

1.2 Selection of Aircraft

The design presented herein, has been oriented to the installation of an air-worthy breadboard on the SH-3A weapons system. This weapons system was selected for the following reasons:

a. It is presently an operational ship based airborne weapons system with known capabilities.

b. This vehicle utilizes the automatic stabilization equipment, manufactured by Hamilton Standard Electronics Department.

c. The SH-3A operational requirements provide for ample design goals in both the navigational and flight control modes of operation.

d. The pilot and crew fatigue encountered on typical ASW missions, justify greatly the concept of automatic flight path control.

e. The system is produced by Sikorsky Aircraft, a Division of United Aircraft.

1.3 Flight Path Concept

The concept of a flight path is not new. Its application to low speed helicopter/VTOL aircraft requires that we modify our thinking in order to clearly visualize the problems related to their flight characteristics and mission profiles.

1.3.1 Land Operation

Normally any aircraft designated to fly from one station to another will fly a specific flight plan. A precise flight path may readily be defined, with the knowledge of the exact runway that is to be used and what approach pattern best suits the aircraft characteristics. The landing or takeoff heading is defined by necessity, and the approach or climbout by standard procedures. It may be concluded that a precisely defined altitude profile, and position profile, may be generated to specify a flight path between two runways fixed on the earth. Strategically located navigational aids, now in use, may provide flight path crosschecks during critical phases of the flight.

1.3.2 ASW Utilization

The SH-3A ASW mission profile is not defined at any given instant during dipping operations. The short range between transitions, and variable wind direction, create problems not encountered during land based operations. The transition heading, both to and from hover, may be conveniently defined as a line in space which rotates about a specific point on the ocean. The direction, at any given instant, depends upon wind direction. Safety of flight procedures dictate that cross wind transitions of greater than ten degrees are undesirable.

The flight path defined in this report attempts to take into account the problems of short flight distances, and variable wind directions. It should be noted that system limitations exist, due in part to the GFE systems available, and the limited authority of the SH-3A control system. However, the system has capabilities which may be extended with minimum support equipment development. Briefly; the equipment which requires improvement, not only for flight path control, but for all modes of operation:

a. Altimeter (Radar and barometric)
b. True airspeed system
c. Autopilot system (extended authority and couplers)
d. Doppler accuracy
e. Power management control
f. Navigational displays (plotters and indicators)

1.4 FPC Description Reference SK52217

1.4.1 The Flight Path Control is an integrated navigation and stabilization system for helicopters. It incorporates a strapped down inertial navigation system which obtains vehicle acceleration and angular rates from six body mounted accelerometers and gyros. The acceleration and angular rate signals are supplied to a digital computer which resolves the acceleration information into an inertial coordinate reference frame. The digital computer double integrates the acceleration to generate a continuous indication of position in inertial space. The position of the helicopter is converted from inertial coordinates to present position earth fixed latitude and longitude. The strapped down inertial system is aided by doppler velocity signals which are used to erect and align the system on a moving base.

The FPC contains a stored flight plan which when compared to the present position of the helicopter generates command signals to automatically "fly" the vehicle to its preprogrammed destination. These command signals are applied through a modified SH-3 Helicopter Automatic Stabilization Equipment autopilot to actuate the control surfaces.

The FPC can be overriden at anytime by the pilot who can command a flight in any manner. The FPC can be reprogrammed to a limited extent in the air. The system is capable of storing several flight plans which can be selected by the pilot. A completely new flight program can be inserted into the computer by modifying the program on the flight line.

1.4.2 A Brief Description of the FPC Performance Features are:

1. Prior to takeoff a series of manual inputs must be inserted into the FPC. The coarse erection and alignment of the inertial navigation system will be performed. The pilot will manually take off and fly the helicopter to cruise altitude and then initiate the FPC. The FPC will perform fine erection and alignment of the strapped down system.

2. The FPC will compute the wind velocity, the flight path and distance to the first dunk point. It will fly the helicopter at a constant speed down wind of the dunk point and then fly a transition to hover at the dunk point.

3. When the first dunk point is achieved, the pilot will insert position fix data to update his inertial navigation system. The computer will determine the flight path to the next dunk point. The take-off from hover will be initiated by the pilot and will be automatically flown.

A series of pilot option buttons have been incorporated to enable the pilot to modify his flight path while under automatic flight. The option selected will be acted upon during automatic flight except during transitions to and from hover, and during the initial portion of the flight to the first dunk. One option will be accepted by the computer at any given instant. If an option is selected during a transition, only the last option will become effective when either the "prepare for takeoff" is pressed or the first point after takeoff is reached.

The following options are available for use during automatic flight:

a. Skip one dunk
b. Skip two dunks
c. Skip three dunks
d. Fly to new dunk point
e. Compute new pattern(based upon new point)

The flight to the first dunk is unique because no wind information exists during the initial phase of flight. The FPC wind direction computation relies upon approximately 30% of the range to the first dunk point to sum up wind components. During this portion of the flight, a pilot option will not be acted upon. However, when the vehicle reaches a point which is .7 the distance to the dunk point, the last option selected will become effective.

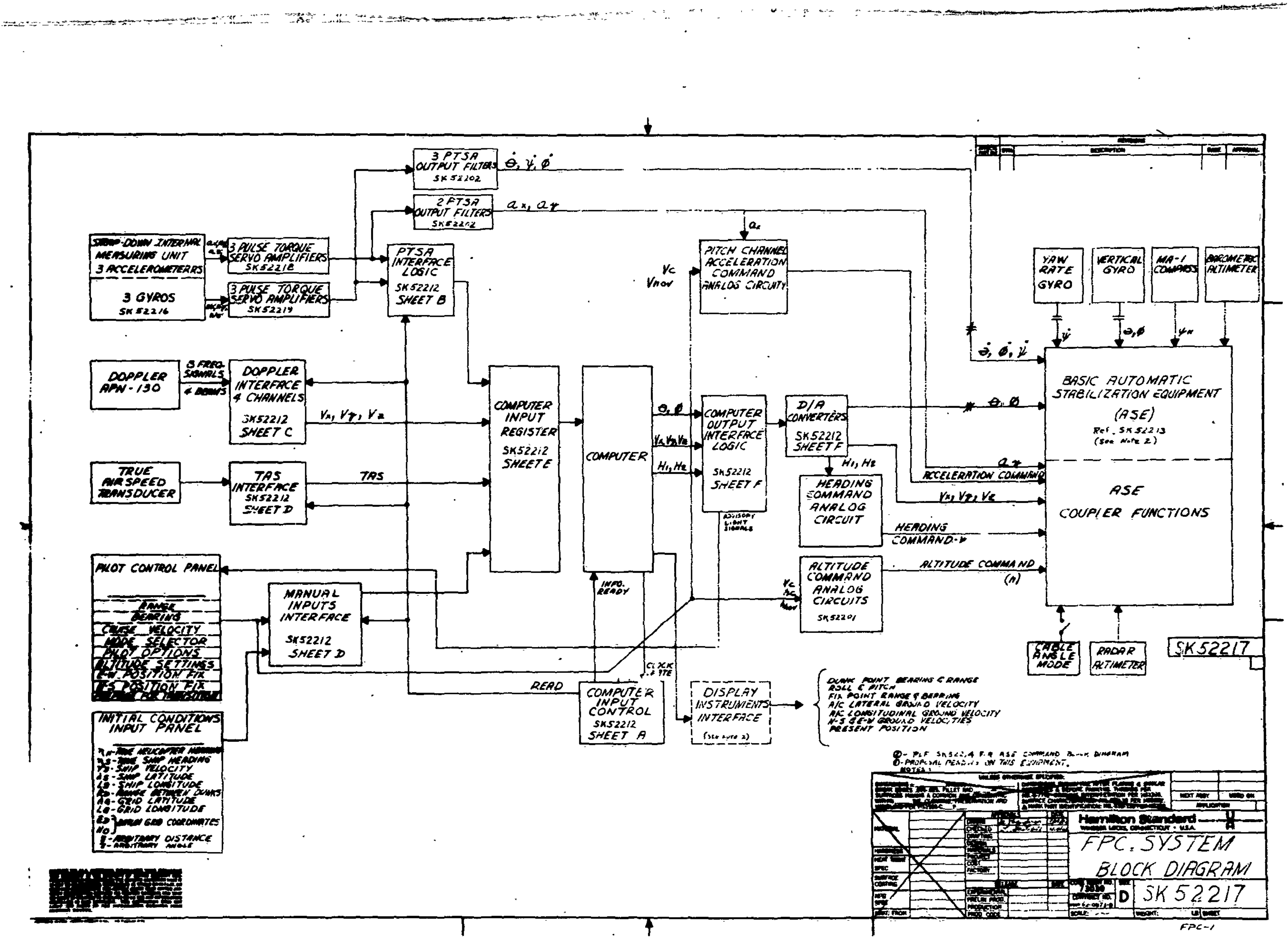
STRAP-DOWN INTERNAL MEASURING UNIT 3 ACCELEROMETERS
3 GYROS SK52216
3 PULSE TORQUE SERVO AMPLIFIERS SK52218
3 PULSE TORQUE SERVO AMPLIFIERS SK52219
3 PTSA OUTPUT FILTERS SK52202
2 PTSA OUTPUT FILTERS SK52202
$\dot{\theta}, \dot{\psi}, \dot{\phi}$
a_x, a_y
PTSA INTERFACE LOGIC SK52212 SHEET B
DOPPLER APN-130
3 FREQ. SIGNALS
4 BEAMS
DOPPLER INTERFACE 4 CHANNELS SK52212 SHEET C
V_x, V_y, V_z
TRUE AIRSPEED TRANSDUCER
TAS INTERFACE SK52212 SHEET D
TAS
PILOT CONTROL PANEL
RANGE
BEARING
CRUISE VELOCITY
MODE SELECTOR
PILOT OPTIONS
ALTITUDE SETTINGS
E-W POSITION FIX
N-S POSITION FIX
INITIAL CONDITIONS INPUT PANEL
TRUE HELICOPTER HEADING
TRUE SHIP HEADING
SHIP VELOCITY
SHIP LATITUDE
SHIP LONGITUDE
RANGE BETWEEN DUNKS
GRID LATITUDE
GRID LONGITUDE
GRID COORDINATES
ARBITRARY DISTANCE
ARBITRARY ANGLE
MANUAL INPUTS INTERFACE SK52212 SHEET D
COMPUTER INPUT REGISTER SK52212 SHEET E
COMPUTER
INFO. READY
READ
CLOCK
COMPUTER INPUT CONTROL SK52212 SHEET A
θ, ϕ
V_x, V_y, V_z
H_1, H_2
V_c
V_{nav}
a_x
PITCH CHANNEL ACCELERATION COMMAND ANALOG CIRCUITY
COMPUTER OUTPUT INTERFACE LOGIC SK52212 SHEET F
ADVISORY LIGHT SIGNALS
D/A CONVERTERS SK52212 SHEET F
HEADING COMMAND ANALOG CIRCUIT
ALTITUDE COMMAND ANALOG CIRCUITS SK52201
DISPLAY INSTRUMENTS INTERFACE (See note 2)
DUNK POINT BEARING & RANGE
ROLL & PITCH
FIX POINT RANGE & BEARING
A/C LATERAL GROUND VELOCITY
A/C LONGITUDINAL GROUND VELOCITY
N-S & E-W GROUND VELOCITIES
PRESENT POSITION
YAW RATE GYRO
VERTICAL GYRO
MA-1 COMPASS
BAROMETRIC ALTIMETER
$\dot{\psi}$
θ, ϕ
ψ_M
$\dot{\theta}, \dot{\phi}, \dot{\psi}$
ACCELERATION COMMAND
HEADING COMMAND-ψ
ALTITUDE COMMAND (h)
BASIC AUTOMATIC STABILIZATION EQUIPMENT (ASE) Ref. SK52213 (See Note 2)
ASE COUPLER FUNCTIONS
CABLE ANGLE MODE
RADAR ALTIMETER
SK52217
NOTES:
①- REF SK52214 FOR ASE COMMAND BLOCK DIAGRAM
②- PROPOSAL PENDING ON THIS EQUIPMENT.
UNLESS OTHERWISE SPECIFIED
NEXT ASSY
USED ON
APPLICATION
Hamilton Standard
WINDSOR LOCKS, CONNECTICUT • U.S.A.
FPC, SYSTEM BLOCK DIAGRAM
D
SK 52217
FPC-1

2.0 SUMMARY

The summary is composed of three sections; a report scope which describes the contents of the report, a conclusion which defines the results of the design study, and a statement of completed task which defines the work completed.

2.1 Scope of Report

This report describes the analysis and design of a helicopter guidance system known as a Flight Path Control (FPC). The FPC integrates a strapped down inertial navigation concept to indicate the helicopter position and a digitally commanded autopilot to signal the helicopter control surfaces to guide it on a pre-programmed or pilot commanded flight path.

The report discusses the detailed design. The strapped down inertial navigation is detailed which includes a description of the basic computational frame of reference, and a proposed method of erection and alignment on a moving base. A detailed description of the Inertial Measurement System; the inertial instruments, gyros and accelerometers, the pulse torque amplifier, the inertial instrument package and the instrument calibration procedures is provided.

The basic flight path concepts including the flight path calculations, implementation and control electronics are defined.

The digital system simulation, digital computer specification, input-output interface design and computer program are summarized.

An insight is provided into the system and component errors and the sensor cost reduction trade-off study. The flight test power supply and electronics packages are described. Also defined are the GFE instruments.

It was necessary to limit the amount of detail presented in this report. Therefore, some subjects are discussed in summary form and others which were details having no specific bearing on conclusions are omitted entirely.

2.2 Design Conclusions

The FPC design has resulted in a system which will automatically maneuver an ASW helicopter through a preprogrammed flight path including transitions to and from hover. The over-all analysis and design can be separated into subsystems which are discussed below.

2.2.1 Navigation System

The basic strapped down navigation computations will be performed in the inertial frame of reference using an ellipsoid of revolution as an earth model with a homogenous gravitational field. There will be two modes of erection and alignment, coarse and fine. The coarse erection and alignment will be performed for three minutes on the carrier deck. It will use self-contained accelerometer data for erection and external ships heading for alignment. The fine erection and alignment will be performed in the air using external doppler velocity and earth's rate damping. The total erection and alignment time will be 15 to 30 minutes depending on the magnitude of the initial and sustained errors.

The position errors accumulated by the strapped down navigation were computed based on typical present day tactical limitations. The main source of position error is the inertial gyro drift rate shift which can be .1°/Hr.

The gyro drift rate shift is canceled during fine erection and alignment. It is estimated that a 2.5 nautical mile (Root Sum Square) position error will be accumulated during the first hour of the test flight. There will be a 1.5 nautical mile (RSS) error during each hour of flight test in a pure inertial mode.

2.2.2 Inertial Measurement System (IMS)

The inertial measurement system is the heart of the gimbal-less inertial navigation system. The performance of the inertial instruments, single degree of freedom gyros and accelerometers are the limiting influence in the position error. The FPC position requirements dictate the use of a .015°/hr. gyro to yield a 1.5 nautical mile C.E.P.

The accelerometers used for the FPC are existing units with readily obtainable requirements. The accelerometer dynamic range extends from 10^{-5}g threshold to 2.5g maximum input.

The pulse torque amplifiers used in conjunction with the gyros and accelerometers generate digitalized data (serial pulse train) which is a direct indication of angular rate and acceleration. These pulse torque amplifiers are a specialized digital to analog converter. The pulse torque amplifier has a scale factor stability of one part in 100,000 and an bias stability of one part in a million. It is designed to operate at 130°F ± 5°F with the output bridge regulated to 150°F ± .1°F to achieve these stability criteria.

A detail calibration procedure has been derived to define the instrument characteristics such as bias, scale factor and orthogonality. The procedure requires the rotation of the inertial package through various orientations and angular rates and the the appropriate parameters are computed.

A solid conduction inertial package was designed to contain the gyros and accelerometers . Its special features include a control to regulate the temperature across the instruments to ± .1°F, a weight of 11 pounds, ease of calibration and simplicity of design.

2.2.3 Flight Path Control

The FPC contains a computer controlled autopilot designed to pilot the helicopter automatically through a wide variety of ASW patterns. The FPC will calculate each successive dunk point in a pattern centered on the search datum, and maneuver the vehicle over each dunk point in turn.

The basic units of the system are:

1. The Dunk Pattern and Flight Path Computer, which accepts inputs from the pilot and navigation section, generates and routes digital commands.
2. The Analog Command Generators which develop the analog command signals.

3. A modified Automatic Stabilization Equipment, which provides both implementation of the maneuvers and maintains the vehicle in a dynamically stable mode.

The FPC will function in an ASW pattern with a minimum range of 5,000 yards between successive dunk points, a cruise velocity between 60 and 100 knots, a hovering altitude of 20 to 100 feet and a cruise altitude between 100 and 200 feet. Velocities above 100 knots are possible but the minimum range (5,000 yards) between dunk points must be increased to allow sufficient maneuvering room.

The FPC will automatically command and maintain various flight modes such as:

1. A constant cruise velocity.
2. Level flight at preselected altitude.
3. A predetermined fixed distance transistion to hover from cruise.
4. A transition from hover to cruise.
5. A coordinated turn.
6. Homing on a preselected point.

Through the blending of navigational, computational, and autopilot functions, it is possible to provide a wide range of pilot options and overriding capabilities, thus enabling the pilot to skip dunk points, leave and re-enter the pattern at any time, or to start a new pattern centered on a datum point of his choice. Upon leaving the pattern, the pilot may insert a selected point in the FPC and be flown automatically to this point, terminating in a hover over it.

Much of the flexibility in the program stems from the fact that the pattern is realized by homing on successive points rather than by dead reckoning methods. Also, the system operates at low authority levels, consistent with automatic flight practices; this gives the pilot ultimate control over the vehicle at all times. Finally, pilot opinion has been a prime factor in all design considerations; automatic maneuvers were designed to duplicate, as nearly as possible existing manual ASW maneuvers.

2.2.4 Digital Equipment Design

The digital simulation studies indicate that a high speed, parallel word digital computer will be required to resolve the strapped down system equations. It should have a 4096 word memory capacity with a word length of 30 bits (29 bit plus a sign bit). The operation times shall be

Addition -- less than 24 microseconds including access time

Multiplciation -- less than 150 microseconds

with the time as small as possible. The digital computer must perform fourth order Runge-Kutta integration to minimize dynamic errors. The iteration time will be 200 milliseconds. The channelized digital system was compared to a centralized processing unit to perform the digital coupler functions. The central processing unit is the best approach because it results in less hardware because of its ability to time-share computation. The analog coupler is used in the system since it was in existence and required no design. The digital input-output interface was designed. The data input-output operates under direct authority of the computer in a synchronous mode.

2.2.5 General Systems Design

The use of the inertial navigation sensors to provide stability augmentation signals to the autopilot will result in a cost reduction when compared to a system containing both inertial and autopilot sensors. The reliability will be slightly improved because several of the analog sensors are retained for redundancy.

The flight test power supp.y will consist of three commercial DC supplies, two integral DC supplies and a 400 cps A. C. supply.

The electronics package will consist of six commercial type consoles and a pilot's control panel. The combined weight of the four items will be approximately 550 pounds.

2.3 Statement of Task Completion

Hamilton Standard Electronics Department has designed an integrated flight path control system in fulfillment of Bureau of Naval Weapons Contract Number NOW 62-0873D.

In accordance with the Statement of Work dated March 9, 1961, HSED has accomplished the following:

1. A four-channel autopilot system has been designed by modifying the existing SH-3A Automatic Stabilization Equipment. The coupler functions are an integrated part of this hardware.
2. A series of digital signals are available for display of aircraft performance.
3. The tie in to government furnished equipment has been reviewed and adapters designed where necessary.
4. A sensor cost reduction trade off study was performed.
5. The relative advantages of analog, channelized digital and centralized digital implementation of the coupler functions have been determined.
6. A detailed investigation of the doppler radar and radar altimeter was performed. All other existing GFE equipment will presently meet the performance objectives and was not studied.
7. This report covers the design of the flight test breadboard.

3.0 DETAIL DESIGN

This section defines the design effort which provides for an integration of a "strapped-down" inertial navigation system, and a flight path control system. The major design efforts are tabulated as follows:

a. Navigation system, which includes erection and alignment.

b. Inertial measurement system.

c. Flight path control design.

d. Digital computer and associated equipment.

e. General systems design including the system error analysis.

3.1 Navigation System

3.1.1 Introduction

The task of directing one's course from one location to another, through calculations using position, velocity, and acceleration is divided into two functions; one function, commonly referred to as navigation, deals with the necessary calculations to determine one's instantaneous position and the second function is the directing and is called guidance or control. This section of the report deals only with the navigation portion of the above task, i.e. the calculations and related equations necessary to determine one's location at any time after the flight has begun.

Included is a description of the alignment procedure on a moving base and the calculations necessary for an inertial navigation system mechanized by a digital computer and inertial sensors which are mounted in a fixed orientation within the helicopter, i.e. a "strapped down" inertial navigation system. (The alignment procedure on a fixed base is also included.) The strapped down navigation system departs from the present state of inertial navigation systems in that a stable platform is not required because the resolution of acceleration from the accelerometer axes to the space integration (computation) axes is performed by the digital computer.

The "strapped-down" system is aligned and erected to a computational reference frame that is defined by the earth's geometrical model.

It is generally realized that complexity of the basic navigation calculations (those calculations that are necessary assuming perfect conditions) must be significantly increased due to non-ideal inputs and instruments; hence, considerable attention will be given to developing the proposed navigation formulation from the basic system in order to compensate for anticipated errors from various sources.

3.1.2 Design Conclusions

Because of the inherent non-linear characteristics of a digitally controlled fixed-frame inertial guidance system, normal servo techniques do not provide a valid dynamic analysis of the system processes. The ability of the proposed system to perform as stated is, therefore, contingent on the verification of the design hypothesis by either digital simulation or actual flight tests.

The primary conclusions that resulted from the study of the navigation requirements of the FPC considering tactical and accuracy specifications are:

1. Navigation computations will be performed in the inertial reference frame.

2. An ellipsoid of revolution will be used as the earth model with a gravitational field based on a homogeneously distributed mass within.

3. Coarse erection and alignment of the system on the carrier deck will be performed using inertial sensor derived gravity components with external heading and present position information.

4. Fine erection and alignment in air will be performed using external doppler velocity information and earth's rate.

5. The total erection and alignment time will be 15 to 30 minutes depending on the magnitude of initial condition errors.

6. The gyro drift components will be compensated through the use of doppler velocity information and an internally generated earth rate signal in a gyro feedback loop.

3.1.3 Selection of Computational Frame of Reference

The choice of the reference frame in which the sensed accelerations are to be expressed to enable their integration for the determination of position was restricted to two frames (1) an inertial frame and (2) a present position frame (one related to the instantaneous location of the craft in earth coordinates). Other conceivable reference frames were not considered at length because they seemed to contain fewer advantages than the two proposed frames. Specifically, the two

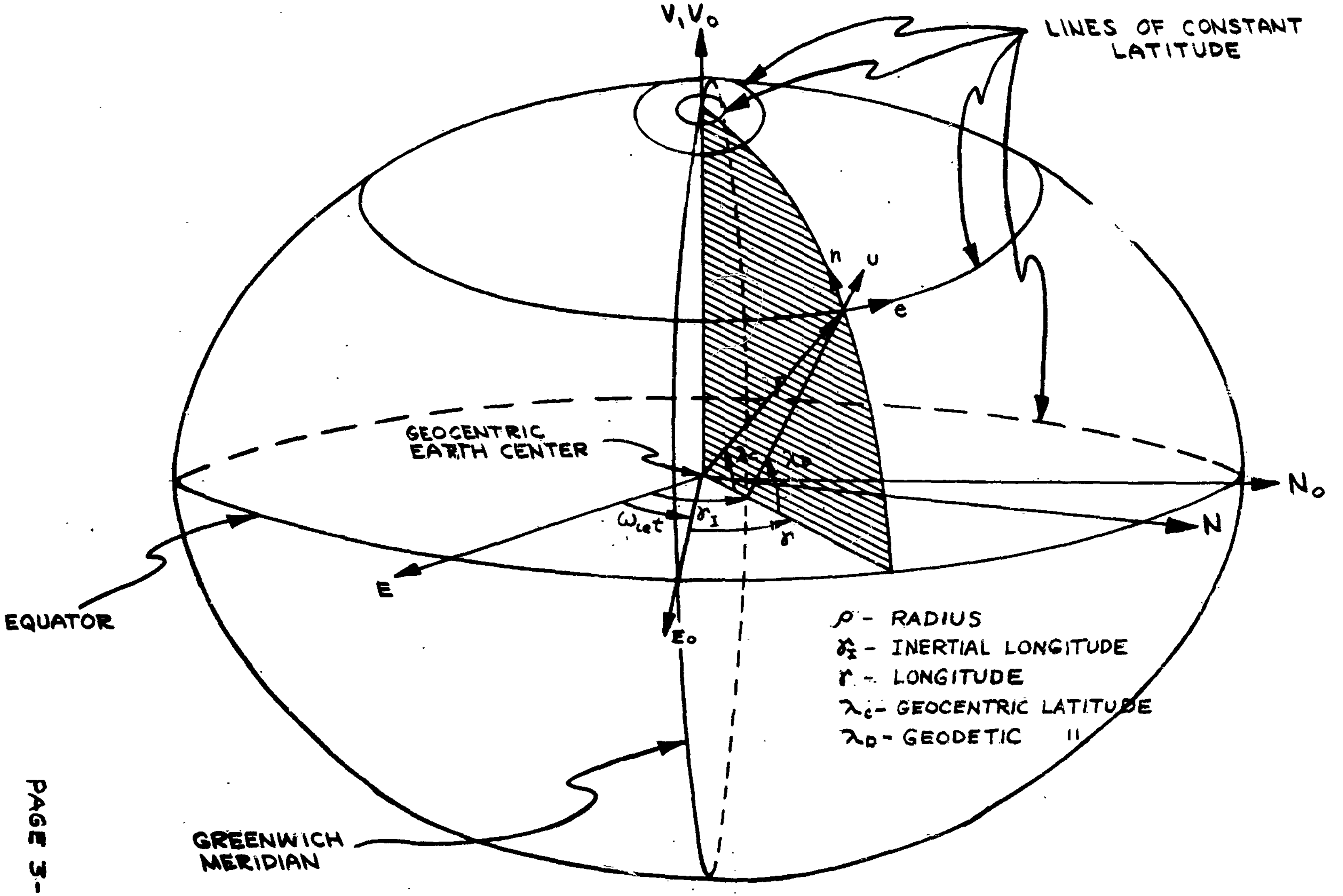
V, V₀
LINES OF CONSTANT LATITUDE
n
u
e
GEOCENTRIC EARTH CENTER
N₀
N
E
Eo
ω_ie t
γ_I
γ
λ_c
λ_D
ρ
EQUATOR
GREENWICH MERIDIAN
ρ - RADIUS
γ_I - INERTIAL LONGITUDE
γ - LONGITUDE
λ_c - GEOCENTRIC LATITUDE
λ_D - GEODETIC "

FIGURE 1
PICTORAL REPRESENTATION OF COORDINATE SYSTEMS RELATED TO THE EARTH MODEL ISOMETRIC PROJ.

PICTORAL REPRESENTATION OF THE COORDINATE SYSTEMS RELATED TO THE EARTH MODEL - ORTHOGRAPHIC PROJECTIONS

FIGURE 2

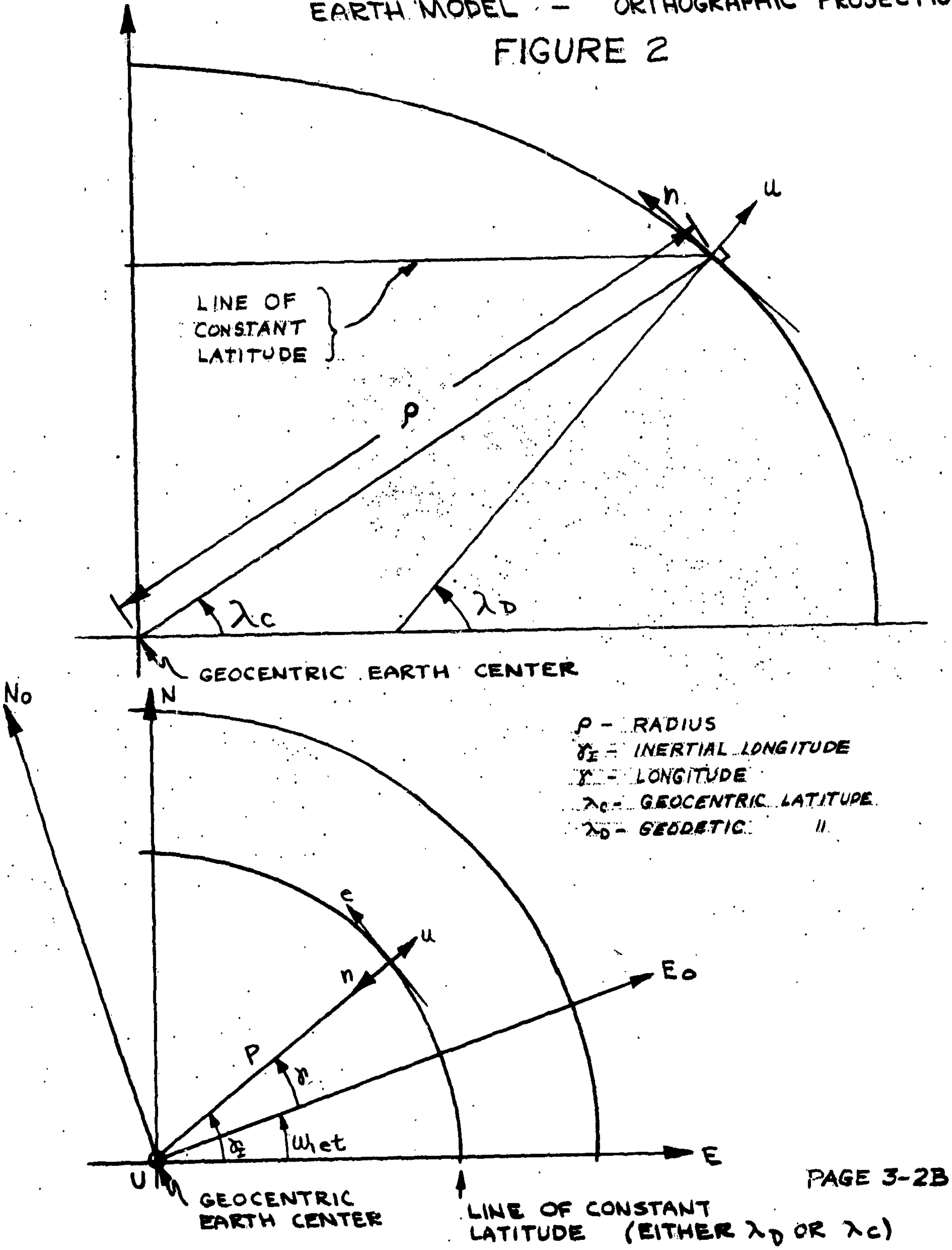
n
u
LINE OF CONSTANT LATITUDE
ρ
λc
λD
GEOCENTRIC EARTH CENTER
No
N
ρ - RADIUS
γI - INERTIAL LONGITUDE
γ - LONGITUDE
λC - GEOCENTRIC LATITUDE
λD - GEODETIC "
e
u
n
Eo
P
γ
γI
ωie t
E
U
GEOCENTRIC EARTH CENTER
LINE OF CONSTANT LATITUDE (EITHER λD OR λC)

frames considered were an inertial frame centered at the center of the earth model chosen (hence it is implicity assumed that the earth's center is moving in a straight line) and a present position frame whose coordinates are latitude, longitude, and distance from the center of the earth model.

The obvious advantage of the inertial frame is that once the sensed accelerations are properly resolved and gravitational attraction compensation has been accomplished then there exists a linear relationship between the true acceleration along a given axis and the displacement along the same axis. This condition does not hold for the present position in that due to its relative motion with respect to an inertial frame products of the unknown quantities appear; hence, the required integrations become much more complex.

A major disadvantage of the inertial frame is that a somewhat complicated calculation is necessary to determine the proper gravitational attraction compensation for each acceleration component. However, for the present position reference frame it might be possible to eliminate the need of using gravitational attraction compensation by eliminating the need of the acceleration along the axis containing the gravitational attraction. This would be accomplished by duplicating the procedure of a stable platform type of navigation system; thus, only the horizontal acceleration components would be used and either an external altitude reference or the assumption that the flight would take place on the earth's surface would necessarily be involved.

It was first thought that the present position scheme would be inherently more accurate than the inertial; however, upon closer examination, it was decided that this was incorrect. Therefore, because of the much less complicated integration that is necessary and because the total number of calculations appears to be smaller, the inertial frame has been chosen as the frame in which the position integrations shall be accomplished.

3.1.4 Description of Basic Navigation System

In this report the "basic navigation system" is the terminology used to describe the calculations that would be necessary if there were no error sources, i.e. perfect instruments, perfect knowledge of initial conditions, perfect integrations, and many others. The following figure (Fig.3) shows those operations that are essential for navigation using only measurements of acceleration and angular rates.

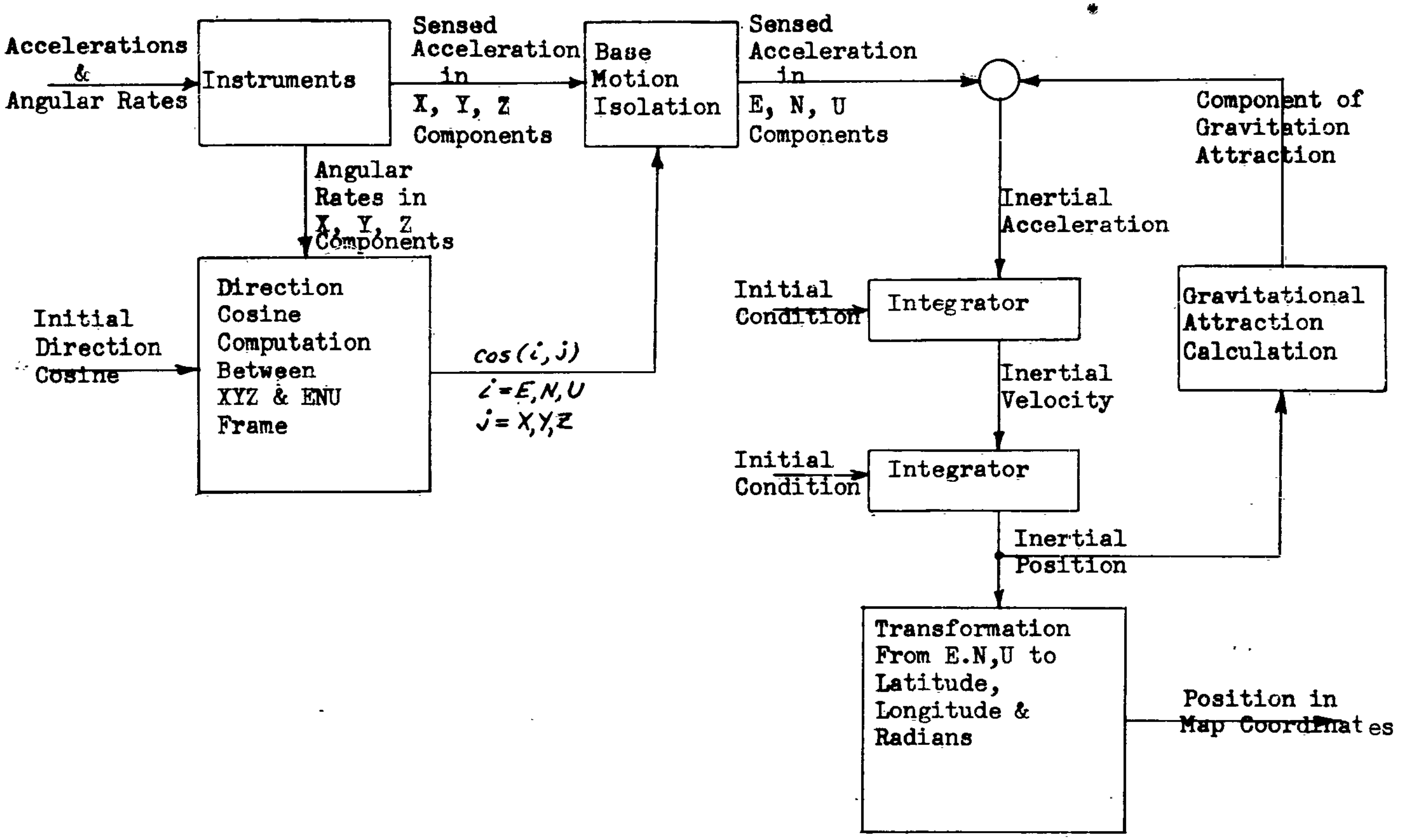
Accelerations
&
Angular Rates
Instruments
Sensed
Acceleration
in
X, Y, Z
Components
Base
Motion
Isolation
Sensed
Acceleration
in
E, N, U
Components
Angular
Rates in
X, Y, Z
Components
Initial
Direction
Cosine
Direction
Cosine
Computation
Between
XYZ & ENU
Frame
cos (i, j)
i = E, N, U
j = X, Y, Z
Component of
Gravitation
Attraction
Inertial
Acceleration
Initial
Condition
Integrator
Inertial
Velocity
Initial
Condition
Integrator
Inertial
Position
Gravitational
Attraction
Calculation
Transformation
From E.N,U to
Latitude,
Longitude &
Radians
Position in
Map Coordinates

Figure 3

3.1.4 (Continued)

The diagram is intended to be self-explanatory but a short description does not seem superfluous. The angular rate and sensed acceleration (true acceleration plus gravitational attraction) are sensed by two orthogonal arrays of instruments parallel to one another (gyros and accelerometers); thus, the angular rates and sensed accelerations are indicated by the vectorial sum of their respective components. The angular rate components are then used to obtain the solutions of a set of integral equations relating orientation of the instrument coordinate (XYZ) system to inertial (ENU) coordinate systems, viz, the direction cosines between the two systems. These direction cosines then become the inputs to the box labeled "Base Motion Isolation". The function of Base Motion Isolation is to reflect the sensed accelerations from the frame of the instruments (XYZ) to the inertial coordinate system (ENU), i.e., it is a matrix multiplication used to resolve the sensed accelerations into the coordinate frame in which the integrations will be done. Now that the sensed accelerations are in the ENU frame, the component due to gravitational attraction is removed prior to integration; the resulting signal represents the inertial acceleration (or true acceleration) of the craft. As can be seen from Figure 3 the gravitational attraction compensation is a function of the inertial position coordinates. The true acceleration is now integrated once to obtain inertial velocity and then a second time to yield the inertial position coordinates of the helicopter. As stated previously these inertial coordinates are used to calculate the gravitational attraction compensation; they are also operated on to produce the corresponding position information in map coordinates.

The remaining portions of this section (3.1) shall be directed towards a more specific discussion of the proposed navigation system.

3.1.5 Erection and Alignment

3.1.5.1 General Description

The erection and alignment process of a fixed-frame inertial guidance system yields the initial values of the direction cosines that relate the system instrument axes to the computational axes, i.e., provides accurate knowledge of the instrument axes orientation in the computational reference frame. Since the computational frame is coincident with the physical geometric reference (the Hayford ellipsoid of revolution), the required information is obtained through the measurement and mathematical resolution of physical quantities. Reference to Figure 3 will show that the erection and alignment process must provide the instantaneous relationship between the system instrument axes, which may be at any attitude near the surface of the earth, and the earth centered inertial reference frame.

For a fixed base system, this relationship is derived in a two-step process which utilizes craft latitude and longitude to define the location of the present position coordinates with respect to the inertial reference frame, and accelerometer and gyro outputs to define the orientation of the instrument axes with respect to the present position coordinates.

The second step accomplishes the same results as erecting and aligning a platform system to a local vertical-local north reference. This step is performed in a inertial system (on a fixed base) by direct measurement of gravity and earth's rate. In the general case, the relative magnitude of the gravity components sensed by each accelerometer allow the determination of the direction cosines between the instrument axes and the local vertical. The outputs of the accelerometers and gyros are used, together with the knowledge that there is no earth rate component along the local east vector, to generate the other six direction cosines defining the spatial relationship between the instrument axes and the local north-local east axes.

In the absence of external disturbances, measurement accuracies in the order of 1 x 10^{-4} g are possible with available accelerometers. Earth rate component information may be obtained to the zero drift tolerances of state-of-the-art rate gyros, approximately .01°/hr. Physical measurements with these accuracies permit erection and alignment of inertial guidance system to within 30 seconds of vertical and 5 mili radians of true north within several minutes.

3.1.5.2 Environmental conditions aboard medium weight carriers.

It is intended that the Flight Path Control be used on aircraft carrier based helicopters. The condition found on a ship at sea are far from ideal for the erection and alignment of an inertial navigation system, platform or fixed-frame. A ship underway on a calm sea is subject to the random motions resulting from normal maneuvers as well as the low frequency perturbations that result from inexact steering (helmsman wander). Given sufficient time, periodic motions may be filtered to any desired magnitude, minimizing their effect on the alignment process. The effects of non-periodic motions due to turns, acceleration, deceleration, etc. cannot be completely eliminated by filtering since a steady offset of the output quantity results, yielding erroneous component information to the erection and alignment system. Compound these effects with a disturbed sea and accurate alignment of an inertial system on the flight deck becomes difficult.

The repetitive pitching and rolling motions induced by the sea cause centripetal accelerations at all locations on the ship other than the center of rotation. These accelerations, proportional to sine^2 and/or cosine^2, are unidirectional yielding steady acceleration components which prevent accurate determination of the local gravity vector position and magnitude by accelerometer measurements or closed loop leveling techniques. Because of the tight coupling between the erection and alignment modes, the resulting errors in leveling define the minimum limits of alignment accuracy.

Consider the separate acceleration components that are sensed by an accelerometer mounted on the flight deck of a carrier parallel to the longitudinal axis. In the general case, the accelerometer will be displaced from the ship's centers of rotation both vertically and horizontally resulting in cross-coupling due to pitch, roll, and yaw.

The output of this accelerometer is composed of:

1. Longitudinal acceleration modified by pitch and yaw angles.
2. Gravity component variation due to pitch and roll angles.
3. Centripetal acceleration due to pitching modified by yaw angle.
4. Centripetal acceleration due to yaw accelerations modified by pitch and roll angles.

5. Centripetal acceleration due to roll while the ship is pitched.
6. Tangential acceleration due to yaw rates.
7. Tangential acceleration due to pitching and rolling.

Using the relationship's defined in Figure 4, the accelerations sensed by the longitudinal accelerometer in the sensor package are:

$$
\begin{aligned}
\ddot{a}\ \text{Long} = {} & \ddot{X}\cos\psi\cos\phi + \ddot{Y}\sin\psi - \ddot{Z}\sin\phi - g\sin\phi \\
& - \ddot{\psi}(R_p^2+Ry_2^2)^{\frac{1}{2}}\sin[\tan^{-1}Rp/Ry_2]\cos\phi \\
& + \dot{\psi}^2(Rp^2+Rr_2^2)^{\frac{1}{2}}\cos[\tan^{-1}Rp/Rr_2]\cos\phi \\
& + \ddot{\phi}(Ry^2+Rr_1^2)^{\frac{1}{2}}\sin[\tan^{-1}Ry/Rr_1]\cos\psi \\
& - \dot{\phi}^2(Ry^2+Rr_1^2)^{\frac{1}{2}}\cos[\tan^{-1}Ry/Rr_1]\cos\psi \\
& + [\ddot{\theta}(Ry^2+Rp^2)^{\frac{1}{2}}\sin(\tan^{-1}Rp/Ry) + \dot{\theta}^2(Ry^2+Rp^2)^{\frac{1}{2}}\cos(\tan^{-1}Rp/Ry)]\sin\phi \\
& - [\ddot{\theta}(RY^2+Rp^2)^{\frac{1}{2}}\cos(\tan^{-1}Rp/Ry) + \dot{\theta}^2(Ry^2+Rp^2)^{\frac{1}{2}}\sin(\tan^{-1}Rp/Ry)]\sin\psi
\end{aligned}
$$

It will be noted that the sixth (6th) and eighth (8th) terms are always positive, independent of ships motions while the remaining terms change sign with each craft oscillation. It is the positive terms in this expression that prevent accurate determination of the gravity-derived signals using filtering techniques. For operation on a medium weight carrier in a state 5 sea, typical values of craft motions are:

Pitch	$-\phi$	$= .046$ rad $[\sin(.5t+\xi_\phi)]$
Roll	$-\theta$	$= .082$ rad $[\sin(.45t+\xi_\theta)]$
Yaw	$-\psi$	$= .026$ rad $[\sin(.05t+\xi_\psi)]$
Heave accelerations	$-\ddot{Z}$	$= .54 \text{ft/sec}^2[\sin(.47t+\xi_z)]$
Surge accelerations	$-\ddot{X}$	$= .40 \text{ft/sec}^2[\sin(t+\xi_x)]$
Sway accelerations	$-\ddot{Y}$	$= .60 \text{ft/sec}^2[\sin(.6t+\xi_y)]$

Typical values of the distances shown are:

$Ry = 80$ ft.
$Rr_1 = 440$ ft.
$Rr_2 = 100$ ft.
$Rp = 50$ ft.

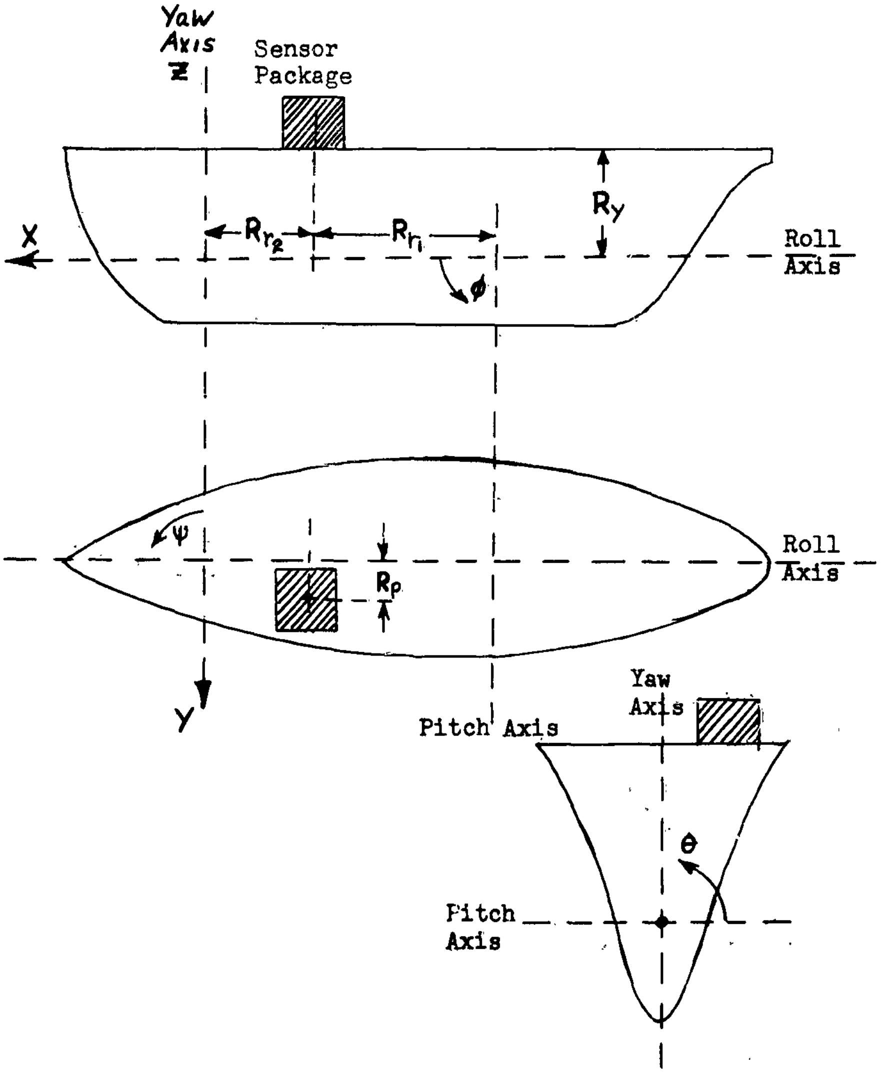
Yaw Axis Z
Sensor Package
X
R_{r_2}
R_{r_1}
R_y
ϕ
Roll Axis
ψ
R_p
Roll Axis
Y
Pitch Axis
Yaw Axis
θ
Pitch Axis

Figure 4
Definition of relationships between sensor package location and centers of rotation of aircraft carrier.

The resulting expression for the output of the longitudinal accelerometer, using small angle approximations, is then:

$$\begin{aligned}\ddot{a}_{Long} = {} & .40\sin(t+\xi_x) + .6\sin(.6t+\xi_y)[.026\sin(.05t+\xi_\psi)] \\ & -.54\sin(.47t+\xi_z)[.046\sin(.5t+\xi_\phi)] - 32.2[.046\sin(.5t+\xi_\phi)] \\ & +.65\times10^{-4}\sin(.05t+\xi_\psi)(112)(.446)+(.13\times10^{-2})^2\cos^2(.05t+\xi_\psi)(112)(.89) \\ & -.0135\sin(.5t+\xi_\phi)(446)(.182) \\ & -(.027)^2\cos^2(.5t+\xi_\phi)(446)(.984) \\ & +[-.0166\sin(.45t+\xi_\theta)(94.2)(.53)+(.0369)^2\cos^2(.45t+\xi_\theta)(.848)(94.2)] \\ & \qquad (.046\sin\{.5t+\xi_\phi\}) \\ & -[+.0166\sin(.45t+\xi_\theta)(94.2)(.848)+(.0369)^2\cos^2(.45t+\xi_\theta)(.53)(94.2)] \\ & \qquad (.026\sin\{.05t+\xi_\psi\})\end{aligned}$$

Assuming all phase angles equal zero and calculating the r.m.s. magnitudes, the separate components of the acceleration are approximately:

$$\begin{aligned}\ddot{a}_{Long} \cong {} & \pm .4 \pm .0156 \mp .0248 \mp 1.48 \pm .00324 + .000169 \\ & \pm 1.08 - .321 \mp .038 \pm .005 \mp .0345 \mp .00176 \ (\text{ft/sec}^2)\end{aligned}$$

The two terms of non-varying sign have magnitudes of +.00169 ft/sec^2 and - .321 ft/sec.^{2}. The first of these due to yaw rates, is insignificant when compared to the second which is caused by the pitching excursions of the ship.. Centripetal acceleration components of this magnitude cause approximately a 0.5° error in system erection.

Similar cross-coupling terms of non-varying sign are present in the outputs of the vertical and lateral accelerometers mounted in the sensor package at the same location. For this reason, any purely inertial system located at unspecified locations on the deck of a ship to be erected only by open or closed loop filtering techniques will seek a position determined by the average-apparent vertical not the true vertical. This will introduce large errors in the system erection and alignment which will be present even if the ship is steaming at a truly constant heading and velocity in a disturbed sea.

The results of the above derivation, based on a discrete frequency representation of a ship's motions is complicated by the fact that disturbed seas which cause these motions actually occur as a spectrum with energy distribution covering a broad frequency band. The center point and shape of this spectrum vary with wind velocity, duration and fetch. For any one set of wind conditions, this spectrum as viewed from a moving vessel changes in frequency range and contour for each ship's velocity and heading (head sea, beam sea, quartering sea, following sea, etc.) due to the varying frequency of encounter.

The most widely accepted representation of sea conditions is that generated by Neuman et. al. which is based on the hypothesis that a seaway is composed of an infinite number of wave systems which vary in frequency and direction of travel. The sea state representation is expressed as a power spectral density based on a fully developed sea as determined by measurements at a fixed point. The spectrum for a state 3 sea, given in Figure 5 can be expressed by the relationship:

$$[A(w)]^2 = (c/w^2)\ e^{-2g/v^2w^2}$$

where $[A(w)]^2$ is the energy spectrum in ft.^{2} sec.

C is a constant

w is the wave frequency in rad/sec

g is the accelerations of gravity in ft/sec.^{2}

v is the wind velocity ft/sec.

Because w is given as wave frequency at a fixed point, it must be modified to reflect the ship's velocity and heading.

Since $w = kc$
and $v = K(V \pm C)$ for head or following seas

where v is the frequency of encounter in rad/sec
v is the ship's velocity in ft/sec.
c is the wave clerity in ft/sec.

then $\frac{v}{w} = \frac{V}{C} \pm 1$

and $v = (\frac{V}{C} \pm 1)\ W$

NO. 340 -20 DIETZGEN GRAPH PAPER
20X20 PER INCH

EUGENE DIETZGEN CO.
MADE IN U. S. A.

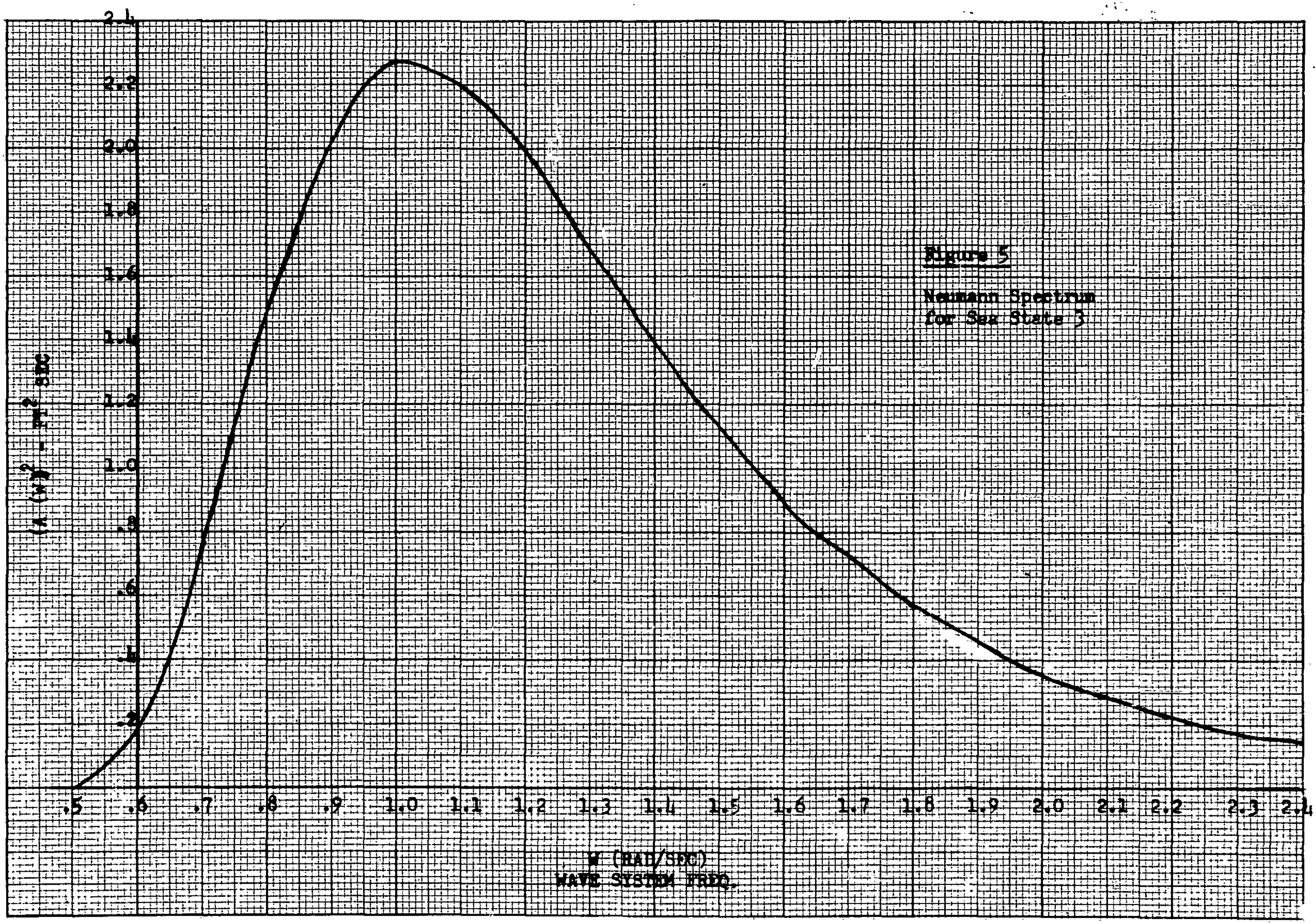

Figure 5

Neumann Spectrum
for Sea State 3

The Neumann spectrum may therefore be recalculated replacing v for W for each velocity condition desired. Figure 6 shows the resulting spectrum as it affects the longitudinal axis of the ship spectrum for a velocity of 35 kts in a following sea. As would be expected the peak energy is concentrated at a much lower frequency with a decrease in the over-all spectral density. Bringing the ship about at the same velocity would cause the spectrum of encounter to shift upward in frequency to its fixed point configuration at the beam sea condition and shift to a much higher frequency as the ship moves through the quartering sea to a head sea condition.

It is therefore possible, and probable, for the encounter spectrum of a given sea state to contain high frequency wave disturbances or wave disturbances with periods approaching that of a Schuler tuned system ($T \cong 84.4$ minutes). These may well occur in low sea states when all tactical operations are possible and therefore must be considered in the design of an erection and alignment system.

The energy distribution of these widely varying wave forcing functions is modified by the inherent dynamics of the operations ship resulting in peak energy concentrations for pitch and roll angles, and heave, surge, and sway accelerations (Figure 7). The corresponding crafts motions and acceleration in these axes are therefore greatest near the peak energy points with reduced magnitude at higher and lower frequencies.

Of primary concern are the low frequency components which are the most difficult to attenuate through filtering techniques because of the long averaging times required. The spectra of ship motions and accelerations, corresponding to the energy spectra of Figure 7, are shown in Figure 8. For the sea state, ship velocity, and heading conditions which existed when these measurements were made, the significant perturbations occurred between .3 rad/sec and 2 rad/sec. For other environmental conditions significant disturbances may be expected to range between 0.1 rad/sec and 4 rad/sec. Since the period of oscillation corresponding to 0.1 rad/sec is 62 sec., an averaging time period of approximately 600 sec (10 minutes) will be required to attenuate this to one tenth of its value.

The effect of ship's dynamics about the yaw axis modifies the encounter energy spectrum in a much different way. The yaw axis energy and motion spectra (Figure 9) determined from measurements made with the same environmental conditions as the previous data, indicates significant yaw axis excursions

NO. 340 -20 DIETZGEN GRAPH PAPER
20 X 20 PER INCH
EUGENE DIETZGEN CO.
MADE IN U. S. A.

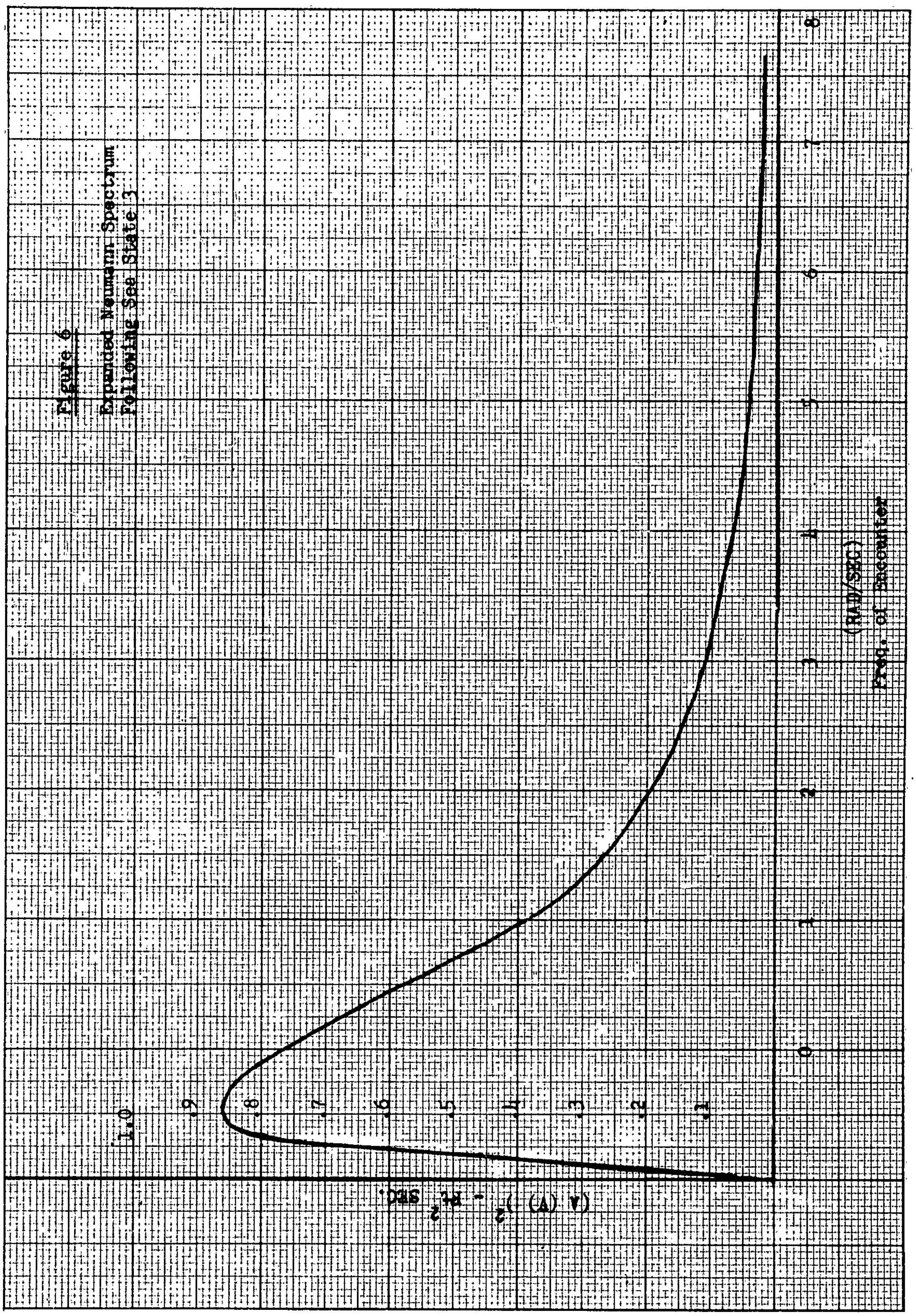

Figure 6

Expanded Neumann Spectrum Following Sea State 3

EUGENE DIETZGEN CO
MADE IN U.S.A.

NO. 340 -20 DIETZGEN GRAPH PAPER
20 X 20 PER INCH

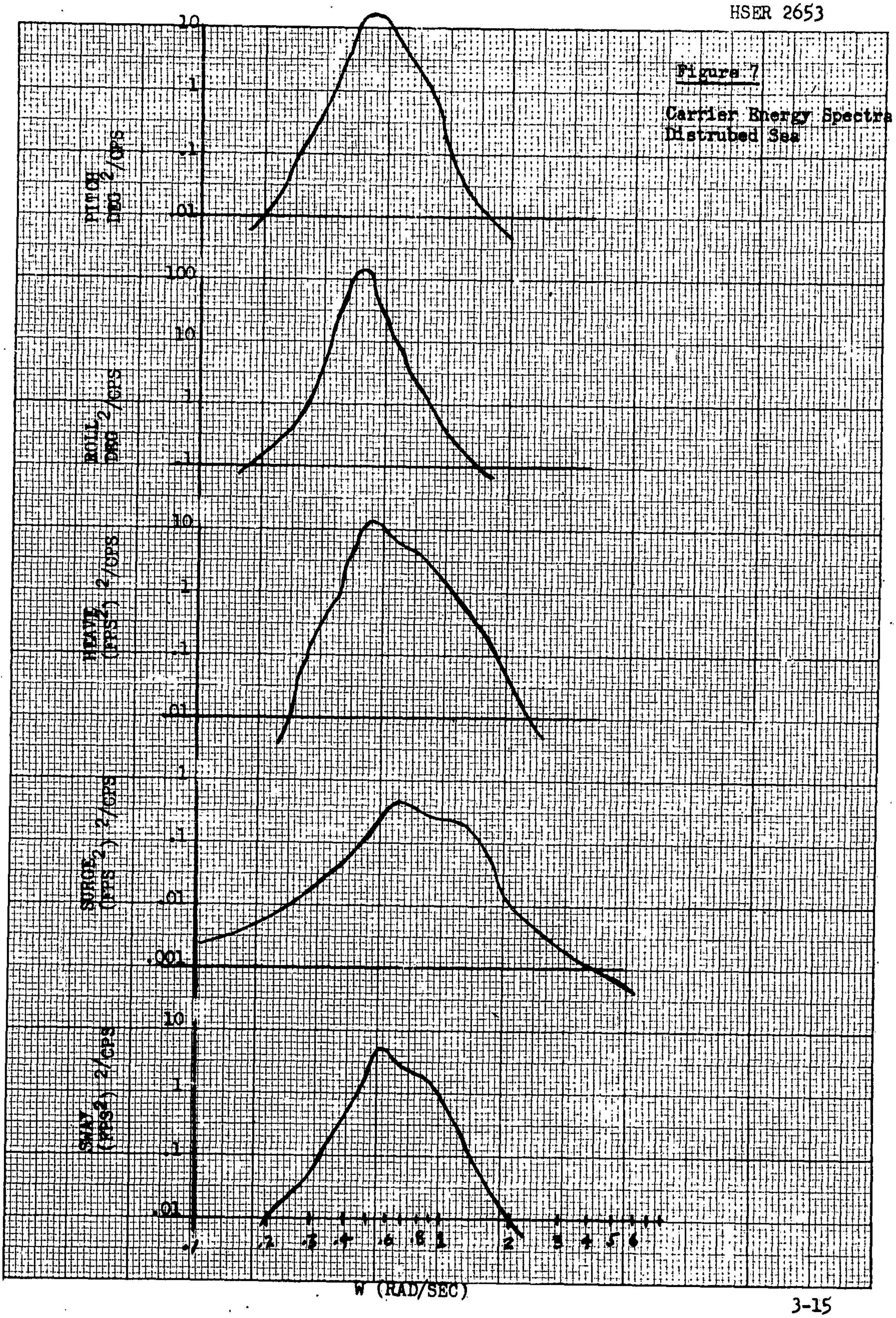

Figure 7

Carrier Energy Spectra
Distrubed Sea

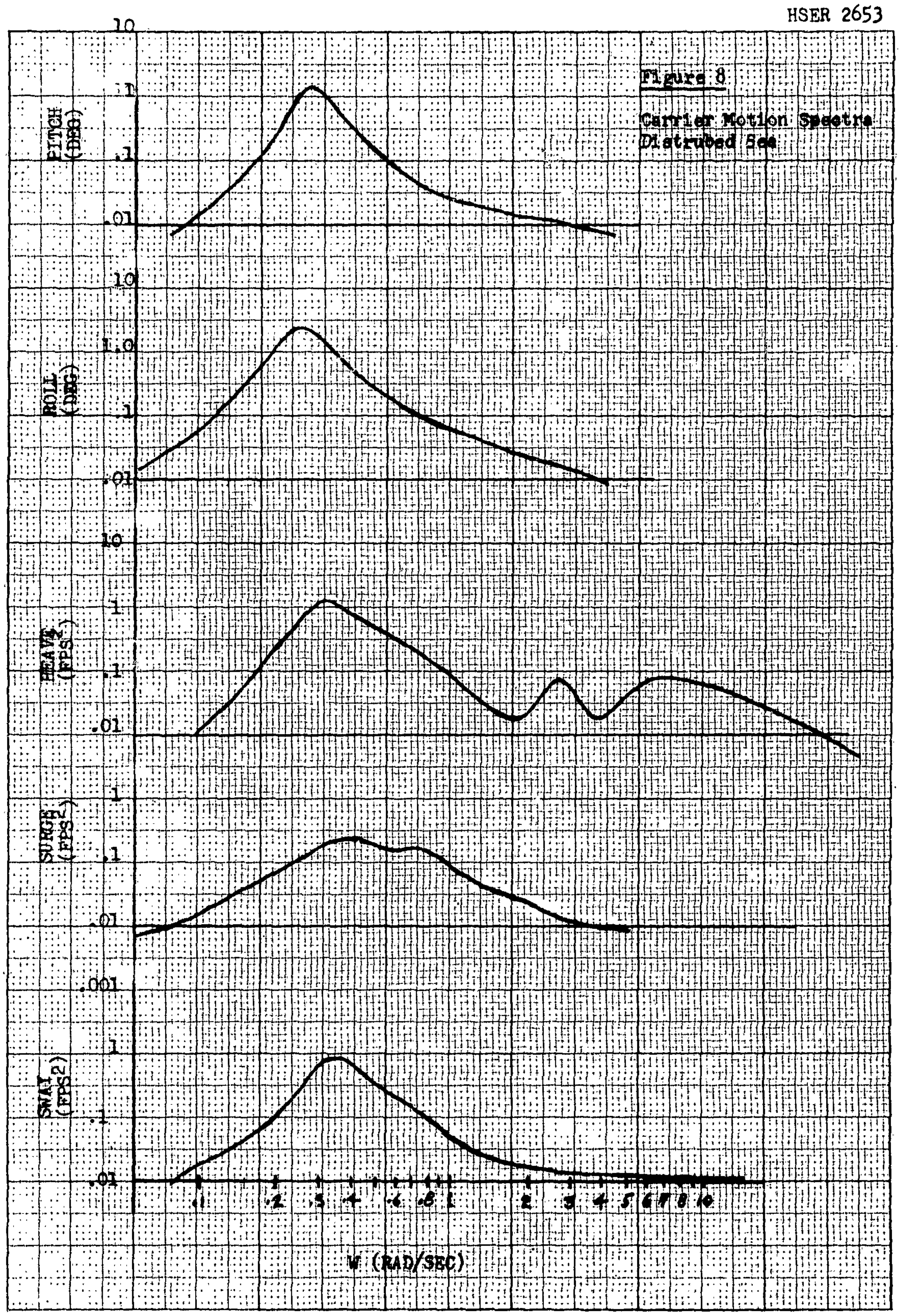

Figure 8

Carrier Motion Spectra
Distrubed Sea

EUGENE DIETZGEN CO.
MADE IN U.S.A.

NO. 340-20 DIETZGEN GRAPH PAPER
20X20 PER INCH

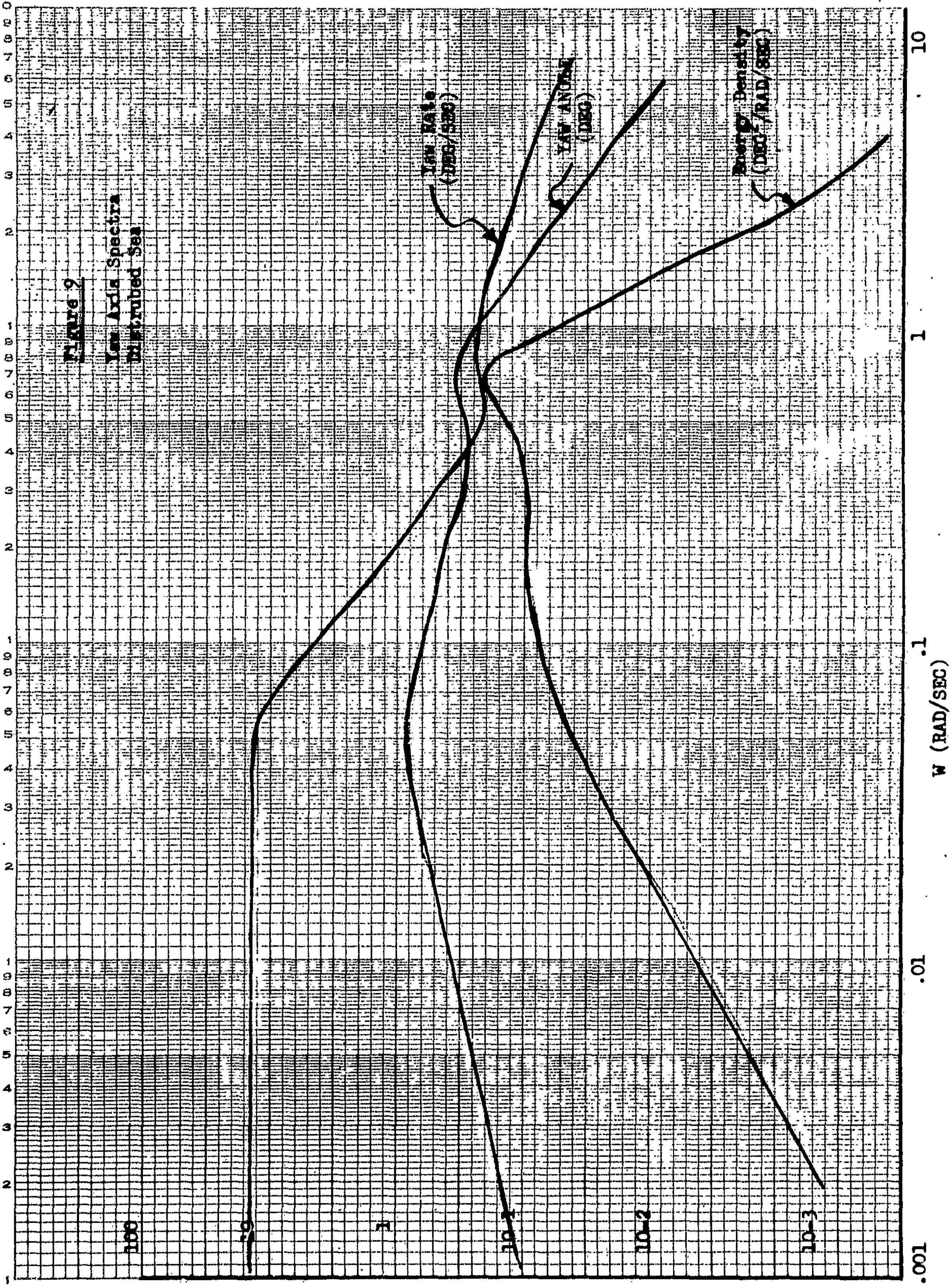

Figure 9

Yaw Axis Spectra
Disturbed Sea

EUGENE DIETZGEN CO.
EUGENE DIETZGEN GRAPH PAPER
SEMI-LOGARITHMIC
4 CYCLES X 10 DIVISIONS PER INCH

well below0.001 rad/sec (period $\cong$ 100 minutes) and yaw rates equal to earth rate (.004 °/sec) at frequencies of approximately .01 rad/sec (period $\cong$ 10 minutes). Averaging over 10 cycles to obtain reduction in amplitude by approximately 10/1 would therefore require 100 minutes.

Additional perturbations that must be considered when determining the total disturbances to a carrier based inertial system are:

(1) Natural ship's vibrations.
(2) Longitudinal and torsional bending due to ship and sea motions.
(3) The effects of the expansion joints along the length of the ship.

It is theoretically possible to compensate for many of the external disturbances using ship derived pitch, roll, heading and velocity signals when location of the inertial system is known with respect to the centers of rotation of the ship.

For the specific tactical situation of the Flight Path Controller, the helicopters equipped with the inertial systems may be located at random areas of the flight decks so this type of compensation cannot even be considered.

3.1.5.3 Self-Contained Gyrocompassing Inertial Systems

The several methods proposed for erection and alignment of local level geometric reference guidance systems whether platform or fixed frame, all reduce basically to low band pass closed loop systems which reduce the magnitude of unwanted input disturbances by filtering (or averaging) processes. The band width of this closed loop must be optimized for two conflicting requirements:

1. Minimization of solution time with a given set of input disturbances.
2. Minimization of the forced dynamic errors resulting from the input disturbances.

The erection and alignment mode of self-contained local level inertial systems, are generally designed as shown in the simplified block diagram of Figure 10. These systems whether they are

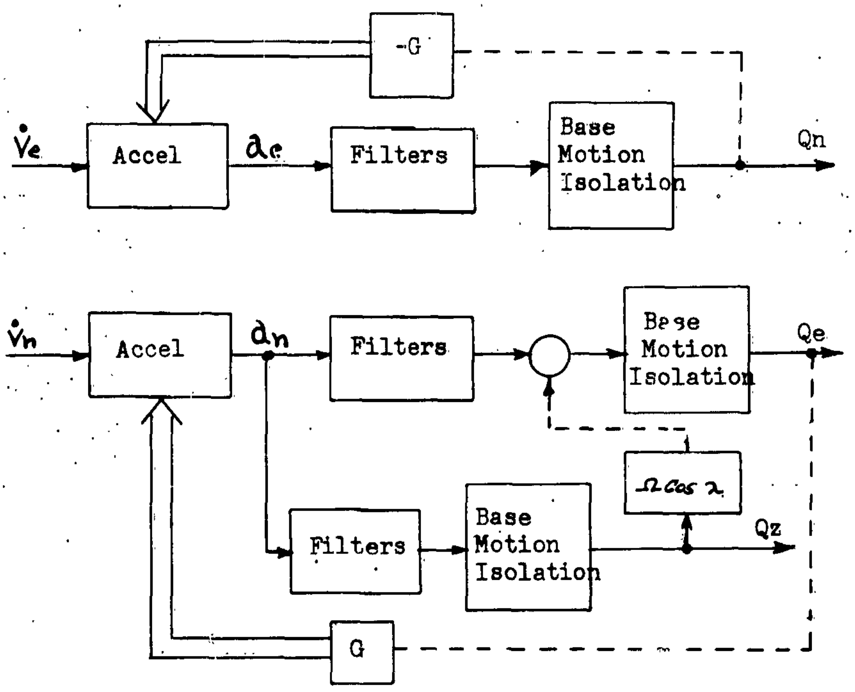
-G
$\dot{V}_e$
Accel
a_e
Filters
Base Motion Isolation
Qn
$\dot{V}_n$
Accel
a_n
Filters
Base Motion Isolation
Qe
$\Omega \cos \lambda$
Filters
Base Motion Isolation
Qz
G

Figure 10

classified as acceleration-coupled with internal filtering or velocity coupled with internal feedback, are essentially equivalent and are designed to have maximum input distrubance attenuation characteristics with minimum time constant filters.

An example of the dynamic response of the erection and alignment modes of a typical system may be obtained from analysis of the system shown in the simplified block diagram of Figure 11. This system contains second order filters with the loop gains adjusted to yield critical damping of the major leveling loop dynamics. The filter time constants are chosen to provide adequate attenuation of pitch and roll disturbances and results in a leveling time of approximately 5 minutes for pitch and roll motions of 10 degrees. It will be noticed, however, that attenuation of yaw axis motions is very small and that there is no provision to attenuate the steady tangential accelerations that result from the pitching and rolling motions.

The gyro compassing loop dynamic response is obtained using the closed loop response of the East leveling loop in the forward path as shown in Figure 12. The root locus plot shows the closed loop response to consist of a pair of dominant complex roots, with a subordinate complex pair and a high frequency lag. The loop gain (which must vary as a function of latitude) is adjusted to yield a well damped system.

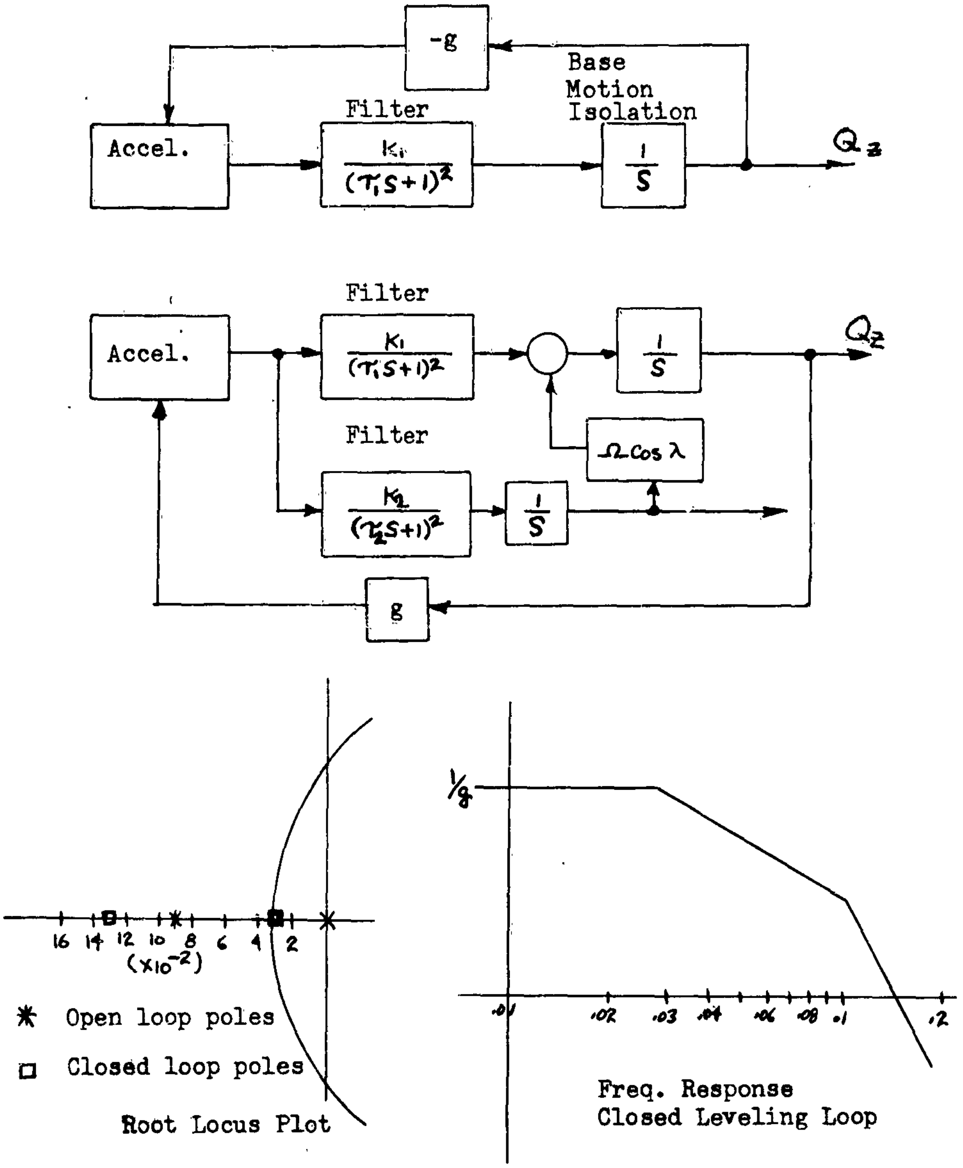
-g
Base
Motion
Isolation
Filter
Accel.
$\frac{K_1}{(T_1S+1)^2}$
$\frac{1}{S}$
Q_z
Filter
Accel.
$\frac{K_1}{(T_1S+1)^2}$
$\frac{1}{S}$
Q_z
Filter
$\Omega \cos \lambda$
$\frac{K_2}{(T_2S+1)^2}$
$\frac{1}{S}$
g
16 14 12 10 8 6 4 2
$(\times 10^{-2})$
$1/g$
.01 .02 .03 .04 .06 .08 .1 .2

✱ Open loop poles

☐ Closed loop poles

Root Locus Plot

Freq. Response
Closed Leveling Loop

Figure 11

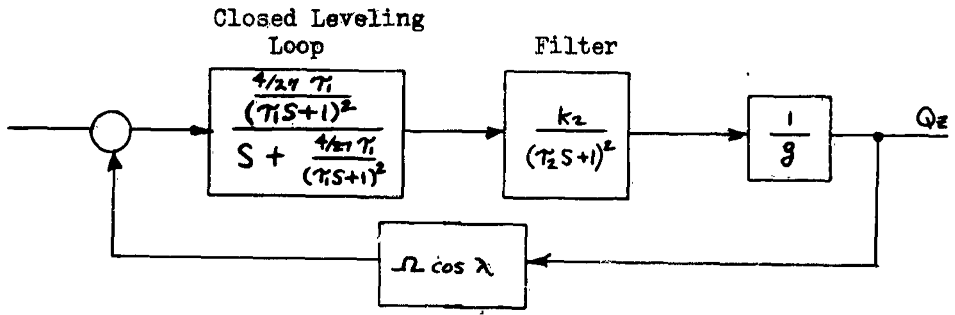
Closed Leveling Loop
Filter
$\frac{4/27\,\tau_1}{(\tau_1 S+1)^2} \Big/ \left(S + \frac{4/27\,\tau_1}{(\tau_1 S+1)^2}\right)$
$\frac{k_2}{(\tau_2 S+1)^2}$
$\frac{1}{g}$
Q_z
$\Omega \cos \lambda$

Simplified gyro compassing loop; which reduces to:

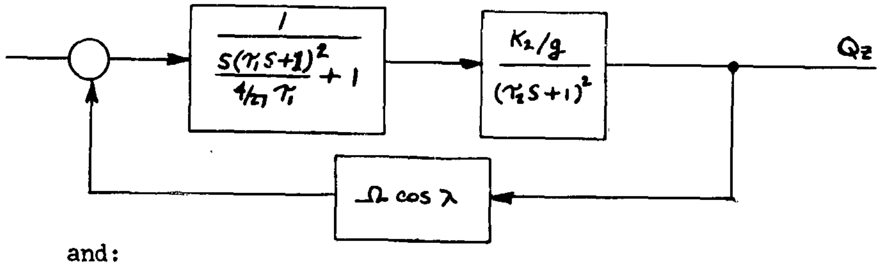
$\frac{1}{\frac{S(\tau_1 S+1)^2}{4/27\,\tau_1}+1}$
$\frac{K_2/g}{(\tau_2 S+1)^2}$
Q_z
$\Omega \cos \lambda$

and:

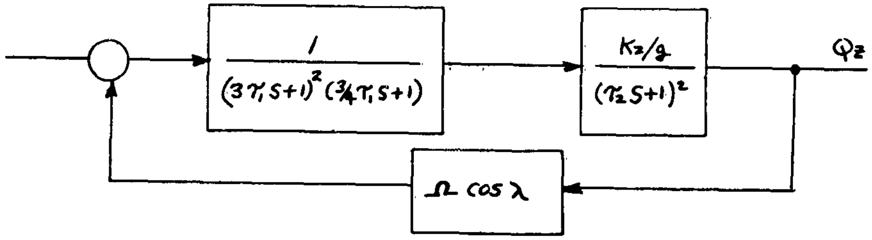
$\frac{1}{(3\tau_1 S+1)^2(3/4\,\tau_1 S+1)}$
$\frac{K_2/g}{(\tau_2 S+1)^2}$
Q_z
$\Omega \cos \lambda$

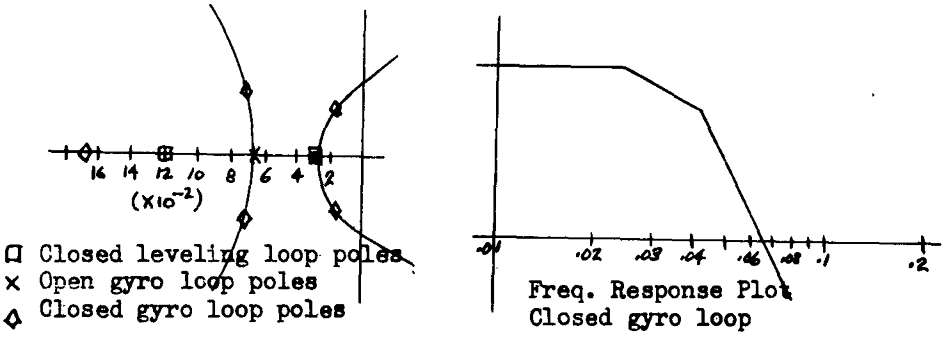

Root Locus Plot

Freq. Response Plot
Closed gyro loop

Figure 12

With $K_2 \cos \lambda$ equal to 65, the leveling time for 5 degrees initial misalignment is approximately 15 minutes.

In this loop also, there is no provision to remove the steady acceleration component caused by ship motions. It is evident that no low pass filter can be designed to eliminate the cosine^2 tangential acceleration components yet pass the steady-state earth rate and gravity signals. If it is possible to reduce these effects by some other means such as location of the instrument package, then filtering is practical for sea state-ship's velocity heading conditions which result in relatively high frequency oscillatory motions.

3.1.5.4 External Velocity Inputs

The difficulties encountered in aligning self-contained inertial systems on a moving base which requires separation of the earth rotational rate of 0.004°/sec. from sinusoidal base rates of approximately 1°/sec. may be alleviated through comparison of computed inertial parameters with equivalent externally measured parameters. The logical choice of external inputs is craft velocity which may be obtained from doppler velocity instruments with good long term accuracy and may be compared with the velocity information generated by the inertial system which has good short term accuracy. The comparison may be made on quantities of equivalent magnitude reducing the signal separation problem.

External velocity information is introduced into the inertial system to control system damping and resonant frequency. Judicious choice of the magnitudes of these quantities provides maximum attenuation of inertial system errors in the shortest time with greatest accuracy. Simplification of the block diagram of the basic fixed frame inertial system (refer to Figure 13) permits linear analysis of the position tracking loops. By assuming a constant value of gravitational attraction and a constant value for the earth's radius (spherical earth), the three interacting loops may be separated into independent single axis systems.

Each position tracking loop of the basic system maybe represented as in Figure 13. The two integrators, velocity and position, are represented using Laplace notation as:

$$\mathcal{L}\left[\int dt\right] = \frac{1}{s}$$

The G/R feedback is derived as the component of gravitational field force sensed by an I axis accelerometer (see Figure 14) in the earth fixed reference frame. From fundamental feedback theory, the transfer function of this loop is:

$$\frac{I}{A_I} = \frac{1}{S^2 + G/R}$$

which indicates an undamped second order system with Schuler Tuning ($\mathcal{T}$ = 84.4 minutes)

Introduction of external velocity information into this loop is accomplished as in Figure 15. The difference signal Δv fed back through the gain C_1 controls primarily the damping of the loop and fed forward through the gain C_2 controls the resonant frequency.

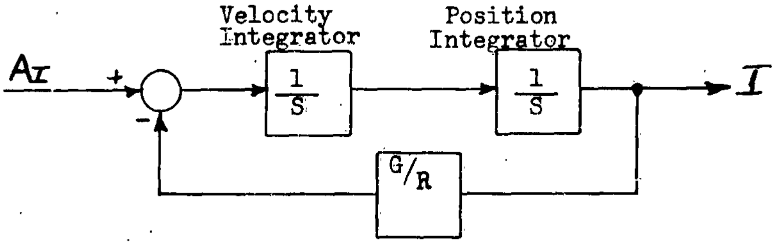
Velocity Integrator
Position Integrator
A_I
+
−
$\frac{1}{S}$
$\frac{1}{S}$
I
G/R

Single Axis Representation of Position Tracking Loop
Figure 13

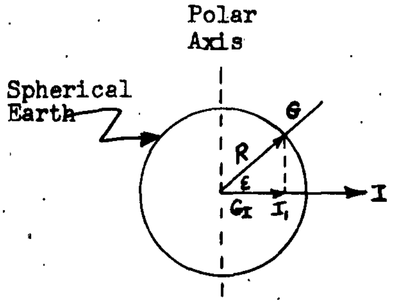
Polar Axis
Spherical Earth
G
R
ε
G_I
I_1
I

$$G_I = G \cos(\varepsilon) = G\frac{I_1}{R}$$

$$G_I = I_1\left(\frac{G}{R}\right)$$

Derivation of G/R Feedback
Figure 14

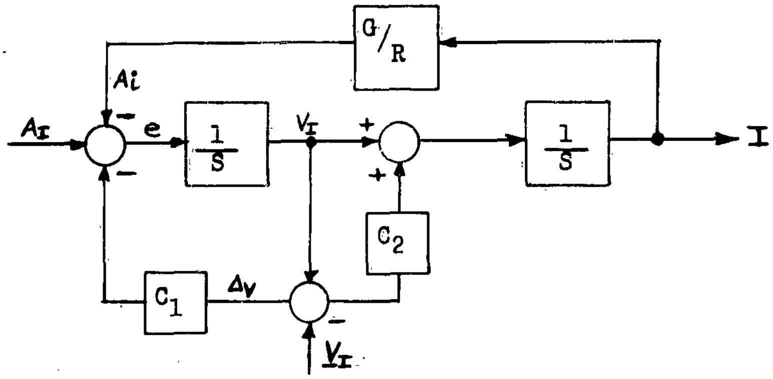

Position Tracking Loop with External Velocity Input

Figure 15

Writing the loop equations:

$$e = A_I - Ai - C_1 \Delta V$$

$$A_i = A_I - C_1 \Delta V - e$$

$$\Delta V = e/s - V_I$$

$$\left[e\left(\frac{1}{s}\right) + C_2 \Delta V\right]\left(\frac{1}{s}\right)\left(\frac{G}{R}\right) = A_I - C_1 \Delta V - e$$

Let $A_I = 0$ to determine stability, then $V_I = 0$ (no motion in inertial space)

$$\left(\frac{e}{s^2} + C_2 \frac{e}{s^2}\right) \frac{G}{R} = - C_1 \frac{e}{s} - e$$

$$\left[s^2 + C_1 s + (1 + C_2) \frac{G}{R}\right] e = 0$$

which is as expected.

If the external velocity has an error e_v, the loop equations become:

$$\left[\frac{e}{s^2} + C_2 \left(\frac{e}{s^2} - \frac{e_v}{s}\right)\right]\frac{G}{R} = A_I - C_1 \left(\frac{e}{s} - e_v\right) - e$$

where $\Delta V = e/s - e_V$

Letting $A_I = 0$ as before, then:

$$\left[s^2 + C_1 s + (1 + C_2)\frac{G}{R}\right] e = s\left(C_2 \frac{G}{R} + C_1 s\right) e_v$$

OR:

$$e/e_V = \left[s\left(C_2 \frac{G}{R} + C_1 s\right)\right] / \left[s^2 + C_1 s + (1 + C_2)\frac{G}{R}\right]$$

This indicates that the acceleration error (e) will exhibit a damped oscillatory characteristic to initial disturbances but will have no steady-state error due to doppler velocity calibration errors.

If it is desired that the system settle in 30 minutes and be damped to 0.5 of critical,

$$w_d = \frac{1}{360} \text{ sec.}$$

$$w_n = \frac{1}{360\sqrt{1 - .25}} = .00321 \text{ rad/sec}$$

since

$$w_n^2 = \frac{G}{R}(1 + C_2)$$

$$C_2 = 5.71$$

and

$$C_1 = 2\zeta w_n = 2\,(.5)\,(.00321) = .00321$$

then

$$\frac{e}{\bar{e}_v} = \frac{.85\,s\,(\,.3655 \times 10^{-3}s + 1\,)}{\left(\frac{s}{3.21 \times 10^{-3}}\right)^2 + \frac{2(\,.5)\,s}{3.21 \times 10^{-3}} + 1}$$

In this case, an external perturbation of 1 knot in the doppler velocity signal at frequencies greater than 0.005 rad/sec result in an acceleration error (e) of approximately 0.0054 ft/sec.^{2}. The transfer function $\frac{e}{\bar{e}v}$ is shown in Figure 16.

The corresponding inertial velocity error due to doppler velocity error is given by:

$$\frac{V}{e_v} = \frac{(C_2\frac{G}{R} + C_1 s\,)}{s^2 + C_1 s + (\,1 + C_2\,)\frac{G}{R}}$$

which, for the above case yields:

$$\frac{V}{\bar{e}_v} = \frac{8.79 \times 10^{-6}\left(\frac{s}{2.74 \times 10^{-3}} + 1\right)}{s^2 + 3.21 \times 10^{-3}s + 10.32 \times 10^{-6}}$$

and is plotted in Figure 17. For doppler error frequencies below 0.001 rad/sec. the inertial velocity error will equal

NO. 340-L35 DIETZGEN GRAPH PAPER
LOGARITHMIC
3 CYCLES X 5 CYCLES

EUGENE DIETZGEN CO.
MADE IN U. S. A.

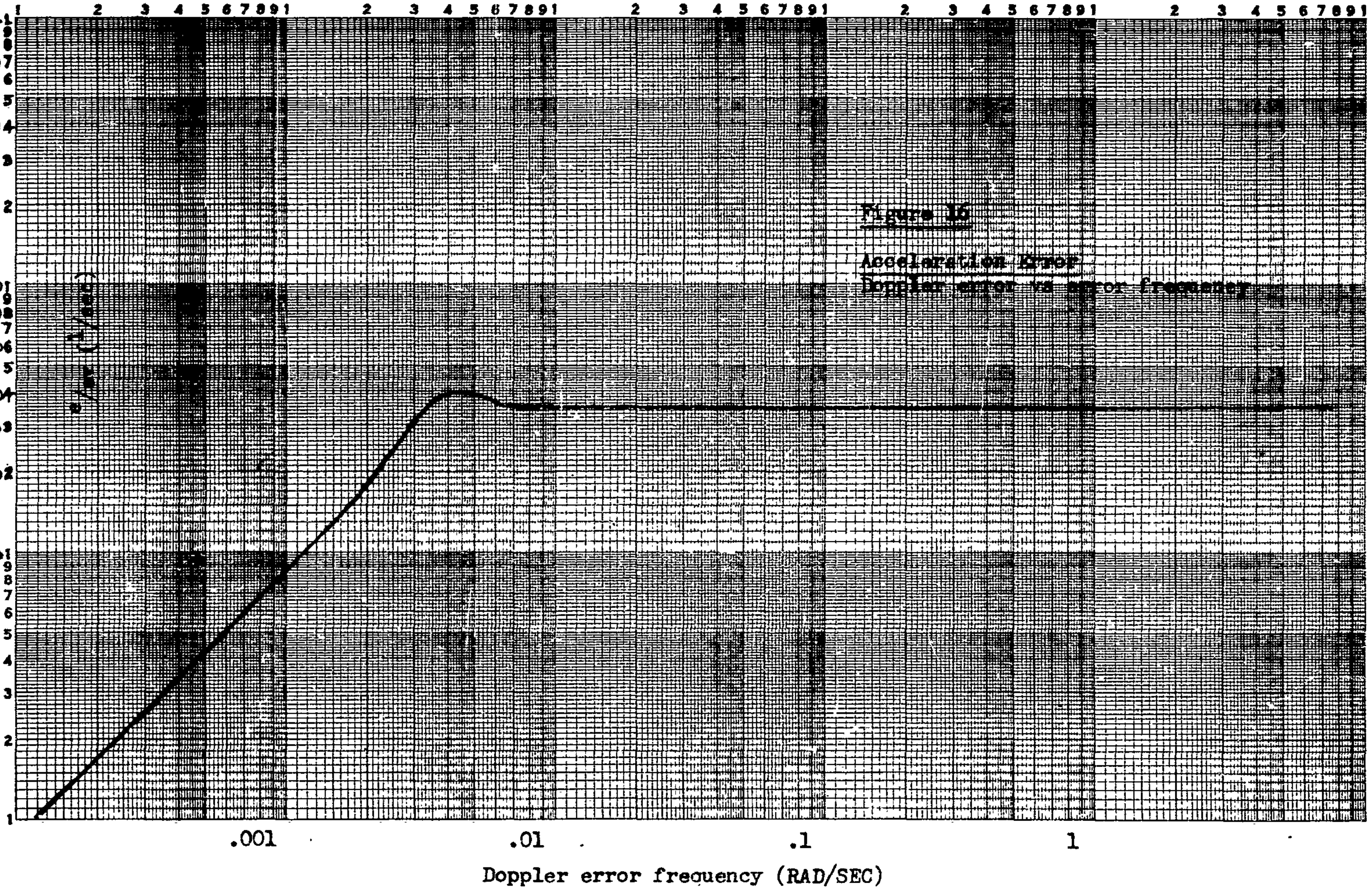

Figure 16

Acceleration Error
Doppler error vs error frequency

NO. 340-L35 DIETZGEN GRAPH PAPER
LOGARITHMIC
3 CYCLES X 5 CYCLES

EUGENE DIETZGEN CO.
MADE IN U. S. A.

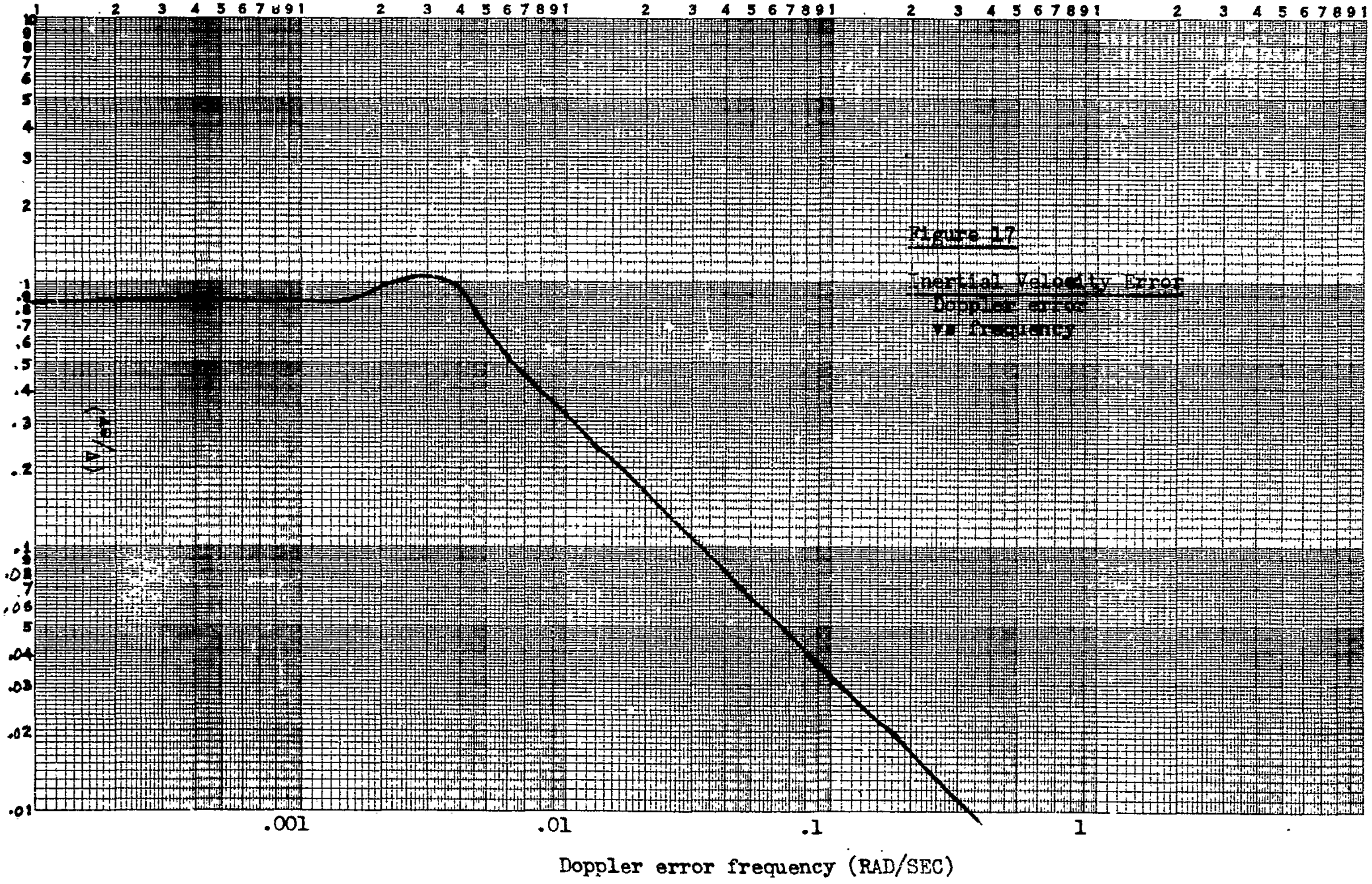

Figure 17

Inertial Velocity Error
Doppler error
vs frequency

approximately 85% of the doppler velocity error, indicating that the steady state accuracy of the doppler inertial system, is dependent on the basic accuracy of the doppler information, i.e., on the accuracy of the basic instrument and resolution of the beam velocities into airframe velocities. Since the instantaneous information from any doppler-velocity system occurs with a normal probability distribution about the actual velocity, the information fed to the inertial system must be short term averaged to reduce the effects of the variation. The averaging time must be kept to a minimum, however, so that changes in actual craft velocity are not significantly attenuated but are passed directly to the velocity comparison network.

Use of external velocity information will not only aid the reduction of initial disturbances to the inertial system by tuning the tracking loop but will constrain the inertial errors which normally tend to accumulate with time since the long-term accuracy of a doppler-inertial system is proportional to inherent accuracy of the doppler system.

3.1.5.5 FPC Erection and Alignment System

Due to the errors that arise from simple filtering techniques for erection and alignment of a carrier based inertial guidance system, the design of the FPC was based on the philosophy that this approach would be sufficient only for coarse erection where knowledge of the local gravity vector position within 1 degree is tolerable. More accurate information on the true vertical position must therefore be obtained by other means during the fine erection and alignment mode.

Implementation of the coarse erection process in a fixed frame system entails the use of gyros and accelerometers with a filtering process similar to the closed loop process of a platform system. Because the inertial sensors are hard mounted to the base, however, the action of the base motion isolation function is accomplished with the use of the gyro outputs feeding a sub-routine in the computer program. The resulting isolated accelerometer outputs are then averaged to yield the relationship between the average-apparent-vertical and the instantaneous system axes.

The coarse erection process is actually performed as shown in Figure 18 and is accomplished as two separate functions. Since the instrument axes are in motion, as is the apparent vertical, due to perturbations of the base; it is necessary to obtain the average position of the apparent vertical with respect to a set of reference axes. At the end of the coarse erection process, the spatial relationship between the instantaneous instrument axes and the reference axes are combined with the relationship between the reference axes and the average-apparent-vertical to provide the desired information relating the average-apparent-vertical and the instantaneous instrument axes position.

Stated mathematically, the desired relationship is:

$$\cos (x, y, z/\overline{u})$$

where x, y, and z are unit vectors along the respective instrument axes

u is the local vertical unit vector

$\overline{U}$ is the average position of the vertical unit vector

X_0, Y_0 and Z_0 are the reference unit vectors established at $t = t_0$ -2 minutes.

The orientation of the reference axes in the present position coordinate frame is chosen to be the instantaneous orientation of the instruments axes at $t - t_0$ -2 minutes and is established by setting the initial values of the direction cosine matrix of box J to:

$$\mathrm{Cos}(X,Y,Z/X_0,Y_0,Z_0) = \begin{vmatrix} 100 \\ 010 \\ 001 \end{vmatrix} \quad t = t_0 - 2$$

Continuous information from the x, y, z gyros up dates this matrix in accordance with base motion to maintain the validity of the direction cosines. The ouputs of the x, y, x accelerometers, which move with the base, are so resolved on to the reference axes through the use of these direction cosines (Box H) and provide the instantaneous values of acceleration on the X_0, Y_0 and Z_0 axes, i.e.

$$a_{x_0}, a_{y_0}\ a_{z_0}$$

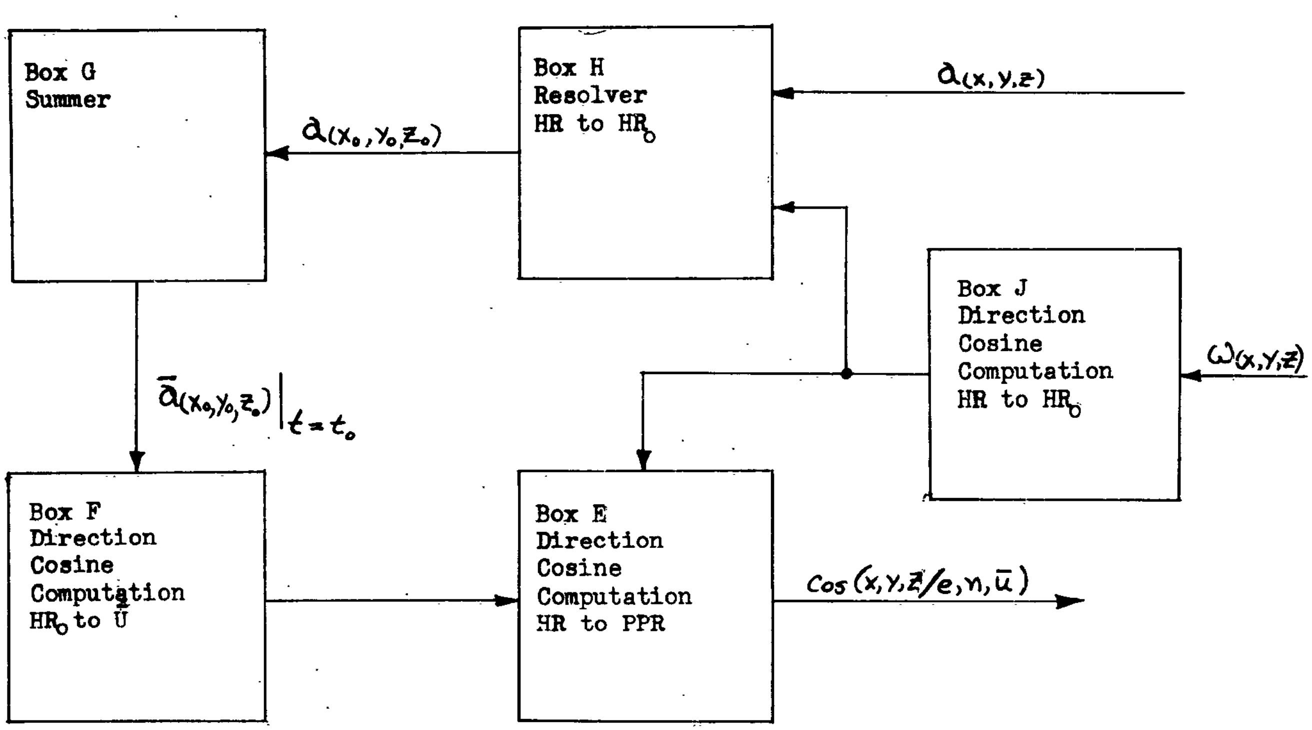
Box G
Summer
Box H
Resolver
HR to HR$_0$
$a(x,y,z)$
$a(x_0,y_0,z_0)$
Box J
Direction
Cosine
Computation
HR to HR$_0$
$\omega(x,y,z)$
$\bar{a}(x_0,y_0,z_0)\Big|_{t=t_0}$
Box F
Direction
Cosine
Computation
HR$_0$ to $\bar{U}$
Box E
Direction
Cosine
Computation
HR to PPR
$\cos(x,y,z/e,n,\bar{u})$

Signal Flow Diagram
Coarse Erection & Alignment (Moving Base)

Figure 18

Summation of these components for a predetermined time interval (Box G) provides the average component values $\bar{a}_{x_0}$, $\bar{a}_{y_0}$ $\bar{a}_{z_0}$ and allows computation (Box F) of the direction cosines between X_0 Y_0 Z_0 and $\bar{U}$; cos $(X_0\ Y_0\ Z_0/\bar{U})$. Combination of the direction cosines cos $(X_0\ Y_0\ Z_0/U)$ with Cos $(X, Y, Z/X_0, Y_0, Z_0)$ at $t = t_0$ in a matrix calculation yields the desired cos $(X, Y, Z/\bar{U})$ from Box E. The time for coarse erection must be optimized for minimum total error. Errors due to periodic ship motions decrease with erection time. Errors introduced by the earth rotation rate, which cannot be accounted for in this process, increase with erection time.

Bias errors introduced by the tangential accelerations of the sensors are independent of time. Consideration of the effects of these error sources had led to the choice of a coarse erection time of 2 minutes.

The coarse alignment process involves the computation of the direction cosines which relate the local east, local north vectors to the instrument axes, cos (e, n/X, Y, Z,) utilizing heading information from the ship's compass and knowledge of the helicopter orientation on the flight deck of the carrier. This computation is performed as indicated in Box E during the last computation cycle of the digital computer before $t = t_0$. The ship's heading information is combined with the helicopter orientation angle to provide the horizontal component of the helicopter, and inertial system, heading angle. This information is reflected onto the X-Y plane of the instrument axes according to the instantaneous pitch and roll angles of the ship as determined by the coarse erection process. Trigonometric manipulation of the resulting angles permits the calculation of the direction cosines; cos (e, n/X, Y, Z). Determination of the signs of several computed functions is based on the knowledge that the helicopter and ship are in an upright condition on the surface of the earth and that deviation from the vertical will be between ± 90°.

Coarse alignment accuracy is expected to be approximately ±5° of true North. Shipboard gyrocompass specifications require heading accuracies of ± 0.5°. Discussion with personnel at the ASW shipboard equipment group at Bu Weps confirmed that the estimated helicopter orientation should be accurate to within ±5°. Combining these expected errors with an estimated computer error of 0.1° yields the composite 5° error.

The relationship between the earth centered inertial reference frame and the present position frame of local east, local north, local vertical cos (e, n, u/E_0 N_0 U_0) is determined through use of spherical trigonometry equations and the Hayford representation of the earth's geoid (See Figure 20). The external information required is geographic latitude and longitude as determined by the ship's navigation system. Inaccuracies in ship's latitude and longitude obtained by dead reckoning navigation systems may be as large as 20 miles which will introduce errors of approximately 20 minutes of arc into the composite inertial erection and alignment information

Coarse erection and alignment direction cosines are shown in Figure 19.

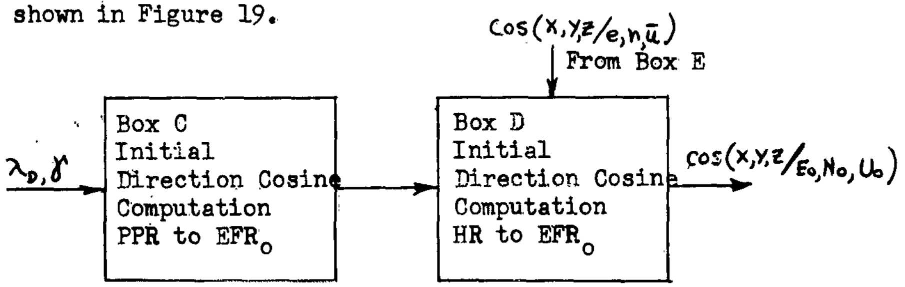
$\cos(x,y,z/e,n,\bar{u})$
From Box E
λ_D, γ
Box C
Initial
Direction Cosine
Computation
PPR to EFR_0
Box D
Initial
Direction Cosine
Computation
HR to EFR_0
$\cos(x,y,z/E_0,N_0,U_0)$

Figure 19

This error will be removed during the fine erection and alignment mode to be described later.

Signal flow of the final stage of coarse erection and alignment. direction cosines is shown in Figure 19

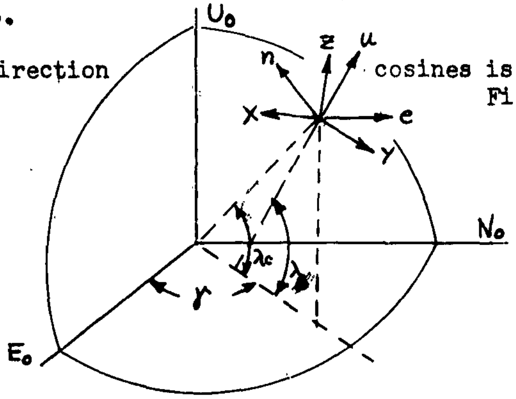
U_0
z
u
n
X
e
Y
N_0
λ_c
λ_D
γ
E_0

Pictorial Relationship between E, N, U, e, n, u, and X, Y, Z coordinate reference frames.

Figure 20

Matrix multiplication (Box D) of the direction cosines relating the instrument axes to the present position axes, cos $(X, Y, Z/e, n, \bar{u})$ and the direction cosines relating present position to the inertial reference frame, cos $(e, n, u/ E_0 N_0 U_0)$ provides the relationship between instrument axes and inertial reference frame required for the coarse erection and alignment of the inertial system to the inertial reference, i. e./

$$\cos(X,Y,ZYE_0N_0U_0) = \cos(X,Y,Z/e,n,\bar{u}) \quad \cos(e,n,u/E_0N_0U_0)$$

3.1.5.6 Fine Erection and Alignment

Because of the magnitude of the errors expected in the coarse erection and alignment information, it is imperative that the fine erection and alignment process be as fast and as accurate as possible. As stated in a previous section of this report, doppler velocity information will be utilized to help achieve this aim. The simplified signal flow diagram in Figure 21 shows the basic system configuration and method of doppler tie-in to the position tracking (gravity compensation) loop. Linear analysis of this loop specified that coefficient C_4 be set to a value of 5.71 to increase the natural frequency of the servo-synthesized pendulum to 0.00321 rad/sec for a settling time of approximately 35 minutes. C_3 is made equal to 0.00321 to yield a damping ratio of 0.5 of critical. The response of this system to a step of acceleration is given in Figure 22. The error in computed inertial velocity is equal to 85% of the steady state error in the doppler system as shown in Figure 17.

The initial conditions of velocity and position of the helicopter at the start of the fine erection and alignment processes are computed in inertial coordinates using external information supplied from the ship's navigation system, i.e., latitude, longitude, ship's velocity, ship's heading, helicopter orientation angle, and parameters defining the Hayford earth model representation. The error in these initial conditions, dependent on the accuracy of the inputs to the computer program, contributes to the initial disturbance of the position tracking loop in addition to the error in the acceleration input. Use of the doppler inertial velocity error as feedback and feedforward allows tuning and damping of the position tracking loop to reduce the effects of the initial loop errors.

Simplified Signal Flow Diagram
Doppler-Inertial Fine Erection Process

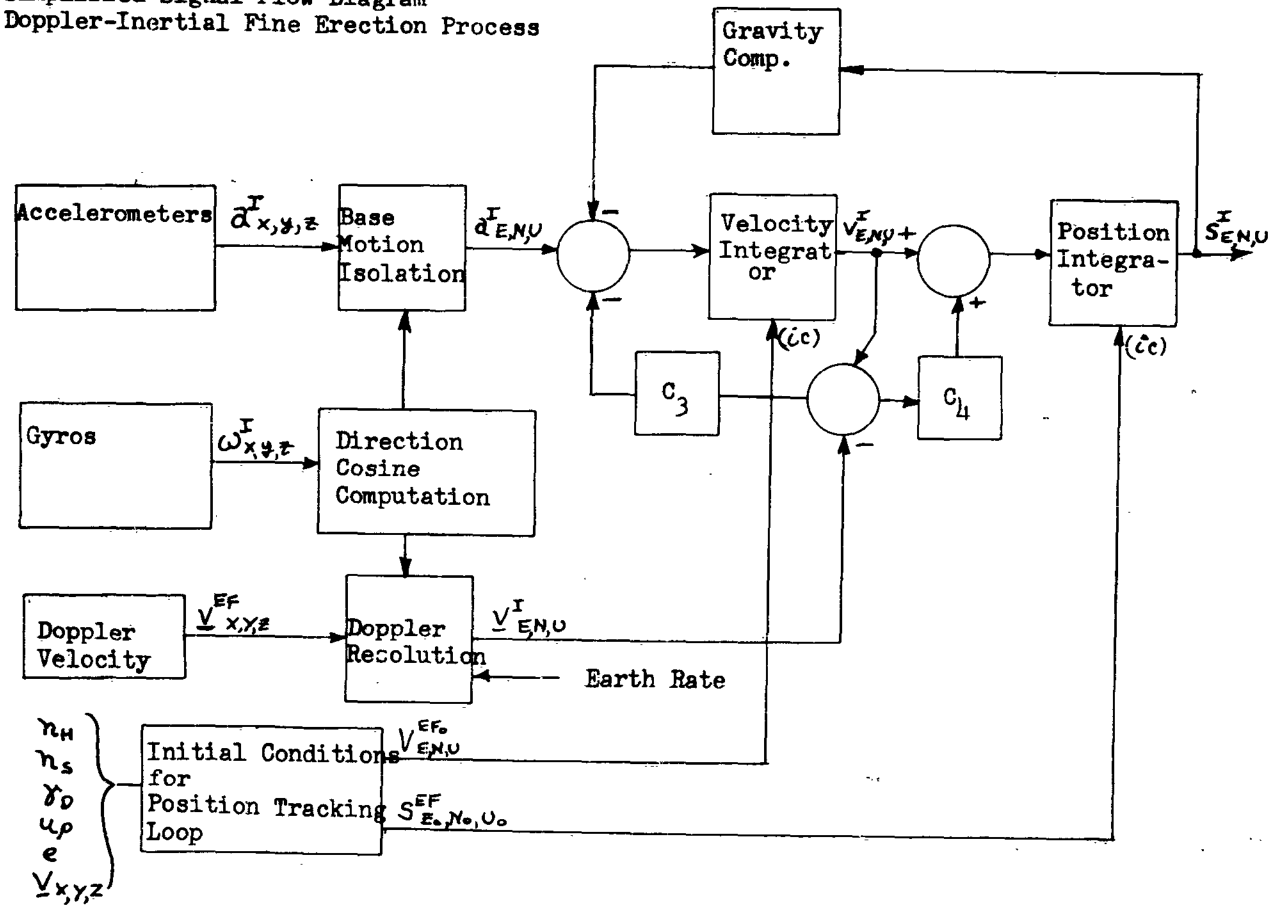
Gravity Comp.
Accelerometers
$a^I_{x,y,z}$
Base Motion Isolation
$a^I_{E,N,U}$
−
−
Velocity Integrator
$V^I_{E,N,U}$
+
+
Position Integrator
$S^I_{E,N,U}$
(ic)
(ic)
C_3
C_4
−
Gyros
$\omega^I_{x,y,z}$
Direction Cosine Computation
Doppler Velocity
$\underline{V}^{EF}_{x,y,z}$
Doppler Resolution
$\underline{V}^I_{E,N,U}$
Earth Rate
n_H
n_s
γ_D
u_ρ
e
$\underline{V}_{x,y,z}$
Initial Conditions for Position Tracking Loop
$V^{EF_0}_{E,N,U}$
$S^{EF}_{E_0,N_0,U_0}$

Figure 21

NO. 340 -20 DIETZGEN GRAPH PAPER
20X20 PER INCH

EUGENE DIETZGEN CO.
MADE IN U. S. A.

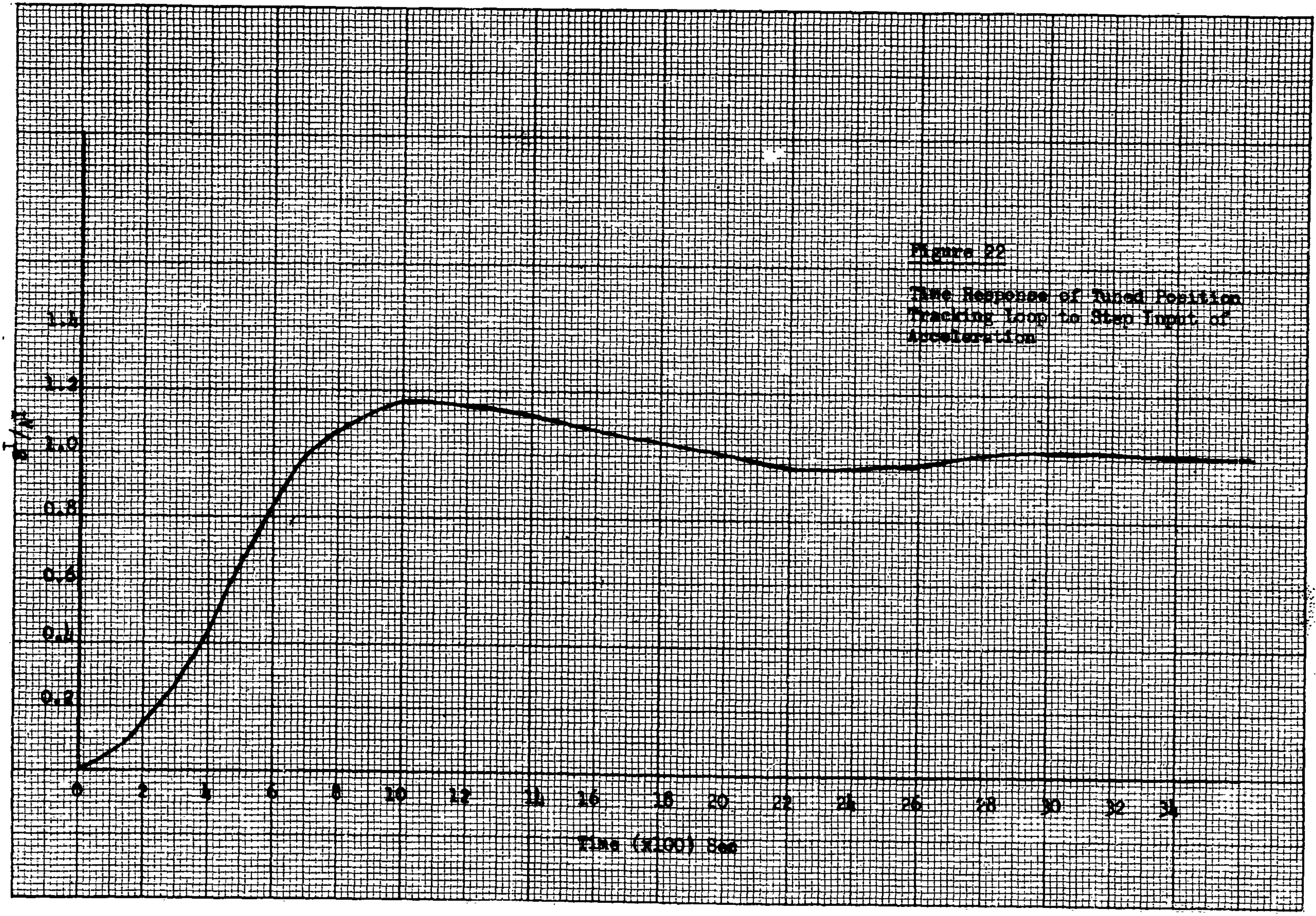

Figure 22

Time Response of Tuned Position Tracking Loop to Step Input of Acceleration

Reference to Figure 21 will show that in this simplified form no provision has been made to correct the errors in the initial values of the direction cosines which provide base motion isolation. Although these direction cosines are continually updated by rate gyro information to reflect changes in the attitude of the sensor package, initial errors will remain unless they are corrected by external information. These errors are similar to an inaccurately erected platform and result in erroneous acceleration information to the position tracking loop causing continuous forced dynamic errors in these loops.

The final system design of the FPC Navigation System is shown in simplified signal flow form on SK52200. The doppler velocity and inertially derived velocity are self-resolved into east, north, and vertical components in the earth fixed reference frame. Comparison of these velocities provide velocity component errors which are resolved into equivalent angular rate errors. Resolution of these errors to corresponding gyro rate errors by inertially derived direction cosines provide the necessary corrections for inertial error reduction of the base motion isolation direction cosines. Multiplication of the correction signals by coefficient $C1_1$ and algebraic subtraction from the corresponding rate gyro outputs provide the short term, fast response required for optimum erection and alignment. Integration of the correction signals $(\frac{C2}{s})$ and subtraction from the rate gyro outputs result in reduction of the steady-state errors caused by gyro drift.

Self resolution of the doppler velocity signals by inertially derived quantities to provide the required correction signals is a boot-strap process with the total error directly related to the accuracy of the doppler-velocity system. Gyro and accelerometer ouputs provide the inertially derived velocity components which are tranformed, through the use of a very accurate internally gnerated earth rate signal, and compared with the resolved doppler velocity signals. It is primarily through the use of the internal earth rate signal that the drift rates of the individual gyros are determined and the correction signals generated.

Reduction of the inital condition errors in the base motion isolation direction cosines is a transient condition with the correction signals supplied primarily through the proportional (C_1) path to the gyro output summation networks.

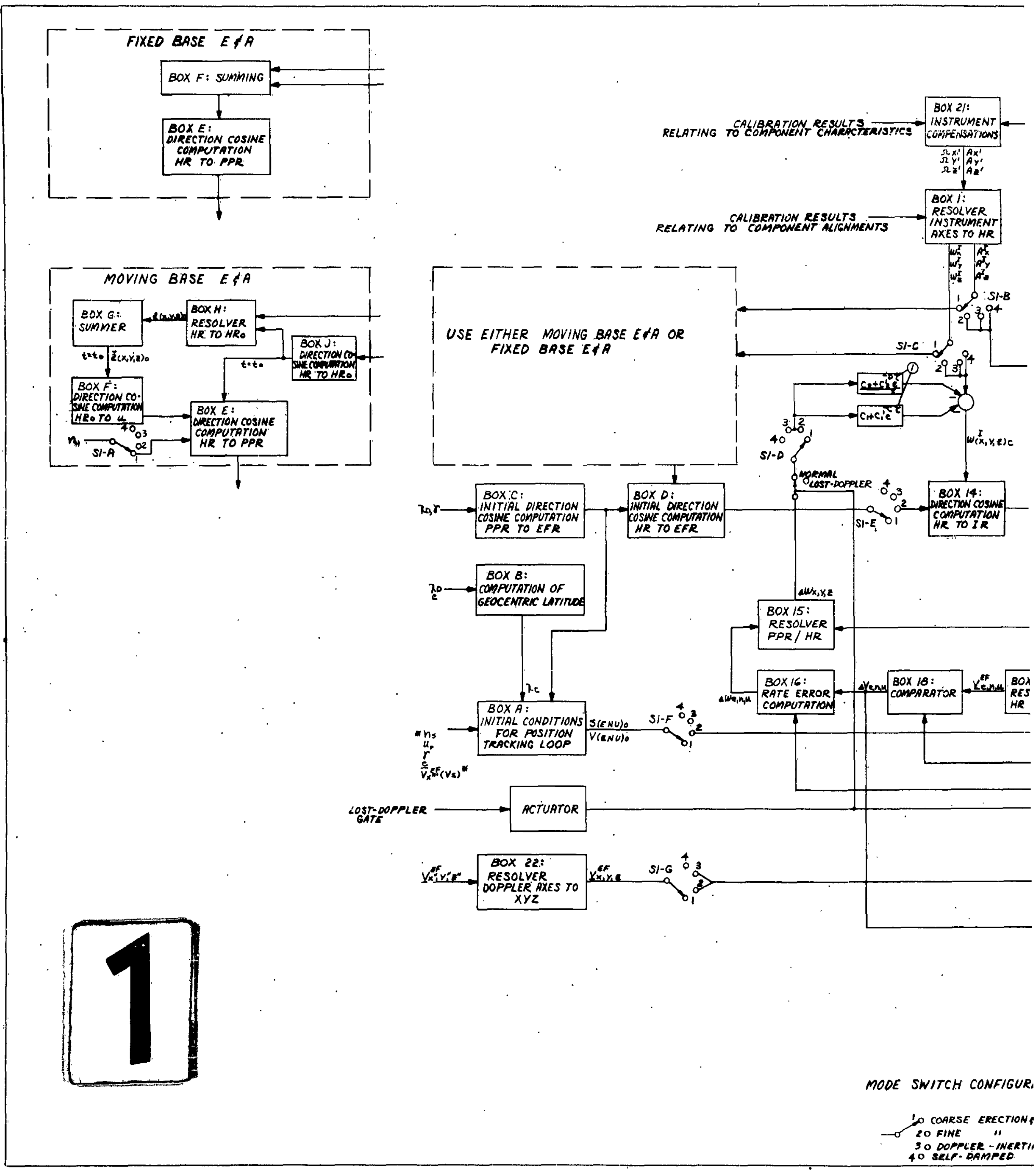
FIXED BASE E & A
BOX F: SUMMING
BOX E: DIRECTION COSINE COMPUTATION HR TO PPR
MOVING BASE E & A
BOX G: SUMMER
BOX H: RESOLVER HR TO HR₀
BOX J: DIRECTION COSINE COMPUTATION HR TO HR₀
BOX F: DIRECTION COSINE COMPUTATION HR₀ TO u
BOX E: DIRECTION COSINE COMPUTATION HR TO PPR
t=t₀
t=t₀
S1-A
USE EITHER MOVING BASE E & A OR FIXED BASE E & A
CALIBRATION RESULTS RELATING TO COMPONENT CHARACTERISTICS
BOX 21: INSTRUMENT COMPENSATIONS
CALIBRATION RESULTS RELATING TO COMPONENT ALIGNMENTS
BOX 1: RESOLVER INSTRUMENT AXES TO HR
S1-B
S1-C
S1-D
NORMAL
LOST-DOPPLER
S1-E
BOX C: INITIAL DIRECTION COSINE COMPUTATION PPR TO EFR
BOX D: INITIAL DIRECTION COSINE COMPUTATION HR TO EFR
BOX 14: DIRECTION COSINE COMPUTATION HR TO IR
BOX B: COMPUTATION OF GEOCENTRIC LATITUDE
BOX 15: RESOLVER PPR / HR
BOX 16: RATE ERROR COMPUTATION
BOX 18: COMPARATOR
BOX RES HR
BOX A: INITIAL CONDITIONS FOR POSITION TRACKING LOOP
S(ENU)₀
V(ENU)₀
S1-F
LOST-DOPPLER GATE
ACTUATOR
BOX 22: RESOLVER DOPPLER AXES TO XYZ
S1-G
1
MODE SWITCH CONFIGUR
1o COARSE ERECTION
2o FINE
3o DOPPLER-INERTI
4o SELF-DAMPED

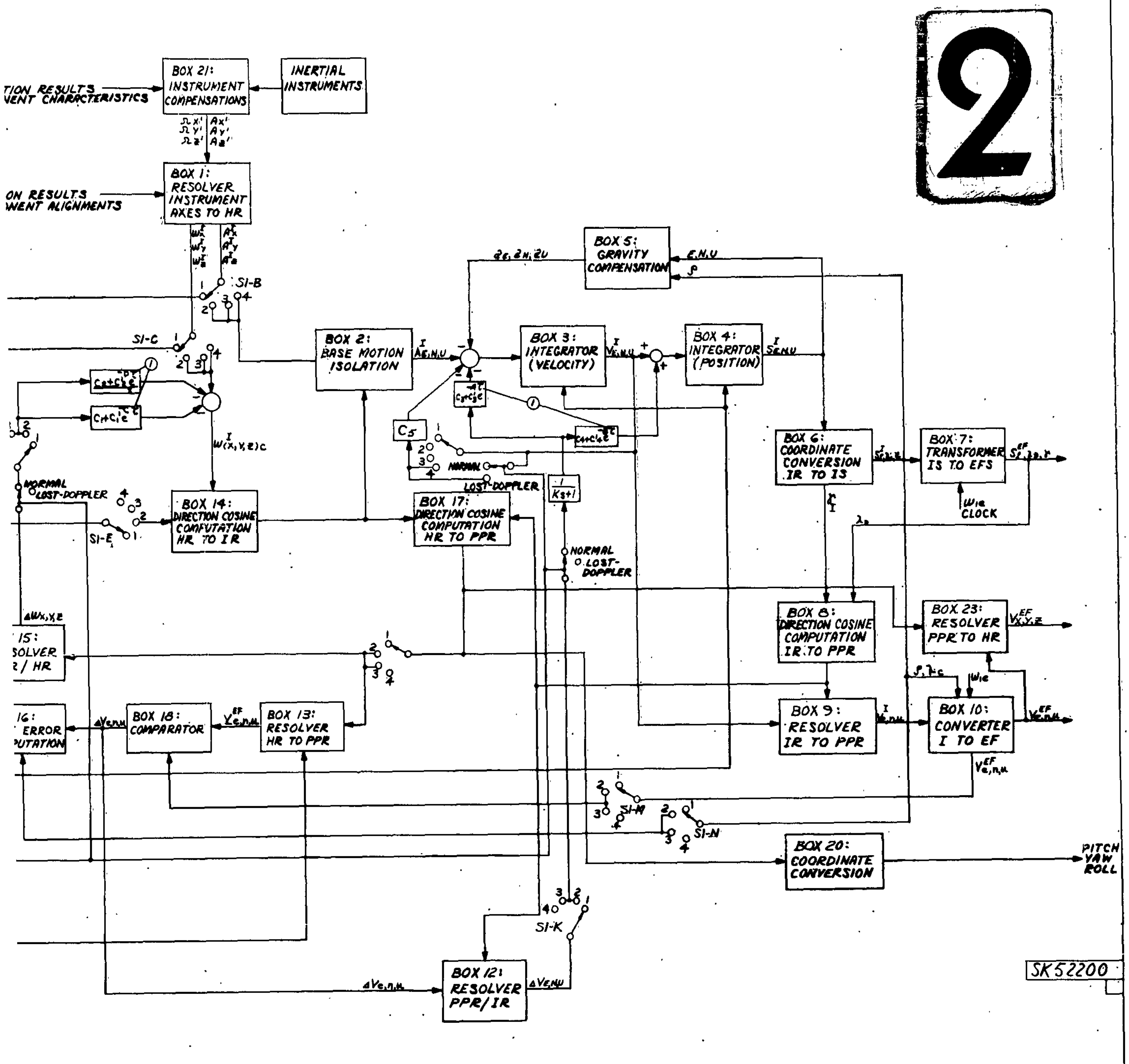
2
TION RESULTS
VENT CHARACTERISTICS
BOX 21: INSTRUMENT COMPENSATIONS
INERTIAL INSTRUMENTS
Ωx' Ωy' Ωz'
Ax' Ay' Az'
ON RESULTS
WENT ALIGNMENTS
BOX 1: RESOLVER INSTRUMENT AXES TO HR
S1-B
S1-C
1
2
3
4
BOX 2: BASE MOTION ISOLATION
$A^I_{E,N,U}$
BOX 5: GRAVITY COMPENSATION
g_E, g_N, g_U
E, N, U
ρ
BOX 3: INTEGRATOR (VELOCITY)
$V^I_{E,N,U}$
BOX 4: INTEGRATOR (POSITION)
$S^I_{E,N,U}$
C_5
NORMAL
LOST-DOPPLER
$\frac{1}{Ks+1}$
$w^I_{(x,y,z)c}$
BOX 14: DIRECTION COSINE COMPUTATION HR TO IR
S1-E
BOX 17: DIRECTION COSINE COMPUTATION HR TO PPR
NORMAL
LOST-DOPPLER
BOX 6: COORDINATE CONVERSION IR TO IS
$S^I_{x,y,z}$
BOX 7: TRANSFORMER IS TO EFS
$S^{EF}_{\lambda,\phi,r}$
w_{ie}
CLOCK
λ_o
BOX 8: DIRECTION COSINE COMPUTATION IR TO PPR
BOX 23: RESOLVER PPR TO HR
$V^{EF}_{X,Y,Z}$
$\Delta w_{x,y,z}$
15: SOLVER R/HR
16: ERROR PUTATION
$\Delta V_{E,N,U}$
BOX 18: COMPARATOR
$V^{EF}_{E,N,U}$
BOX 13: RESOLVER HR TO PPR
BOX 9: RESOLVER IR TO PPR
$V^I_{E,N,U}$
ρ, λc
w_{ie}
BOX 10: CONVERTER I TO EF
$V^{EF}_{E,N,U}$
S1-M
S1-N
BOX 20: COORDINATE CONVERSION
PITCH
YAW
ROLL
S1-K
BOX 12: RESOLVER PPR/IR
$\Delta V_{E,N,U}$
SK52200

2-① DENOTES $\tau = 0$ UNTIL DOPPLER-INERTIAL MODE BEGINS; THEN $\Delta\tau = \Delta t$

1-(*) ASTRISK DENOTES Ω_N & Ω_S NOT TO BE USED ON FIXED BASE E&A

NOTES:

MODE SWITCH CONFIGURATION

1 o COARSE ERECTION & ALIGNMENT
2 o FINE " "
3 o DOPPLER - INERTIAL
4 o SELF-DAMPED

UNLESS OTHERWISE SPECIFIED.

NEXT ASSY	USED ON		
APPLICATION			

HAMILTON STANDARD
DIVISION OF UNITED AIRCRAFT CORPORATION
WINDSOR LOCKS, CONNECTICUT, U.S.A.

BLOCK DIAGRAM,
FPC NAVIGATION LOOP

CODE IDENT NO. 73030
CONTRACT NO. 62-0873-D
SCALE NONE
SK52200
WEIGHT: LB SHEET

1 3-3022-002

FPC-1

Drift rate correction in a steady-state condition and is provided by the continuous output of the integrator path ($\frac{C2}{S}$) which cancels the drift rate component in each gyro output. In the system steady-state condition the velocity error signal decreases to zero resulting in no correction input to either the C_1 or $\frac{C2}{S}$ path. Gross simplification of the Navigation Loop formulation has permitted linearization of the system dynamics. The assumptions of major importance are listed below:

1. The three interacting position tracking loops assumed linear and independent.
2. The three axis velocity resolution assumed non-interacting and linear.
3. The direction cosines relating instrument axes to inertial reference axes and the corresponding base motion isolation function assumed linear and constant.

Dynamic analysis based on these assumptions has allowed specification of the values of the correction coefficients. According to this analysis, optimum settling of the complete system, obtained by setting $C_1 = 0.00498$ and $C_2 = 1.83 \text{ X } 10^4$, will occur in approximately 20 minutes.

In order to reduce the acceleration errors introduced by high frequency tuning of the position tracking loop, the FPC navigation system is designed to operate after the fine erection and alignment mode in a doppler-damped mode in which the tuning C_4 is set to zero and the damping coefficient is adjusted to yield a lightly damped Schuler tuned loop. The transfer function of the ratio of inertial velocity to doppler velocity error is shown in Figure 23 for a damping of 0.09 of critical corresponding to the value of $C_1 = .2225 \text{ X } 10^{-3}$/sec.

The maximum inertial error is equal to approximately 10% of the doppler error at a frequency of 0.00124 rad/sec (the Schuler frequency). Use of the doppler velocity signal in the doppler inertial mode of operation limits the maximum error of the system and prevents cumulative error build-up that occurs in pure inertial systems due to shifts in component bias and drift levels.

A fourth mode of operation is included in the design of the Navigation System which eliminates the use of doppler information after erection and alignment. The system will operate as a purely inertial system with the inherent errors only partially compensated by a very small amount of self-damping.

EUGENE DIETZGEN CO.
MADE IN U. S. A.

NO. 340-L35 DIETZGEN GRAPH PAPER
LOGARITHMIC
3 CYCLES X 5 CYCLES

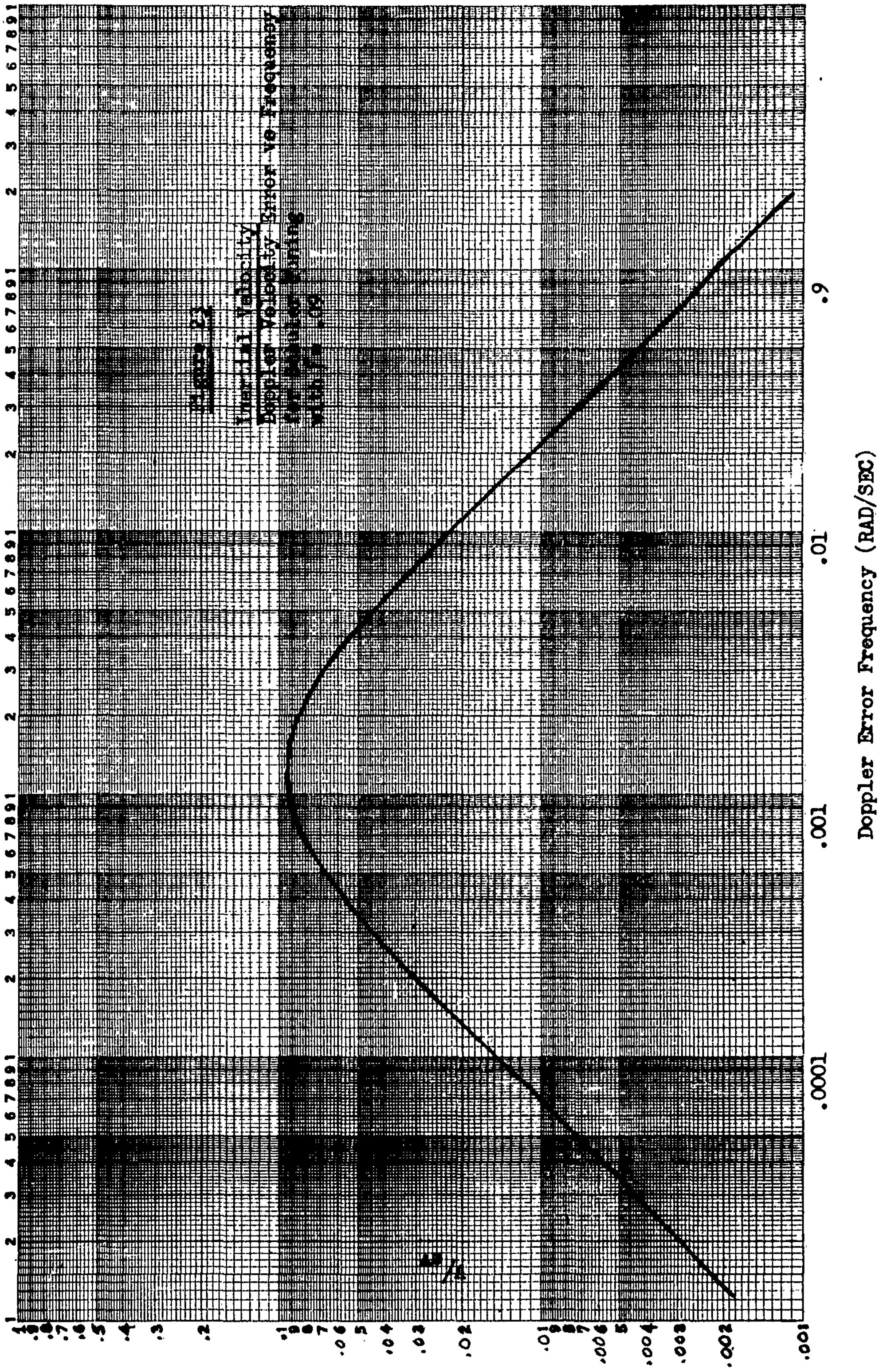

Figure 21

Inertial Velocity
Doppler Velocity Error vs Frequency
For [illegible] Tuning
with [illegible] .09

This mode of operation may be selected manually by the system operator but will be automatically initiated when the doppler return signal is lost by action of the lost-doppler gate signal.

The recommended damping factor for this mode is 0.02 of critical with the final value dependent primarily upon the phase lag introduced into the position tracking loop by the digital computing equipment. To obtain this value of damping, the coefficient C_5 is set equal to 0.0496×10^{-3}/sec.

Because of the possibility of transient disturbances occuring internally to the system during mode switching between the fine erection and alignment and doppler inertial modes, fading circuits have been designed to slowly change the values of the effected coefficients. The changes occur as an exponential decay according to the expression $K\ (1-e^{-\alpha t}\ )$ where the decay times are selected to fade-out the outer loop (gyro correction) before significant changes occur in the inner (Position Tracking) loop. The desired transient time for the outer loop is approximately 15 minutes which requires that the exponential coefficients C and D be equal to 180. The transient for the inner loop should be accomplished in 30 minutes which will be accomplished with values of A and B equal to 360.

Since the outer loop opens completely after the fine erection and alignment process, coefficients C_1' and C_2' must equal 0.00498 and 1.83×10^{-4} respectively. Although the integration gain $C_2 = C_2' e^{DT}$ equals zero at the termination of the transient, the final value of the integrator output will be held to continue the gyro drift cancellation. The coefficient C_4' equals 5.71 and completely opens the doppler feed-forward in the position tracking loop. Coefficient C_3' equals 3.065×10^{-3}/sec. to reduce the loop damping to 0.09 of critical after the fade-out period. The complete system signal flow diagram is given in drawing #SK52200.

3.1.5.7 Operational Procedure

Information generated by the system during the fine erection and alignment process, which consumes the first 20 minutes of flight time, is inaccurate. Although the velocity errors decrease with time, the position errors-latitude, longitude or grid coordinate information are cumulative requiring a position fix at the termination of this mode of operation. Use of this information will result in large navigation and flight path errors.

The suggested operational procedure for the FPC Navigation System is as follows:

1. Two minutes before takeoff, the coarse erection and alignment process is initiated.
2. In the interval beforetakeoff, ship's velocity, heading, and present position information is inserted into the computer.
3. Immediately after termination of the coarse erection and alignment, the system automatically switches into the self-damped mode for a period of time sufficient to allow take-off and cruise beyond the deck area of the carrier. Since doppler information is very inaccurate while the helicopter is over the ship and cannot be used for erecting and aligning the system, it is imperative that the helicopter takeoff and cruise over the side as soon after completion of coarse erection and alignment as possible.
4. Initiation of the fine erection and alignment process may be performed automatically or manually by the system operator after the helicopter is in a smooth cruise mode. The flight profile should be restricted to minimum course and velocity changes or to a hovering condition during this mode to reduce the external distrubances to the system.
5. Normal operation in the doppler inertial mode commences after completion of the fine erection and alignment process and should continue for the duration of the fade-out time (30 minutes). Termination of fine erection and alignment may be determined by a logic circuit which indicates when the three gyro correction signals have been reduced to zero or a minimum acceptable threshold. A position fix is required at this time to update the indicated position of the helicopter. This fix must be made external to the Navigation System between the Position Loop output and the Flight Path Controller input, to prevent generation of a transient input to the Schuler tuned loops.
6. Operation in the self-damped mode will normally occur only if the doppler system is inaccurate or inoperative. Inoperative doppler will cause automatic transition to the delf-damped mode.

3.1.5.8 Sources of System Error

The major sources of system error will be:

1. Variation of the earth's surface from the Hayford ellipsoid of revolution representation of the earth's geoid.
2. Effects of gravity anomalies.
3. Inherent errors in the doppler velocity system.
4. Variation between true helicopter velocity and indicated helicopter velocity due to continuous ocean currents.

3.2 Inertial Measurement System

3.2.1 Introduction

The inertial measurement system consists of the following major areas:

a. Gyro and accelerometer inertial instruments
b. Pulse torque servo amplifiers
c. Instrument calibration and alignment
d. Inertial instrument package design

The function of the major components cited above dictate the ultimate performance of a gimbal-less inertial navigation system. The design criteria is basically established by the vehicle dynamics, tactical environment, and the navigational accuracies desired.

3.2.1.1 Instruments

The repeatability of the gyro and accelerometer coefficients from one calibration test to the next is an important indication of a navigation system's performance. In this application, tactical considerations place a heavy burden on gyro performance. At present, no low cost gyro meets the ultimate long term stability requirements for an operational system. Many gyro manufacturers are concentrating their efforts in this particular area, and substantial headway is being made.

3.2.1.2 Pulse Torquing

Pulse torquing is a term used to designate the digitalization of the current used to torque single degree of freedom gyros and accelerometers. The present design utilizes several unique circuit developments that allow for satisfaction of requirements without serious compromise. The following basic requirements apply principally to gyros, as they are the most difficult to satisfy in a no gimbal configuration:

a. Adequately high maximum torque to handle any possible sustained input angular rates.

b. Adequately small pulse size to provide necessary resolution.

c. Practical pulse frequencies from the point of view of an electromagnetic torquer.

d. Sufficiently low and steady torquer power input so that mechanical distortions due to changes in thermal gradient patterns will be minimized.

e. Dynamic stability of the servo loop and sufficiently fast response must be maintained.

3.2.1.3 Instrument Calibration and Alignment

The calibration procedure provides values for the instrument characteristics, such as bias, scale factor, etc., in order that corrections to instrument outputs can be made in the system computer. Even after this compensation has been accomplished, the signals must not yet be used in the base motion isolation because they are indications of motion vector components along an orthogonal set of axes. This problem introduces the need for alignment, or resolving the compensated outputs onto an orthogonal set of axes. The system of orthogonal axes chosen against an accurate reference may be referred as the ideal instrument coordinate system.

3.2.1.4 Inertial Package

Since inertial grade instrument accuracies depend greatly on thermal and dimensional stability, the packaging concepts must inherently concentrate on a thermally stable configuration. Three package configurations were considered, solid conduction, forced liquid convection, and Helium Hi-pressure. Each configuration was considered on the basis of the following criteria:

a. Weight
b. Volume

c. Power required
d. Manufacturing feasibility
e. Reliability
f. Warm-up time
g. Temperature repeatability
h. Estimated cost
i. Instrument calibration
j. Maintenance

3.2.2 Design Conclusions

The inertial measurement system defined herein has been designed to utilize the inertial sensors to the greatest extent feasible. It is considered that the pulse torque amplifiers, inertial measurement package, and associated temperature controls satisfy all design criteria established for this sytem. No inherent limitations exist for the various methods of calibration and alignment with the exception of package to doppler alignment.

The major area of concern lies with the gyro long term drift performance. The FPC accuracy requirements dictate the use of a .015 degree per hour gyro. This would yield a circular error probability (CEP) of 1.5 nautical miles in present position. Present gyros will yield a CEP of 6 to 8 nautical miles.

The alignment of the inertial sensor package to doppler antenna axes may be easily solved by the use of a planar array antenna. This will enable the inertial sensor package and the doppler antenna to become an integral unit. This is not feasible with the present AN/APN-130 doppler system, and a possible method is presented in this section.

3.2.3 Gyros

The gyros are the most critical component in the flight path control system. The gyros must maintain a very low drift rate over a four hour mission period. In addition, their mission to mission shift, that is, the drift rate shift when de-energized and re-energized must be small and predictable. The gyro requirements were reviewed with all of the major gyro manufacturers known to HSED. The results of this study are discussed below.

3.2.3.1 The drift rate of a gyro is composed of a constant term and a time varying term

$$W_d = W_c + W_r (t)$$

Eighty percent of the constant drift rate will be eliminated during the fine erection and alignment by using the earth's rate reference and the doppler velocity reference to establish the aircraft velocity and angular rate. The remaining drift rate (20%) will contribute the major portion of the navigation error and is composed of

> Wce the effective constant drift term which is 20% of the manufacturer's constant drift rate shift.

The drift rate terms are based on manufacturer drift rate terms and accelerations which are assumed to be $7x10^{-3}$g in the X and Y gyros and 1g in the Z gyro. This assumes that the helicopter flies a relatively level flight with zero pitch angle.

The various drift rate components are defined for the purpose of this report as one sigma values as follows:

Wce = effective constant drift rate
Wce = 20% Wc = 20% (WB + WM + WA)
WB = Bias uncertainty (°/Hr.)
WM = Mass unbalance drift (°/Hr/g)
WA = Anisoelastic Drift ($°/Hr/g^2$)

The comparison of the gyros available with HSED requirements are shown in Tables 1 and 2.

3.2.3.2 The time varying drift rate (wr) is composed of three components.

TABLE 1
EFFECTIVE CONSTANT DRIFT (ω_{CE}) "X" AND "Y" GYROS

COMPANY	HSED REQ'T.	SPERRY	NORDEN	NORTRONICS	KEARFOTT	HONEYWELL
Unit Design.	N/A	SIG 1041	203	HIG-5	001	GG 87
ω_B °/Hr.	.06	.5	.3	1°	2	1
ω_M °/Hr.	.3	.5	.3	3	2	2
ω_A °/Hr/g^2	8	.01	.02	.02	.02	.2
$\omega_C = \omega_{Dr} + \omega_M u + \omega_A$	.06214	.5035	.3021	1.0210	2.0140	1.0140
ω_{Ce}	.01243	.10070	.06042	.20420	.40280	.20280

TABLE 2
EFFECTIVE CONSTANT DRIFT "Z" GYRO (ACCEL. 1G)

COMPANY	HSD REQ'T.	SPERRY	NORDEN	NORTRONICS	KEARFOTT	HONEYWELL
Unit Design.	N/A	SIG 1041	203	HIG -5	001	GG 87
ω_B °/Hr.	.03	.5	.3	1	2	1
ω_M °/Hr/g	.03	.5	.3	3	2	2
ω_A °/Hr/g^2	.002	.01	.02	.02	.02	.2
$\omega_C = \omega_{Dr} + \omega_{MU} + \omega_A$	.062	1.01	.62	2.02	4.02	3.2
ω_{Ce}	.0122	.202	.124	.404	.804	.64

$$Wr = W_{Dt} + W_{\mu} t + W_{\rho} t$$

Where W_{Dt} = time varying drift rate shift (°/Hr.)
$W_{\mu t}$ = time varying mass unbalance drift rate (°/Hr/g)
$W_{\rho t}$ = pure random drift.

The comparison of the time varying drift rate of various gyros with HSED requirements is shown in Tables 3 and 4.

3.2.3.3. Table 5 shows the combined effective constant drift rate and the time varying drift rate. The effective constant drift rate is shown for two levels of compensation, 80% and 90%. Also, shown are torquer power, voltage and current characteristics.

3.2.4 Accelerometer (Reference Table 6)

The inertial accelerometer requirements for the flight path control are less stringent than the gyro. Since the maximum accleration will be slightly more than one "g", the dynamic range of the instrument is an order of magnitude less than that expected from an accelerometer mounted in a missle strapped down guidance system. The accelerometer requirements were generated such that the accumulative distance error due to accelerometer bias and threshold were negligible.

The selection of the accelerometers will be based upon the error contributed by the accelerometer as reflected by Δa_f.

Where $\Delta a_f = a_t + a_b + a_f \Delta k_p + \frac{\Delta Kt}{Kt} \; af$

and a_t = threshold in g units

a_b = bias error in g units

Δ_{kp} = pick-off scale factor stability per unit

$\frac{\Delta k_t}{k_t}$ af in a_f units.

k_t = torquer scale factor

TABLE 3
EFFECTIVE TIME VARYING DRIFT "X" AND "Y" GYROS

COMPANY	HSD REQ'T.	SPERRY	NORDEN	NORTRONICS	KEARFOTT	HONEYWELL
Unit Design.	N/A	SIG 1041	203	HIG-5	001	GG-87
ω_{Dt} °/Hr.	.001	.01	.04	.1	.2	1
$\omega_{\mu t}$ °/Hr/g	.01	.01	.04	.2	.2	2
ω_{pt} °/Hr.	.001	.01	.02	.15	.1	.05
$\omega_r = \omega_{Dt} + \omega_{\mu t} + \omega_{pt}$	.00207	.02007	.06028	.2514	.3014	1.064

TABLE 4
EFFECTIVE TIME VARYING DRIFT "Z" GYRO (ACCEL. = 1G)

COMPANY	HSD REQ'T.	SPERRY	NORDEN	NORTRONICS	KEARFOTT	HONEYWELL
Unit Design.	N/A	SIG 1041	203	HIG-5	001	GG-87
ω_{Dt} °/Hr.	.0008	.01	.04	.1	.2	1
$\omega_{\mu t}$ °/Hr/g	.0008	.01	.04	.2	.2	2
ω_{pt} °/Hr.	.0008	.01	.02	.15	.1	.05
$\omega_r = \omega_{Dt} + \omega_{\mu t} + \omega_{pt}$	.0024	.03	.1	.35	.5	3.05

TABLE 5

GYRO IMPORTANT CHARACTERISTICS "X" AND "Y" GYROS

COMPANY	HSED REQ'T	SPERRY	NORDEN	NORTRONICS	KEAR-FOTT	HONEYWELL
Unit Design.	N/A	SIG 1041	203	HIG 5	001	GG 87
ω_d (°/Hr) with 80% drift comp.	.0145	.12077	.12070	.4556	.7052	1.2072
ω_d with 90% drift comp.	.0145	.07042	.09049	.3535	.5028	1.1654
Torquer Current (ma.)	100 Max.	50	93	90	95	90
Torquer Voltage	50 Max.	12	40	15	16	15
Torquer Pwr. (Watts)	3 Max.	.6	3.5	1.4	1.5	1.4
Characteristic Time (Msec.)	20 Max.	6	40	1	1	.6

TABLE 6
ACCELEROMETER REQUIREMENTS

$$\Delta a = at + ab + a_f \Delta Kp + \frac{\Delta Kt}{Kt} af$$

COMPANY	HSED REQ'T	KEARFOTT	HONEYWELL	DONNER
Unit Design.	N/A	C702401-005	GG177	4310
at (g)	10^{-6}	$5x10^{-7}$	$3x10^{-6}$	10^{-5}
ab (g)	$3x10^{-5}$	$3x10^{-5}$	$6x10^{-5}$	10^{-4}
Δkp (Dimensionless)	$5x10^{-4}$	10^{-4}	$1.5x10^{-4}$	$2x10^{-4}$
$\Delta kt/_{kt}$ (Dimensionless)	10^{-4}	10^{-5}	10^{-5}	$3x10^{-5}$
$\Delta kpaf$ (g)	$3.5x10^{-6}$	$7x10^{-7}$	$1.05x10^{-6}$	$1.4x10^{-6}$
$(\Delta kt/kt)$ af (g)	$7x10^{-7}$	$7x10^{-8}$	$7x10^{-8}$	$2.1x10^{-7}$
$\Delta a = (at + ab + \Delta kpaf + \frac{\Delta kt}{kt} af)$ (g)	$3.5x10^{-5}$	$3.127x10^{-5}$	$6.4x10^{-5}$	$1.116x10^{-4}$

3.2.5 Calibration Program for the SANE Inertial Measurement System.

3.2.5.1 The object of the calibration program is to provide signals from the gyro/accelerometer package that are orthogonal and error-free. The two tasks involved are:

1. Compensating the instruments for errors of bias and unbalance, and obtaining scale factors.

2. Resolving the individual instrument axes (x, y, and z) to an orthogonal set (X, Y, Z).

The various symbols used in this phase of the report are reiterated as follows:

i	A subscript used to denote the instruments axes, x, y, z.
J	A subscript used to denote the ideal package orthogonal coordinate system X, Y, Z. The Z axis points upward.
β	The Package face pointing downward (used when obtaining constants).
S_i^a	is the scale factor for the i-axis accelerometer. The units are FT/SEC/PULSE.
S_i^g	is the scale factor for the i-axis gyro. The units are Radians/Pulse.
B_i^a	is the bias term for the i-axis accelerometer. It is the output that is obtained for no input to the unit. Units: FT/Sec^2.
B_i^g	is the bias term for the i-axis gyro. It is a drift rate in radians/sec. The Predictable portion is in one direction and can be compensated. . The random drift cannot be compensated, but it is assumed that the errors will average out over a period of time.

Definitions (Cont.)

λ is latitude

U_i^s is a drift rate due to an acceleration acting on a mass unbalance along the spin axis of the i-gyro. See Figure 24a.

U_i^i is a drift rate due to an acceleration acting on a mass unbalance along the input axis of the i-gyro. Ref. Figure 24b.

Gyro Mass Unbalances

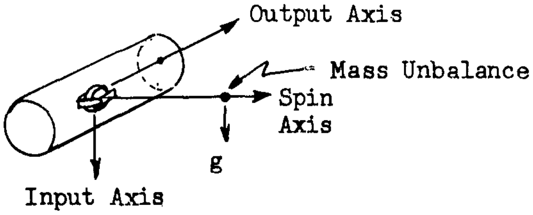
Output Axis
Mass Unbalance
Spin Axis
g
Input Axis

24a U_i^s Mass unbalance due to gravity acting on mass along spin axis. Assumed positive according to the right hand rule about the output axis.

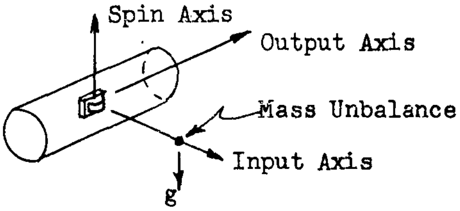
Spin Axis
Output Axis
Mass Unbalance
Input Axis
g

24b U_i^i Mass unbalance due to gravity acting on mass input axis - assumed positive as above.

Figure 24

$b_{i,J}$ A set of direction cosines relating the instrument axes to the ideal package coordinates.

b_{iJ}^i A set of direction cosines derived from the above, and used in resolution to the ideal package coordinates.

μ is the local vertical.

Υ is polar North

θ_T is calibration table rotation in radians.

3.2.5.2 Methods of Compensation for Instrument Errors and Misalignment.

3.2.5.2.1 Instrument Compensations: Accelerometers

The output of an accelerometer may be expressed as the net number of pulses (C) counted over a period of time (t) due to the applied acceleration and the bias accelerations.

$$S_i^A \frac{C}{t} = -g \operatorname{Cos}(i,\beta) + B_i^A$$

An output is assumed positive if the applied acceleration tends to move the package in the positive i direction. It should be noted that the gravitational field is equivalent to an acceleration in the upward direction.

For example: The case where the i axis is upward,

$\beta = -i$, $\therefore$ Cos $(i,\beta) = -1$, and a positive acceleration results.

In the SANE computer program, the uncorrected outputs from the accelerometers will be fed into an area of the computer - designated Box 21 on SK 52200 - where the raw pulse data will be scaled and corrected, giving the true acceleration components in the direction of the input of each accelerometer. This operation utilizes the following set of compensation equations:

$$\boxed{\begin{aligned} a_x &= S_x^A \frac{C_x}{\Delta t} - B_x^A \\ a_y &= S_y^A \frac{C_y}{\Delta t} - B_y^A \\ a_z &= S_z^A \frac{C_z}{\Delta t} - B_z^A \end{aligned}} \quad \text{1/2 Box 21}$$

After compensation as outlined above, the acceleration components are resolved to an orthogonal set, a_x, a_y, a_z in Box 1. This computation is outlined in Section 3.2.5.3. The method to obtain the constants S_I^a and B_I^a will be derived in Section 3.2.5.4.2.

3.2.5.2.2 Instrument Compensations: Gyros

The output of a single degree of freedom, pulse torqued, integrating gyro consists of the net number of pulses (C) counted over a period of time (Δ t) due to the torques about the output axis. The torques about the output axis are, in general due to:

Normal gyroscopic reaction to an angular velocity about the input axis. This is assumed positive if the applied angular velocity is about the input axis according to the right-hand rule:

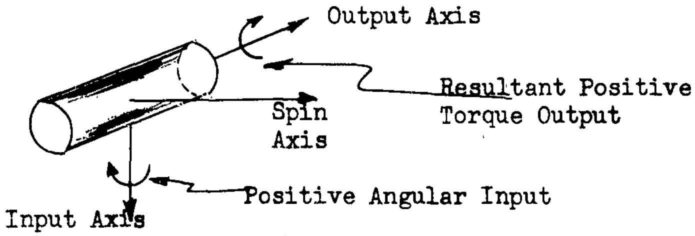

The other outputs: U_I^s, U_I^i, B_I^g, have been defined previously. The general calibration equation for the gyro is:

$$*\,S_i^g C = \left[\theta_T + \omega_{ie}\Delta t \cos(\lambda)\right]\cos(i,\beta) - U_i^i \Delta t \cos(\beta,s) + U_i^s t \cos(\beta,i) + B_i^g \Delta t$$

The sign conventions used agree with those outlined in Figure 24. The outputs from the gyros are fed into Box 21 on SK 52200. The raw pulse data is converted by scale factor and corrected for bias. The unbalance terms must be multiplied by the component of acceleration that causes them. This information is obtained from the compensated outputs of the accelerometers. Below are the gyro compensation equations:

*NOTE: In the general equation above, s refers to spin reference axis, i refers to input axis.

1/2
Box 21

$$\boxed{\begin{aligned}\omega_x &= S_x^G \frac{c}{\Delta t} + U_x^i a_y + U_x^s a_x - B_x^G \\ \omega_y &= S_y^G \frac{c}{\Delta t} - U_y^i a_x + U_y^s a_y - B_y^G \\ \omega_z &= S_z^G \frac{c}{\Delta t} - U_z^i a_y + U_z^s a_z - B_z^G\end{aligned}}$$

In the above gyro compensation equations, the signs of the unbalance terms were determined as outlined bebelow. First, the orientation of the gyros as in the physical package is assumed as in Figure 25 below:

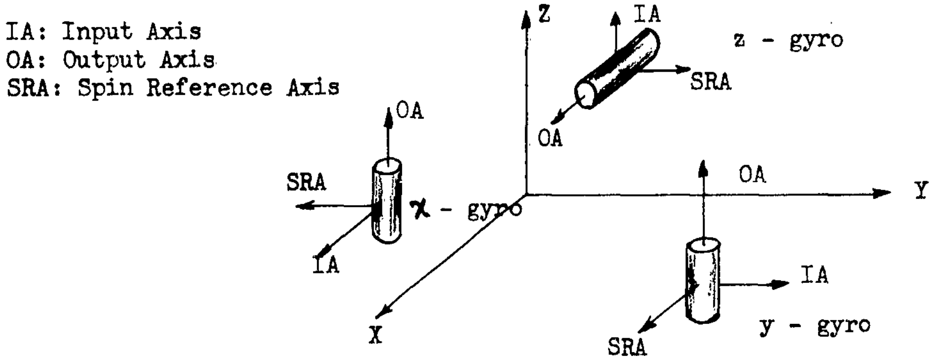

Figure 25 - Definition of Package Orientation

This orientation has the advantage of minimizing errors due to unbalances. Since the output axes of the x and y gyros point vertically upward, there will be minimum unbalance due to gravity. The z gyro must have its input axis pointing upward, but the output axis is in the direction of maximum expected horizontal acceleration, thus minimizing U_z^i as much as possible.

The unbalance, U_x^i, resulting from an acceleration in the positive y direction is seen to be negative about the output axis.

U_x^s, due to positive a_x is negative

U_y^i, due to positive a_x is positive

U_y^s, due to positive a_y is negative

U_z^i, due to positive a_y is positive

U_z^s, due to positive a_z is negative

Since the compensation equation has the purpose of subtracting out the unbalances, the sign of each will be opposite to that above.

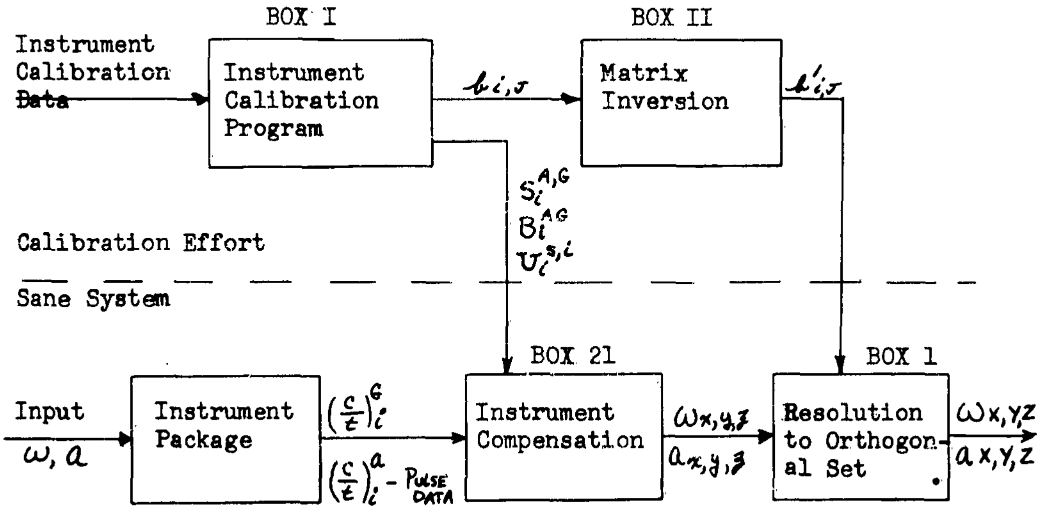
BOX I
Instrument Calibration ~~Data~~
Instrument Calibration Program
$b_{i,j}$
BOX II
Matrix Inversion
$b'_{i,j}$
$S_i^{A,G}$
B_i^{AG}
$U_i^{s,i}$
Calibration Effort
Sane System
BOX 21
BOX 1
Input
ω, a
Instrument Package
$(\frac{c}{t})_i^G$
$(\frac{c}{t})_i^a$ - PULSE DATA
Instrument Compensation
$\omega_{x,y,z}$
$a_{x,y,z}$
Resolution to Orthogonal Set
$\omega_{x,y,z}$
$a_{x,y,z}$

Figure 26 Calibration Program of SANE System

3.2.5.3 Resolution of the instrument outputs to an orthogonal set.

It is assumed that the physical location of the inertial sensors in the package will be such that the instrument axes will not line up with the ideal X, Y, Z axes, nor will they form an orthogonal set within themselves.

The SANE computer compensates for the misalignments by solving a set of equations solved explicitly for $A_{X,Y,Z}$, or $W_{X,Y,Z}$ in terms of known quantities.

The outputs of the instruments can be written as follows:

$$\begin{aligned} Fx &= FX\ bxX + FY\ bxY + FZ\ bxZ \\ Fy &= FX\ byX + FY\ byY + FZ\ byZ \\ Fz &= FX\ bzX + FY\ bzY + FZ\ bzZ \end{aligned}$$

where F is either an acceleration A, or angular rate W. b_{iJ} are cosine terms relating the instrument axis to the ideal axis. (obtained through testing).

In order to solve the equations for $S_{X,Y,Z}$, the method following Cramer's rule is used.

$$F_X = \frac{Dx}{D}, \quad F_Y = \frac{DY}{D}, \quad F_Z = \frac{DZ}{D}$$

where D is the determinant of the b_{iJ} terms:

$$D = \begin{vmatrix} bxX & bxY & bxZ \\ byX & byY & byZ \\ bzX & bzY & bzZ \end{vmatrix}$$

and D_X is obtained by replacing the X column by the column of S_i terms. For example,

S_X may be solved in terms of the instrument outputs:

$$F_X = \frac{\begin{vmatrix} Fx & bxY & bxZ \\ Fy & byY & byZ \\ Fz & bzY & bzZ \end{vmatrix}}{D}$$

expanding the numerator:

$$F_X = Fx \frac{\begin{vmatrix} byY & byZ \\ bzY & bzZ \end{vmatrix}}{D} - Fy \frac{\begin{vmatrix} bxY & bxZ \\ bzY & bzZ \end{vmatrix}}{D} + Fz \frac{\begin{vmatrix} bxY & bxZ \\ byY & byZ \end{vmatrix}}{D}$$

Defining the terms multiplying $S_{x,\ y}$ and $_z$ as b'_{xX}, $b'yX$, and $b'zX$ respectively, the compensation equations can now be written in terms of these b'_{IJ}'s

BOX 1

$$\boxed{\begin{array}{l} F_X = Fx\ b'nX + Fy\ b'yX + Fz\ b'zX \\ F_Y = Fx\ b'xY + Fy\ b'yY + Fz\ b'zY \\ F_Z = Fx\ b'xZ + Fy\ b'yZ + Fz\ b'zZ \end{array}}$$

One set of these equations is used for gyro misalignment and one set for accelerometers.

The complete set of b'_{iJ} may be obtained from the given set of b_{iJ} by the following summary:

$$b'xX = \frac{\begin{vmatrix} byY & byZ \\ bzY & bzZ \end{vmatrix}}{D} \qquad b'yX = -\frac{\begin{vmatrix} bxY & bxZ \\ bzY & bzZ \end{vmatrix}}{D} \qquad b'zX = \frac{\begin{vmatrix} bxY & bxZ \\ byY & byZ \end{vmatrix}}{D}$$

$$b'xY = -\frac{\begin{vmatrix} byX & byZ \\ bzX & bzZ \end{vmatrix}}{D} \qquad b'yY = \frac{\begin{vmatrix} bxX & bxZ \\ bzX & bzZ \end{vmatrix}}{D} \qquad b'zY = -\frac{\begin{vmatrix} bxX & bxZ \\ byX & byZ \end{vmatrix}}{D}$$

$$b'xZ = \frac{\begin{vmatrix} byX & byY \\ bzX & bzY \end{vmatrix}}{D} \qquad b'yZ = -\frac{\begin{vmatrix} bxX & bxY \\ bzX & bzY \end{vmatrix}}{D} \qquad b'zZ = \frac{\begin{vmatrix} bxX & bxY \\ byX & bzY \end{vmatrix}}{D}$$

$$\text{Where } D = \begin{vmatrix} bxX & bxY & bxZ \\ byX & byY & byZ \\ bzX & bzY & bzZ \end{vmatrix}$$

BOX II

It now remains to determine through testing, the biJ constants of the individual instrument package.

3.2.5.4 Obtaining instrument compensation constants.

3.2.5.4.1 Gyroscope tests.

By orienting the instrument package with one axis facing downward and then another, information regarding scale factor, bias and misalignment can be obtained. The equations for the outputs in each orientation can be solved by simple algebra. The complete procedure is developed below.

The package is oriented with the listed face or axis pointing downward. The net positive pulse count C and the time t is recorded for each test. When the rate table is used, the angle appears as plus or minus for CCW and CW rotations, and there is to be an integral number of revolutions. A typical value would be 4π radians at 2.5°/sec.

The x gyro tests are as follows:

Test #	1	2	1'	2'	3	4	5	6
θ_T	$+\theta$	$-\theta$	0	0	$+\theta$	$-\theta$	$+\theta$	$-\theta$
β	+X	+X	+X	-X	Y	Y	-Z	-Z

Where B is the face pointing downward.

The equations defining each test run are:

1. $S_x^G C_1 = -\theta - W_{iet_1} \operatorname{Sin} \lambda A + U_x^s t_1 + B_x^G t_1$

2. $S_x^G C_2 = +\theta - W_{iet_2} \operatorname{Sin} \lambda A + U_x^s t_2 + B_x^G t_2$

1' $S_x^G C_{1'} = -W_{iet_{1'}} \operatorname{Sin} \lambda A + U_x^s t_{1'} + B_x^G t_{1'}$

2' $S_x^G C_{2'} = W_{iet_{2'}} \operatorname{Sin} \lambda A - U_x^s t_{2'} + B_x^G t_{2'}$

3. $S_x^G C_3 = -(\theta + W_{iet_3} \operatorname{Sin} \lambda A) \operatorname{Cos}(x, Y) + U_x^i t_3 + B_x^G t_3$

4. $S_x^G C_4 = -(\theta + W_{iet_4} \operatorname{Sin} \lambda A) \operatorname{Cos}(x, Y) + U_x^i t_4 + B_x^G t_4$

5. $S_x^G C_5 = -(\theta + W_{iet_5} \operatorname{Sin} \lambda A) \operatorname{Cos}(x, -z) + B_x^G t_5$

6. $S_x^G C_6 = -(\theta + W_{iet_6} \operatorname{Sin} \lambda A) \operatorname{Cos}(x, -z) + B_x^G t_6$

Solving the equations for the χ gyro, the following parameters of the χ gyro are determined:

$$S_x^G = \frac{\theta(t_1+t_2)}{C_2t_1-C_1t_2}$$

$$B_x^G = \frac{S_x^G(C_1't_2'+C_2't_1')}{2\,t_1't_2'}$$

$$\text{Cos}(x, Y) = \frac{S_x^G\,(C_4t_3-C_3t_4)}{\theta(t_3+t_4)}$$

$$U_x^S = \frac{S_x^G\,(C_1't_2'-C_2't_1')}{2\,t_1't_2'} + \text{Wie Sin}\,\lambda A$$

$$U_x^i = \frac{S_x^G\,(C_3t_4+C_4t_3)}{2\,t_3t_4} - B_x^G - \frac{\theta(t_3-t_4)}{2\,t_3t_4}\text{Cos}(x,Y) + \text{Wie}\,\text{Sin}\,\lambda A\,\text{Cos}(X,Y)$$

$$\text{Cos}(x, -z) = \frac{S_x^G\,(C_6t_5-C_5t_6)}{\theta(t_5+t_6)}$$

We have seen the complete solution of equations for the χ -gyro. For the remaining gyros and accelerometers, the algebra of solution and the equations resulting from the various orientations are similar. These will not be listed as well as the resulting formulas for the desired constants. These derivations are available in a special report "Calibration Program for the SANE System."

3.2.5.4.2 Accelerometer Tests

The known input used in these tests is the local gravity vector. By using various orientations of the package, the vector is applied along the three axes of each accelerometer. From the resulting equations, the scale factor, bias, and misalignment terms can be found.

The X - accelerometer tests result in the following:

Test #	19	20	21	22	23	24
β	X	-X	Y	-Y	Z	-Z

19 $S_x^A C_{19} = -g\ t19 + B_X^A\ t19$

20 $S_x^A C_{20} = g\ t\ 20 + B_X^A\ t20$

21 $S_x^A C21 = -g\ \mathrm{Cos}_A\ (x, Y)\ t21 + B_x^A\ t21$

24 $S_x^A C_{24} = -g\ \mathrm{Cos}_A\ (x, -z)\ t24 + B_x^A\ t24$

The X - accelerometer constants are

$$S_x^A = \frac{2g t_{19}\ t_{20}}{C_{20}\ t_{19} - C_{19} t_{20}}$$

$$B_x^A = \frac{S_x^A\ (C_{20} t_{19} + C_{19} t_{20})}{2\ t19 t_{20}}$$

$$\mathrm{Cos}_A\ (x, Y) = \frac{-S_x^A C21}{g\ t_{21}} + \frac{B_x^A}{g}$$

$$\mathrm{Cos}_A\ (x, -z) = \frac{-S_x^A C24}{g\ t_{24}} + \frac{B_x^A}{g}$$

The y and z accelerometer formulations are identical and will not be shown.

3.2.5.5 Implementation of the SANE calibration program.

3.2.5.5.1 General

The SANE calibration program will, to a large extent, follow the techniques used by Corporate Systems Center, Division of United Aircraft, in their calibration testing and data processing of a strapped-down inertial system. This section will describe the method used by CSC, and will point out the modifications and adaptations necessary to implement the calibration of the SANE inertial package.

3.2.5.5.2 Detailed Program

The experimental model will be built and tested. The five major pieces of equipment used for data taking will be:

1. The inertial package, consisting of 3 gyros and 3 accelerometers.

2. The calibration table: a level surface aligned within ± 2 seconds of the gravity vector and an Elinco Hysteresis Synchronous Motor to drive the table at an angular rate of plus or minus 2.5°/sec.

3. The electronics cabinet, consisting of power supplies, temperature controls, time reference, and the pulse torque servo amplifiers.

4. The record logic package: used to sum the output pulses of the 6 inertial components and transmit this information in binary form to the tape recorder.

5. The tape recorder: a Potter Model 3280, 7 channel unit used to record, in binary form, the outputs of the gyros and accelerometers.

In order to obtain sufficient data for computation of scale factors, bias mass unbalances, and sensor misalignment direction cosines, the inertial package is placed in various orientations, both with and without angular rotation. The output of the inertial components is recorded on the 7 channel recorder. This tape is then taken to the UAC Research Center where the data is read off the tape and analyzed on the IBM 7090 Computer. The desired information is automatically printed out on the line printer. Reference Figure 27.

3.2.5.5.3 SANE System Modifications

The SANE package will be of a round or oval shape with three mounting feet. In order to orient the package as required, a calibration fixture will have to be designed and built. The requirements for the fixture are that the external surfaces must be at right angles to each other, (within reasonable tolerances as discussed below). Also, the internal mount for the inertial package must allow for positioning of the package.

To determine the allowable tolerance on machined surfaces of the fixture, it is assumed that the permissible angular error of the fixture is 1/10 the maximum tolerable error for SANE system misalignment. This has been previously determined as 3.45 minutes of arc. 1/10 of this is .345 minutes. The tolerance in inches per foot can be found from $e = \ell \tan \alpha$, $\ell = 1$ ft., $\alpha = .345'$ $e = \tan .345 = .0001$ feet/foot or, e max. = .0012"/foot. A rough sketch of the fixture is shown below.

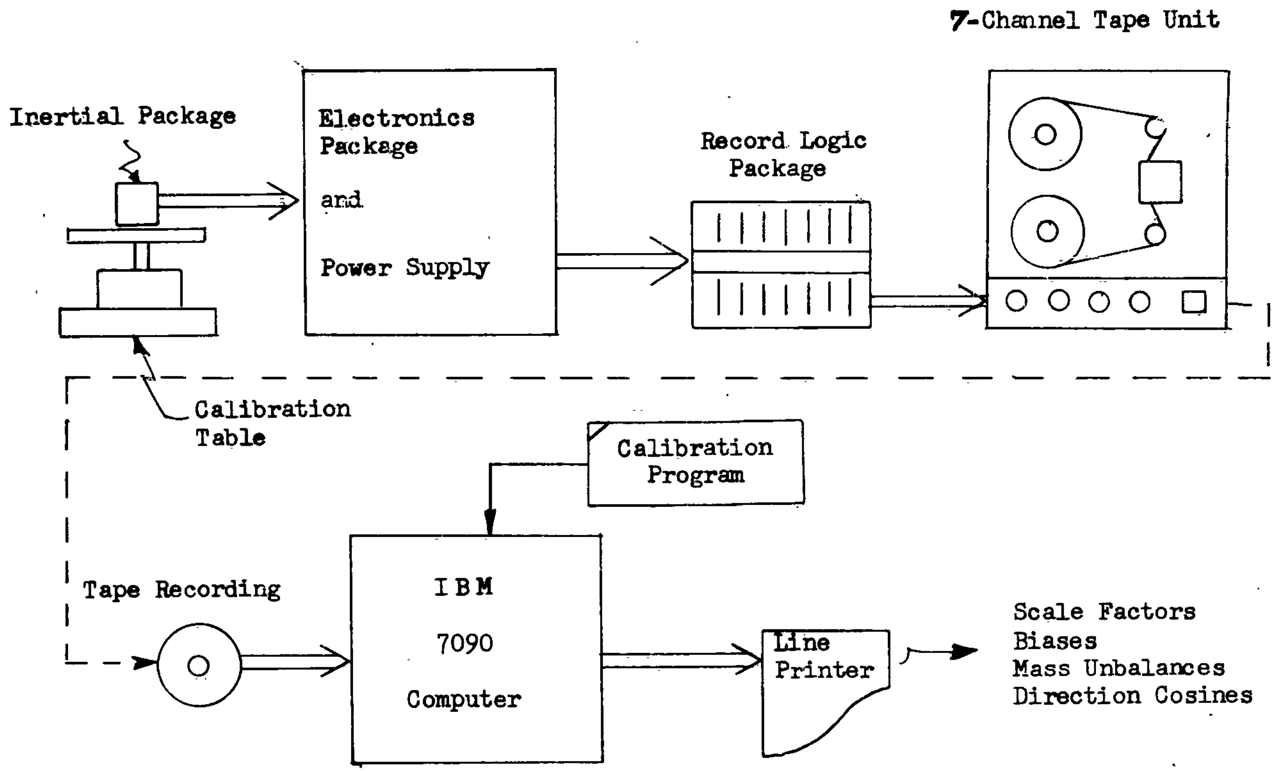
7-Channel Tape Unit
Inertial Package
Electronics Package
and
Power Supply
Record Logic Package
Calibration Table
Calibration Program
Tape Recording
I B M
7090
Computer
Line Printer
Scale Factors
Biases
Mass Unbalances
Direction Cosines

SANE Calibration Program Data Reduction

Figure 27

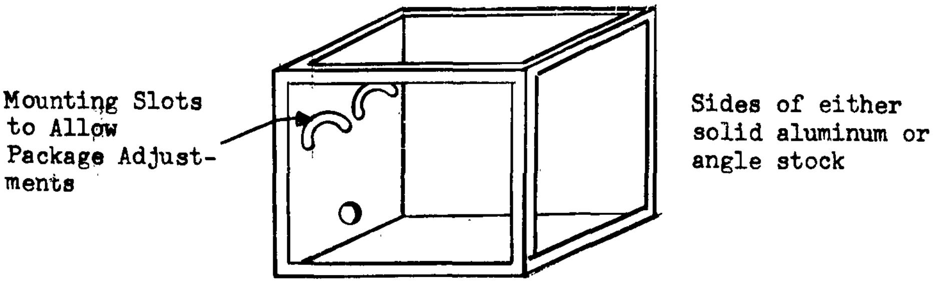
Mounting Slots to Allow Package Adjustments
Sides of either solid aluminum or angle stock

FIGURE 28

3.2.5.6 **Alignment** of the inertial package with the doppler axes.

3.2.5.6.1 General

If the doppler velocity signals are to be used for correcting or aligning the SANE/FPC system, the coordinate systems defined by the inertial package and the doppler must be aligned.

3.2.5.6.2 Maximum Angular Error

Neglecting the errors inherent in the doppler system (approximately ± 2%), and assuming that ± 0.1 nautical miles would be an acceptable error after 1 hour of travel at 100 knots, the two axes will have a maximum misalignment of ± 3.45 minutes of arc.

3.2.5.6.3 AN/APN-130 Alignment Method

Referring to NAVYWEPS 16-30APN130-2, Service Instructions Handbook for the AN/APN-130 (v) Radar Navigation Set, the following method is used to align the doppler to the craft axes:

a. The craft is leveled both longitudinally and laterally, using jacks.

b. A piece of straight aluminum angle stock is placed across the boresighting pads of the external antenna surfaces.

c. A clinometer is placed on the aluminum stock. The angle measured laterally should be 12° ± 1° from the horizontal.

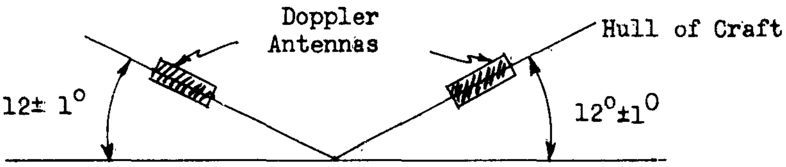

FIGURE 29

Note: The angle has been brought within ± 1° by shimming the antenna mounts. The actual angle, within these limits but having some error, is measured and recorded.

d. A similar method is used for longitudinal error where the antennas should be horizontal ± 25'.

e. A scale factor is determined for each antenna misalignment, and the Signal Data Converter Velocity Computer Module of the AN/APN-130 is adjusted to correct for the misalignments. It should be noted that there are no markings or reference surfaces on the AN/APN-130 package corresponding to the true doppler axes. Since the doppler is resolved to the craft axes, alignment of the inertial package to the craft axes should align the doppler with the SANE/FPC system.

3.2.5.6.4 Craft Leveling

Since craft leveling is used in aligning the doppler, the method used should be examined. Referring to page 1-29 of NAVWEPS 01-230HLC-2-1 General Information for the SH-3 Helicopter;

A leveling plate is permanently attached to the floor in the center of the cargo door.

A plumb bob is hung from a leveling slot above the door.

The plate has marks for each 1/4 degree, and is numbered for each degree. Markings are in the longitudinal direction only and have a range of ± 4°. See sketch.

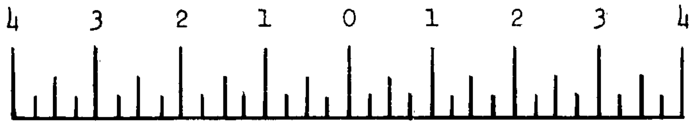

It is estimated that this scale could be set at some value with an accuracy of better than ± 1.5 minutes of arc.

3.2.5.6.5 Alignment Methods

Outlined below are descriptions of a number of alignment methods that could be used either in whole or in part. A summary of the methods along with advantages and disadvantages of each is given in Table 7.

The use of an optical alignment method appears to be of sufficient accuracy for this task, and could be used, assuming that the SH-3 design provides visual accessibility of the inertial package from the outside.

During the initial testing and calibration of the inertial package, reference would be made to a two sided optically flat mirror. The two surfaces, 90° apart will determine the ideal X, Y, Z axes of the instrument package.

The instrument used in conjunction with the mirror surfaces is an Auto-collimator, or a Theodolite with auto-collimation features.

A device known as a "Blitz wheel" is used as part of an operational check on the doppler. The device consists of a rough surfaced revolving reflector of the doppler signals. System operation and scale factor is usually checked with this method.

By positioning the Blitz wheel such that maximum velocity in, for example, the forward or x-direction, the true doppler axes could be determined. Modifications would have to be made to the existing Blitz wheel in order to accurately define the axis of the Blitz wheel. For the optical alignment scheme, this would mean the installation of a mirror cube on the Blitz wheel.

It is also possible to align the inertial package using the resolved outputs of the accelerometers. The craft must be leveled as described previously. The package is then oriented for minimum a_X and a_Y outputs. When this condition is reached, the package is then level, or, the Z axis of the package is in line with the craft vertical.

For the alignment of another axis, the craft must be tilted about one axis. Let us assume a pitched down attitude of about 15°. The package is then aligned until there is minimum output from the Y-axis accelerometer. The exact value of the tilt angle is unimportant. However, for a larger angle, up to 90°, the error is smaller.

Error analysis for accelerometer leveling. We assume that the maximum allowable angular error is 3.5 minutes of arc. For the case where the craft is level, the X and Y accelerometers should be perpendicular to the gravity vector. In this instance, the output would be the sum of bias stability, threshold and resolution errors in addition to the output due to misalignment. This means that we cannot align any closer than the angle corresponding to the spurious outputs.

Our present requirements are for accelerometers having a combined error of 7.58×10^{-5} g. It is possible that we may obtain better. The input to an accelerometer near horizontal is g sin α . To find α , the deviation from horizontal due to accelerometer errors, we set

$$g \text{ SIN } \alpha = 7.58 \times 10^{-5} \text{ g}$$
$$\text{SIN } \alpha = 7.58 \times 10^{-5}$$

α is approximately 7.58×10^{-5} radians
$= (7.58 \times 10^{-5})\ (57.3)\ 60 \text{ minutes} = 0.26 \text{ minutes}$

Comparing this with the maximum allowable error of 3.5 minutes, this means that we have an accuracy ratio of better than 13:1 between the test method and the desired accuracy. For the case where the craft is tilted, the input to the y accelerometer is g $\text{SIN}\,\alpha\,\text{SIN}\,\theta$ where θ is the craft tilt angle. From the General Information Handbook for the SH-3 NAVWEPS 01-230WLC-2-1, the maximum allowable tilt angle, while the craft is on the ground, is 15° about the pitch axis.

Taking $\theta = 15^{\circ}$, and the accelerometer errors as before,

$$g \text{ SIN } \alpha \text{ SIN } 15^{\circ} = 7.58 \times 10^{-5} g$$

$$\text{SIN}\alpha = \frac{7.58 \times 10^{-5}}{\text{SIN } 15^{\circ}} = \frac{7.58 \times 10^{-5}}{.25882} = 2.93\text{x}10^{-4}$$

$$\text{SIN}\alpha \qquad = (2.93\text{x}10^{-4})\ (57.3)\ 60 = \underline{1.01 \text{ min.}}$$

Thus, the minimum detectable angle is about 1 minute, giving an accuracy ratio of about 3.5:1 between this test method and the maximum allowable error.

Mention should be given to the possibility of using spirit levels or bubble levels. This could give us the vertical axis of the package mounted in a level craft without much difficulty. Some other method would have to be employed to provide us with the alignment of the X or Y axis. The accuracy of bubble levels vary, but as an example, the bubble level used in the Keuffel & Esser, KE-2 Theodolite, has an accuracy of 20 seconds. This should be adequate for our purposes.

3.2.5.7 Summary

Table 7 summarizes the methods described in this report. It can be seen that no one method stands out as being ideal. The best method may be a combination. The simplest leveling method, using a bubble level could be combined with either the inertial or the Blitz wheel method of determining directional orientation. The inertial leveling procedure has sufficient accuracy to be combined with one optical sighting from either craft axis or Blitz wheel doppler axis alignment. It is apparent that leveling the inertial package poses no great problems, however, none of the methods described provide an ideal directional alignment in X and Y axes. Use of flight test data for this is being investigated.

Table 7

PROPOSED ALIGNMENT METHODS - SUMMARY

DOPPLER/CRAFT/INERTIAL PACKAGE

	Advantage	Problems
Optical	High Accuracy (±.5 seconds arc)	Presently there is no known visual access to inertial package. Mirrors must be mounted on package.
Blitz Wheel	Gives true doppler axis	Requires (1) optical sight. Obtaining Blitz wheel axis. Does not provide vertical axis.
Inertial	No optical sighting. No additional equipment. Can give vertical with no tilting of craft.	Requires tilting of craft about 10°. Maximum allowable is 15°. Equipment must be operating. Error close to maximum allowable.
Spirit Leveling	No optical sighting needed to obtain vertical. Equipment doesn't have to be turned on.	Gives vertical axis only.
		Note: All methods depend on craft leveling accuracy (estimated ± 1.5 min.)

3.2.6 Pulse Torque Servo Amplifier

3.2.6.1 Introduction

Pulse torquing is a term used to designate the digitalization of current used to torque single-degree-of-freedom gyros and accelerometers. Basically, the PTA accepts an analog error-signal input from a gyro or accelerometer and performs an analog to digital conversion on the input. The PTA accomplishes a servo restraining function and provides an output proportional to acceleration or velocity, depending on the type of inertial sensor used. This output information is in discrete pulse form, which is highly desirable, for the accuracy due to counting accurately controlled pulses exceeds that of attempting to measure analog currents.

The study program just completed was to redesign an existing PTA to meet the new environmental requirements.

3.2.6.2 Specifications

The following are requirements to be met by the PTA:

1. To operate in an environment controlled to 130° ±5°F for coarse temperature control, and to 150° ±1°F for the fine temperature control.

2. To have error contributions smaller than or equal to 1×10^{-5} g/g "Scale Factor Stability" and 1×10^{-6}g "Bias Stability" for a one sigma (1σ), 24 hours of continuous operation at normal operating temperatures.

3. To accept maximum linear acceleration inputs to 2.5 g's for accelerometers and maximum angular velocities of 20°/sec for gyros.

4. Have capability of driving the inertial-sensor torquer winding with up to 40 volts at 4 watts.

5. To withstand the severest helicopter environmental conditions.

6. Torquer power to be constant.

7. Operation at a maximum loop gain consistent with loop stability.

3.2.6.3 Conclusions

Since a previously designed PTA which is capable of operation at 70°F and at a lower torquer power, has operated satisfactorily in this application, it is beleived that the additional requirements can be satisfied without much difficulty and a minimum amount of redesign.

3.2.6.4 Design Considerations

Design requirements of the PTA are very stringent and resulted in the utilization of several unique circuits. The following are part of the requirements imposed on the PTA.

1. Adequately high maximum torque to handle high angular input rates. A maximum of 2.5 g's for the accelerometer and an angular rate of 20°/second for the gyro.

2. Adequately small pulse width to provide the necessary resolution.

3. The use of pulse frequencies which are compatible with the electromagnetic torquers of the inertial sensors, yet optimum for system performance.

4. Torquer power to be kept to a minimum and to be constant.

5. The requirement for high loop gain, dynamic stability and fast response of the servo loop.

6. Ambient temperature to be approximately 150°F.

3.2.6.5 Design and Development Efforts

The development program of the PTA has been to attempt an improvement in an overall system performance and to meet the "Linearity", "Equivalency" and "Scale Factor Stability" requirements.

The Electrical design and developments were to:

1. Eliminate the possibility of all bridge transistors being "on" or "off" simultaneously. Since the current regulator input is from the bridge sensing resistor any transients produced will severely limit the ability of the regulator to meet its functional requirements.

2. Reduce intercircuit coupling of signals.

3. Test the gain linearity and sensitivity of the push-pull stages with a dummy load. Repeat as loaded under normal operating conditions. Since the normal load includes the half wave demodulator, this information would be helpful in evaluating the performance of such a device.

4. Redesign the 25 milliamp accelerometer bridge for use with the accelerometer requiring a torquer current of 12.5 milliamps.

5. Attempt to reduce or eliminate the number of trim pots located within the current regulator circuitry.

6. Set up test procedures for testing "Scale Factor" and "Equivalency Stability" for both open and closed loop operation.

7. Determine optimum circuit layout for minimum coupling. Finalize exact components which are to be fine temperature controlled, keeping in mind the need for proper inter-board impedance matching.

8. Consider the possible use of shielding to improve or maintain existing performance.

9. Design changes have been incorporated in the existing 70°F accelerometer P.T.S.A. and preliminary test have proven satisfactory with an ambient temperature of 150°F. Since operation of the 70°F design has previously met system specifications, a minimum effort should be expended to finalize the design of the higher temperature unit. Some of the problem areas and their respective detrimental effects due to the increase in temperature are listed as follows:

a. Power dissipation of resistive components must be derated by approximately 20%.

b. All semiconductors have a smaller maximum power dissipation. Power reduction of approximately 15%.

c. Thermal noise agitation-voltages in resistive components, which is proportional to the square root of temperature in degrees Kelvin, are increased by approximately 6%.

d. Switching ability of semiconductors is adversely effected. Leakage currents increase. For "bulk" type currents this amounts to an increase in leakage by approximately a factor of 16 over room temperature operation.

10. Due to the high voltage developed across the gyro torquerwinding the semiconductors are being pushed. Initial design philosophy was to incorporate four layer devices as bridge elements. Though satisfactory operation and data have been achieved at 70°F, four layer devices are inherently slower, have higher leakage and have a higher saturation resistance than do transistors. It has, therefore, been decided to design and develop a transistorized power output bridge. The major problems with transistors is that high voltage, high speed, high current and two units in one header are difficult to obtain simultaneously. To solve the high voltage problem, a bridge was designed incorporating eight transistors. The transistors will be grouped, two in a series, shunted by a large value resistance thereby reducing the voltage requirement by a factor of two. Various transistor manufacturers have been consulted, and to date this appears to be the most satisfactory solution. The type of semiconductor specified are planar and are available two per header.

3.2.6.6 Conclusions

The finalization of circuitry for both the gyro and accelerometer PTA, compatible with the temperature requirements, require additional development on their respective room temperature versions. An attempt will be made to meet or exceed the specified system requirements. Since the initial design concept was specifically for missle application, it is felt that the specifications pertaining to loop gain and "Scale-Factor Stability" can be relaxed somewhat. Tests will be conducted to measure "Scale Factor" and Bias Stability in an open loop configuration. Later similar measurements including linearity will be made under closed-loop operation.

In the present design, at room temperature the occurrence of spikes on the bridge sensing resistor have been eliminated. It is felt that the contribution due to an increase in ambient temperature will be insignificant, after the appropriate compensation.

3.2.7 Inertial Instrument Package

The design of a small lightweight inertial instrument package was emphasized. There were two approaches considered; a liquid convection system and a solid conduction system. A detail design was completed on each system. The units were designed to the following specification.

Inertial Instrument Package

Ambient Temperature: 0-150°F, 0-150°F mounting, 0-125°F Ambient Air

Core Temperature: 180 ± 1°F to be held to ± 0.1°F at any point

"G" Loading: 3G maximum, non-shock

Vibration: .006" double amplitude at 5-50 cps
5 G's at 50 - 500 cps

Gyros: 3 at 1.0 # each sealed if required.

Accelerometers: 3 at .25# each sealed if required.

Instrument Alignment: ± 0° 3' 0" initial
± 0° 0' 1" environmental

Package/Frame
Alignment: ± 1°

Warm Up Time: 30 minutes maximum

Interchangeability: All instruments replaceable and interchangeable.

Expected Operational Life: Heaters 1 year continuous
instruments 500 hours continuous

Type Duty: Continuous and interrupted

Shelf Life: 1 year storage

Pressure/Humidity: Normal under 1000 ft.

System Seal: Dust, Salt Spray

Shield, Magnetic: Netic-Conetic

3.2.7.1 The Liquid System (Reference 18X590809)

The liquid convection mode of thermal control at first appeared to have more advantages in rigid temperature control, (the liquid flow rate could be designed to yield any reasonable constant temperature difference across an instrument), in weight, and in ability to withstand external temperature differentials. As design of the liquid system was nearing completion, however, it became apparent that the desired weight level could not be met, and that reliability was considerably reduced due to seal problems and to possible field abuse. Erection and alignment becomes more of a problem, and laboratory tests run on some filler materials proved discouraging. With sufficient development time and with the improvement of polyurethenes, the liquid system still holds future promise of better temperature control at weights excelled those possible with a solid core.

In this method a coolant (glycol) is pumped through an annular space around each instrument by a simple impeller powered by two motors (for redundancy). The flow rate of ten feet per second would result in only a .1°F temperature rise of fluid from entrance to exit of annulus. The fluid is collected from all the instruments, mixed and then directed by a solenoid-controlled valve through a tube attached to the package skin. Here the fluid surrenders its heat to the skin, which radiates the heat to the surroundings. The package weight would approach 14 pounds. Any temperature differential imposed across the package outer skin would not be "felt" by any instrument, since this heat flux would be mixed, and thereby balanced, by the fluid. The pump, the valve and the flow patterns throughout the package ducts ensure continued mixing of the fluid.

Limitations and restrictions of this design include the quantity and difficulty of sealing the complex fluid passages, stringent assembly techniques required, difficulty of field maintenance, proneness to failure due to field abuse, and a required cyclic overhaul (which could only be accomplished at the factory). Any state-of-the art advances in sub-miniaturization would not be enjoyed by simply modifying this design as much as would the solid package, since the fluid system tends to control the package volume required rather than the instrument size.

The package skin is made of netic-conetic material, which assures magnetic attenuation of approximately 120,000 to one.

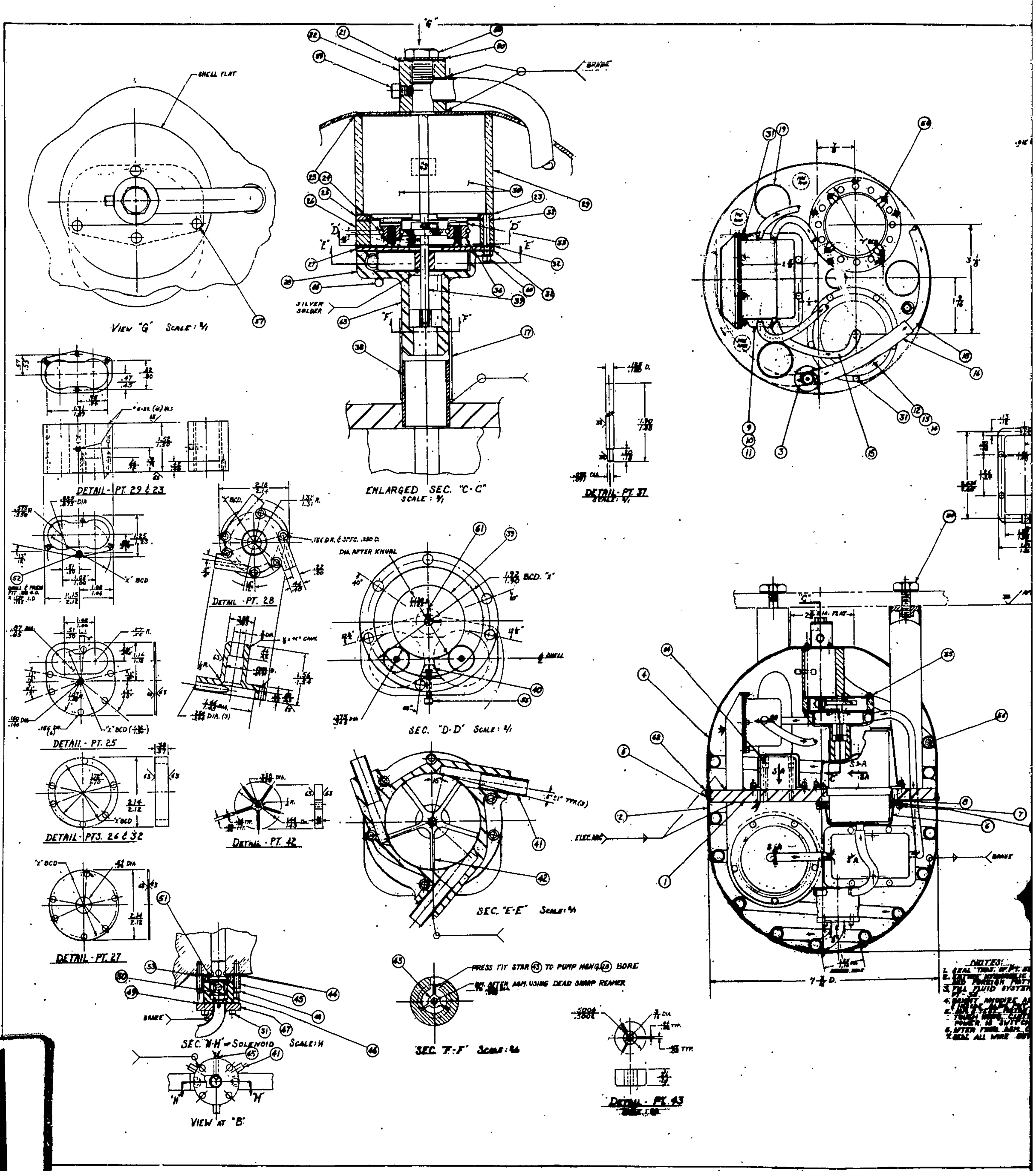
"G"
SHELL FLAT
View "G" Scale: 4/1
BRAKE
SILVER SOLDER
ENLARGED SEC. "C-C"
SCALE: 4/1
DETAIL - PT. 37
DETAIL - PT. 29 & 23
DETAIL - PT. 28
DIA. AFTER KNURL
SEC. "D-D" Scale: 4/1
DETAIL - PT. 25
DETAIL - PTS. 26 & 32
DETAIL - PT. 42
SEC. "E-E" Scale: 4/1
DETAIL - PT. 27
SEC. "H-H" - SOLENOID Scale: 4/1
VIEW AT "B"
PRESS FIT STAR 43 TO PUMP HANG. 28 BORE
SEC. "F-F" Scale: 4/1
DETAIL - PT. 43
ELEC. ARC
BRAKE
7 1/8 D.
NOTES:

1

2

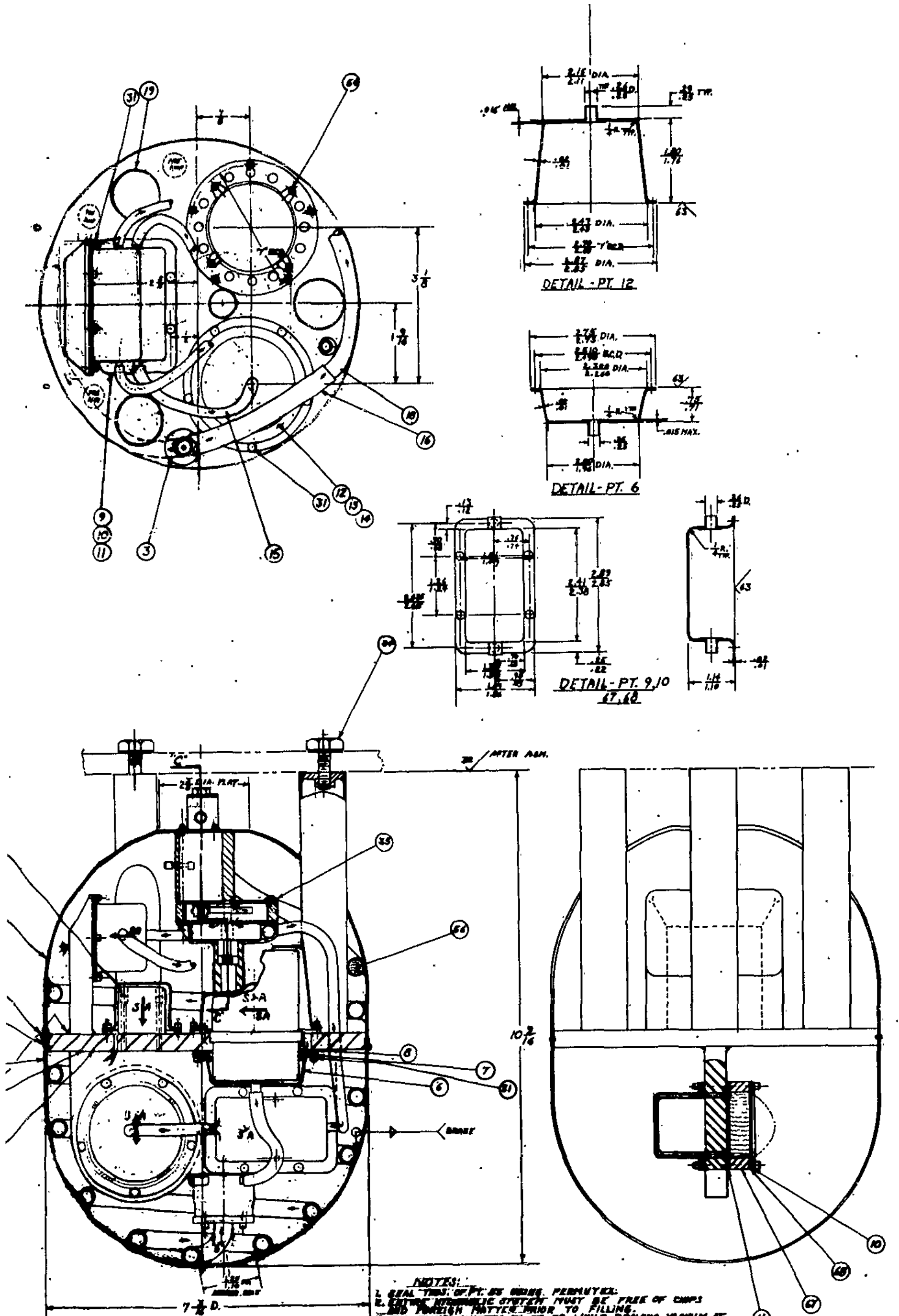

NOTES:
1. SEAL THDS. OF PT. 55 USING PERMATEX.
2. ENTIRE HYDRAULIC SYSTEM MUST BE FREE OF CHIPS AND FOREIGN MATTER PRIOR TO FILLING.
3. FILL FLUID SYSTEM AT PT. 59 WHILE DRAWING VACUUM AT PT. 54.
4. BRIGHT ANODIZE ALUMINUM PTS.. PAINT OUTSIDE PTS. 2 & 4 FLAT BLACK [illegible]
5. [illegible] PUMP ASM. AS SEPARATE UNIT. IMPELLER NOT TO TOUCH [illegible]. CLUTCH PT. 36 TO DISENGAGE PT. 39 WHEN ITS MOTOR POWER IS SWITCHED OFF. TEST RUN FOR 5 HR. MINIMUM.
6. AFTER FINAL ASM. CEMENT ALL PLASTIC HOSE CONNECTIONS USING GLYPTAL.
7. SEAL ALL WIRE OUTLETS USING SILICON RUBBER CEMENT.

PT. NO.	NAME	QTY.	MAT'L / DESCRIPT.
68	DIAPHRAGM	1	BUNA "N" RUBBER .010 THK.
67	RESERVOIR	1	ALUM.
66	SENSOR, COARSE	1	
65	SENSOR, FINE	1	
64	SCREW	12	#2-56 × 3/16 LG SOC HD
63	HEATER WIRE	1	
62	SCREW	16	#6 SELF-TAP
61	SET. SCR.	2	#4-40 × 3/16 LG. SOC. HD CUP PT.
60	SCREW	3	#6-32 × 3/8 LG. SOC. HD.
59	SCREW	1	1/4-28 × 1/4 LG
58	BOLT	1	5/16-24 × 3/4 LG
57	SCREW	4	#6-32 × 3/8 LG SOC. HD.
56	FLUID	AR	ETHYLENE GLYCOL
55	SCREW	1	#6-32 × 3/8 LG. SOC. HD.
54	SERVO CLAMP	12	
53	ADAPTOR	1	ALUM.
52	BUSHING	1	"OILITE"
51	PLUNGER	1	STL.
50	SPRING	1	
49	GASKET	1	.060 THK. NEOPRENE
48	SCREW	2	#6-32 × 3/4 LG SOC. HD.
47	CAP	1	STL.
46	COIL	1	
45	VALVE BODY	1	ALUM.
44	GASKET	2	.010 THK. NEOPRENE
43	STAR	1	"OILITE" SINTERED BRONZE ROD 1/2 DIA.
42	IMPELLER	1	CRES.
41	TUBE	6	ALUM .250 O.D. × .010-.015 WALL
40	RETAINER	1	ALUM.
39	DRIVE DISC	1	ALUM.
38	TUBE	1	5/8 O.D. × 1/2 I.D.
37	SHAFT	1	CRES.
36	CLUTCH	2	ALUM.
35	NUT	3	#6-32
34	BOLT	3	5/16-24 NF
33	THRUST BEARING	2	MPB #33T 1/8 I.D. × 5/16 O.D. MINIATURE
32	GASKET	3	.010 NEOPRENE
31	CAP SCREW	14	SOC. HD. #6-32 × 1/2 LG.
30	MOTOR, SERVO	2	MODEL 6A5, [illegible] @ 12,000 RPM. 24VDC .9A , WESTERN GEAR Co.
29	MOTOR HOUSING	1	ALUM.
28	PUMP HOUSING	1	ALUM.
27	BAFFLE PLATE	1	ALUM.
26	GEAR HOUSING	1	ALUM.
25	BACK PLATE	1	ALUM.
24	"O" RING SEAL	2	PARKER #2-10
23	GASKET	2	.010 THK. NEOPRENE
22	FILL VALVE	1	STL
21	GASKET	1	.040-.060 THK. NEOPRENE
20	WASHER	1	ALUM
19	LEG	3	1" O.D. × .020 WALL TITANIUM
18	UPPER COIL	1	STL. TUBING .015-.025 WALL
17	TUBING	AR	PVC 1/4 I.D. × 3/4 O.D.
16	TUBING	AR	PVC REINFORCED 3/8 I.D. × 1/2 O.D.
15	TUBING	AR	PVC REINFORCED 1/4 I.D. × 3/8 OD
14	GYRO GASKET, UPPER	3	.060 THK. NEOPRENE
13	GYRO LOCK RING, UPR	3	ALUM. .030 THK.
12	GYRO CAP, UPPER	3	ALUM.
11	ACCEL. GASKET	4	.060 THK. NEOPRENE
10	ACCEL. LOCK RING	4	ALUM. .030 THK.
9	ACCEL. CAP	3	ALUM.
8	GYRO GASKET, LWR.	3	.060 THK. NEOPRENE
7	GYRO LOCK RING, LWR.	3	ALUM. .030 THK.
6	GYRO CAP, LOWER	3	SPUN ALUM.
5	DUST SEAL	1	1/8 × 1/4 × 23 LG. BUNA "N" RUBBER
4	UPPER SHELL	1	(SEE PT. 2)
3	LOWER COIL	1	STL. TUBING .015-.025 WALL
2	LOWER SHELL	1	NETIC-CONETIC .040 THK ; PERFECTION MICA CORP.
1	WELDMENT	1	BERYLLIUM

UNLESS OTHERWISE SPECIFIED:

NEXT ASSY	USED ON
APPLICATION	

Hamilton Standard
WINDSOR LOCKS, CONNECTICUT • U.S.A.

SDIMU - FPC
LIQUID CONVECTION

18X 590809

FPC-1

3.2.7.2 The Solid System Reference 18X590805 and SK52216

With the recognition of the listed short comings of the sophisticated liquid convection system, a review of concepts was made and the shortcomings of the solid system re-evaluated. A formula was developed to ascertain the need for additional thermal filtering. A detailed analysis indicated that an additional thermalfilter would not be needed provided the present filtering could be improved. With no additional rings of conductive metal, as assumed 8°F temperature difference across the outside of the package was found to create less than the maximum allowable .1°F across any instrument. This was reflected in a lower weight than had been originally estimated, and made the weight comparable to the liquid design. Further investigation was therefore implied.

The principle of operation of the solid core is that the instruments are considered to be heat sources buried within a highly conductive, thermal bed. If these heat sources are relatively distributed and have essentially even heat outputs, the core will tend to be nearly isothermal, and will have calculable temperature gradients throughout,

- For an aluminum core closely machined to accept the instruments, the steady-state temperature difference should never exceed ± .04°F which is well within the 0.1°F required.

If magnesium were used for the core, a weight savings of 30% of the core weight (about 3/4 pound) could be evidenced, but the thermal transients would increase so that temperature regulation would be ± .06°F rather than ± .04°F as in aluminum. However, this still remains within specification. Commercially pure magnesium should be used (i.e., Dow B92-52 ingot, 99.878% pure) to retain high thermal conductivity. Dow lists 99.9% pure magnesium conductivity as $91^{BTU}/FT/FT^2/°F/HR$. For the breadboard model, however, aluminum is recommended because of its ease of machining and thermal stability at elevated temperatures.

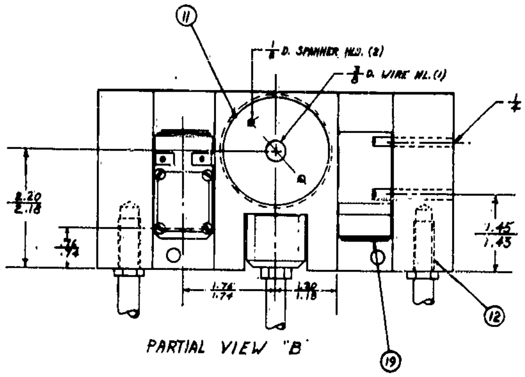
11
1/8 D. SPANNER HLS. (2)
3/8 D. WIRE HL. (1)
1/4
2.20/2.18
.76/.74
1.45/1.43
1.76/1.74
1.20/1.18
12
19

PARTIAL VIEW "B"

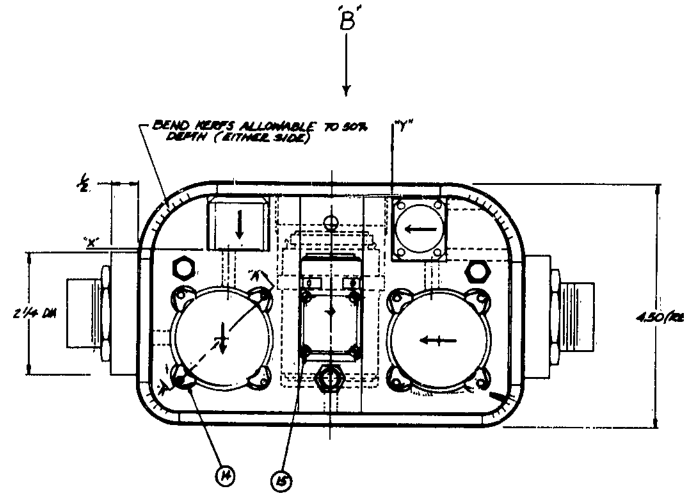
'B'
BEND KERFS ALLOWABLE TO 50% DEPTH (EITHER SIDE)
"Y"
1/2
"X"
"A"
"A"
2 1/4 DIA
4.50 (RE
14
15

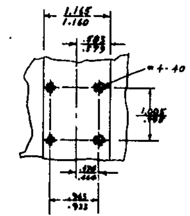
1.165/1.160
.583/.575
#4-40
1.005/.995
.450/.440
.945/.935

TYP. ACCEL. MACHINING

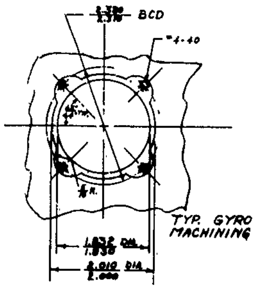
2.320/2.310 BCD
#4-40
45° TYP.
1/16 R.
1.832 DIA./1.830
2.010 DIA./2.000

TYP. GYRO MACHINING

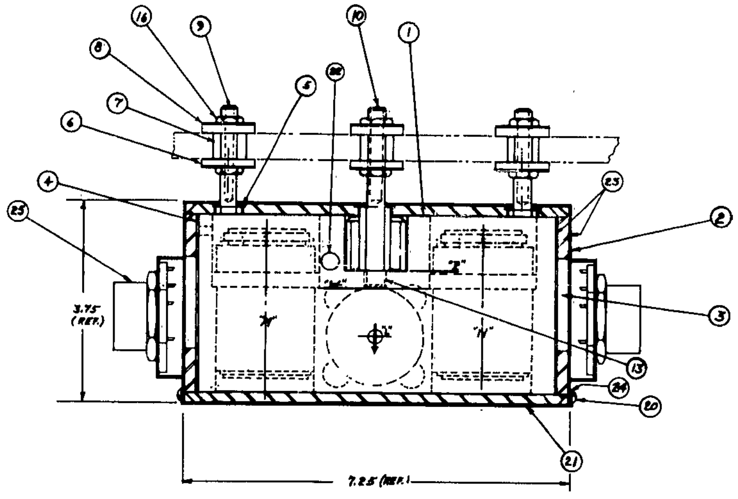
16
9
10
1
8
7
6
5
22
4
25
23
2
3
"Z"
"M"
"N"
"L"
3.75 (REF.)
13
24
20
21
7.25 (REF.)

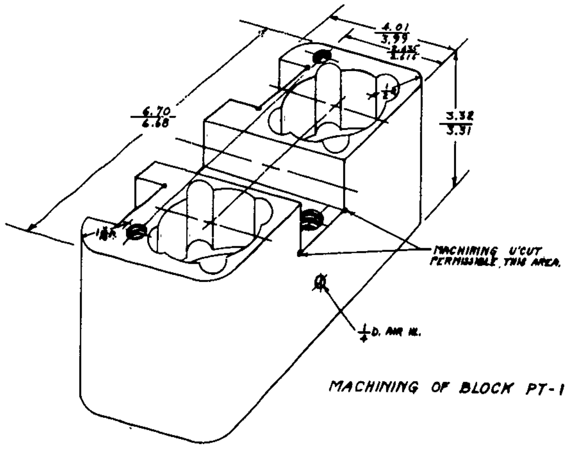
4.01/3.99
2.430/2.410
6.70/6.68
3.32/3.31
1/2 R.
1/8 R.
MACHINING U'CUT PERMISSIBLE THIS AREA.
1/4 D. AIR HL.

MACHINING OF BLOCK PT-1

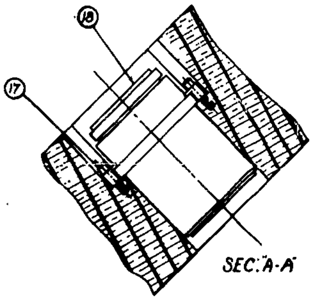

SEC."A-A"

NOTES:

1. COAT ALL INSTRUMENT SURFACES ADJAC.
USING PT-23 PRIOR TO ASSEM. AND A
2. PACK ALL GAPS OR VOIDS BETWEEN INSTR
3. SEAL ALL EXPOSED JOINTS WITH PT-2
4. SURFACES "W" & "X" TO BE PARALLEL
WITHIN .0004 "/IN.
5. AXES "M" & "N" TO BE PARALLEL WITHIN
PERPENDICULAR WITH AXIS "L" WITHIN
6. AXIS "L" TO BE PERPENDICULAR TO SURF
TO SURFS. "X" & "Y". WITHIN .0008 "/IN.
7. AXIS "M" & "N" TO BE PARALLEL TO SURFS.
& PERPENDICULAR TO SURF "X" WITHIN
8. PAINT OUTSIDE SURFACES FLAT BLACK.

1

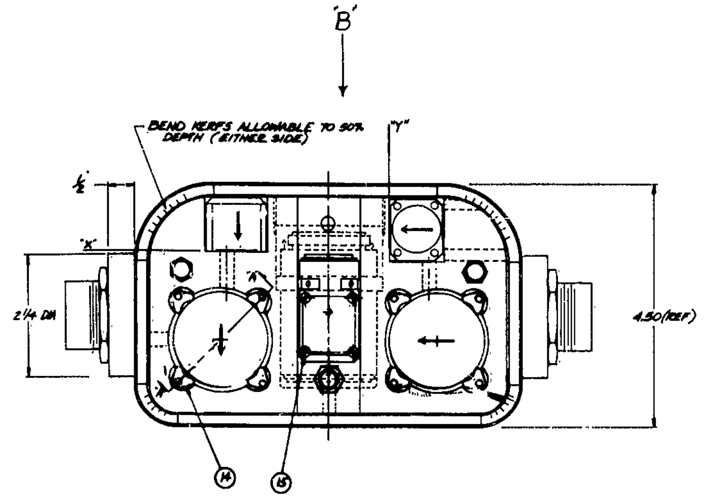

LIST OF PARTS

PT	NAME	QTY.	DESCRIPT. (MAT'L
1	BLOCK	1	AA-6061 T-6
2	SHIELD	1	NETIC-CONETIC (.040) PERFECTION MICA CORP.
3	INSULATION	AR	3/4 EXT. AA DFPI PLYWOOD
4	HEATER, FINE	1	
5	SEAL	3	RUBBER 3/4 I.D. x 1 1/4 O.D. x 1/4 THK. 30-40 DUR BUNA 'N'
6	ISOLATOR	6	RUBBER 3/8 I.D. x 1 O.D. x 1/4 THK. DUR. 20-30 BUNA 'N'
7	BUSHING	3	RUBBER 3/4 I.D. x 1 1/8 O.D. x 1/2 LG DUR. 30-40 BUNA 'N'
8	WASHER	6	STL. 7/16 I.D. x 1 O.D. x .030 THK.
9	LEG	2	CRES. 3/4 HEX. STK. 3" LG
10	LEG	1	CRES 3/4 HEX STK 2 1/2 LG.
11	PLUG	1	AA 6061-T6 2 1/4 O.D. x 1/4 THK.
12	HELI-COIL INSERT	2	3/8-16NC x 1" LG.
13	HELI-COIL INSERT	1	1/2-13NC x 1/4 LG.
14	SERVO CLAMP	12	CAT.# C19SS, STERLING PRECISION CORP.
15	SCREW, ACCEL.	12	#4-40 x 3/8 LG. STL.
16	NUT, MACH.	6	STL. 3/8-16 N.C.
17	SCREW, SOCKET	12	#4-40 x 5/8 LG. CRES.
18	GYROSCOPE	3	SPERRY
19	ACCELEROM.	3	KEARFOTT
20	SCREW, SEALTOP	6	
21	BOTTOM SHIELD	1	NETIC-CONETIC (.040) PERFECTION MICA CORP.
22	SENSOR, TEMP.	1	
23	SILICON GREASE	AR	G.E.
24	SILICON ELASTIC	AR	
25	CONNECTOR	2	BENDIX PIGMY CAT.# PT07A-20-41P

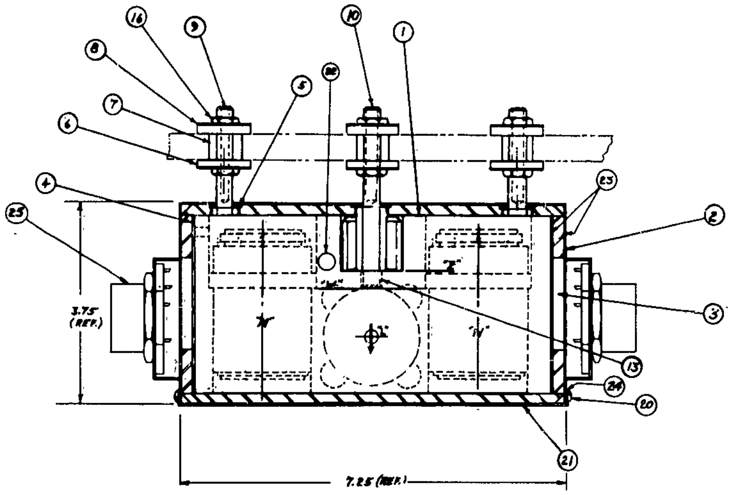

2

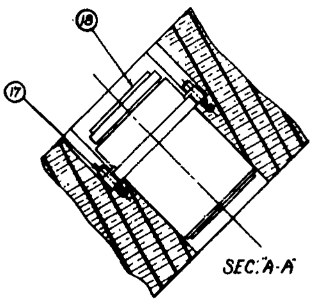

SEC. 'A-A'

NOTES:

1. COAT ALL INSTRUMENT SURFACES ADJACENT TO BLOCK PT-1, USING PT-23 PRIOR TO ASSEM. AND ALL INSULATION SURFACES.
2. PACK ALL GAPS OR VOIDS BETWEEN INSTRUMENTS AND BLOCK WITH PT-23.
3. SEAL ALL EXPOSED JOINTS WITH PT-24.
4. SURFACES "W" & "Z" TO BE PARALLEL WITHIN .0004 "/IN. & PERPENDICULAR TO SURF. "X" & "Y" WITHIN .0004 "/IN.
5. AXES "M" & "N" TO BE PARALLEL WITHIN .0008 "/IN. AND THEIR PLANE PERPENDICULAR WITH AXIS "L" WITHIN .0004 "/IN.
6. AXIS "L" TO BE PERPENDICULAR TO SURF. "X" WITHIN .0008 "/IN. AND PARALLEL TO SURFS. "Z" & "Y" WITHIN .0008 "/IN.
7. AXIS "M" & "N" TO BE PARALLEL TO SURFS. "X" & "Y" WITHIN .0008 "/IN. & PERPENDICULAR TO SURF "Z" WITHIN .0008 "/IN.
8. PAINT OUTSIDE SURFACES FLAT BLACK.

UNLESS OTHERWISE SPECIFIED:
DIMENSIONS ± ____ ANGLES ± ____
BREAK EDGES .005-.015. FILLET RAD ____
SURFACES HAVING A COMMON AXIS CONCENTRIC WITHIN ____ TIR. CLEANING, PRESERVATION AND HANDLING PER HS1989-C ____ P ____
DIMENSIONS SHOWN ARE AFTER PLATING & SIMILAR PROCESSES & BEFORE PAINTING. THREADS PER MIL-S-7742. DRAWING INTERPRETATION PER HS1380. SURFACE CHARACTERISTICS: MIL-STD-10 PER HS1082. △ MARK PART IDENTIFICATION: MIL-STD-130 PER HS333.

NEXT ASSY	USED ON
APPLICATION	

		APPROVALS		DATE
MATERIAL		DRAWN		
		CHECKED		
		DRAFTING		
		DESIGN		
HARDNESS		MATERIALS		
HEAT TREAT SPEC		PROJECT		
		COST		
		FACTORY		
SURFACE COATING		RELEASE		DATE
MFG SPEC		EXPERIMENTAL		
		PRELIM PROD.		
		PRODUCTION		
MAKE FROM		PROD. CODE		

Hamilton Standard
WINDSOR LOCKS, CONNECTICUT • U.S.A.

STRAP-DOWN INERTIAL MEASURING UNIT, FPC

CODE IDENT NO. 73030
CONTRACT NO.
SIZE
18X590805
SCALE: 1/1
WEIGHT: CALC. 11.2 LB
SHEET

FPC-1

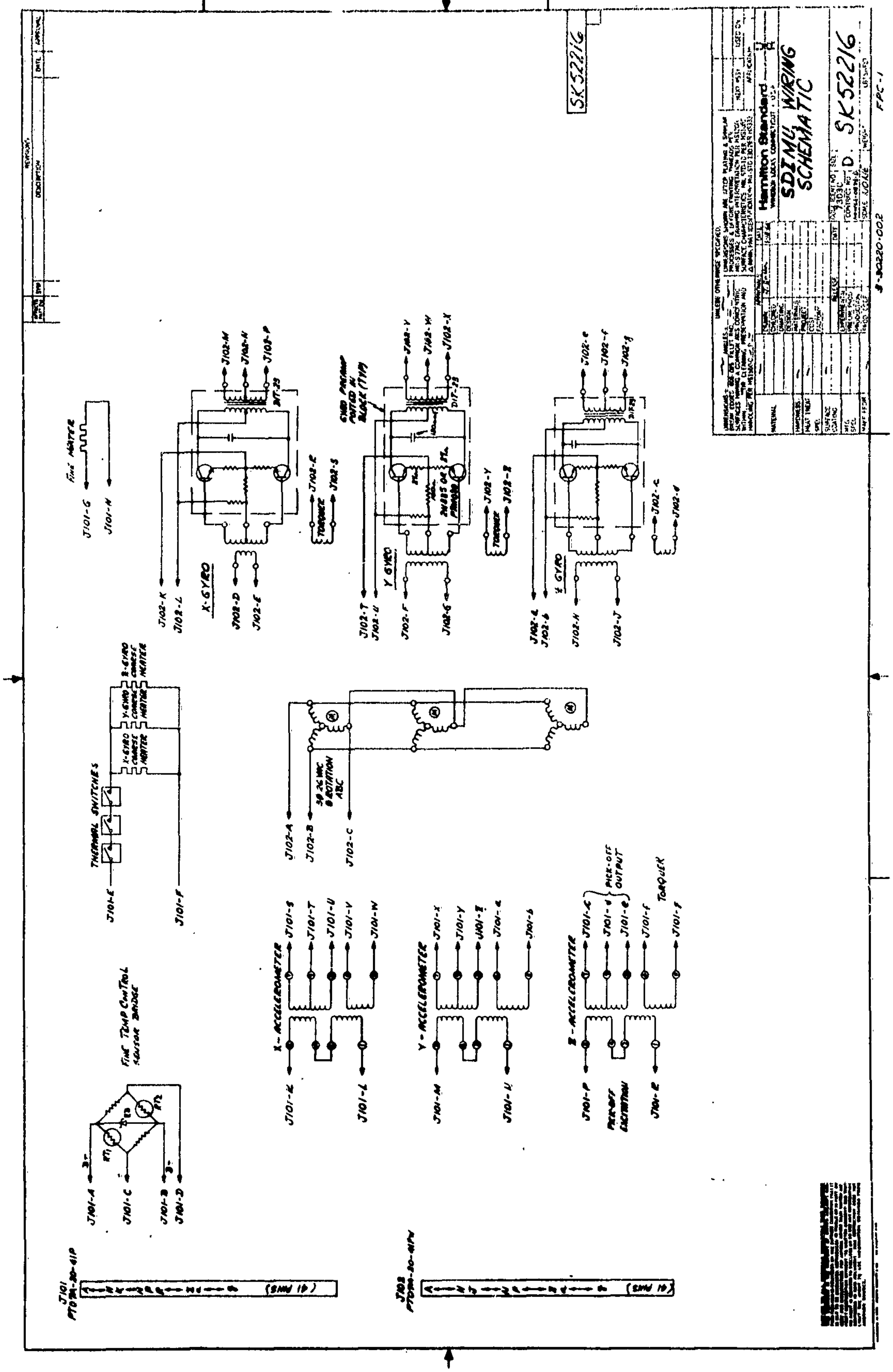
SK52216
Hamilton Standard
SDIMU WIRING SCHEMATIC
SK52216
FPC-1
X-GYRO
Y GYRO
Z GYRO
J102-K
J102-L
J102-D
J102-E
J102-M
J102-N
J102-P
J102-R
J102-S
TORQUER
J102-T
J102-U
J102-F
J102-G
J102-V
J102-W
J102-X
J102-Y
J102-Z
J102-a
J102-b
J102-H
J102-J
J102-e
J102-f
J102-g
J102-c
J102-d
GYRO PREAMP POTTED IN BLOCK (TYP)
FINE HEATER
J101-G
J101-H
THERMAL SWITCHES
X-GYRO COARSE HEATER
Y-GYRO COARSE HEATER
Z-GYRO COARSE HEATER
J101-E
J101-F
J102-A
J102-B
J102-C
3Ø 26 VAC
Ø ROTATION ABC
FINE TEMP CONTROL SENSOR BRIDGE
RT1
RT2
J101-A
J101-C
J101-B
J101-D
X-ACCELEROMETER
J101-K
J101-L
J101-S
J101-T
J101-U
J101-V
J101-W
Y-ACCELEROMETER
J101-M
J101-N
J101-X
J101-Y
J101-Z
J101-a
J101-b
Z-ACCELEROMETER
J101-P
J101-R
J101-c
J101-d
J101-e
J101-f
J101-g
PICK-OFF OUTPUT
PICK-OFF EXCITATION
TORQUER
J101
J102

Warm Up

Warm up time occurs exponentially, and should be achieved within thirty minutes by using the heaters enclosed within the gyros, the instruments being protected by individual thermo-switches.

Time Constants

Time constants for a temperature fluctuation at the surface of the core to be sensed by the temperature sensor buried 1/2 inch within the core would be four seconds. This should be entirely satisfactory, since the sensor will sense the bed temperature and will respond within a relatively short time, preventing large on-off heater oscillation about the nominal temperature.

The core is surrounded with a layer of insulation to act as a thermal barrier which controls the amount of heat flux reaching the outer skin. All but two per cent of the heat leaves the package by radiation and convection occurring at the outer skin. This few per cent escapes via the three legs, and the leg resistance is adequate to prevent a 15°F temperature gradient at the mounting surface from creating a .1°F temperature gradient within the package. A resistance heater type temperature control regulates the aluminum block temperature by means of an electronic temperature controller. The package skin is a netic conetic covering designed to attenuate a DC magnetic field by a factor of 120,000 to 1. This material can be fabricated, formed, machined, and subjected to blows without affecting its magnetic shielding properties.

Since the type and strength of magnetic fields which may be encountered is unknown, an optimum thickness of .015 conetic over .025 netic material was selected. This would reduce a 60 cycle field of 500 gauss by about 30,000 to 1. The weight of the shield is approximately two pounds, and package weight could be reduced if thinner material could be used and less magnetic attenuation could be tolerated. The same material could possibly, by coordination with instrument vendors, be cased over the individual instruments. Approximately one-half pound could be saved from present package design by doing this.

Stresses

Stresses in the core remain easily within material limits, both for aluminum and for magnesium. Deflection under a 3-g load remain less than the maximum tolerable of one second of arc.

Vibration

For this particular application, the prime vibration source is between 10 and 20 cps. It is desired to isolate all frequencies above one or two cps to reduce anisoelastic drift error in the gyros. The vibration isolation is compounded because no damping is desired such that all accelerations will be detected. Commercial isolators tend to resonate under our load at ten to 14 cps, which is in the middle of the band to be isolated(rotor blade vibration). The apparent solution, then, is to use a soft mounting with adjustable rigidity, so that the resonant frequency of the mounts can be shifted to either side of the prime source by adjusting while on a shaker table. Such a system has been provided. Adjustable mounting bolts can change the amount of pre-load on the mount and thereby change the transmissibility of the mount.

Future Prospects

With the present aluminum core, the package weighs around 11.2 pounds. Some additional design effort could probably reduce this to 9 pounds, and the incorporation of a magnesium core in place of aluminum (beryllium is also a possibility) could yield an 8.5 pound package that would meet the present specifications. Further improvements in the state-of-the-art by instrument vendors would directly affect the weight and/or size of the package.

It, therefore, seems an entirely reasonable prediction at this time that an eight-pound strap-down inertial package, complete and mounted, is possible in the future without stressing the present state-of-the-art in instrument manufacture.

3.3 Flight Path Control Design

3.3.1 Introduction

The Flight Path Control is a computer-controlled autopilot designed to pilot a vehicle automatically through any of a wide variety of ASW patterns. Once a pattern has been selected and programmed into the computer, and a search datum point inserted, the FPC will calculate each successive dunk point in a pattern centered on the search datum, and maneuver the vehicle into a hover over each dunk point in turn.

The basic units of the system are:

1. The Dunk Pattern and Flight Path Computer, which accepts inputs from the pilot and Navigational Computer generates and routes digital commands.
2. The Analog Command Generators, located in the Computer-Flight Control interface develops the analog command signals.
3. The FPC-1 Modified Automatic Stabilization Equipment (FPC-1/ASE), provides both implementation of the necessary maneuvers, and maintains the vehicle in a dynamically stable mode.

3.3.2 Design Conclusions

The FPC will function in any ASW pattern with a minimum range of 5000 yards between successive dunk points, a cruise velocity between 60 and 100 knots, a hovering altitude of 20 to 100 feet, and a cruising altitude of 100 to 200 feet. Velocities above 100 knots would be possible contingent upon an increase in the minimum range between dunk points to allow sufficient maneuvering room. The FPC will be capable of commanding all the maneuvers necessary to realize a pattern and will sequence them in the proper order.

The maneuvers used are: transition to hover, transition to cruise, coordinated turns (CW and CCW), and the homing maneuver.

Through the blending of navigational, computational, and autopilot functions, it is possible to provide a wide range of pilot options and overriding abilities, thus enabling the pilot to skip dunk points, leave and re-enter the pattern at any time, or to start a new pattern centered on a datum point of his choice. Upon leaving the pattern, the pilot may insert a selected point in the FPC and be flown automatically to this point, terminating in a hover over it.

Much of the flexibility in the program stems from the fact that the pattern is realized by homing on successive points rather than by dead reckoning methods. Also, the system operates at low authority levels, consistent with automatic flight practices; this gives the pilot ultimate control over the vehicle at all times. Finally, pilot opinion has been a prime factor in all design considerations; automatic maneuvers were designed to duplicate, as nearly as possible, existing manual ASW maneuvers.

3.3.3 Design Considerations

3.3.3.1 Basic Flight Path Concepts

The basic flight path concepts evolved from consideration of the operating limitations imposed upon the vehicle[41] and the definition of the mission; i.e. the vehicle must be able to function in a wide variety of ASW patterns without exceeding its operating limitations.

3.3.3.1.1 Operation Limitations

The following vehicle operating limitations are pertinent to the establishment of the basic flight path concepts:

(a) All transitions shall be performed with the vehicle headed into the wind.

(b) The maximum permissible roll angle is 30 degrees.

(c) The maximum permissible acceleration is ± 1.5 g.

(d) The maximum permissible vertical rate is 900 ft/min. (Vertical rates above this value are safe, but uncomfortable.)

(e) The maximum permissible forward speed is 150 knots.

(f) Hovering turns shall not exceed a rate of 24 deg/sec. (360 degrees in 15 seconds).

3.3.3.1.2 Mission Requirements

The system will be capable of operating in ASW missions whose range between successive dunk points is 5000 yards or greater. Design objectives will be to minimize time required to complete a given pattern, and minimize fuel consumption, yet eliminate all abrupt maneuvers, and provide as much flexibility in the program as possible. The principal implication is that both the number and complexity of maneuvers required should be kept to a minimum.

3.3.3.2 Flight Path Implementation

The basic unit used in implementing the flight path will be the Hamilton Standard Automatic Stabilization Equipment (ASE),[42] a four axis control system (pitch, roll, yaw, collective). The ASE Basic Channels will be used to maintain stability of flight; the Coupler functions will be modified to accept FPC inputs. Whenever possible, the Coupler path gains will be preserved and the modifications will be restricted to the Coupler inputs. This will allow the use of the ASE, a proven piece of equipment, in close to its existing form. The implementation design effort would then be centralized in the Analog Command Generator section, where the computer outputs would be processed and fed out in usable analog form.

3.3.4 Basic Flight Path Concepts

3.3.4.1 Dunk Point to Dunk Point Flight Path

The basic problem is to maneuver the vehicle from a hover at some dunk point, A, (see Figure 30A) to a hover at the next dunk point, B. The transition to cruise and the transition to hover must both be performed with the vehicle headed into the wind. The transition to cruise will be completed in a distance, a, and the transition to hover in a distance, b. Therefore, the problem reduces to finding a flight path between Point C, at velocity Vc into the wind, and Point D, at velocity Vc into the wind. (Vc is the selected cruise velocity). Several approaches to this problem are shown in Figure 30.

Figure 30B is a one-maneuver flight path: a continuous turn of varying radius. Typically, this maneuver would be some form of a spiral, which would be highly uneconomical both timewise and fuelwise. Moreover, it would be difficult to implement a varying radius turn with sufficient accuracy.

Figure 30C is a three-maneuver flight path: two 180-degree constant radius turns (radius r depends upon location of B with respect to A), and one straight flight. This would be much easier to implement, but it has several distinct disadvantages. If B is nearly upwind of A, r becomes smaller than the turning capabilities of the vehicle. If B is essentially crosswind from A, r approaches $\overline{AB}/2$ and the distance traveled while turning becomes $\pi \overline{AB}/2 = 1.57\ \overline{AB}$; when the straight flight distances (2a + 2b) are added to this, the total distance traveled can easily become greater than twice $\overline{AB}$. Since turning is a time-consuming maneuver, and two 180 degree turns must be made, this flight path will not be suitable from considerations of time and fuel.

The flight path of Figure 30D is a modification of Figure 30C. A fixed turn radius, r_o, is used for all flights. The angle through which the vehicle turns is kept to a minimum for a particular value of r_o. This

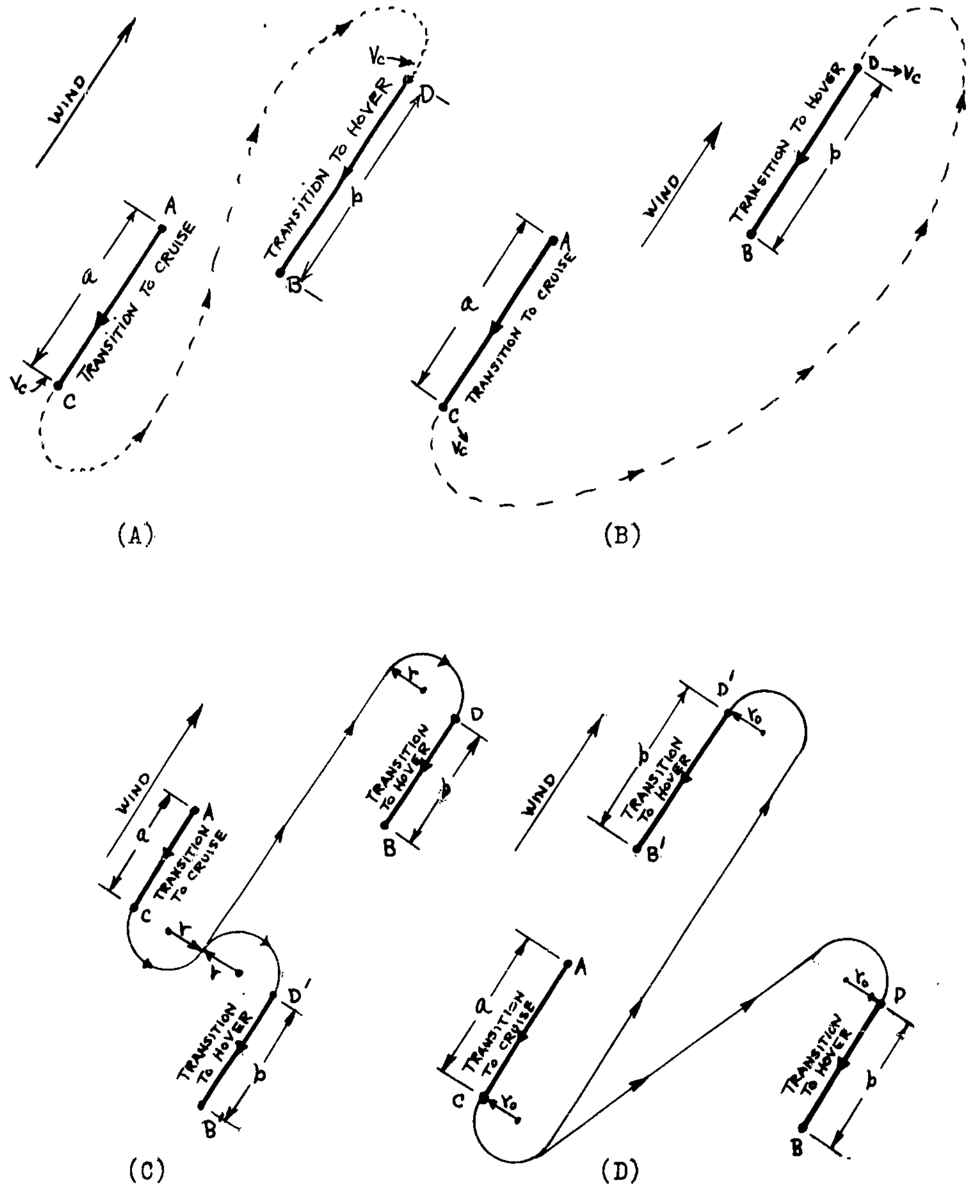
WIND
A
a
TRANSITION TO CRUISE
C
V_c
TRANSITION TO HOVER
D
b
B
(A)
(B)
r
r_0
D'
B'
(C)
(D)

Figure 30
Possible Dunk Point-To-Dunk Point Flight Paths

will in effect minimize the time required for the flight, the distance traveled, and the fuel consumption for a particular set of values, a, b, r_o. Further optimization involves a tradeoff between time required and fuel consumption, the tradeoff being realized by adjustment of a, b, and r_o, subject to the vehicle operating limitations.

Typically, this flight will require one CW and one CCW turn, each of less than 180 degrees. For the case when B' is nearly upwind of A, this technique is valid, but requires either two CW or two CCW turns of close to 180 degrees. (The direction of the turns depends on whether $\overline{AB}$ is displaced from the wind vector, $\overrightarrow{V_W}$, in a clockwise or counterclockwise sense.)

Flight paths involving three or more turns must necessarily require more time, distance traveled, fuel, computation, and complexity of implementation, and would not represent an optimal choice.

On the basis of these considerations, the path of Figure 30D was selected as the Dunk Point-to-Dunk Point Flight Path.

3.3.4.2 Base-to-First Dunk Point Flight Path

The Base-to-First Dunk Point Flight Path is derived from roughly the same format as the Dunk Point-to Dunk Point Flight Path. The prime difference is that the pilot must perform a manual takeoff from the base, bring the vehicle up to cruise speed and altitude, and engage the FPC. (The reason for this is explained in Section 3.3.4.4.) The initial act of the FPC is to turn the vehicle toward the first dunk point. Again, the transition to hover over the first dunk point must be performed into the wind. Thus, Figure 31A illustrates the requirements of the flight path. Figure 31B shows the two cases encountered in practice. In each case only two turns are required.

3.3.4.3 Pilot Options

Flight paths required for automatic flights initiated by pilot options can be made to correspond to either

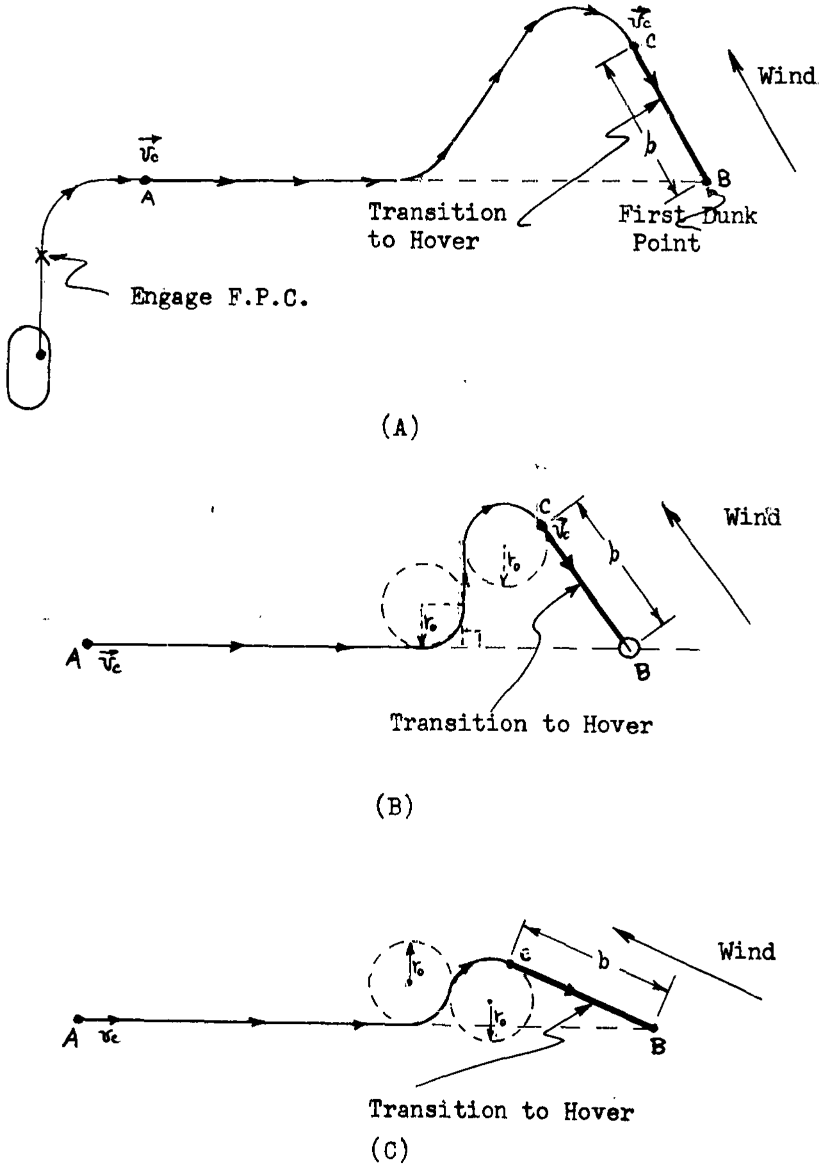
$\vec{v}_c$
C
Wind
b
$\vec{v}_c$
A
B
Transition to Hover
First Dunk Point
Engage F.P.C.
(A)
C
$\vec{v}_c$
Wind
b
r_o
r_o
A
$\vec{v}_c$
B
Transition to Hover
(B)
c
b
Wind
r_o
r_o
A
v_c
B
Transition to Hover
(C)

Figure 31
Base-To-First Dunk Point Flight Path

(3.3.4.1) or (3.3.4.2). If the option is initiated while the vehicle is in a hover, (3.3.4.1) will suffice. For exercising options while in the cruise mode, the initial FPC action will be to turn the vehicle toward the pilot-selected point, whereupon the scheme of (3.3.4.2) will be applicable.

3.3.4.4 Wind Computations

As can be seen from the foregoing discussions, the wind is a key factor in the specification of a flight path. It would be a gross oversimplification to assume that the wind would remain a constant in magnitude and direction throughout an entire ASW mission. However, this should be a reasonable assumption for any single dunk point-to-dunk point flight. At the start of the mission, the vehicle is essentially without information as to the wind magnitude and direction. This necessitates the manual takeoff at the start of the mission. During the straight flight toward the first dunk point, average values of the wind components are calculated and the rest of the base-to-first dunk point flight may then be calculated. While in hover at the first dunk point, the same wind values are used to compute the path to the second dunk point. On the straight segment of the flight toward the second dunk point, average wind values are computed to be used on the next dunk point-to-dunk point flight.

Obviously this is not the best way of treating the wind, yet several factors make it necessary. For the optimal flight path chosen, all calculations must be made at the start of the dunk point-to-dunk point flight, while the vehicle is in a hover. (This necessitates the assumption that the wind remains constant throughout the flight from one point to the next, but also introduces a certain amount of symmetry into the path, greatly reducing the number of computations required.) Since the vehicle's airspeed sensors do not function in a hover, the wind must be pre-calculated on the straight segment of flight toward the dunk point over which the flight path calculations will be made. Thus, the wind values unavoidably lag one flight segment behind.

Another ramification of this is that the vehicle may transition to hover along one calculated wind vector, yet leave the hover on another calculated wind vector. This should present no problem, since hovering turns of up to 24 deg/sec are permitted.

There is an alternative solution to this problem: all flights can be treated like the flight to the first dunk point. In this case, the vehicle would leave a hover on the same calculated wind vector on which it performed the transition to hover. It would then turn toward the next dunk point and, on the straight flight toward that point, calculate a new set of average wind values. Next, it would calculate the rest of the flight path to the next dunk point in the manner of Section (3.3.4.2.) using the newly calculated wind values. In general, this is a five-maneuver flight path: three turns and two straight flights. It would require more computation than the method of Section (3.3.4.1) and more complex implementation. The flight time, distance traveled, and fuel consumption would also increase.

The fact that any flight path chosen requires the prediction of the wind at the next dunk point makes the flight with the least number of maneuvers, (3.3.4.1), the best compromise.

The data required for the wind computations are: V_e^{EF} and V_n^{EF}, the groundspeed velocities; ψ, the heading or yaw angle; and V_{TAS}, the true airspeed.

The components of the instantaneous wind velocity (see Figure 32) are:

$$\Phi n = V_n^{EF} - V_{TAS} \cos \psi$$

$$\Phi e = V^{EF} - V_{TAS} \sin \psi$$

and $$|\Phi| = \sqrt{\Phi e^2 + \Phi n^2}$$

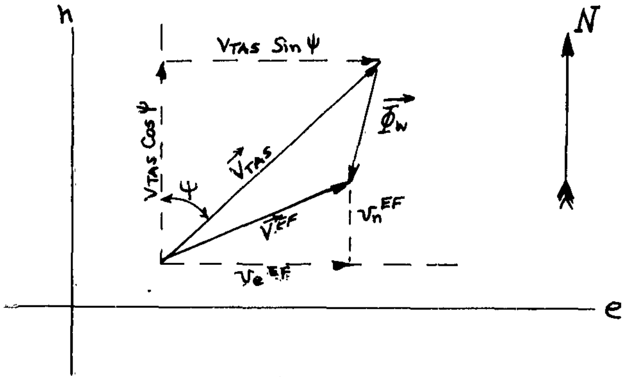
h
N
e
$V_{TAS}\sin\psi$
$V_{TAS}\cos\psi$
$\vec{V}_{TAS}$
$\vec{\Phi}_W$
ψ
$\vec{V}^{EF}$
V_n^{EF}
V_e^{EF}

Figure 32

Wind Computation Vector Diagram

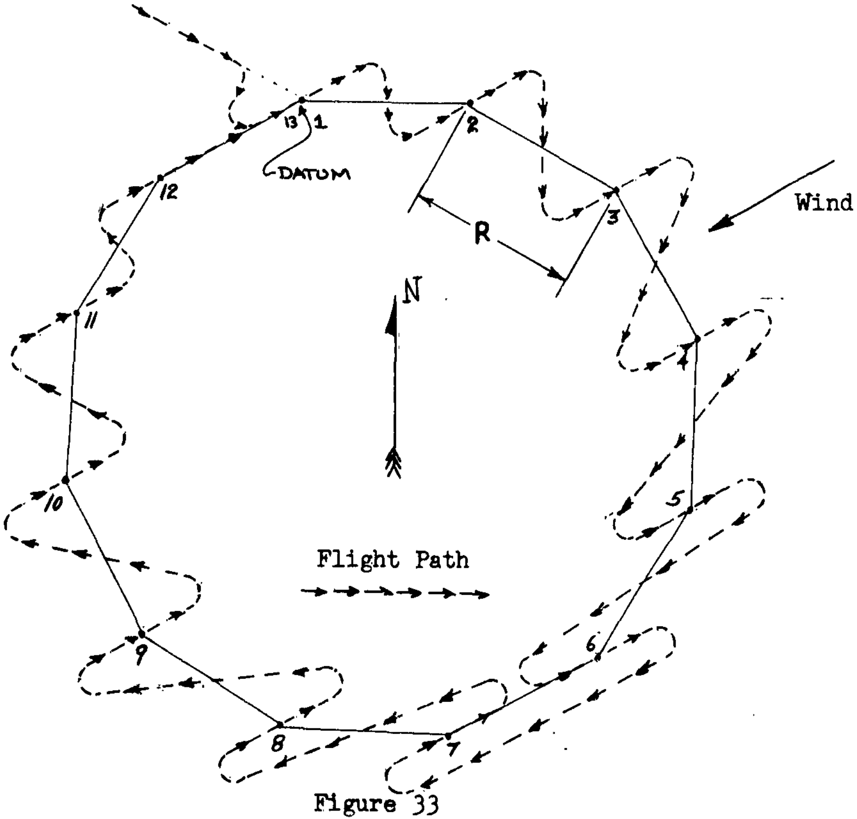
1
2
3
4
5
6
7
8
9
10
11
12
13
DATUM
R
N
Wind
Flight Path

Figure 33
Flight Test Dunk Pattern

If these quantities are computed k times, the average values are given by:

$$\bar{\Phi}_n = \frac{1}{K} \sum_{j=1}^{k} \Phi_{nj}$$

$$\Phi_e = \frac{1}{K} \sum_{j=1}^{k} \Phi_{ej}$$

Since the wind components are used for the purpose of generating the sine and consine of the wind angle, Φ_w, the average magnitude must be defined as:

$$|\bar{\Phi}| = \sqrt{\bar{\Phi}_e^{2} + \bar{\Phi}_n^{2}}$$

For a wind angle, Φ_w, measured clockwise from North:

$$\cos \Phi_w = \frac{\bar{\Phi}_n}{|\bar{\Phi}|} \qquad \text{sine } \Phi_w = \frac{\bar{\Phi}_e}{|\bar{\Phi}|}$$

3.3.4.5 Dunk Pattern for Flight Test Purposes

The pattern of Figure 33 was selected for flight test purposes. The range between dunk points, R, is a constant, 5000 yards or greater. If the prevailing winds throughout the mission remain in one general direction, this pattern should present the most varied set of wind conditions with respect to the bearing from each dunk point to the next, and should bring about all the variations in the flight path of Section (3.3.4.1); i.e. the four different sequences of turning maneuvers; CW-CCW, CCW-CW, CW-CW, and CCW-CCW.

3.3.5 Flight Path Calculations

All flight path calculations will be referenced to an earth-fixed east-north grid, whose origin is at some longitude and latitude, E_{orig}, N_{orig}.

3.3.5.1 Flight Test Dunk Pattern

Table 8 gives the necessary computations to generate the desired pattern about some datum point, (e_o, n_o).

TABLE 8

Dunk Point (k)	e_{dk}	n_{dk}
Datum	e_o	n_o
1	e_o	n_o
2	e_o+R	n_o
3	$e_o+1.86605R$	$n_o-0.5R$
4	$e_o+2.36605R$	$n_o-1.36605R$
5	$e_o+2.36605R$	$n_o-2.36605R$
6	$e_o+1.86605R$	$n_o-3.23210R$
7	e_o+R	$n_o-3.73210R$
8	e_o	$n_o-3.73210R$
9	$e_o-0.86605R$	$n_o-3.23210R$
10	$e_o-1.36605R$	$n_o-2.36605R$
11	$e_o-1.36605R$	$n_o-1.36605R$
12	$e_o-0.86605R$	$n_o-0.5R$
13	e_o	n_o

3.3.5.2 Dunk Point-to Dunk Point Flight Path

As will be shown in Section (3.3.6.1.1), knowledge of only four points is required to realize the flight path. (See Figure 34.) While the vehicle is hovering over dunk point e_{dk} it will most likely be drifting with the water current and will not be located at the calculated value of e_{dk}. Thus, the present position at the start of the calculations, (e_h, n_h) must be used. The point (e_a, n_a) which marks the end of the transition to cruise must be known, as well as the point (e_T, n_T) where the vehicle starts to turn toward the next dunk point. Finally, the coordinates of the next dunk point, $(e_{D_{k+1}}, n_{D_{k+1}}) = (e_D, n_D)$ must be obtained from Table 8.

The calculations for the two cases of Section (3.3.4.1) are greatly simplified if they are carried

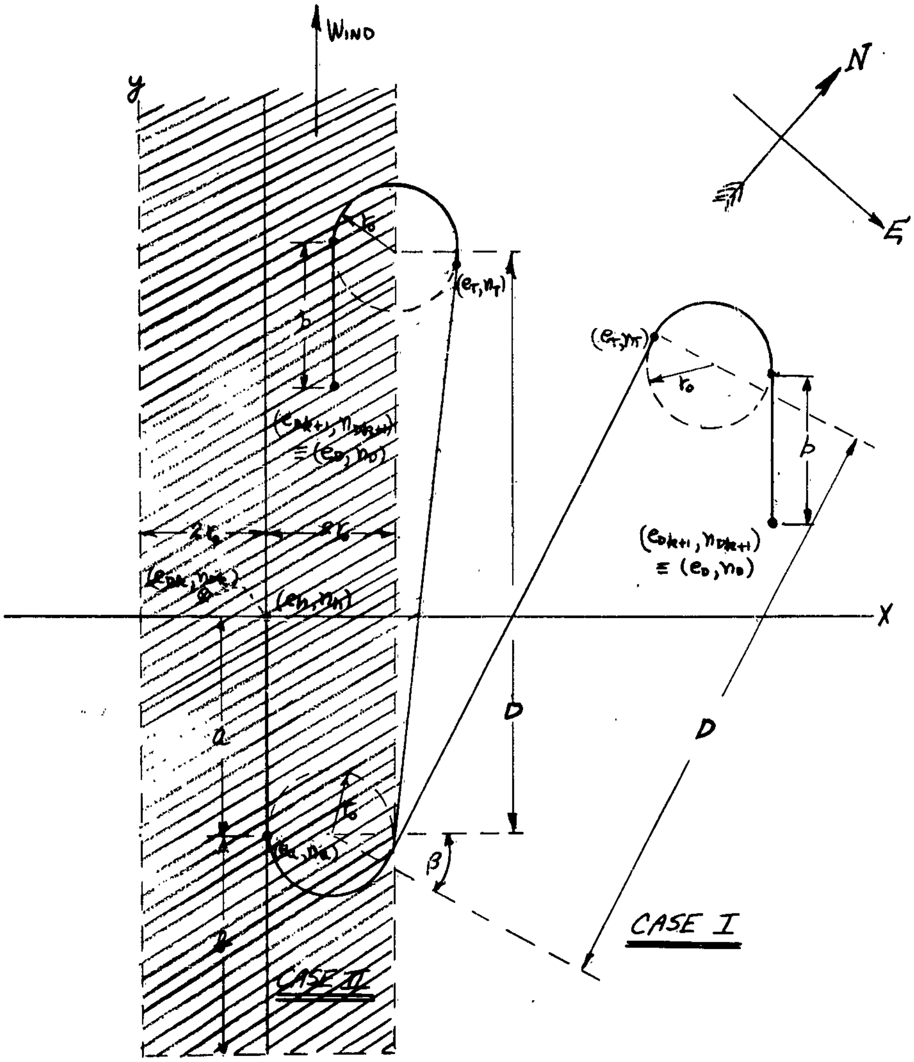
WIND
y
X
N
E
r_0
(e_T, n_T)
b
(e_{Dk+1}, n_{Dk+1})
$\equiv (e_D, n_D)$
$2r_0$
(e_{Dk}, n_{Dk})
(e_h, n_h)
a
D
β
CASE II
CASE I

Figure 34

Detail Diagram - Dunk Point-To-Dunk Point Flight Path out in an (x, y) coordinate system, centered on (e_h, n_h) with the y axis in the direction of the wind. (x, y) coordinates will use the same subscripts as the corresponding (e, n) coordinates. The computations are carried out in the following order:

(1) $x_D = (e_D - e_h) \cos \Phi_w - (n_D - n_h) \sin \Phi_w$

(2) $y_D = (e_D - e_h) \sin \Phi_w + (n_D - n_h) \cos \Phi_w$

Case I:

$|x_D| > 2\, r_o$, or $|x_D| \leqslant 2\, r_o$, $(y_D + a + b) < 0$

(3a) $D = \sqrt{\{|x_D| - 2\, r_o\}^2 + (y_D + a + b)^2}$

(4a) $x_T = \operatorname{sgn} x_D \left\{ (|x_D| - r_o) - \frac{2\, r_o^2}{D^2}(|x_D| - 2r_o) - \frac{r_o}{D^2}(y_D + a + b)\sqrt{D^2 - 4\, r_o^2} \right\}$

(5a) $y_T = (y_D + b) - \frac{2\, r_o^2}{D^2}(y_D + a + b) + \frac{r_o}{D^2}(|x_D| - 2\, r_o)\sqrt{D^2 - 4\, r_o^2}$

or

Case II:

$|x_D| \leqslant 2\, r_o$, $(y_D + a + b) > 0$

(3b) $D = \sqrt{|x_D|^2 + (y_D + a + b)^2}$

(4b) $x_T = \operatorname{sgn} x_D \left\{ (|x_D| - r_o) + \frac{r_o}{D}(y_D + a + b) \right\}$

(5b) $y_T = (y_D + b) - \frac{r_o}{D}|x_D|$

(6) $X_a = 0$

(7) $y_a = -a$

(8) $e_a = e_n - a \sin \Phi_W$

(9) $n_a = n_h - a \cos \Phi_W$

(10) $e_T = e_h + x_T \cos \Phi_W + y_T \sin \Phi_W$

(11) $n_T = n_h - x_T \sin \Phi_W + y_T \cos \Phi_W$

Equations (8) - (11), together with the determination of (e_h, n_h) from the navigation system and (e_D, n_D) from the dunk pattern computations, constitute the four required points.

3.3.5.3 Base-to-First Dunk Point Flight Path

Again knowledge of four points is requied to realize the flight path (See Figure 35) Point A of Figure 31, which will be called (e_i, n_i). (Actually, any point on the line $\overline{AB}$ will suffice, and the actual (e_i, n_i) used will be the present position of the vehicle on the line $\overline{AB}$ when the calculations are begun); the first dunk point $(e_{D1}, n_{D1}) = (e_D, n_D)$; and the points (e_s, n_s) and (e_T, n_T) of Figure 35.

The calculations for the cases of Section (3.3.4.2) are greatly simplified if they are carried out in an (x, y) coordinate system, centered on (e_D, n_D) with the y axis in the direction of line $\overrightarrow{AB}$ of Figure 31, or the direction $\overrightarrow{(e_D, n_D)\ (e_j, n_j)}$. (x, y) coordinates will use the same subscripts as the corresponding (e, n) coordinates. The computations will be carried out in the following order:

(1) $$a_1 = \frac{(e_i - e_D)}{\sqrt{(e_i - e_D)^2 + (n_i + n_D)^2}}$$

(2) $$a_2 = \frac{(n_i - n_D)}{\sqrt{(e_i - e_D)^2 + (n_i - n_D)^2}}$$

(3) $c_1 = a_1 \sin \Phi_W + a_2 \cos \Phi_W$

(4) $c_2 = a_2 \sin \Phi_W - a_1 \cos \Phi_W$

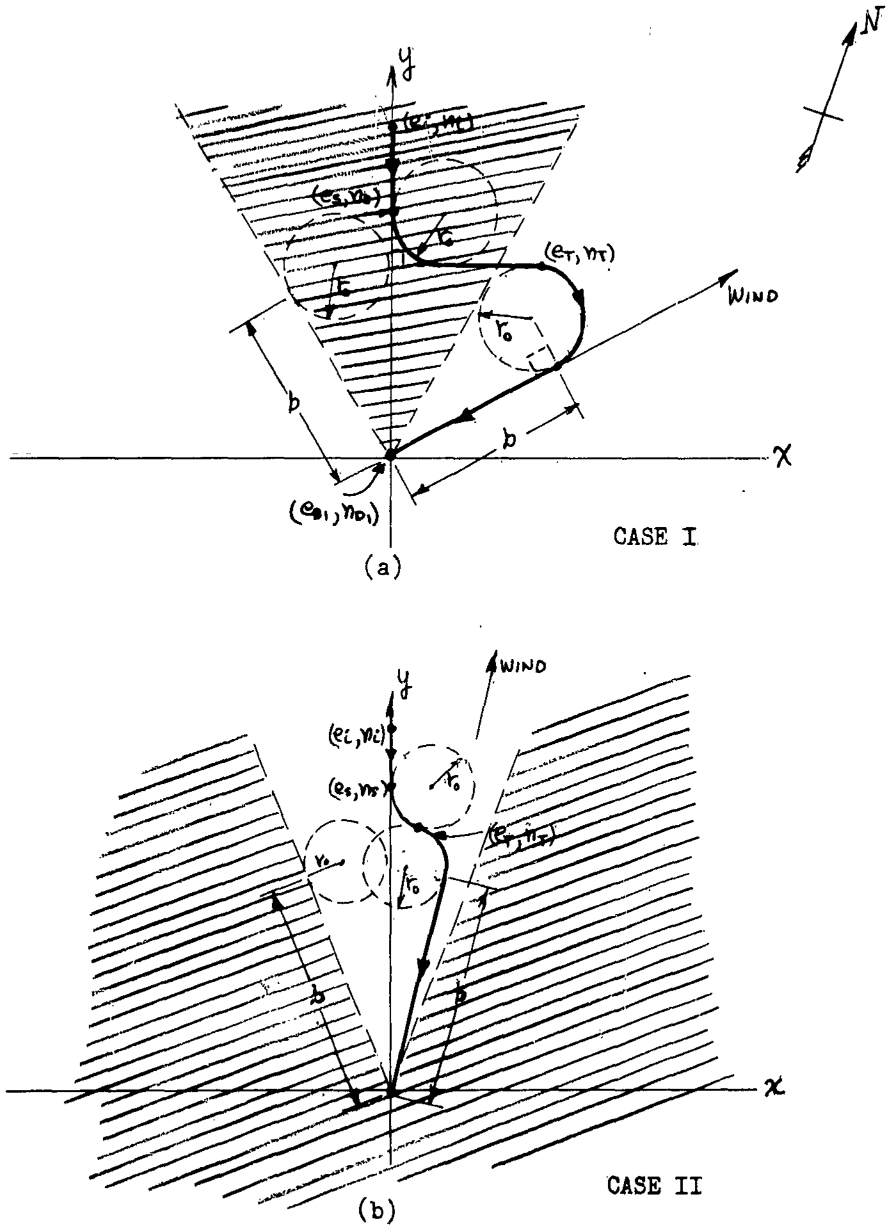
N
y
(e_i, n_i)
(e_s, n_s)
r_c
r_c
(e_T, n_T)
WIND
r_o
b
b
x
(e_{D1}, n_{D1})
CASE I
(a)
WIND
y
(e_i, n_i)
(e_s, n_s)
r_o
r_o
r_o
(e_T, n_T)
b
b
x
CASE II
(b)

Figure 35
Detail Diagram - Base-To-First Dunk Point Flight Path

Case I:

$$|c_2| \geqslant \frac{2br_o}{b^2+r_o^2}, \quad \underline{\text{or}} \quad |c_2| < \frac{2br_o}{b^2+r_o^2}, \quad c_1 < 0.$$

(5) $x_s = 0$

(6) $y_s = bc_1 + r_o(2 + |c_2|)$

(7) $x_T = \mathrm{sgn}\, c_2 \left\{ b|c_2| - r_o c_1 \right\}$

(8) $y_T = y_s - r_o$

or

Case II:

$$|c_2| < \frac{2br_o}{b^2+r_o^2}, \quad c_1 > 0$$

(9) $V = \mathrm{sgn}\, c_2 \left\{ b\, |c_2| - r_o c_1 \right\}$

(10) $W = bc_1 + r_o|c_2|$

(11) $x_s = 0$

(12) $y_s = w + \sqrt{4r_o^2 - \left\{ r_o - (\mathrm{sgn}\, c_2)V \right\}^2}$

(13) $x_T = \frac{1}{2}\, \mathrm{sgn}\, c_2 \left\{ b\, |c_2| + r_o(1-c_1) \right\}$

(14) $y_T = \frac{1}{2}\, (y_s + W)$

(15) $e_s = e_D + y_s a_1$

(16) $h_s = n_D + y_s a_2$

(17) $e_T = e_D + y_T a_1 + X_T a_2$

(18) $n_T = n_D + y_T a_2 - X_T a_1$

Equations (15) - (18), together with the value of (e_i, n_i) from the navigation system, and (e_{D1}, n_{D1}) from dunk pattern computations, constitute the four required points to realize the flight path.

3.3.5.4 Pilot Options

By substituting the pilot-selected point for (e_D, n_D), an optional flight, starting from either hover or cruise mode can be realized by use of the computations in Section (3.3.5.2) or (3.3.5.3). Note: If a negative number should appear under the radical sign in Section (3.3.5.2), Equation (3a), it means that there is not sufficient maneuvering room to realize the pattern (i.e. the two turn circles overlap), and that the dunk point must be rejected in favor of the next successive one. Also, the pattern for Section (3.3.5.3) must be calculated at a time when $y > y_s$, in order that the pattern may be realizable. Case II of Section (3.3.5.2) will always be realizable.

Derivations of the flight path equations appear in Appendix 5.3.1.

3.3.6 Flight Path Implementation

3.3.6.1 Command Sequences and Associated Computations

3.3.6.1.1 Sequence of Commands - Dunk Point-to-Dunk Point Flight Path

For the dunk point-to-dunk point flight path, the commands will be issued in the following order:

(a) Transistion to cruise; home on (e_a, n_a). Track to (e_a, n_a).

(b) Home on (e_T, n_T); track to (e_T, n_T).

(c) Home on (e_D, n_D); track to a distance b from (e_D, n_D).

(d) Transition to hover; home on (e_D, n_D); track to (e_D, n_D).

As a result of these commands:

1. The vehicle will accelerate to cruise velocity, V_c, and climb to cruise altitude, h_c. The homing command will keep the vehicle headed into

the calculated wind vector. Initial alignment with the wind vector will be accomplished by means of a hovering turn, using only the yaw channel. The tracking computation will mark the end of the transition.

2. The homing command will turn the vehicle to the proper heading to fly it to (e_T, n_T). If the heading error, Ψerr, is greater than 10 degrees, the command will result in a coordinated turn of radius r_o, terminating at the proper heading. If the heading error is less than 10 degrees, the vehicle will be yawed to the proper heading. The tracking computation will terminate the maneuver at (e_T, n_T).

3. The homing command will perform the same function as in (b). The tracking computation will terminate the maneuver at a distance b from (eD, nD).

4. The vehicle will decelerate to zero velocity (V_{hov}), and descend to hover altitude, h_{hov}). The homing command will trim out the coordinated (or yawed) turn of (c), heading the vehicle toward the dunk point (e_D, n_D); if the vehicle was on track at (e_T, n_T), the resulting heading should correspond to the calculated wind vector. Errors resulting from missing the calculated track at (e_T, n_T) will be discussed in Section (3.3.6.1.5).

3.3.6.1.2 Sequence of Commands - Base-to-First Dunk Point Flight Path

This mode of flight starts with the vehicle at cruise velocity and altitude. The order of commands is:

(a) Home on (e_D, n_D); track Ψerr to zero. (This places the vehicle on the line $\overline{AB}$ of Figure 2.)

(b) Calculate the flight path to (e_D, n_D).

(c) Home on (e_S, n_S); track to (e_S, n_S).

(d) Home on (e_T, n_T); track to (e_T, n_T).

(e) Home on (e_D, n_D); track to a distance b from (e_D, n_D).

(f) Transition to hover; home on (e_D, n_D); track to (e_D, n_D).

The results of commands (c) through (f) are discussed in the previous section.

3.3.6.1.3 Sequence of Commands - Pilot Options

For optional flights, initiated from hover or cruise, the methods of the previous two sections will be used, with the pilot-selected point substituted for (e_D, n_D).

3.3.6.1.4 Associated Computations

There are two computations associated with these commands; one is required for tracking to a point, and the other for the heading error. For tracking to a distance d from a point (e_j, n_j), the quantity T must be reduced to an arbitrarily small value, δ. T is defined as:

$$T = \sqrt{(e_p-e_j)^2 + (n_p-n_j)^2} = d,$$

where (e_p, n_p) are the present position corrdinates of the vehicle. The heading error, Ψerr, is defined by the equation:

$$\text{sine } \Psi err = g_1h_2 - g_2h_1$$

where:

$$g_1 = \frac{V_e}{\sqrt{V_e^2+V_n^2}}, \quad g2 = \frac{V_n}{\sqrt{V_e^2+V_n^2}}$$

and:

$$h_1 = \frac{(e_j-e_p)}{\sqrt{(e_j-e_p)^2 + (n_j-n_p)^2}}, \quad h2 = \frac{(n_j-n_e)}{\sqrt{(n_j-n_p)^2 + (e_j-e_p)^2}}$$

In the limit as Ψerr $\longrightarrow$ 0, sin Ψerr $\longrightarrow$ Ψerr $\longrightarrow$ 0. Again the actual tracking will be to some arbitrarily small value, δ. (The tracking of Ψerr is used only on the flight to the first dunk point, before wind values have been calculated. Although called a heading error, it is actually a bearing error, and satisfying the relationship Ψerr $\longrightarrow$ 0 will induce a crab angle in the vehicle. When the wind values are calculated and the system changes over to true heading commands, no transient heading commands should result, since the vehicle will still be traveling along line $\overline{AB}$ of Figure 31, and the analog circuitry will command the same crab angle as was previously flown.)

3.3.6.1.5 Flight Path Errors

Transitions to hover are always initiated at a distance b from the dunk point, while homing on the dunk point. Since b is the distance required for the transition, the position error at the dunk point should be negligible, amounting to the difference between the arc length of the final heading correction at the start of the transition and its chord. This correction will be a large radius (yawed) turn of less than 10 degrees in most cases, so that the difference between arc length and chord will be negligible.

The only error that need be considered is the angular deviation from the calculated wind vector at the dunk point. This error arises from two sources: passing through (e_T, n_T) on an incorrect heading, and the inability to hold to a constant turn radius, r_o. The analytical expression for the error is rather complex in form, and affords little insight to the magnitude of the error. However, with suitable assumptions and approximations, it is possible to develop simpler expression for the bounding value of the error. With reference to Figure 36, if the vehicle flies the correct track a-a' and turns with radius r_o, the wind error, $\Delta\Phi$, will be zero. However, if there is a heading error, ϕ, such that the vehicle flies the track c-c' to (e_T, n_T) and then turns with a radius $r \neq r_o$, there will be a wind error $\Delta\Phi$, such that, for small values of ϕ:

$$\Delta \Phi_{max} = \phi \frac{r_o}{b}$$

Since b will be greater than r_o, this will amount to a reduction of the original error at (e_T, n_T).

This simplified form carries one assumption with it. Let the wind be constant in direction only. During the flight toward (e_T, n_T) let the magnitude increase above its pre-calculated value. This will cause an error ϕ in the direction shown in Figure 36, and an associated error, $\Delta \Phi$. However, this stronger wind will tend to increase the turn radius to a value larger than r_o, and this will tend to diminish the error, $\Delta \Phi$. Hence, if we make the assumption that the primary source of error in the turn radius is the wind, then that portion of the error caused by ϕ, or the value of $\Delta \Phi$ max previously given.

The derivation of the error expression and its bounding value is presented in Appendix 5.3.2.

3.3.6.2 Definition of Maneuvers

3.3.6.2.1 Transition to Hover; Transition to Cruise

As a part of the programmed flight path, the vehicle is required to perform smooth transitions between the cruise mode at groundspeed V_c and altitude h_c, and the hover mode at zero groundspeed and altitude h_{hov}. The transition time, t_D, should be kept as small as possible. The transition distance should be repeatable for any particular set of parameters V_c, h_c, h_{hov}.

Both the transition to cruise and hover will be performed along the same altitude-velocity profile (Figure 37). The profile equation is:

$$h = h_{hov} + \frac{V}{V_c} (h_c - h_{hov})$$

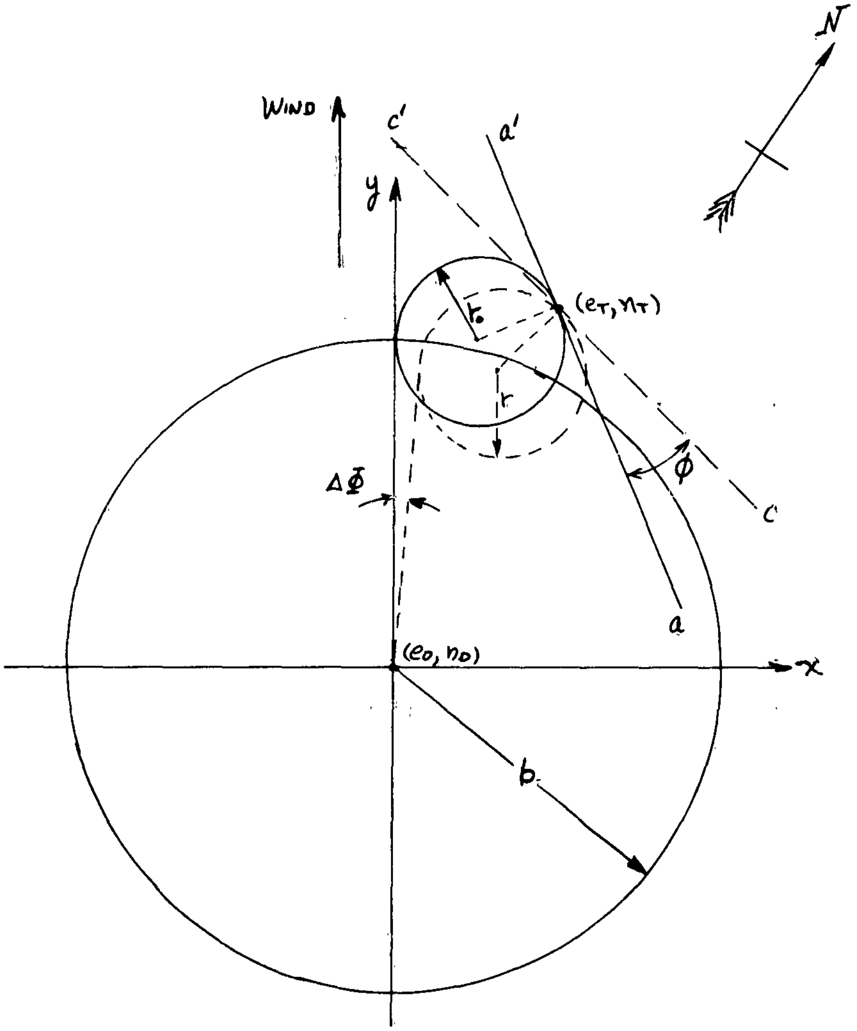
WIND
y
c'
a'
N
r₀
(e_T, n_T)
r
$\Delta\Phi$
ϕ
c
a
(e_0, n_0)
x
b

Figure 36

Flight Path Errors

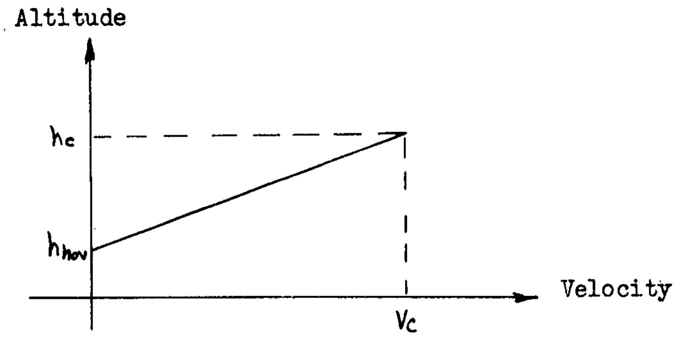

Figure 37

Transition Profile

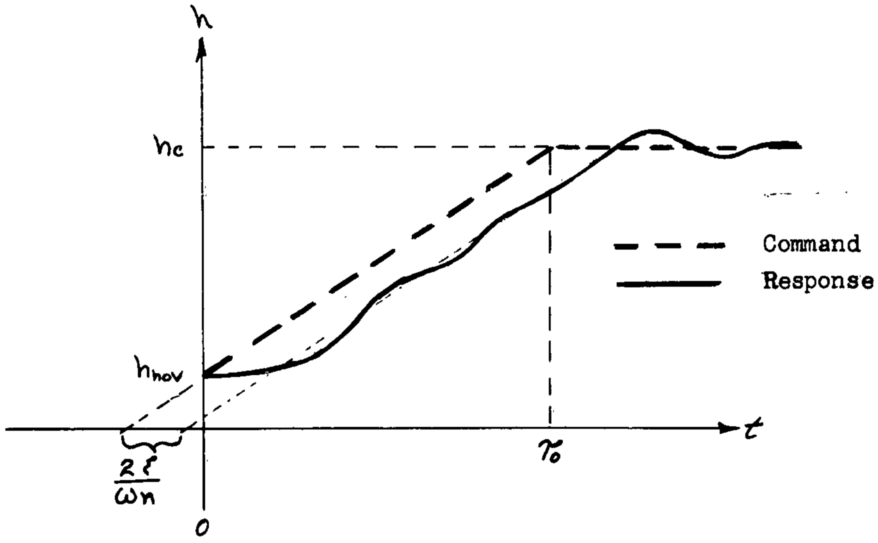

Figure 38

Altitude Channel Response to Transition Command

From this equation, it is apparent that the vertical velocity is proportional to the longitudinal acceleration; and that, for constant longitudinal acceleration, there is no vertical acceleration. For this profile, and for pitch angles of less than 10 degrees, the ground track longitudinal acceleration and velocity may be specified by a_x and V_x of the inertial measurement unit to within 2%.

Thus, the requirements for the transitions may be met by commanding a constant acceleration or deceleration, $\pm a_o$, as measured by the X accelerometer, as long as the velocity error is greater than some arbitrarily small value $V_{\varepsilon o}$ (≈ 5 knots). When the velocity error gets below $V_{\varepsilon o}$, the transition will be faded out by commanding an acceleration or deceleration proportional to the velocity error, V_ε. The altitude command would be slaved to the measured forward speed through analog circuitry, which would generate the profile equation. To be more specific, a transition to cruise would be initiated by command V_c. The initially large velocity error would effect a constant acceleration, a_o, until the velocity reaches ($V_c - V_{\varepsilon o}$), at which point the acceleration command would proportionally fade out ($a_{comm} = a_o \frac{V_\varepsilon}{V_{\varepsilon o}}$). The transition to hover would be initiated by commanding zero groundspeed (V_{hov}), and would be carried out at a constant deceleration, $-a_o$.

The time required for a transition of this type is:

$$t_D = V_c/a_o$$

and the transition distance is:

$$a = b = 1/2\ a_o\ t_D^2 = V_c^2/2a_o.$$

A nominal acceleration of $\pm$ 2 knots/sec was chosen for this system, since it results in a suitable range of transition times, distances, and vertical velocities:

VALUES FOR A TYPICAL ASW MISSION

a_o	V_c	h_c	h_{hov}	t_D	a = b	V_z
± Kt/sec	60 kt	200 ft	40 ft	30 sec	510 yds	320 fpm
± Kt/sec	80 kt	200 ft	40 ft	40 sec	900 yds	240 fpm
± Kt/sec	100 kt	200 ft	40 ft	50 sec	1410 yds	192 fpm

There are several advantages of this method of performing transitions. By controlling acceleration, it is possible to accurately predict both transition time and distance; this cannot be done in the existing ASE transition since only zero groundspeed and h_{hov} are commanded, and there is no attempt made to program the velocity vs. time; hence, the transition time and distance can be neither controlled nor predicted accurately. This method also eliminates the need of entering the transition to hover at a particular gate point (e.g. 60 knots and 150 feet). Finally, the acceleration may change much faster than either velocity or position. This allows a much tighter control loop, and greater position accuracy, since any acceleration errors must be integrated twice before they produce position errors.

This method is not exceptionally difficult to implement, since there are points in the ASE, into which it is convenient to put the necessary acceleration, velocity, and altitude commands. The ASE Basic Channels will be used to provide incremental dynamic stability about the slowly varying transition profile commands. Let us assume that, with the ASE functioning, the vehicle's altitude response may be represented by some equivalent second order transfer function:

$$H_{(S)} = H_{comm}(S) \frac{W_n^2}{s^2+2\zeta W_n S+W_n^2}$$

The transition profile altitude command is given by a ramp. For the purpose of mathematical simplicity let us assume that:

$$h_{comm}(t) \begin{cases} \frac{h_o}{\tau_o} & 0 \leq t \leq \tau_o \\ h_o & t \geqslant \tau_o \end{cases}$$

Therefore:

$$H_{comm}(s) = \frac{1}{s^2} \cdot \frac{h_o}{\tau_o}(1 - e^{-\tau_o s})$$

and:

$$H(s) = \frac{h_o}{\tau_o} \cdot \frac{1}{s^2} \cdot \frac{\omega_n^2}{s^2 + 2\xi\omega_n s + \omega_n^2}(1 - e^{-\tau_o s})$$

$$= \frac{h_o}{\tau_o} \cdot \frac{1}{s^2} \cdot \frac{\omega_n^2}{(s + \xi\omega_n)^2 + (\omega_n\sqrt{1-\xi^2})^2}$$

Thus:

$$h(t) = \frac{h_o}{\tau_o}\Big[\Big(t - \frac{2\xi}{\omega_n}$$

$$+ \frac{1}{\omega_n\sqrt{1-\xi^2}} e^{-\xi\omega_n t} \sin\Big\{\omega_n\sqrt{1-\xi^2}\,t - 2\tan^{-1}\Big(-\frac{\sqrt{1-\xi^2}}{\xi}\Big)\Big\}\Big)u(t)$$

$$- t - \tau_o - \frac{2\xi}{\omega_n}$$

$$+ \frac{1}{\omega_n\sqrt{1-\xi^2}} e^{-\xi\omega_n(t-\tau_o)} \sin\Big\{\omega_n\sqrt{1-\xi^2}(t-\tau_o) - 2\tan^{-1}\Big(-\frac{\sqrt{1-\xi^2}}{\xi}\Big)\Big\}\Big)u(t-\tau_o)\Big]$$

If we assume that the transient response dies out before t $= \tau_o$, then the response may be represented by Figure 38. For a well damped system, it consists primarily of a time lag of $\frac{2\zeta}{W_n}$ seconds in altitude.

3.3.6.2.2 Coordinated Turns

A coordinated turn is one in which all the resultant forces are in the direction of the vehicle Z axis. This condition is represented in Figure 39. For a coordinated turn:

(a) $T \sin \phi = M w^2 r_o = M V_c^2/r_o$

(b) $T \cos \phi = M_g$

(a) $\div$ (b) $\tan \phi = V_c^2/r_o g$

or:

$$r_o = V_c^2/g \tan \phi$$

In order to maintain a constant altitude, the lift force must be:

$$T = Mg \sqrt{1 + \tan^2 \phi}$$

Coordinated turns will be carried out by commanding a fixed roll angle, using the ASE Pitch and Collective Channels to maintain forward speed and altitude. Since the command for a coordinated turn results from a heading error (Yaw Channel), the roll angle command will be supplied through suitable Yaw-Roll crossfeed circuitry, which will command the fixed roll angle whenever the heading error is greater than 10 degrees, and zero roll angle at all other times. The heading error signal will produce an error signal in the Yaw Channel to assist in the turn. The Roll Channel Stick Trim circuitry may have to be modified to provide a smoother "roll-in" and "roll-out".

For this system, a roll angle of 26 degrees was chosen, resulting in the following values:

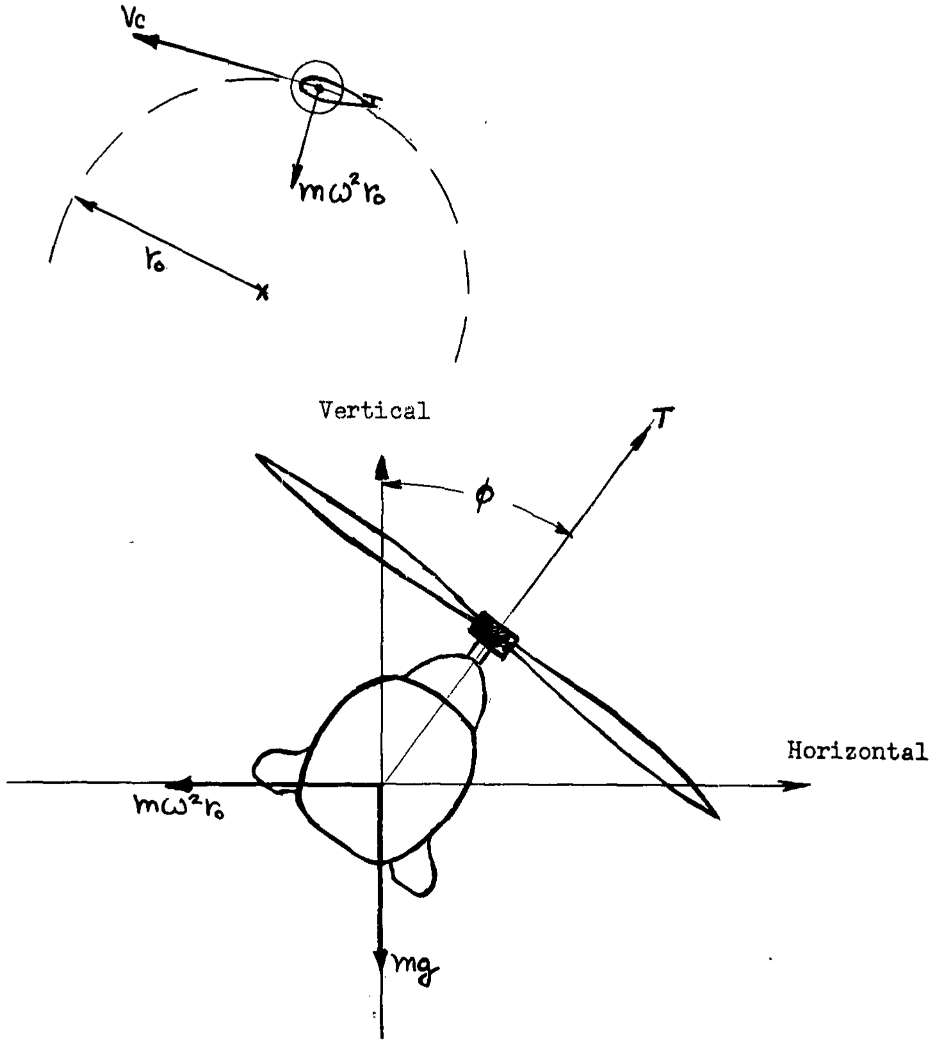
Vc
mω²r₀
r₀
Vertical
T
φ
Horizontal
mω²r₀
mg

Figure #39
Coordinated Turn Force Diagram

ϕ	V_c	r_o	(Turn Rate)
25 deg	60 knots	232 yds.	8.6 deg/sec
25 deg	80 knots	412 yds.	6.5 deg/sec
25 deg	100 knots	644 yds.	5.2 deg/sec

It was necessary that a substantially large roll angle be used. From Figure 34, Case I, we must have $D \geqslant 2r_o$ for the pattern to be realizable. Thus, there is some minimum value of R, the range between dunk points, which will produce this condition. If we consider the case when $D = 2r_o$ (the turn circles are tangent), then the distance between dunk points, ℓ, is given by the expression:

$$\ell = \sqrt{\left[2r_o(1+\cos\beta)\right]^2 + (a + b + 2r_o \sin\beta)^2}$$

$$\ell = \sqrt{(a + b)^2 + 4r_o(a + b)\sin\beta + 8r_o^2(1 + \cos\beta)}$$

and the maximum value of this expression is given by:

$$\ell_{\max} = \ell \bigg|_{\frac{\partial \ell}{\partial \beta} = 0} = \bigg|_{\tan\beta = \frac{a + b}{2r_o}}$$

or

$$\ell_{\max} = 2r_o\left[1 + \sqrt{1 + \left(\frac{a + b}{2r_o}\right)^2}\,\right]$$

For a cruise velocity of 100 knots, where $r_o = 644$ yards, and $a = b = 1410$ yards:

$$\ell_{\max} = 1288\ (1 + \sqrt{1 + (2820/1288)^2}\ ) = 4380 \text{ yards.}$$

Thus, a minimum distance of 4380 yards between dunk points is required to fly the pattern at 100 knots. Smaller roll angles would result in an increase of this distance. In order to provide an insurance factor (approximately 15%), the system will be restricted to patterns in which R is 5000 yards or greater.

It is apparent that, in the presence of a wind disturbance, this method is only an approximation to a coordinated turn which describes a circle of fixed radius, with respect to the ground. However, it appears that it will provide sufficient coordination and accuracy for this system. Roll angle, altitude, and groundspeed will be held constant at the expense of coordination and flight path accuracy; however, this appears to be the best approximate method with regard to accuracy, complexity, and necessary implementation.

Any proposed refinements of this method should be directed toward the generation of a "Turn Computer", which would provide simultaneous control of all five axes: pitch, roll, collective, yaw and power setting. This would of necessity be a complex system, requiring rather extensive implementation, as it must perform the following functions:

(a) Maintain $\left|\overrightarrow{V_c}\right|$ at desired value.

(b) Maintain $\left|\frac{d\overrightarrow{V_c}}{dt}\right|$ at desired value.

(c) Maintain $\frac{d\overrightarrow{V_c}}{dt} \times \overrightarrow{V_c} = 0$.

(d) Maintain h_c at desired value.

(e) Keep turn coordinated by commanding the appropriate interrelation of control parameters, such that the lateral (Y) accelerometer is maintained at a null.

This represents an exact method of implementing coordinated turns. Other approximate methods can be generated, but these in general require considerably more complexity and implementation than the method chosen, and they generally result in a tradeoff between accuracy of the flight path and coordination of the turn. They also require accurate knowledge of the instantaneous wind speed and direction. Rather than attempt any of these methods, the goal for a more sophisticated system should be the generation of a "Turn Computer".

3.3.6.2.3 The Homing Maneuver

The command to home on a point will be generated from a bearing command plus a crab angle correction. It will be a heading command referenced to the MA-1 Compass system. Calculation of the heading command, ψ_{comm}, is illustrated in Figure 40.

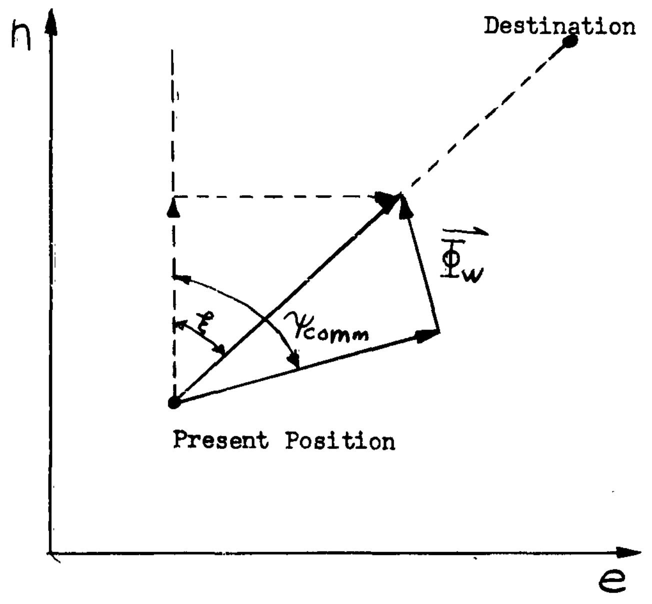
n
Destination
$\vec{\Phi}_w$
ξ
ψ_{comm}
Present Position
e

FIGURE 40

Heading Command Vector Diagram

Using the bearing to the target point, ξ, and the commanded cruise velocity, V_c, the computer generates the two quantities:

$$H_1 = V_c \cos\xi - \Phi_n$$
$$H_2 = V_c \sin\xi - \Phi_e$$

These signals will be passed through D/A converters and used to drive a servo-resolver to the shaft angle, ψ comm. The heading error signal generated by ψcomm and the MA-1 Compass will be used to actuate the Yaw-Roll crossfeed to provide the coordinated turn command, and the Yaw Channel for heading hold capabilities. Although it would be more desirable to use bearing commands, it was deemed more necessary to remove the computer from the feedback path of the dynamic control loop. Thus, the computer is used to generate a heading command rather than a bearing error. The computer is not used as the summing point for error signal generation; however, the only other vehicle instrument suitable for this application (the MA-1 Compass) is a heading indicator. Hence, the necessity of using heading commands. A more refined system would place the computer back in the feedback path by generating a bearing error from the bearing to the target point and the groundspeed velocities derived from the navigation section and removing the MA-1 compass. This will be implemented on the final system.

3.3.7 Flight Control Electronics

3.3.7.1 The Standard ASE Package

The basic building block of the FPC-1 Electronics package will be the Hamilton Standard ASE (Ref. SK 52213). It is a four-axis unit (pitch, roll, yaw, collective) with basic channels for dynamic stability control, and coupler channels for such functions as heading hold, forward speed and drift speed control, altitude hold, automatic transition to hover, and a cable angle and altitude mode for sonar dipping. Briefly, the ASE operates as follows:

3.3.7.1.1 Pitch Channel Operation

Automatic attitude stabilization is maintained in the pitch attitude at all times after pressing the ASE engage button on the ASE control panel. When the vehicle is displaced from its normal flight attitude,

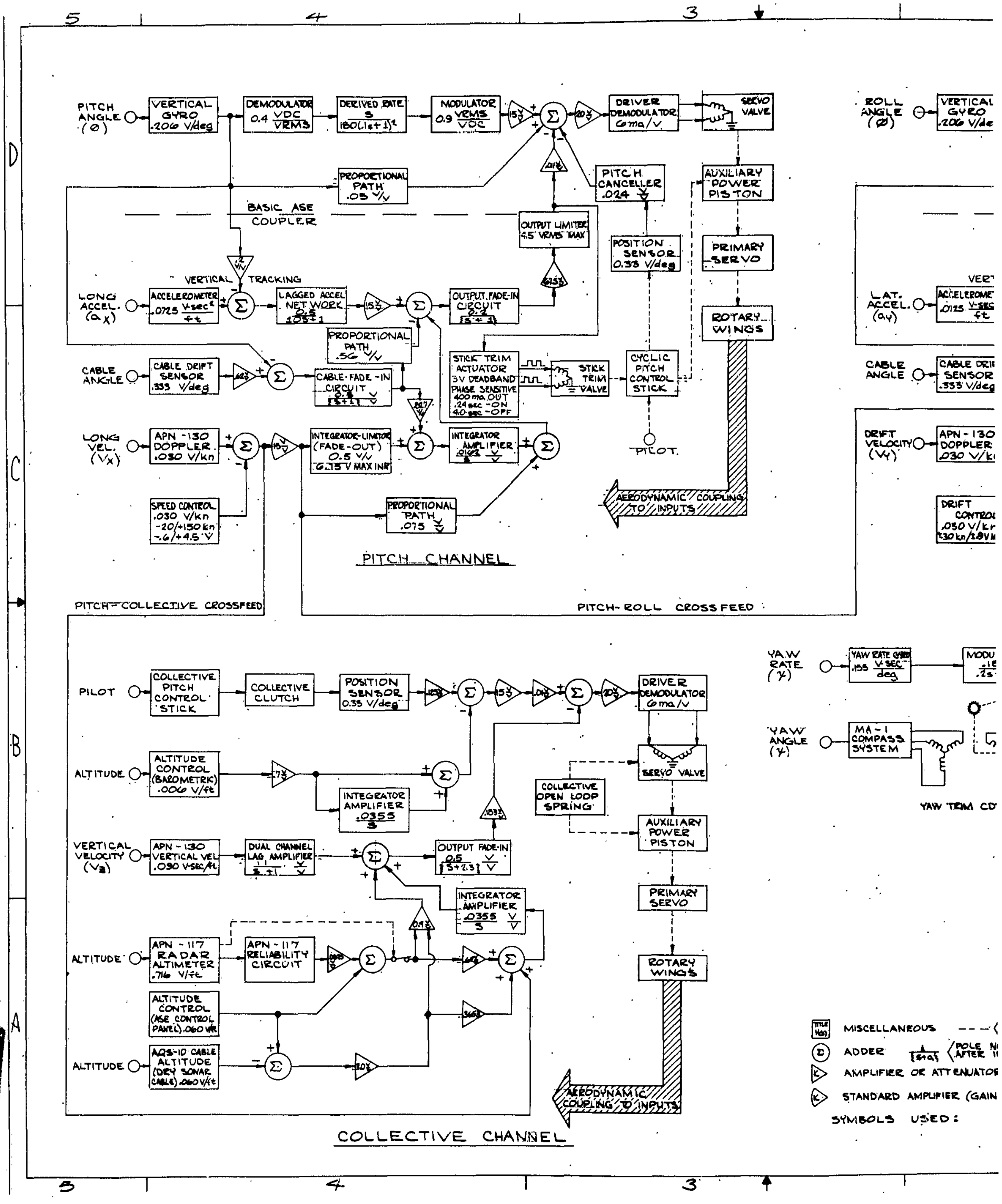

5
4
3
D
C
B
A
PITCH ANGLE (θ)
VERTICAL GYRO .206 V/deg
DEMODULATOR 0.4 VDC/VRMS
DERIVED RATE S/180(.1s+1)²
MODULATOR 0.9 VRMS/VDC
15%
20%
DRIVER DEMODULATOR 6 ma/V
SERVO VALVE
AUXILIARY POWER PISTON
PRIMARY SERVO
ROTARY WINGS
PROPORTIONAL PATH .05 V/V
.01%
PITCH CANCELLER .024 V/V
BASIC ASE COUPLER
OUTPUT LIMITER 4.5 VRMS MAX
POSITION SENSOR 0.33 V/deg
VERTICAL TRACKING
LONG ACCEL. (ax)
ACCELEROMETER .0725 V-sec²/ft
LAGGED ACCEL NETWORK 0.5/10S+1
15%
OUTPUT FADE-IN CIRCUIT 0.2/(S+1)
.0725
PROPORTIONAL PATH .56 V/V
CABLE ANGLE
CABLE DRIFT SENSOR .333 V/deg
.623
CABLE FADE-IN CIRCUIT 0.5/(S+1) V/V
.827 V/V
STICK TRIM ACTUATOR 3V DEADBAND PHASE SENSITIVE 400 ma OUT .24 sec - ON 4.0 sec - OFF
STICK TRIM VALVE
CYCLIC PITCH CONTROL STICK
PILOT
LONG VEL. (Vx)
APN-130 DOPPLER .030 V/kn
15%
INTEGRATOR-LIMITER (FADE-OUT) 0.5 V/V 6.75 V MAX INP
INTEGRATOR AMPLIFIER .0163/S V/V
SPEED CONTROL .030 V/kn -20/+150 kn -.6/+4.5 V
PROPORTIONAL PATH .075 V/V
AERODYNAMIC COUPLING TO INPUTS
PITCH CHANNEL
PITCH-COLLECTIVE CROSSFEED
PITCH-ROLL CROSSFEED
ROLL ANGLE (Ø)
VERTICAL GYRO .206 V/de
LAT. ACCEL. (ay)
ACCELEROME .0125 V-SEC/ft
CABLE ANGLE
CABLE DRI SENSOR .333 V/deg
DRIFT VELOCITY (Vy)
APN-130 DOPPLER .030 V/k
DRIFT CONTROL .030 V/kn 30 kn/±.9V
YAW RATE (ψ)
YAW RATE GYRO .155 V-SEC/deg
MODU
YAW ANGLE (ψ)
MA-1 COMPASS SYSTEM
YAW TRIM CO
PILOT
COLLECTIVE PITCH CONTROL STICK
COLLECTIVE CLUTCH
POSITION SENSOR 0.33 V/deg
.125
15%
.01%
20%
DRIVER DEMODULATOR 6 ma/V
SERVO VALVE
COLLECTIVE OPEN LOOP SPRING
AUXILIARY POWER PISTON
PRIMARY SERVO
ROTARY WINGS
ALTITUDE
ALTITUDE CONTROL (BAROMETRIC) .006 V/ft
.7%
INTEGRATOR AMPLIFIER .0355/S
.033
VERTICAL VELOCITY (Vz)
APN-130 VERTICAL VEL .090 V-sec/ft
DUAL CHANNEL LAG AMPLIFIER 1/(S+1) V/V
OUTPUT FADE-IN 0.5/(S+2.3) V/V
INTEGRATOR AMPLIFIER .0355/S V/V
0.1%
ALTITUDE
APN-117 RADAR ALTIMETER .716 V/ft
APN-117 RELIABILITY CIRCUIT
.08
.46
ALTITUDE CONTROL (ASE CONTROL PANEL) .060 V/ft
.46
ALTITUDE
AQS-10 CABLE ALTITUDE (DRY SONAR CABLE) .060 V/ft
.10%
AERODYNAMIC COUPLING TO INPUTS
COLLECTIVE CHANNEL
MISCELLANEOUS
ADDER
1/(τs+1) (POLE N AFTER
AMPLIFIER OR ATTENUATOR
STANDARD AMPLIFIER (GAIN
SYMBOLS USED:

1

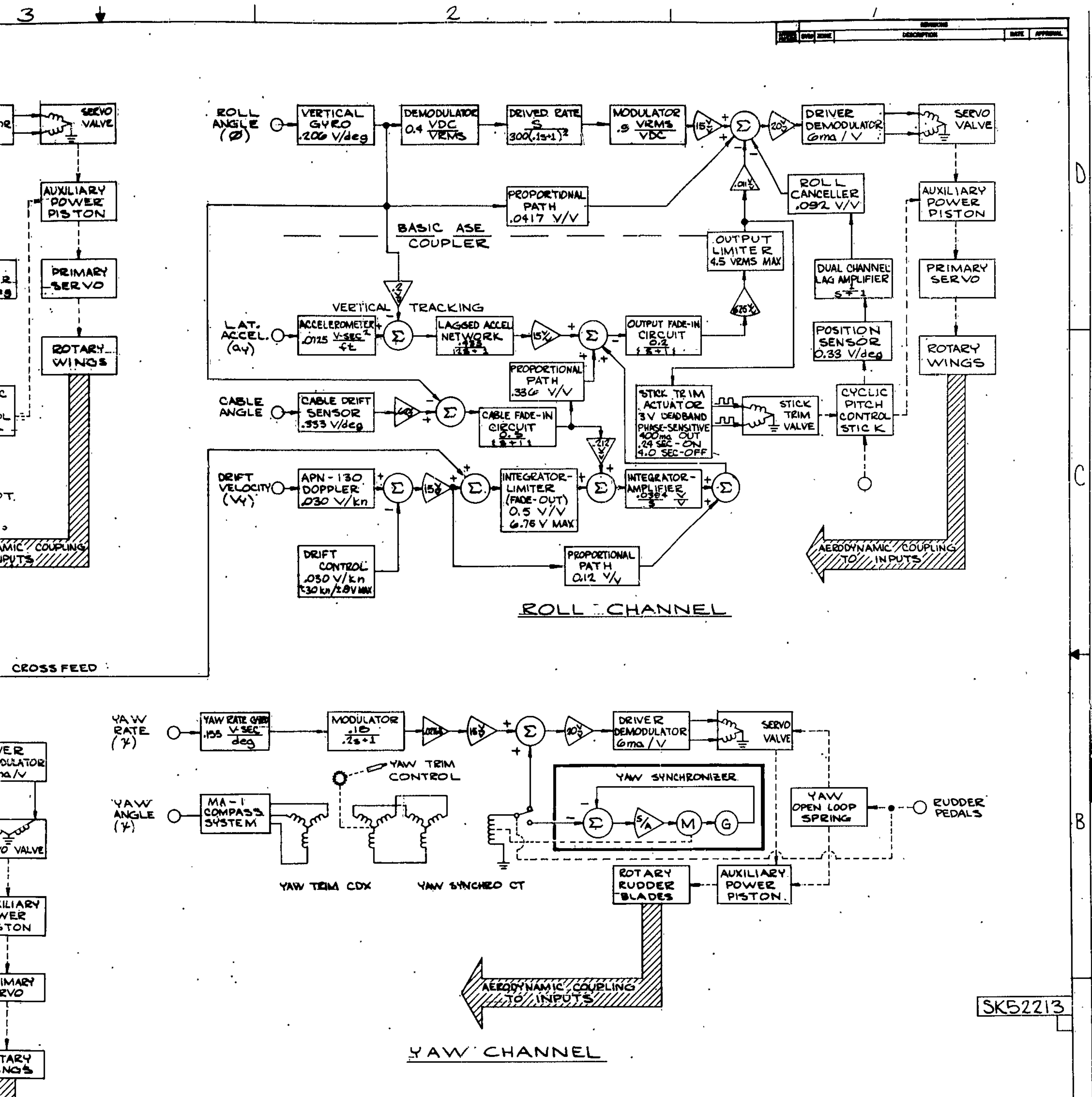
ROLL ANGLE (Ø)
VERTICAL GYRO .206 V/deg
DEMODULATOR 0.4 VDC/VRMS
DRIVED RATE S/300(.1s+1)²
MODULATOR .5 VRMS/VDC
15
20
DRIVER DEMODULATOR 6ma / V
SERVO VALVE
PROPORTIONAL PATH .0417 V/V
.011
ROLL CANCELLER .092 V/V
AUXILIARY POWER PISTON
BASIC ASE COUPLER
OUTPUT LIMITER 4.5 VRMS MAX
DUAL CHANNEL LAG AMPLIFIER 1/s+1
PRIMARY SERVO
.625
POSITION SENSOR 0.33 V/deg
ROTARY WINGS
VERTICAL TRACKING
LAT. ACCEL. (ay)
ACCELEROMETER .0125 V-sec²/ft
LAGGED ACCEL NETWORK .425/.12s+1
15
OUTPUT FADE-IN CIRCUIT 0.2/s+1
PROPORTIONAL PATH .336 V/V
STICK TRIM ACTUATOR 3 V DEADBAND PHASE-SENSITIVE 400ma OUT .24 SEC - ON 4.0 SEC - OFF
STICK TRIM VALVE
CYCLIC PITCH CONTROL STICK
CABLE ANGLE
CABLE DRIFT SENSOR .333 V/deg
CABLE FADE-IN CIRCUIT 0.5/s+1
.212
DRIFT VELOCITY (Vd)
APN-130 DOPPLER .030 V/kn
15
INTEGRATOR-LIMITER (FADE-OUT) 0.5 V/V 6.76 V MAX
INTEGRATOR-AMPLIFIER .0384/s V/V
DRIFT CONTROL .030 V/kn ±30 kn/±.8V MAX
PROPORTIONAL PATH 0.12 V/V
AERODYNAMIC COUPLING TO INPUTS
ROLL CHANNEL
CROSS FEED
YAW RATE (ψ)
YAW RATE GYRO .155 V-SEC/deg
MODULATOR .18/.2s+1
15
20
DRIVER DEMODULATOR 6ma / V
SERVO VALVE
YAW TRIM CONTROL
YAW ANGLE (ψ)
MA-1 COMPASS SYSTEM
YAW SYNCHRONIZER
5/A
M
G
YAW OPEN LOOP SPRING
RUDDER PEDALS
YAW TRIM CDX
YAW SYNCHRO CT
ROTARY RUDDER BLADES
AUXILIARY POWER PISTON
AERODYNAMIC COUPLING TO INPUTS
YAW CHANNEL
SERVO VALVE
AUXILIARY POWER PISTON
PRIMARY SERVO
ROTARY WINGS
AERODYNAMIC COUPLING INPUTS
3
2
1
D
C
B
A
SK52213
2

SYMBOLS USED:

TITLE HDR MISCELLANEOUS

Σ ADDER

▷K AMPLIFIER OR ATTENUATOR (GAIN = K)

▷K STANDARD AMPLIFIER (GAIN = K)

– – – (MECHANICAL CONNECTION

$\frac{1}{\tau s + 1}$ (POLE NON-EXISTENT AFTER INITIAL FADE-IN

NOTES:

1- REF SK52214 FOR FPC-1 MODIFIED ASE BLOCK DIAGRAM.

UNLESS OTHERWISE SPECIFIED:

DIMENSIONS ± ~ ANGLES ± ~ BREAK EDGES .005-.015 FILLET RAD ~ – ~ SURFACES HAVING A COMMON AXIS CONCENTRIC WITHIN ~ TIR. CLEANING, PRESERVATION AND HANDLING PER HS1500-C ~

DIMENSIONS SHOWN ARE AFTER PLATING & SIMILAR PROCESSES & BEFORE PAINTING. THREADS PER MIL-S-7742. DRAWING INTERPRETATION PER HS1300. SURFACE CHARACTERISTICS: MIL-STD-10 PER HS1000. △ MARK PART IDENTIFICATION: MIL-STD-130 PER HS333.

NEXT ASSY	USED ON
APPLICATION	

		APPROVALS		DATE
MATERIAL	~	DRAWN		
		CHECKED		
		DRAFTING		
		DESIGN		
HARDNESS	~	MATERIALS		
HEAT TREAT SPEC	~	PROJECT		
		COST		
		FACTORY		
SURFACE COATING	~	RELEASE		DATE
MFG SPEC	~	EXPERIMENTAL		
		PRELIM PROD.		
		PRODUCTION		
MAKE FROM	~	PROD. CODE		

Hamilton Standard
WINDSOR LOCKS, CONNECTICUT • U.S.A.

STANDARD ASE
BLOCK DIAGRAM

CODE IDENT NO. 73030
CONTRACT NO.
SIZE J
SK52213
SCALE: NONE
WEIGHT: LB
SHEET

3-30220-002 1 NOW 62-0873-D FPC-1

the vertical gyro feeds a signal proportional to the fuselage attitude with reference to the horizon into the pitch ASE amplifier module contained in the amplifier. Within the pitch ASE amplifier module, this proportional signal is fed in parallel paths. One path is a straight proportional feed-through and the other is fed to a derived rate network. The purpose of the derived rate network is to determine the rate at which the vehicle has been displaced. At the output of the derived rate network, the proportional feed-through and derived rate signals are mixed and compared to the proportional signal developed by the position sensor. The position sensor is phased oppositely to the vertical gyro signal and will cancel the vertical gyro signal when the vehicle is at the selected attitude as reflected by the position of the cyclic pitch control stick. The resultant rate plus proportional signal is the attitude error signal. This attitude error signal is amplified and demodulated to provide an output to excite a solenoid of the pitch servo valve. As the servo valve corrects the attitude error through the auxiliary power piston, primary servo, and rotary wings, the attitude error signal diminishes. When the vehicle is repositioned to its original attitude, the vertical gyro output signal is returned to its original value.

While ASE is engaged, the coupler may be engaged by pressing the CPLR engage button on the ASE control panel. During coupler operation of the pitch channel, one of two modes may be used, doppler or cable angle. During the doppler mode, the coupler will seek and retain selected fore-and-aft speeds during automatic cruise flight and automatic transition from forward flight to a hover over the sonar transducer. This is accomplished by placing the CYC CPLR switch on the ASE control panel in the DOPP position. During this mode, the pitch (velocity heading) actual ground speed signal from the radar navigation set is compared with the selected signal established by the SPEED control on the ASE control panel. Any difference between these signals is the error signal. This error signal is fed to the pitch coupler integrator module as the proportional doppler error signal. Therefore, this error signal represents the proportion that the vehicle has been displaced from its preselected groundspeed. The proportional doppler error signal splits and a portion is fed through the integrator limiter circuit to the integrator amplifier circuit to provide the system with zero steady state error. The integral signal output of the integrator amplifier circuit is added to the other portion of proportional doppler error signal, and the resultant proportional doppler error plus integral signal is transformer coupled to an output fade-in and amplifier-limiter circuit in the pitch coupler amplifier module. During the doppler mode, an accelerometer develops a signal proportional to the acceleration of the vehicle. Prior to the output fade-in and amplifier-limiter circuit, the output signal from the accelerometer is added to the proportional doppler error plus integral signal, providing a large correction signal proportional to acceleration. The output fade-in circuit provides for a smooth initial build-up of the signal to avoid any abrupt vehicle jump due to possible large existing errors when the coupler is engaged. The signal from the output fade-in circuits is coupled to a standard amplifier and output limiter circuit. This circuit amplifies and limits the output signal to a level approximately 3/4 the total authority of ASE. The coupler output attitude error signal is coupled to a stick trim actuator circuit which excites a solenoid of the pitch stick trim valve to automatically reposition the cyclic pitch control stick, extending the authority of the pitch channel. The coupler output attitude error signal is also coupled to the pitch ASE amplifier module. In the ASE amplifier module, the coupler attitude limiter circuit, the output signal from the accelerometer error signal is processed in a similar manner as the basic ASE attitude error signal.

During the cable angle mode, the coupler will maintain the sonar cable perpendicular to the horizon. This is accomplished by placing the CYC.CPLR switch on the ASE control panel in the CABLE ANGLE position. During this mode, the sonar detecting-ranging set develops a signal which is proportional to the angle of the sonar cable, relative to the floor of the vehicle. This signal is compared with the vertical gyro signal in the pitch coupler integrator module. Any difference between these signals is the error signal. This error signal is fed to the pitch coupler integrator module as a proportional cable angle error signal. Therefore, this error signal represents the proportion that the sonar cable has been displaced from true vertical.

The proportional cable angle error signal is processed in a similar manner as the proportional doppler error signal, including the operation of the integrator amplifier accelerometer and stick trim actuator circuits.

3.3.7.1.2 Roll Channel Operation

Automatic attitude stabilization is maintained in the roll attitude at all times after pressing the ASE engage button on the ASE control panel. When the vehicle is displaced from its normal flight attitude, the vertical reference feeds a signal proportional to the fuselage attitude with reference to the horizon into the roll ASE amplifier module contained in the amplifier. Within the roll ASE amplifier module, this proportional signal is fed in parallel paths. One path is a straight proportional feed-through and the other is fed to a derived rate network. The purpose of the derived rate network is to determine the rate at which the vehicle has been displaced. At the output of the derived rate network, the proportional feed-through and derived rate signals are mixed, and compared to the proportional signal developed by the position sensor. The proportional signal developed by the position sensor is lagged approximately one second in the dual channel lag amplifier. The position sensor signal is phased oppositely to the vertical reference signal and will cancel the vertical gyro signal when the vehicle is at the selected attitude as reflected by the position of the cyclic pitch control stick. The resultant rate plus proportional signal is the attitude error signal. This attitude error signal is amplified and demodulated to provide an output to excite a solenoid of the roll servo valve. As the servo valve corrects the attitude error through the auxiliary power piston, primary servo, and rotary wings, the attitude error signal diminishes. When the vehicle is repositioned to its original attitude, the vertical gyro output signal is returned to its original value. While ASE is engaged, the coupler may be engaged by pressing the CPLR engage button on the ASE control panel. During coupler operation of the roll channel, one of two modes may be used, doppler or cable angle. During the doppler mode, the coupler will seek and retain selected lateral drift speeds during automatic cruise flight and automatic transition from forward flight to a hover over the sonar transducer. Thisis accomplished by placing the CYC CPLR switch on the ASE control panel in the DOPP position. During this mode, the roll (velocity drift) actual ground drift signal from the radar navigation set is compared with the selected signal established by the DRIFT control on the ASE control panel. Any difference between these signals is the error signal. This error signal is fed to the roll coupler integrator module as the proportional doppler error signal. Therefore, this error signal represents the proportion that the vehicle has been displaced from its preselected ground drift. The proportional doppler error signal splits and a portion is fed through the integrator limiter circuit to the integrator amplifier circuit to provide the system with zero steady state error. The integral signal output of the integrator amplifier circuit is added to the other portion of proportional doppler error signal, and the resultant proportional doppler error plus integral signal is transformer coupled to an output fade-in and amplifier-limiter circuit in the roll coupler amplifier module. During the doppler mode, an accelerometer develops a signal proportional to the acceleration of the vehicle. Prior to the output fade-in and amplifier-limiter circuit, the output signal from the accelerometer is added to the proportional doppler error plus integral signal, providing a large correction signal proportional to acceleration. The output fade-in circuit provides for a smooth initial build-up of the signal to avoid any abrupt vehicle jump due to possible large existing errors when the coupler is engaged. The signal from the output fade-in circuit is coupled to a standard amplifier and output limiter circuit. This circuit amplifies and limits the output signal to a level approximately 3/4 the total authority of ASE. The coupler output attitude error signal is coupled to ~~a~~ stick trim actuator circuit which excites a solenoid of the roll stick trim valve to automatically reposition the cyclic pitch control stick to extend the authority of the roll channel. The coupler output attitude error signal is also coupled to the roll ASE amplifier modules. In the ASE amplifier module, the coupler attitude error signal is processed in a similar manner as the basic ASE attitude error signal.

During the cable angle mode, the coupler will maintain the sonar cable perpendicular to the horizon. This is accomplished by placing the CYC CPLR switch on the ASE control panel in the CABLE ANGLE position. During this mode, the sonar detecting-ranging set develops a signal which is proportional to the angle of the sonar cable. relative to the floor of the vehicle. This signal is compared with the vertical reference signal in the roll coupler integrator module. Any difference between these signals is the error signal. This error signal is fed to the roll coupler integrator module as a proportional cable angle error signal. Therefore, this error signal represents the proportion that the sonar cable has been displaced from true vertical. The proportional cable angle error signal is processed in a similar manner as the proportional doppler error signal, including the operation of the integrator amplifier, accelerometer, and stick trim actuator circuits.

3.3.7.1.3 Collective Channel Operation

While ASE is engaged, the collective channel may be engaged by pressing the BAR ALT engage button on the ASE control panel to stabilize the altitude of the vehicle. When the vehicle is displaced from its normal flight altitude, the barometric altitude control feeds a signal proportional to the new altitude into the collective ASE amplifier module contained in the amplifier. Within the collective ASE amplifier module, this proportional altitude error signal is amplified and demodulated, to provide an output to excite a solenoid of the collective servo valve. As the servo valve corrects the altitude error signal through the auxiliary power piston, primary servo, and rotary wings, the altitude error signal diminishes. When the vehicle is repositioned to its original altitude, the altitude control output signal is returned to its original value. However, as the servo valve corrects the altitude error signal, it places the collective servo system in an open-loop condition. The open-loop condition extends the authority of the collective channel by limiting the mechanical feed-back of the collective servo valve to resultantly reposition the collective pitch control stick. During open-loop operation, the position sensor produces a proportional signal to dampen the collective pitch control stick movement. The pilot may still override the open-loop operation by applying an opposing force on the collective pitch control stick. As the altitude error signal diminishes, the position sensor proportional signal will return the collective pitch control stick to the engage altitude position. While BAR ALT is engaged, and the pilot uses the collective pitch control stick and the BAR REL switch to change altitude, the collective clutch nulls the output of the position sensor.

While BAR ALT is engaged, the coupler may be engaged by pressing the CPLR engage button on the ASE control panel. During coupler operation of the collective channel, one of two modes may be used, radar altitude or cable altitude. During the radar altitude mode, the coupler will seek and retain the selected altitude. This is accomplished by placing the ALT CPLR switch on the ASE control panel in the RDR ALT position. During this mode, the proportional radar altitude signal from the radar altimeter is compared with the signal from the ALTITUDE control on the ASE control panel. Any difference between these signals is the error signal. This error signal is fed to the collective coupler module as the proportional radar altitude error signal. Therefore, this error signal represents the proportion that the vehicle has been displaced from its preselected altitude. The proportional radar altitude error signal splits and a portion is fed to the integrator amplifier circuit. The integral signal output of the integrator amplifier circuit is added to the other portion of the proportional radar altitude error signal. The resultant proportional radar altitude error signal, and the resultant proportional radar altitude error plus integral signal is transformer coupled to an output fade-in circuit. The radar navigation set produces a signal (vertical velocity) proportional to the rate of change in altitude. This rate signal is lagged approximately one second in the dual channel lag amplifier, and transformer coupled to the output fade-in circuit. The coupler rate plus proportional altitude error signal output of the fade-in circuit is coupled to the collective ASE amplifier module and processed in a similar manner as the basic ASE altitude error signal. During the cable altitude mode, the coupler will maintain the vehicle at the selected altitude over the water. This is accomplished by placing the ALT CPLR switch on the ASE control panel in the CABLE ALT position. During this mode, the proportional cable altitude signal from the sonar detecting-ranging set is compared with the signal from the ALTITUDE control on the ASE control panel. Any difference between these signals is the error signal. This signal is fed to the collective coupler module as the proportional cable altitude error signal. Therefore, this signal represents the proportion that the vehicle has been displaced from its preselected altitude. The proportional cable altitude error signal is processed in a similar manner as the radar altitude error signal.

3.3.7.1.4 Yaw Channel Operation

While ASE is engaged, the yaw channel will stabilize the heading of the vehicle. The MA-1 compass system feeds a proportional attitude (heading) signal to a differential synchro in the ASE control panel. The physical position of the differential synchro is controlled by the YAW TRIM control on the ASE control panel. The output of the differential synchro is coupled to the yaw synchronizer. Depending upon the condition of the yaw channel, the signal will become a synchronizing signal or a proportional attitude error signal. During the synchronizing mode (manual turns) of operation, the proportional attitude signal is nulled out and no error signal is coupled to the yaw ASE amplifier module. When the yaw channel is operating normally, the proportional attitude error signal is coupled to the yaw ASE amplifier module. Within the ASE amplifier module, the proportional attitude error signal is added to a rate signal developed by the yaw rate gyro. The resultant rate plus proportional attitude error signal is amplified and demodulated to provide an output to excite a solenoid of the yaw servo valve. As the servo valve corrects the attitude error signal through the auxiliary power piston and the rotary rudder blades, the attitude error signal diminishes. When the vehicle is positioned back to its original attitude, the MA-1 compass system output will return to its original value. As the servo valve corrects the attitude error signal, it places the yaw servo system in an open-loop condition. The open-loop condition extends the authority of the yaw channel by limiting the mechanical feedback of the yaw servo valve to resultantly reposition the yaw pedals. The pilot may override the open-loop operation by applying an opposing force on the pedals.

While ASE is engaged and the pilot uses the yaw pedals to turn manually, he will experience an artifical force feel. The yaw rate gyro will produce a signal proportional to the turning rate of the vehicle. This rate signal is eventually coupled to the servo valve and places the yaw servo system in an open-loop condition, opposite to the turn of the vehicle.

3.3.7.1.5 Crossfed Signals

In the Standard ASE there is a Pitch-Collective Crossfeed signal, which is used to program altitude vs. forward speed for the automatic transition to hover; and a Pitch-Roll Crossfeed to prevent the vehicle from tilting sideways as it finishes the transition.

3.3.7.2 The FPC-1 Modified ASE Package (Ref. SK 52214)

Most of the necessary modifications were made at the inputs of the Standard ASE. The Basic and Coupler Channel path gains were left unchanged, and the new inputs were adjusted to the same scale factor as those which were replaced.

3.3.7.2.1 Pitch Channel

In the Basic Channel, the Vertical Gyro-Derived Rate network has been left in as a back-up sensor network, in parallel with the inertially derived pitch angle and pitch rate. The longitudinal accelerometer and Doppler heading velocity channels were replaced by the inertially derived longitudinal acceleration and velocity. The cable angle channel was left unchanged.

The velocity selector signal from the computer selects the appropriate command velocity, (Ref. SK 52208), and introduces that analog command to a velocity error summing point. The Pitch-Roll crossfeed signal originates

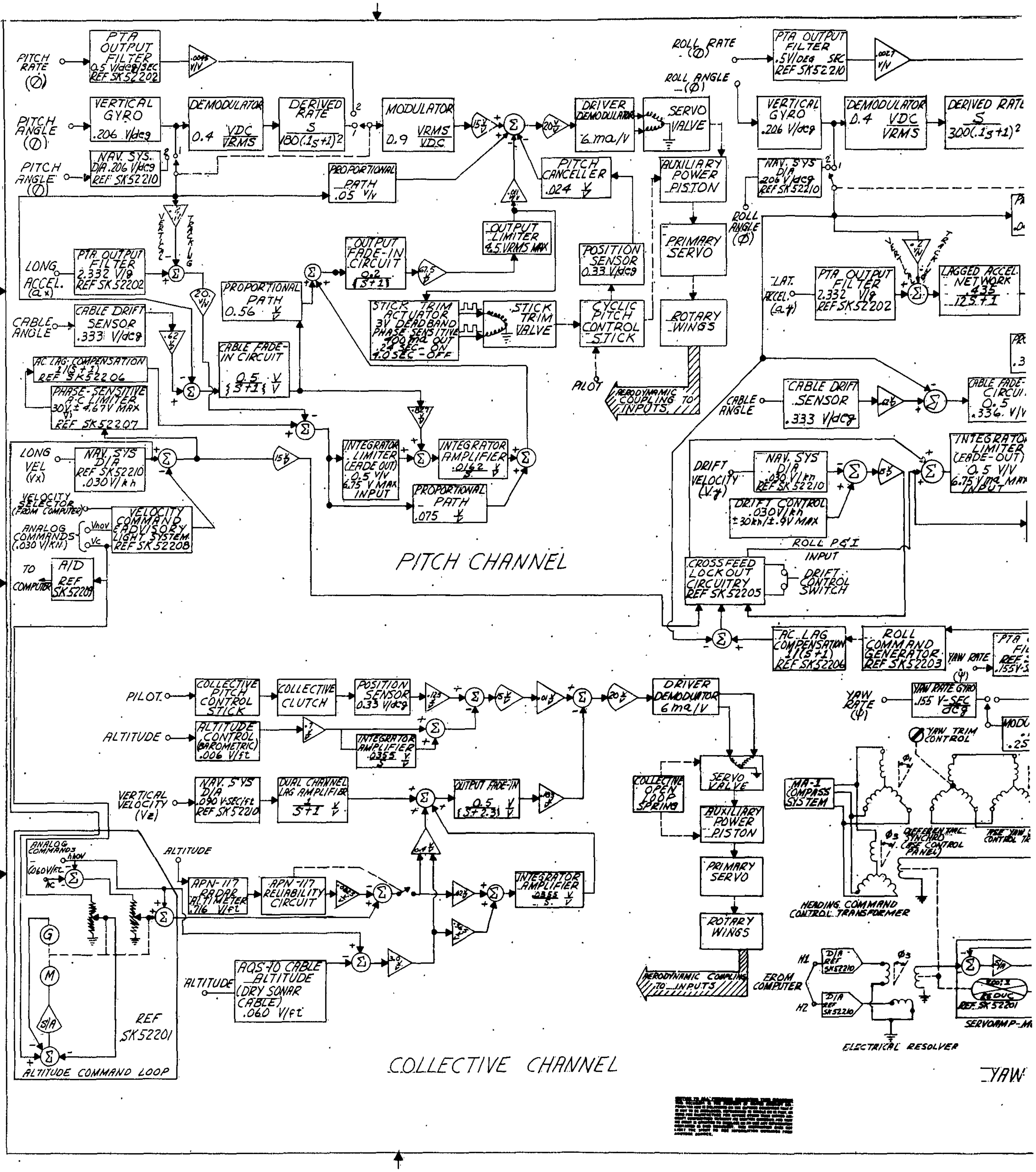
PITCH RATE (Ø)
PTA OUTPUT FILTER 0.5 V/deg/SEC REF SK52202
.0046 V/V
PITCH ANGLE (Ø)
VERTICAL GYRO .206 V/deg
DEMODULATOR 0.4 VDC/VRMS
DERIVED RATE S/180(.1s+1)²
MODULATOR 0.9 VRMS/VDC
15 V/V
DRIVER DEMODULATOR 6 ma/V
SERVO VALVE
PITCH ANGLE (Ø)
NAV. SYS. D/A .206 V/deg REF SK52210
PROPORTIONAL PATH .05 V/V
PITCH CANCELLER .024 V/V
AUXILIARY POWER PISTON
PRIMARY SERVO
ROTARY WINGS
.81 V/V
OUTPUT LIMITER 4.5 VRMS MAX
POSITION SENSOR 0.33 V/deg
CYCLIC PITCH CONTROL STICK
PILOT
AERODYNAMIC COUPLING TO INPUTS
VERTICAL
TRACKING
LONG ACCEL. (ax)
PTA OUTPUT FILTER 2.332 V/g REF SK52202
20 V/V
PROPORTIONAL PATH 0.56 V/V
OUTPUT FADE-IN CIRCUIT 0.2/(S+1)
67.5 V/V
STICK TRIM ACTUATOR 3V DEADBAND PHASE SENSITIVE 400 ma OUT 24 SEC - ON 4.0 SEC - OFF
STICK TRIM VALVE
CABLE ANGLE
CABLE DRIFT SENSOR .333 V/deg
.62 V/V
A.C. LAG COMPENSATION 1/(S+1) REF SK52206
PHASE-SENSITIVE A-C LIMITER 30V ± 4.67V MAX REF SK52207
CABLE FADE-IN CIRCUIT 0.5/(S+1) V/V
.827 V/V
INTEGRATOR LIMITER (FADE OUT) 0.5 V/V 6.75 V MAX INPUT
INTEGRATOR AMPLIFIER .0162/S V/V
PROPORTIONAL PATH .075 V/V
LONG VEL (Vx)
NAV. SYS D/A REF SK52210 .030 V/kh
15 V/V
VELOCITY SELECTOR (FROM COMPUTER)
ANALOG COMMANDS (.030 V/KN.)
Vhov
Vc
VELOCITY COMMAND ADVISORY LIGHT SYSTEM REF SK52208
TO COMPUTER
A/D REF SK52209
PITCH CHANNEL
ROLL RATE (Ø)
PTA OUTPUT FILTER .5 V/deg SEC REF SK52210
.0027 V/V
ROLL ANGLE (Ø)
VERTICAL GYRO .206 V/deg
DEMODULATOR 0.4 VDC/VRMS
DERIVED RATE S/300(.1s+1)²
NAV. SYS D/A .206 V/deg REF SK52210
ROLL ANGLE (Ø)
VERTICAL
TRACKING
LAT. ACCEL. (ay)
PTA OUTPUT FILTER 2.332 V/g REF SK52202
LAGGED ACCEL. NETWORK .435/(.125+1)
CABLE ANGLE
CABLE DRIFT SENSOR .333 V/deg
CABLE FADE-IN CIRCUIT 0.5 .336 V/V
DRIFT VELOCITY (Vy)
NAV. SYS D/A .030 V/kn REF SK52210
DRIFT CONTROL .030 V/kn ±30kn/±.9V MAX
INTEGRATOR LIMITER (FADE-OUT) 0.5 V/V 6.75 V MAX INPUT
ROLL P & I INPUT
CROSSFEED LOCKOUT CIRCUITRY REF SK52205
DRIFT CONTROL SWITCH
A.C. LAG COMPENSATION 1/(S+1) REF SK52206
ROLL COMMAND GENERATOR REF SK52203
YAW RATE (Ψ)
PTA FILTER REF .155 V-S
YAW RATE (Ψ)
YAW RATE GYRO .155 V-SEC/deg
YAW TRIM CONTROL
MODU .25
PILOT
COLLECTIVE PITCH CONTROL STICK
COLLECTIVE CLUTCH
POSITION SENSOR 0.33 V/deg
.123 V/V
15 V/V
.01 V/V
20 V/V
DRIVER DEMODULATOR 6 ma/V
ALTITUDE
ALTITUDE CONTROL (BAROMETRIC) .006 V/ft
.7 V/V
INTEGRATOR AMPLIFIER .0355/S V/V
VERTICAL VELOCITY (Vz)
NAV. SYS D/A .090 V-SEC/ft REF SK52210
DUAL CHANNEL LAG AMPLIFIER 1/(S+1) V/V
OUTPUT FADE-IN 0.5/(S+2.3) V/V
.183 V/V
COLLECTIVE OPEN LOOP SPRING
SERVO VALVE
AUXILIARY POWER PISTON
PRIMARY SERVO
ROTARY WINGS
AERODYNAMIC COUPLING TO INPUTS
ANALOG COMMANDS
hhov
.060 V/ft
hc
G
M
S/A
REF SK52201
ALTITUDE COMMAND LOOP
ALTITUDE
APN-117 RADAR ALTIMETER .716 V/ft
APN-117 RELIABILITY CIRCUIT
.0838 V/V
.64 V/V
.423 V/V
.325 V/V
INTEGRATOR AMPLIFIER .0355/S V/V
ALTITUDE
AQS-10 CABLE ALTITUDE (DRY SONAR CABLE) .060 V/ft
3.0 V/V
COLLECTIVE CHANNEL
MA-1 COMPASS SYSTEM
Ø1
Ø3
DIFFERENTIAL SYNCHRO
USE YAW CONTROL
CABLE CONTROL PANEL
HEADING COMMAND CONTROL TRANSFORMER
H1
H2
D/A REF SK52210
D/A REF SK52210
FROM COMPUTER
ELECTRICAL RESOLVER
REF SK52201
SERVOAMP-M
YAW

1

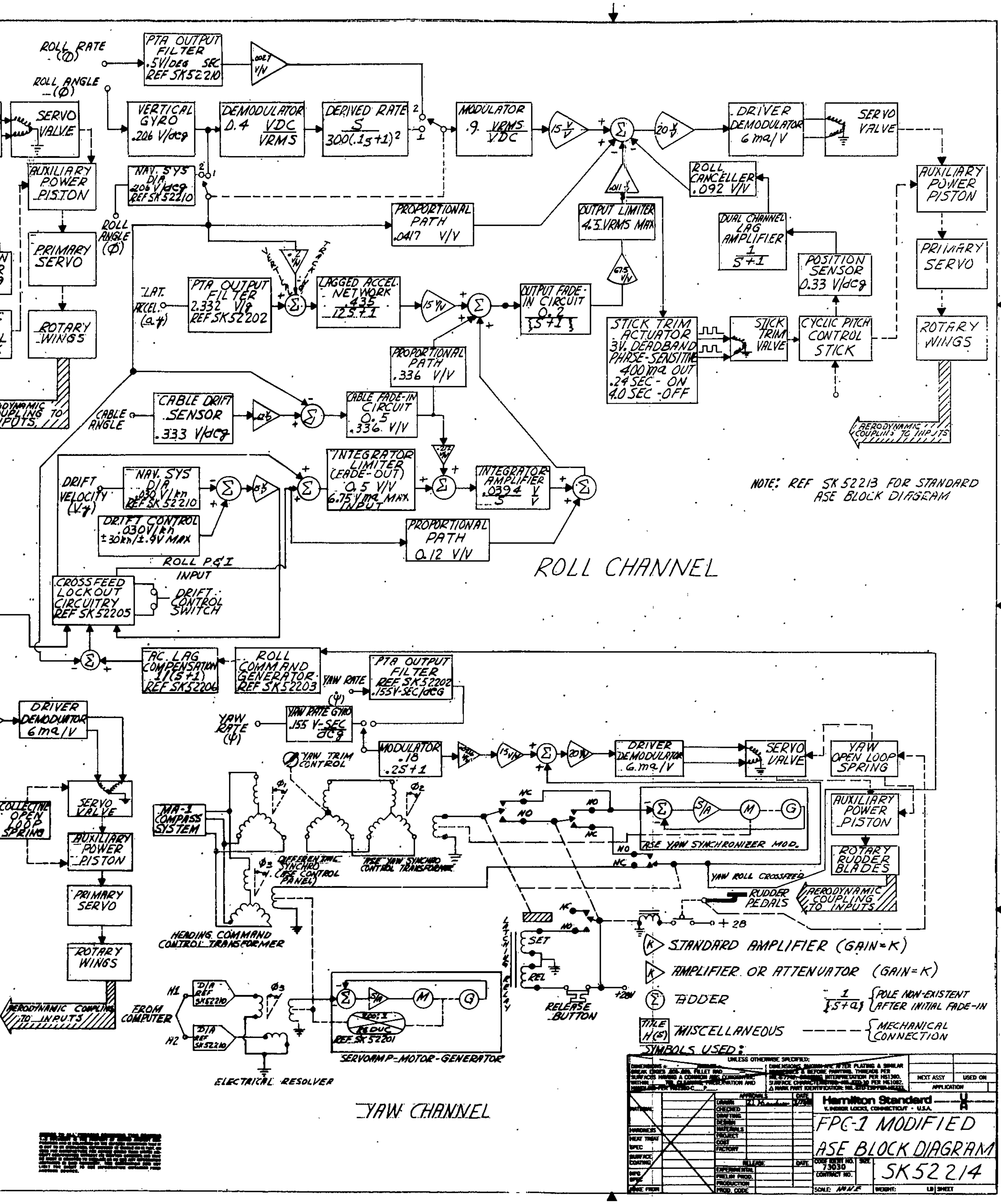
ROLL RATE (Ṗ)
PTA OUTPUT FILTER .5V/DEG SEC REF SK52210
.0027 V/V
ROLL ANGLE (Φ)
SERVO VALVE
VERTICAL GYRO .206 V/deg
DEMODULATOR 0.4 VDC/VRMS
DERIVED RATE S/300(.1S+1)²
MODULATOR .9 VRMS/VDC
15 V/V
20 V/V
DRIVER DEMODULATOR 6 ma/V
SERVO VALVE
AUXILIARY POWER PISTON
NAV. SYS D/A .206 V/deg REF SK52210
ROLL ANGLE (Φ)
PROPORTIONAL PATH .0417 V/V
.011 V/V
OUTPUT LIMITER 4.5 VRMS MAX
ROLL CANCELLER .092 V/V
DUAL CHANNEL LAG AMPLIFIER 1/(S+1)
AUXILIARY POWER PISTON
PRIMARY SERVO
POSITION SENSOR 0.33 V/deg
PRIMARY SERVO
ROTARY WINGS
LAT. ACCEL. (aᵧ)
PTA OUTPUT FILTER 2.332 V/g REF SK52202
LAGGED ACCEL. NETWORK .435/(.125+1)
15 V/V
OUTPUT FADE-IN CIRCUIT 0.2/{S+1}
67.5 V/V
STICK TRIM ACTUATOR 3V. DEADBAND PHASE-SENSITIVE 400 ma OUT .24 SEC - ON 4.0 SEC - OFF
STICK TRIM VALVE
CYCLIC PITCH CONTROL STICK
ROTARY WINGS
AERODYNAMIC COUPLING TO INPUTS
AERODYNAMIC COUPLING TO INPUTS
PROPORTIONAL PATH .336 V/V
CABLE ANGLE
CABLE DRIFT SENSOR .333 V/deg
.26
CABLE FADE-IN CIRCUIT 0.5 .336 V/V
.24 V/V
DRIFT VELOCITY (Vᵧ)
NAV. SYS D/A .030 V/kn REF SK52210
DRIFT CONTROL .030V/kn ±30kn/1.4V MAX
.6
INTEGRATOR LIMITER (FADE-OUT) 0.5 V/V 6.75 V/ma MAX INPUT
INTEGRATOR AMPLIFIER .0394/S V/V
PROPORTIONAL PATH 0.12 V/V
ROLL P&I INPUT
CROSSFEED LOCKOUT CIRCUITRY REF SK52205
DRIFT CONTROL SWITCH
NOTE: REF SK52213 FOR STANDARD ASE BLOCK DIAGRAM
ROLL CHANNEL
AC. LAG COMPENSATION 1/(S+1) REF SK52206
ROLL COMMAND GENERATOR REF SK52203
YAW RATE (Ψ̇)
PTA OUTPUT FILTER REF SK52202 .155V-SEC/deg
YAW RATE (Ψ̇)
YAW RATE GYRO .155 V-SEC/deg
MODULATOR .18/(.2S+1)
15 V/V
20 V/V
DRIVER DEMODULATOR 6 ma/V
SERVO VALVE
YAW OPEN LOOP SPRING
YAW TRIM CONTROL
DRIVER DEMODULATOR 6 ma/V
Φ₁
Φ₂
MA-1 COMPASS SYSTEM
COLLECTIVE OPEN LOOP SPRING
SERVO VALVE
AUXILIARY POWER PISTON
PRIMARY SERVO
ROTARY WINGS
AERODYNAMIC COUPLING TO INPUTS
NC
NO
NO
NC
S/A
M
G
ASE YAW SYNCHRONIZER MOD.
NO
NC
AUXILIARY POWER PISTON
ROTARY RUDDER BLADES
Φ₃
DIFFERENTIAL SYNCHRO (ASE CONTROL PANEL)
ASE YAW SYNCHRO CONTROL TRANSFORMER
YAW ROLL CROSSFEED
RUDDER PEDALS
AERODYNAMIC COUPLING TO INPUTS
HEADING COMMAND CONTROL TRANSFORMER
NC
NO
+28
LATCHING RELAY
SET
REL
RELEASE BUTTON
+28V
K STANDARD AMPLIFIER (GAIN=K)
K AMPLIFIER OR ATTENUATOR (GAIN=K)
Σ ADDER
1/{S+a} {POLE NON-EXISTENT AFTER INITIAL FADE-IN
TITLE H(S) MISCELLANEOUS
------ {MECHANICAL CONNECTION
SYMBOLS USED:
H1
D/A REF SK52210
Φ5
FROM COMPUTER
H2
D/A REF SK52210
S/A
M
G
REDUC
REF SK52201
SERVOAMP-MOTOR-GENERATOR
ELECTRICAL RESOLVER
YAW CHANNEL

UNLESS OTHERWISE SPECIFIED:

NEXT ASSY
USED ON
APPLICATION

APPROVALS
DATE
DRAWN
CHECKED
DRAFTING
DESIGN
MATERIALS
PROJECT
COST
FACTORY

RELEASE
DATE
EXPERIMENTAL
PRELIM PROD.
PRODUCTION
PROD. CODE

MATERIAL
HARDNESS
HEAT TREAT SPEC
SURFACE COATING
MFG SPEC
MAKE FROM

Hamilton Standard
WINDSOR LOCKS, CONNECTICUT · U.S.A.

FPC-1 MODIFIED
ASE BLOCK DIAGRAM

CODE IDENT NO. 73030
CONTRACT NO.
SIZE
SK52214
SCALE: NONE
WEIGHT: LB
SHEET

2

at this point. The velocity error signal is also fed to the Phase-Sensitive AC Limiter, and through a 1-second lag compensation, to the acceleration error sum point. The limiter gives an acceleration command proportional to velocity error up to a limiting value of ± 2 knots/sec at a velocity error of 5 knots. The acceleration error command replaces the velocity error command of the Standard ASE. The Lagged Accelerometer network is not used. The analog cruise velocity command undergoes an A/D conversion, (Ref. SK 52209) and is routed to the computer for use in generating the heading command. The analog signals, V_x and V_c, are crossfed to the Altitude Command Loop, (Ref. SK 52201) in the Collective Channel, where they are used in the development of altitude-velocity profile equation and the associated analog altitude command.

3.3.7.2.2 Collective Channel

In the Collective Channel, the Doppler vertical velocity is replaced by the inertially derived velocity, V_z. The altitude control on the ASE Control Panel is replaced by the output of the Altitude Command Loop, (Ref. SK 52201), which is summed with the AN/APN-117 Radar Altimeter output or the AN/AQS-10 Cable Altitude output to provide an altitude error signal.

3.3.7.2.3 Yaw Channel

The Standard ASE Yaw Channel was retained in full, with the addition of the inertially derived yaw rate. The present yaw rate gyro will serve as a back-up instrument. In parallel with the Standard ASE Yaw Channel is the Heading Command Channel (Ref. SK 52204), which accepts the signals (H_1, H_2) from the computer and uses them to position a control transformer; the control transformer output is compared with the MA-1 Compass output to provide a heading error signal.

The normal condition of the channel is with the Heading Command path ON. When the rudder pedals are depressed, the Heading Command path is turned OFF and the Standard ASE Channel is turned ON in the synchronizing mode. When the pedals are released, the Standard ASE Channel remains ON in a heading hold mode until the RELEASE BUTTON is momentarily depressed. At this time, the Standard ASE Channel is turned OFF and the Heading Command channel is put back into the circuit. This arrangement allows the pilot to override a flight path, turn to a new heading, and hold that heading; then, by pressing the RELEASE BUTTON, he may revert to the original heading command. The error signal at the input to the Yaw Servo Driver-Demodulation Circuitry is crossfed to the Roll Channel-Roll Command Generator to provide a command signal for co-orcinated turns.

3.3.7.2.4 Roll Channel

As in the pitch channel, the Vertical Gyro-Derived Rate Network will serve as a back-up system for the inertially derived roll angle and roll rate. The lateral (Y) accelerometer and Doppler drift velocity channel will be replaced by the inertially derived Y axis accelerometer and velocity.

The Roll Angle Command Section is comprised of the Roll Command Generator (Ref. SK 52203), which can command roll angles of zero degrees and ± 25 degrees; the AC Lag Compensation and the Crossfeed Lockout Circuitry (Ref. SK 52205). It has three modes of operation, the applicable mode being selected by the Crossfeed Lockout circuitry.

When the command for V_c is present and V_x is greater than 50 knots, the Crossfeed Lockout Circuitry passes the signal from the Roll Command Generator. If V_x is less than 50 knots or the command for V_{hov} is present, the Pitch-Roll Crossfeed signal is passed. When the vehicle is in a hover, momentarily depressing the DRIFT CONTROL Switch will place the Drift Control path in operation. This path automatically switches out when the transition to cruise is started.

3.3.7.3 Required Additional Circuitry

The following is a list of the circuitry needed in addition to the Standard ASE Package, in order to implement the Flight Path Control:

(a) Pulse Torque Amplifier (PTA) Output Filter

(b) D/A Converter

(c) A/D Encoder

(d) Velocity Command and Advisory Light System

(e) Phase-Sensitive AC Limiter

(f) AC Lag Compensation Network

(g) Altitude Command Loop

(h) Yaw Channel - Heading Command Loop

(i) Roll Command Generator

(j) Crossfeed Lockout Circuitry

3.3.7.3.1 PTA Output Filter (Ref. SK 52202)

This filter detects the average value of a timewise unsymmetrical square wave. The output (2.332 V/g — 1 g max) shall cover its full range in response to the following input:

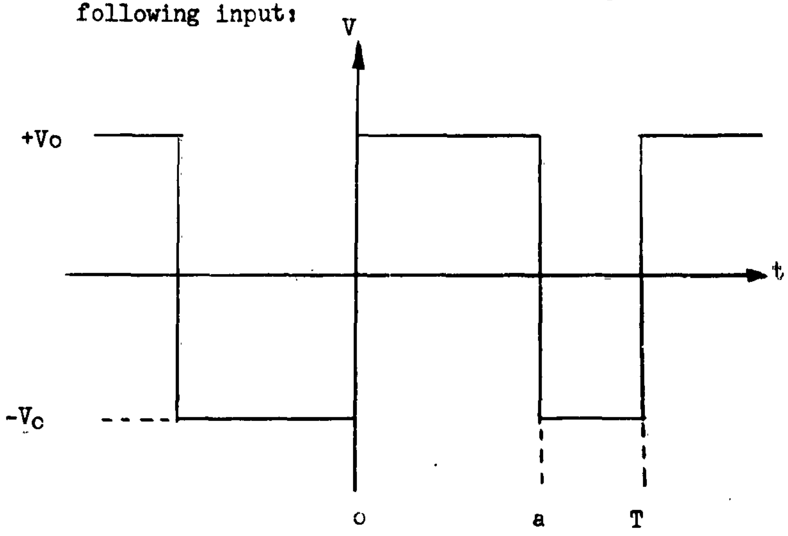

$T = 10^{-3}$ SEC

$.3T \leq a \leq .7T$

REVISIONS			
SYM	DESCRIPTION	DATE	APPROVAL

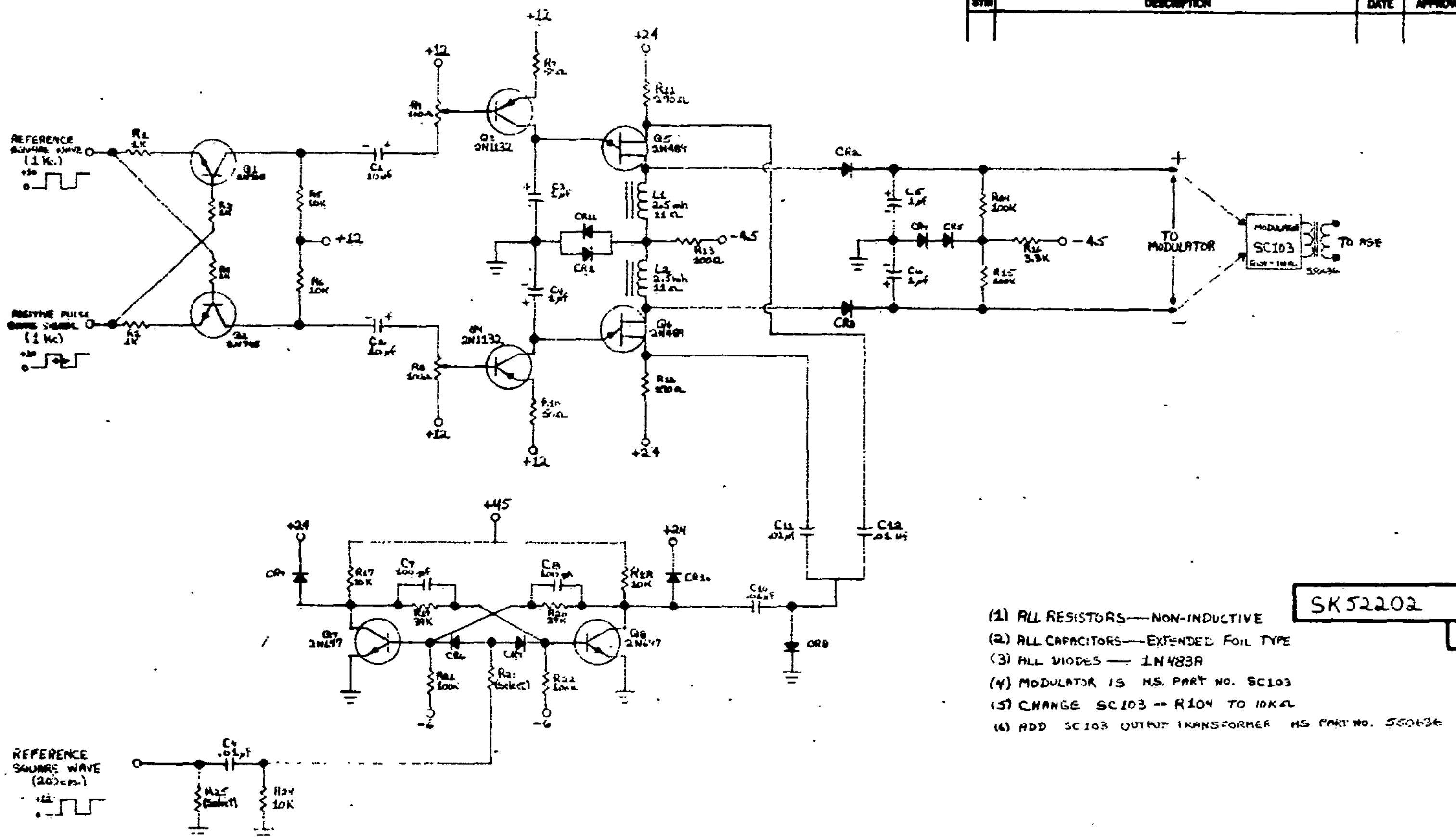
+12
+24
+12
R7 5Ω
R11 270Ω
R9 100Ω
Q3 2N1132
Q5 2N489
REFERENCE SQUARE WAVE (1 Kc.)
+10
0
R1 1K
Q1 2N706
R3 1K
R4 1K
R5 10K
+12
R6 10K
C1 10μf
C2 10μf
C3 1μf
C4 1μf
CR11
CR1
L1 2.5 mh 11 Ω
L2 2.5 mh 11 Ω
R13 100Ω
-4.5
POSITIVE PULSE DRIVE SIGNAL (1 Kc)
+10
0
R2 1K
Q2 2N706
R8 100Ω
Q4 2N1132
R10 5Ω
Q6 2N489
R12 270Ω
+12
+12
+24
CR2
CR3
C5 1μf
C6 1μf
CR4
CR5
R14 100K
R15 100K
R16 3.3K
-4.5
+
-
TO MODULATOR
MODULATOR SC103
TO RSE
550636
+45
+24
CR9
R17 10K
C7 100 pf
R19 39K
Q7 2N697
CR6
CR7
R21 100K
R23 (select)
R22 100K
-6
-6
C8 100 pf
R20 39K
R18 10K
Q8 2N697
+24
CR10
C10 .022μf
CR8
C11 .01μf
C12 .01μf
REFERENCE SQUARE WAVE (20 cps)
+12
0
C9 .01μf
R25 (select)
R24 10K

(1) ALL RESISTORS—NON-INDUCTIVE
(2) ALL CAPACITORS—EXTENDED FOIL TYPE
(3) ALL DIODES — 1N483A
(4) MODULATOR IS H.S. PART NO. SC103
(5) CHANGE SC103 -- R104 TO 10KΩ
(6) ADD SC103 OUTPUT TRANSFORMER HS PART NO. 550636

SK52202

[illegible] IS THE PROPERTY OF UNITED AIRCRAFT CORPORATION AND IS DELIVERED ON THE EXPRESS CONDITION THAT IT IS NOT TO BE DISCLOSED, REPRODUCED IN WHOLE OR IN PART, OR USED FOR MANUFACTURE FOR ANYONE OTHER THAN UNITED AIRCRAFT CORPORATION WITHOUT ITS WRITTEN CONSENT; AND THAT NO RIGHT IS GRANTED TO DISCLOSE OR SO USE ANY INFORMATION CONTAINED IN SAID DOCUMENT. THIS RESTRICTION DOES NOT LIMIT THE RIGHT TO USE INFORMATION OBTAINED FROM ANOTHER SOURCE.

UNLESS OTHERWISE SPECIFIED:
DIMENSIONS ± ______ ANGLES ± ______
BREAK EDGES .005-.025. FILLET RAD ______
SURFACES HAVING A COMMON AXIS CONCENTRIC WITHIN ______ TIR. CLEANING, PRESERVATION AND HANDLING PER HS1550-C ___ P ___
DIMENSIONS SHOWN ARE AFTER PLATING & SIMILAR PROCESSES & BEFORE PAINTING. THREADS PER MIL-S-7742. DRAWING INTERPRETATION PER HS1360. SURFACE CHARACTERISTICS: MIL-STD-10 PER HS1082. △ MARK PART IDENTIFICATION: MIL-STD-130 PER HS333.

NEXT ASSY	USED ON
APPLICATION	

		APPROVALS		DATE
MATERIAL		DRAWN	[illegible]	[illegible]
		CHECKED		
		DRAFTING		
		DESIGN		
HARDNESS		MATERIALS		
HEAT TREAT SPEC		PROJECT		
		COST		
		FACTORY		
SURFACE COATING		RELEASE		DATE
		EXPERIMENTAL		
MFG SPEC		PRELIM PROD.		
		PRODUCTION		
MAKE FROM		PROD. CODE		

Hamilton Standard
WINDSOR LOCKS, CONNECTICUT • U.S.A.

PULSE TORGUE AMPLIFIER—
ELECTRONIC OUTPUT FILTER

CODE IDENT NO.	SIZE	
73030	C	SK52202
CONTRACT NO.		
SCALE:	WEIGHT: LB	SHEET

Now

The filter uses active filtering on the 1 Kc base frequency, by integrating it over 10 cycles; and then averages the resultant 100 cps information with a passive filter. The resulting DC signal is modulated and fed out at a scale factor of 2.332 V/g.

3.3.7.3.2 D/A Converter (Ref. SK 52210)

The D/A Converter will handle 8 bits plus a sign bit. The D/A Converter utilizes an operational amplifier technique using a high gain forward amplifier (-K') and variable feedback $(\frac{R_f}{R})$. The gain of the upper half of the amplifier is (-K'); of the lower half, $-K' (1 + \frac{R_f}{R})$. Therefore, the analog output is given be $\frac{e\ out}{e\ in} = K' \frac{R_f}{R}$. The size of R is controlled by the digital information which is used to switch in the weighted values of resistance making up R. The circuit of SK 52210 has a maximum output of 9 volt AC, for all 8 bits present.

3.3.7.3.3 A/D Encoder (Ref. SK 52209)

This device is used to supply a natural binary signal to the computer, representing the manually set cruise velocity command. It covers the range from 64 to 100 knots in two-knot steps. A potentiomter for the analog cruise velocity command is mounted on the same shaft.

3.3.7.3.4 Velocity Command and Advisory Light System (Ref. SK 52208)

This circuit has two advisory lights: "Switch to Cruise Velocity", and "Switch to Hover Velocity". There are two inputs representing these commands. Two conditions are required to command the appropriate light: (1) the Mode Selector switch must be in the FPC position; and (2) the Velocity Control switch must be in the wrong position (i.e. "Switch to Hover Velocity" light lights only if command for V_c is present).

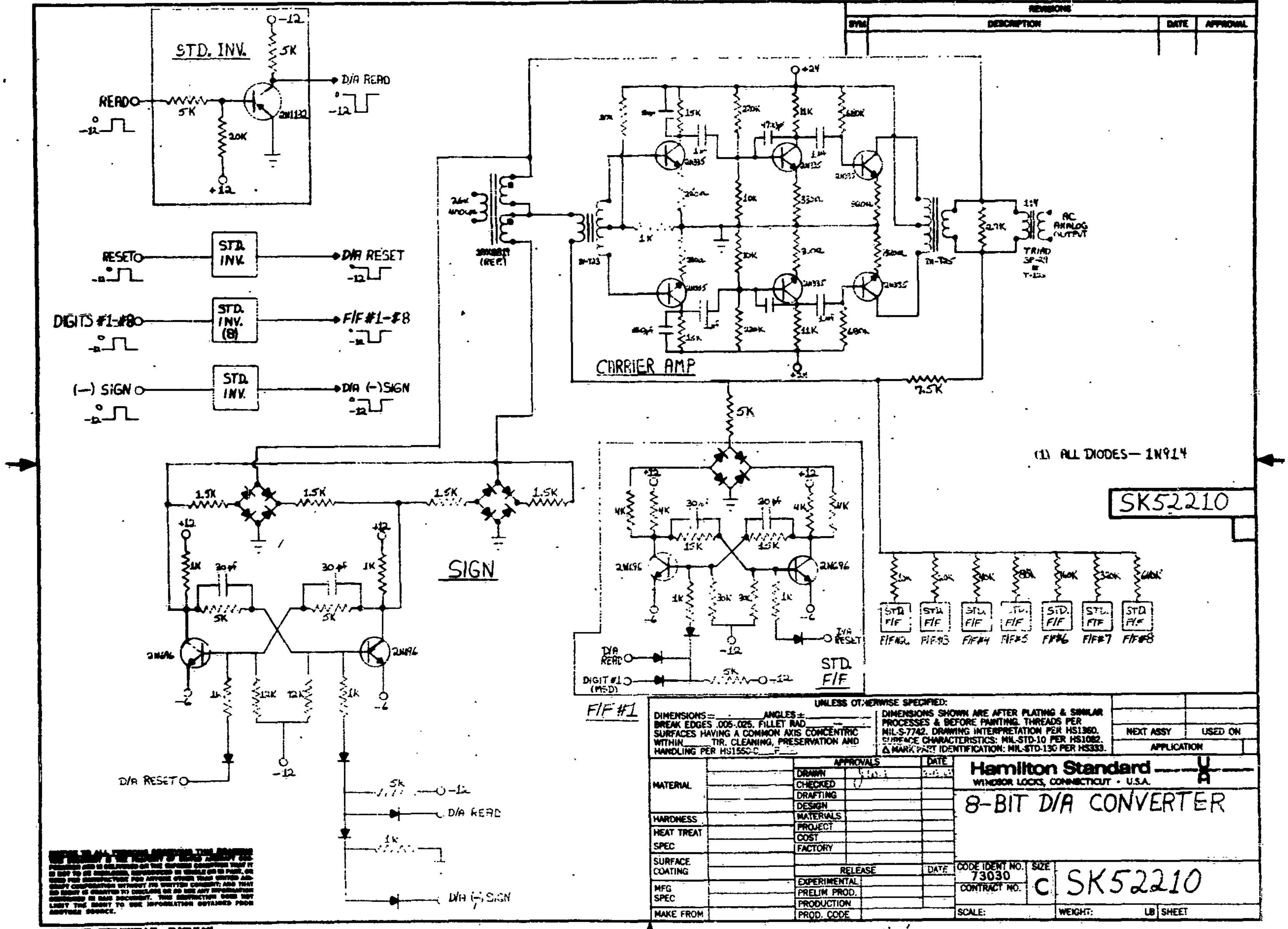
STD. INV.
READ
5K
2N1132
20K
+12
-12
D/A READ
RESET
STD. INV.
D/A RESET
DIGITS #1-#8
STD. INV. (8)
F/F #1-#8
(—) SIGN
D/A (—)SIGN
+24
15K
220K
11K
680K
1K
10K
330Ω
560Ω
2N335
CARRIER AMP
2.7K
1:1
AC ANALOG OUTPUT
TRIAD SP-29 or T-123
7.5K
5K
(REF)
1.5K
SIGN
30pf
2N696
12K
1K
D/A RESET
D/A READ
D/A (-) SIGN
4K
15K
30K
2N696
D/A RESET
D/A READ
DIGIT #1 (MSD)
STD. F/F
F/F #1
STD. F/F
F/F#2
F/F#3
F/F#4
F/F#5
F/F#6
F/F#7
F/F#8
REVISIONS
SYM
DESCRIPTION
DATE
APPROVAL

(1) ALL DIODES— 1N914

SK52210

UNLESS OTHERWISE SPECIFIED:
DIMENSIONS ± ________ ANGLES ± ________
BREAK EDGES .005-.025. FILLET RAD ________
SURFACES HAVING A COMMON AXIS CONCENTRIC WITHIN ______ TIR. CLEANING, PRESERVATION AND HANDLING PER HS1550-C ___ F ___

DIMENSIONS SHOWN ARE AFTER PLATING & SIMILAR PROCESSES & BEFORE PAINTING. THREADS PER MIL-S-7742. DRAWING INTERPRETATION PER HS1360. SURFACE CHARACTERISTICS: MIL-STD-10 PER HS1082. △ MARK PART IDENTIFICATION: MIL-STD-130 PER HS333.

NEXT ASSY	USED ON
APPLICATION	

		APPROVALS		DATE
MATERIAL		DRAWN		
		CHECKED		
		DRAFTING		
		DESIGN		
HARDNESS		MATERIALS		
HEAT TREAT		PROJECT		
SPEC		COST		
		FACTORY		
SURFACE COATING		RELEASE		DATE
		EXPERIMENTAL		
MFG SPEC		PRELIM PROD.		
		PRODUCTION		
MAKE FROM		PROD. CODE		

Hamilton Standard
WINDSOR LOCKS, CONNECTICUT • U.S.A.

8-BIT D/A CONVERTER

CODE IDENT NO. 73030
CONTRACT NO.
SIZE C
SK52210
SCALE:
WEIGHT: LB
SHEET

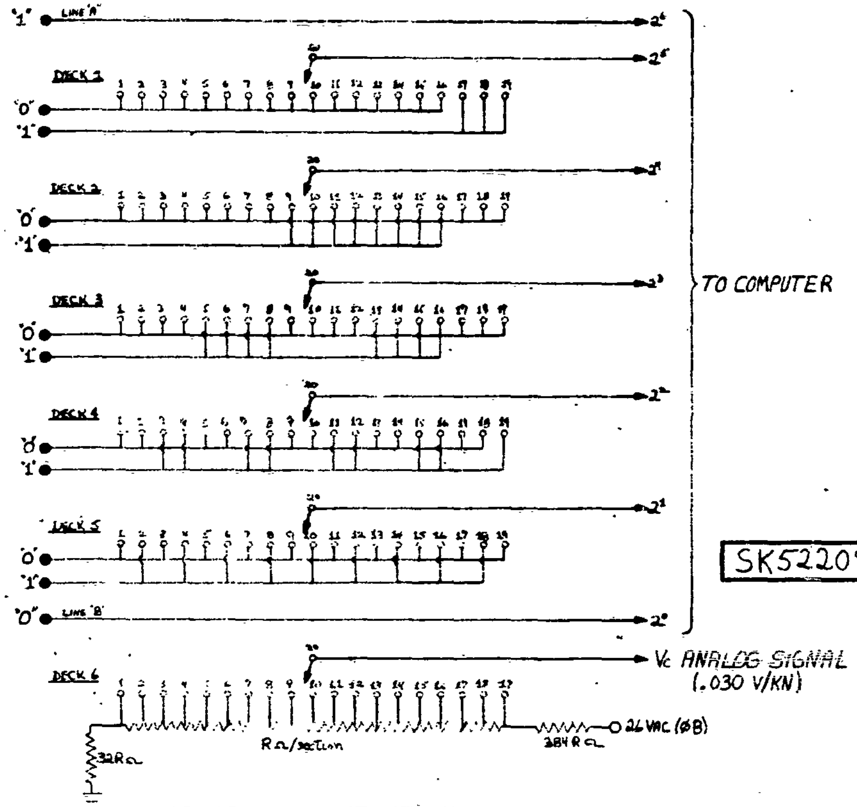
"1"
LINE 'A'
2^6
2^5
DECK 1
"0"
"1"
DECK 2
2^4
DECK 3
2^3
DECK 4
2^2
DECK 5
2^1
LINE 'B'
2^0
TO COMPUTER
DECK 6
V_c ANALOG SIGNAL
(.030 V/KN)
32RΩ
RΩ/section
384 RΩ
24 VAC (ØB)
1 2 3 4 5 6 7 8 9 10 11 12 13 14 15 16 17 18 19
20

SK52209

SWITCH POSITION	SPEED (KNOTS)	LINE 'A' (2^6)	DECK 1 (2^5)	DECK 2 (2^4)	DECK 3 (2^3)	DECK 4 (2^2)	DECK 5 (2^1)	LINE 'B' (2^0)
1	64	1	0	0	0	0	0	0
2	66	1	0	0	0	0	1	0
3	68	1	0	0	0	1	0	0
4	70	1	0	0	0	1	1	0
5	72	1	0	0	1	0	0	0
6	74	1	0	0	1	0	1	0
7	76	1	0	0	1	1	0	0
8	78	1	0	0	1	1	1	0
9	80	1	0	1	0	0	0	0
10	82	1	0	1	0	0	1	0
11	84	1	0	1	0	1	0	0
12	86	1	0	1	0	1	1	0
13	88	1	0	1	1	0	0	0
14	90	1	0	1	1	0	1	0
15	92	1	0	1	1	1	0	0
16	94	1	0	1	1	1	1	0
17	96	1	1	0	0	0	0	0
18	98	1	1	0	0	0	1	0
19	100	1	1	0	0	1	0	0
20	OFF	☒	☒	☒	☒	☒	☒	☒

SWITCH: J-B-T INSTRUMENTS INC.

	NO.	TYPE	O.D.	DEPTH BEHIND PANEL
(1)	MS-20-6	MOLDED	2 5/8"	2 3/8"
(2)	MS-20B-6	BONDED, CURED LAMINATE	2 5/8"	2 15/32"

UNLESS OTHERWISE SPECIFIED:
DIMENSIONS ± ______ ANGLES ± ______
BREAK EDGES .005-.025. FILLET RAD ______
SURFACES HAVING A COMMON AXIS CONCENTRIC WITHIN ______ TIR. CLEANING, PRESERVATION AND HANDLING PER HS1550-C ___ P ___

DIMENSIONS SHOWN ARE AFTER PLATING & SIMILAR PROCESSES & BEFORE PAINTING. THREADS PER MIL-S-7742. DRAWING INTERPRETATION PER HS1360. SURFACE CHARACTERISTICS: MIL-STD-10 PER HS1082. △ MARK PART IDENTIFICATION: MIL-STD-130 PER HS333.

NEXT ASSY	USED ON
APPLICATION	

	APPROVALS	DATE
DRAWN	W.K	3-13-
CHECKED		
DRAFTING		
DESIGN		
MATERIALS		
PROJECT		
COST		
FACTORY		
RELEASE		DATE
EXPERIMENTAL		
PRELIM PROD.		
PRODUCTION		
PROD. CODE		

MATERIAL
HARDNESS
HEAT TREAT SPEC
SURFACE COATING
MFG SPEC
MAKE FROM

Hamilton Standard
WINDSOR LOCKS, CONNECTICUT • U.S.A.

A/D ENCODER - 7-BIT

CODE IDENT NO. 73030
CONTRACT NO.
SIZE C
SK52209
SCALE:
WEIGHT: LB
SHEET

NOW 62-0873-1 FFL-1

SK52208

SYM	DESCRIPTION	DATE	APPROVAL

REVISIONS

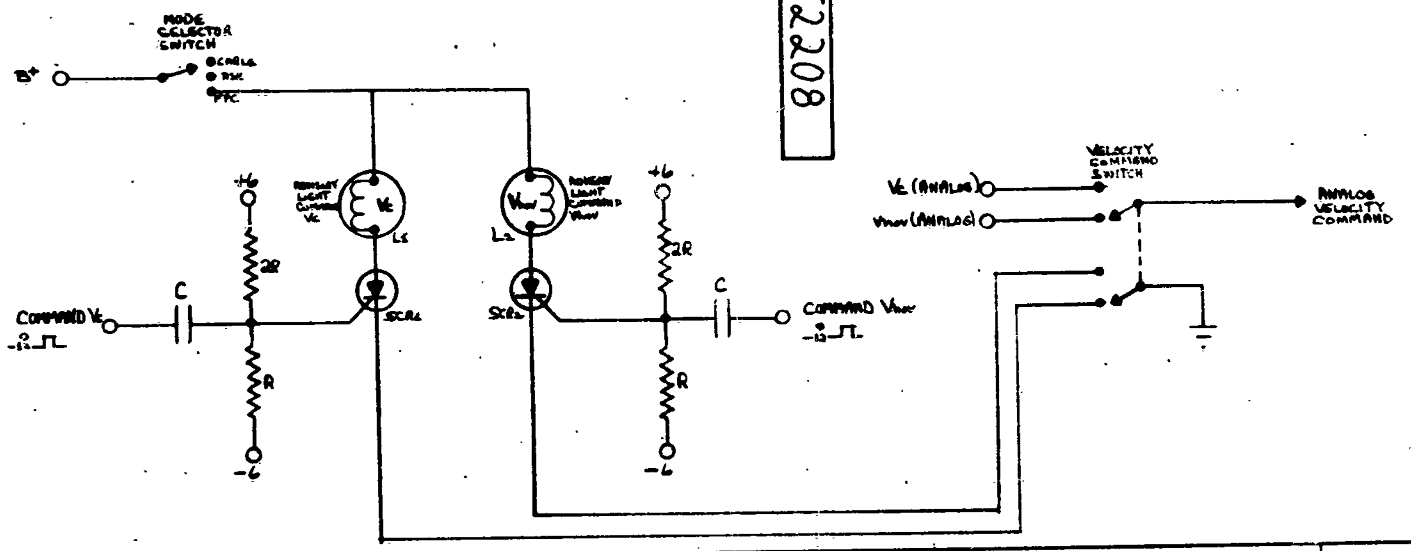
MODE SELECTOR SWITCH
CABLE
TSK
FPC
B+
ROMEAN LIGHT COMMAND Vc
Vc
L1
SCR1
+6
2R
C
R
-6
COMMAND Vc
-12 0
ROMEAN LIGHT COMMAND Vnav
Vnav
L2
SCR2
+6
2R
C
R
-6
COMMAND Vnav
-12 0
VELOCITY COMMAND SWITCH
Vc (ANALOG)
Vnav (ANALOG)
ANALOG VELOCITY COMMAND

UNLESS OTHERWISE SPECIFIED:

DIMENSIONS ± ______ ANGLES ± ______
BREAK EDGES .005-.025. FILLET RAD ______
SURFACES HAVING A COMMON AXIS CONCENTRIC WITHIN ______ TIR. CLEANING, PRESERVATION AND HANDLING PER HS1550-C ___ P ___

DIMENSIONS SHOWN ARE AFTER PLATING & SIMILAR PROCESSES & BEFORE PAINTING. THREADS PER MIL-S-7742. DRAWING INTERPRETATION PER HS1360. SURFACE CHARACTERISTICS: MIL-STD-10 PER HS1082. △ MARK PART IDENTIFICATION: MIL-STD-130 PER HS333.

NEXT ASSY	USED ON
APPLICATION	

		APPROVALS		DATE
MATERIAL		DRAWN	J.W.K	3-13-67
		CHECKED		
		DRAFTING		
		DESIGN		
HARDNESS		MATERIALS		
HEAT TREAT SPEC		PROJECT		
		COST		
		FACTORY		
SURFACE COATING		RELEASE		DATE
		EXPERIMENTAL		
MFG SPEC		PRELIM PROD.		
		PRODUCTION		
MAKE FROM		PROD. CODE		

Hamilton Standard
WINDSOR LOCKS, CONNECTICUT · U.S.A.

VELOCITY COMMAND ADVISORY LIGHT SYSTEM

CODE IDENT NO.	SIZE	
73030	B	SK52208
CONTRACT NO.		
SCALE:	WEIGHT: LB	SHEET

NOW 62-0873-D

FPC-1

NOTICE TO ALL PERSONS RECEIVING THIS DRAWING
THIS DOCUMENT IS THE PROPERTY OF UNITED AIRCRAFT CORPORATION AND IS DELIVERED ON THE EXPRESS CONDITION THAT IT IS NOT TO BE DISCLOSED, REPRODUCED IN WHOLE OR IN PART, OR USED FOR MANUFACTURE FOR ANYONE OTHER THAN UNITED AIRCRAFT CORPORATION WITHOUT ITS WRITTEN CONSENT; AND THAT NO RIGHT IS GRANTED TO DISCLOSE OR SO USE ANY INFORMATION CONTAINED IN SAID DOCUMENT. THIS RESTRICTION DOES NOT LIMIT THE RIGHT TO USE INFORMATION OBTAINED FROM ANOTHER SOURCE.

3.3.7.3.5 Altitude Command Loop (Ref. SK 52201)

The altitude command loop must generate the command $h = h_{hov} + \frac{V_x}{V_c}(h_c - h_{hov})$. It is a servo motor driven multiplier. The analog altitude commands are subtracted to form $(h_c - h_{hov})$; a servo positioning loop is used to generate thr ratio $\frac{V_x}{V_c}$. By linking a potentiometer with the altitude signal to this loop, the product $\frac{V_x}{V_c}(h_c - h_{hov})$ is formed. h_{hov} is added back in to complete the profile equation. The output is passed through a Gain Adjust network, which is a modification of the Phase-Sensitive AC Limiter. This is done to match the scale factor of the command to the non-linear output of the AN/APN 117. The mechanical limits of the potentiometers restrict the altitude command to a range of 20 to 200 feet, even if V_x should become less than zero, or greater than V_c.

3.3.7.3.6 Yaw Channel-Heading Command Loop (Ref. SK 52204)

In this loop the computer signals (H_1, H_2) are passed through D/A converters and used to drive a resolver to the shaft position ψ comm. This resolver is mechanically linked to the Heading Command control transformer, to introduce the analog heading command to the yaw channel.

The switching arrangement allows the heading command channel to be overridden by depressing the rudder pedals. This throws the ASE Yaw Synchro Module into the synchronizing mode to follow the resulting turn to a new heading. When the pedals are released, the ASE Yaw Synchro will hold the new heading until the OVERRIDE RELEASE Button is momentarily depressed. At this time, the system reverts to the heading command mode with the original heading command reinstituted. When the Heading Command Channel is operative, the ASE Yaw Synchro is maintained in a synchronizing mode.

3.3.7.3.7 Roll Command Generator (Ref. SK 52203)

The Roll Command Generator output may be represented by the following diagram:

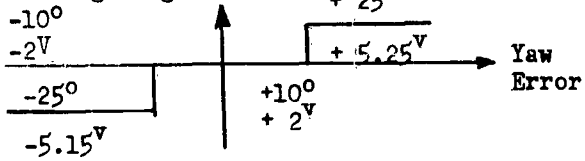

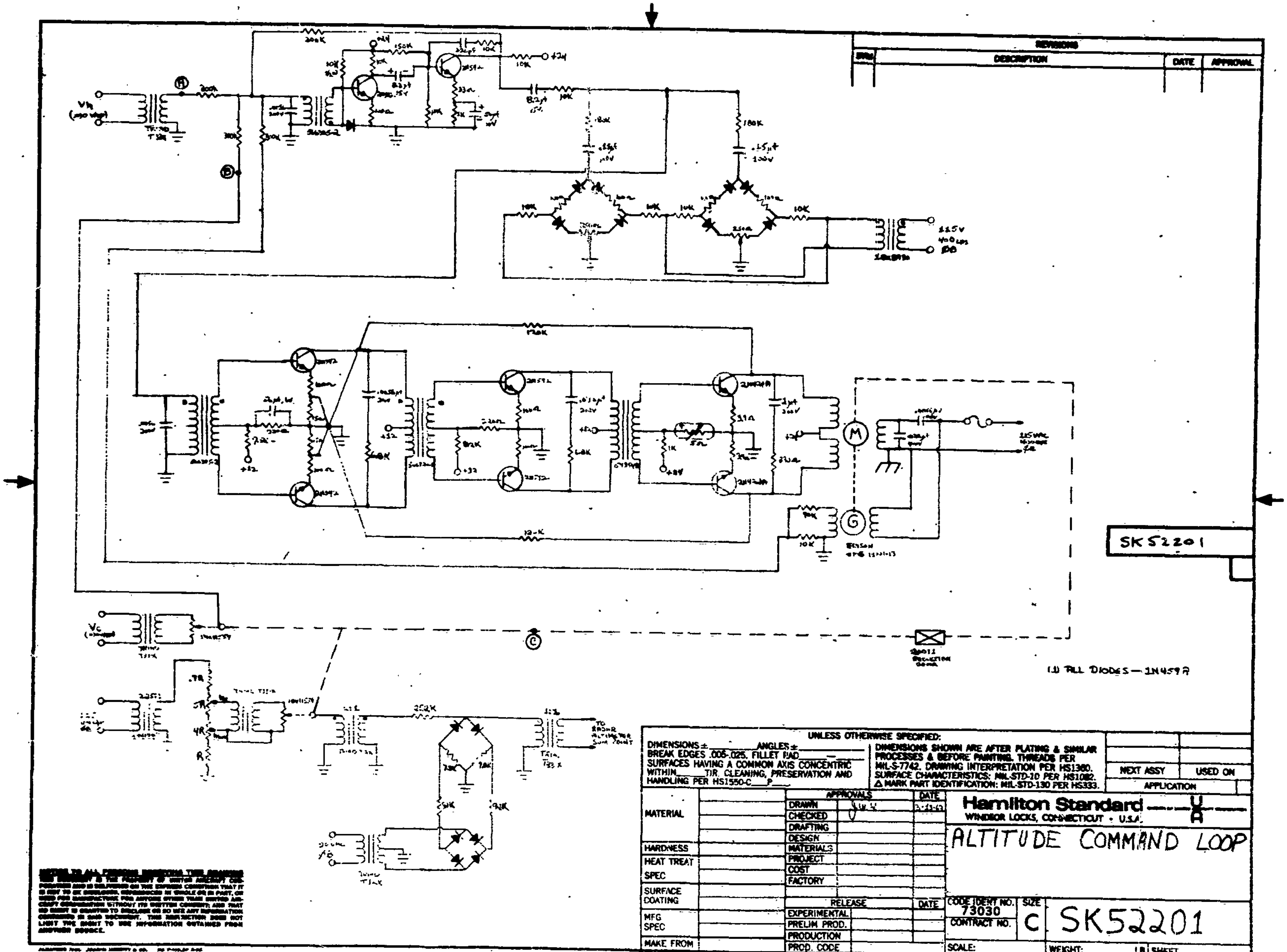
REVISIONS
SYM
DESCRIPTION
DATE
APPROVAL
Vin
(400 cps)
T1200
T 3R
Ⓐ
200K
300K
Ⓑ
300K
SK6265-2
200K
10K
150K
10K
2N1132
8.2μf
15V
2N514
33Ω
100Ω
1K
22μf
10K
10K
+24
8.2μf
15V
10K
180K
.15μf
200V
10K
10K
10K
10K
180K
.15μf
200V
10K
115V
400cps
ØB
SK6829
170K
2N1072
2μf
7.5K
+32
6.8K
2N357
2N357
2N1072
8.2K
+32
6.8K
2N1072A
1K
+48
51Ω
M
G
115VAC
400cps
ØA
10K
12K
10K
Beckman
Vc
T11K
Ⓒ
.7R
.5R
.4R
R
T11K
232K
T11K
T33K
TO
RADAR
ALTIMETER
SUM POINT
51K
91K
T11K
SK52201
(1) ALL DIODES — 1N459A

UNLESS OTHERWISE SPECIFIED:
DIMENSIONS ± ______ ANGLES ± ______
BREAK EDGES .005-.025. FILLET RAD ______
SURFACES HAVING A COMMON AXIS CONCENTRIC WITHIN ______ TIR. CLEANING, PRESERVATION AND HANDLING PER HS1550-C ___ P ___

DIMENSIONS SHOWN ARE AFTER PLATING & SIMILAR PROCESSES & BEFORE PAINTING. THREADS PER MIL-S-7742. DRAWING INTERPRETATION PER HS1360. SURFACE CHARACTERISTICS: MIL-STD-10 PER HS1082.
△ MARK PART IDENTIFICATION: MIL-STD-130 PER HS333.

NEXT ASSY	USED ON
APPLICATION	

MATERIAL		APPROVALS		DATE
		DRAWN	J.W.V.	3-13-62
		CHECKED		
		DRAFTING		
		DESIGN		
HARDNESS		MATERIALS		
HEAT TREAT SPEC		PROJECT		
		COST		
		FACTORY		
SURFACE COATING		RELEASE		DATE
MFG SPEC		EXPERIMENTAL		
		PRELIM PROD.		
		PRODUCTION		
MAKE FROM		PROD. CODE		

Hamilton Standard
WINDSOR LOCKS, CONNECTICUT · U.S.A.

ALTITUDE COMMAND LOOP

CODE IDENT NO. 73030	SIZE	SK52201
CONTRACT NO.	C	
SCALE:	WEIGHT: LB	SHEET

NOTICE TO ALL PERSONS RECEIVING THIS DRAWING
THIS DRAWING IS THE PROPERTY OF UNITED AIRCRAFT CORPORATION AND IS DELIVERED ON THE EXPRESS CONDITION THAT IT IS NOT TO BE DISCLOSED, REPRODUCED IN WHOLE OR IN PART, OR USED FOR MANUFACTURE FOR ANYONE OTHER THAN UNITED AIRCRAFT CORPORATION WITHOUT ITS WRITTEN CONSENT; AND THAT NO RIGHT IS GRANTED TO DISCLOSE OR SO USE ANY INFORMATION CONTAINED IN SAID DOCUMENT. THIS RESTRICTION DOES NOT LIMIT THE RIGHT TO USE INFORMATION OBTAINED FROM ANOTHER SOURCE.

Now 62-0873-D

FPC-1

REVISIONS			
SYM	DESCRIPTION	DATE	APPROVAL

SK52204

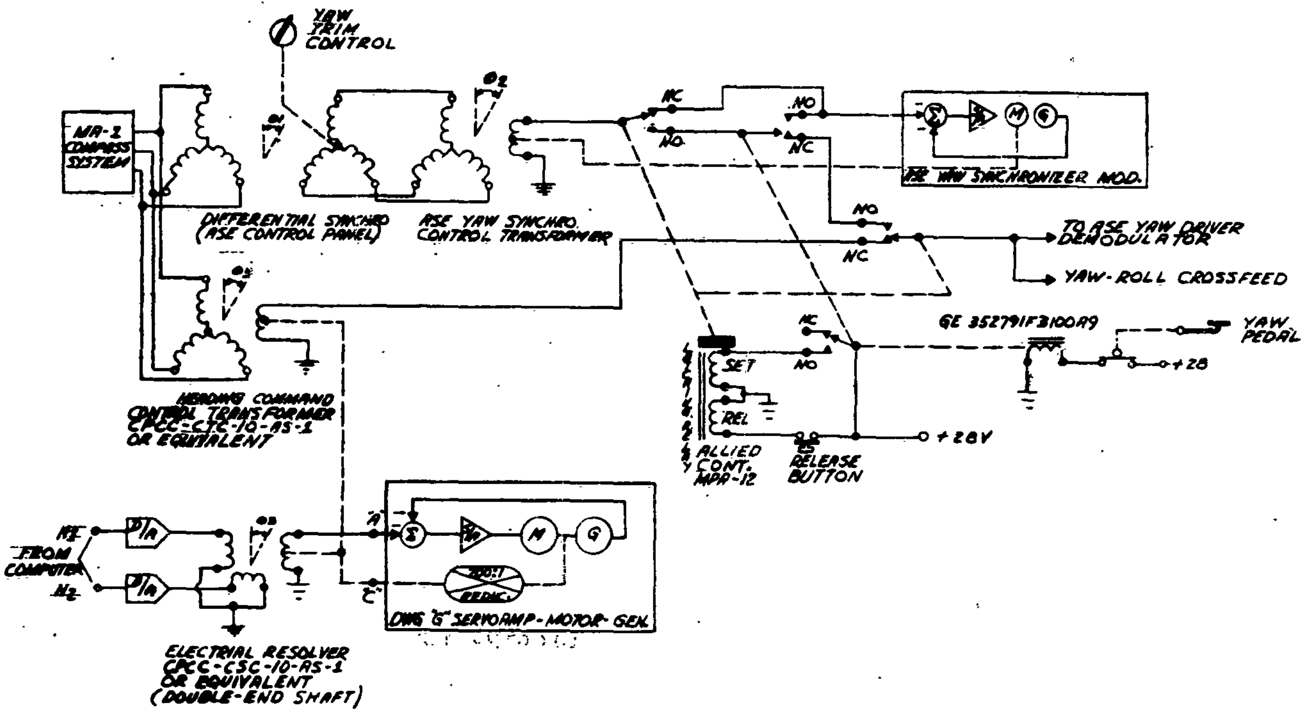
YAW TRIM CONTROL
MA-1 COMPASS SYSTEM
θ1
θ2
θ3
DIFFERENTIAL SYNCHRO (ASE CONTROL PANEL)
ASE YAW SYNCHRO. CONTROL TRANSFORMER
HEADING COMMAND CONTROL TRANSFORMER CPCC-CTC-10-AS-1 OR EQUIVALENT
NC
NO
ASE YAW SYNCHRONIZER MOD.
M
G
TO ASE YAW DRIVER DEMODULATOR
YAW-ROLL CROSSFEED
GE 3S2791F3100A9
YAW PEDAL
+28
SET
REL
ALLIED CONT. MPA-12
RELEASE BUTTON
+28V
H1
FROM COMPUTER
H2
D/A
"A"
"C"
Σ
200:1 REDUC.
DWG "G" SERVOAMP-MOTOR-GEN.
ELECTRIAL RESOLVER CPCC-CSC-10-AS-1 OR EQUIVALENT (DOUBLE-END SHAFT)

UNLESS OTHERWISE SPECIFIED:
DIMENSIONS ± ______ ~~ANGLES ±~~ ______
BREAK EDGES .005-.025. FILLET RAD ______
SURFACES HAVING A COMMON AXIS ~~CONCENTRIC~~
WITHIN ______ TIR. ~~CLEANING, PRESERVATION AND~~
~~HANDLING PER HS1550-C___P___~~

~~DIMENSIONS SHOWN ARE AFTER PLATING & SIMILAR~~
~~PROCESSES & BEFORE PAINTING. THREADS PER~~
~~MIL-S-7742. DRAWING INTERPRETATION PER HS1360.~~
~~SURFACE CHARACTERISTICS: MIL-STD-10 PER HS1082.~~
~~△ MARK PART IDENTIFICATION: MIL-STD-130 PER HS333.~~

NEXT ASSY	USED ON
APPLICATION	

		APPROVALS		DATE
MATERIAL		DRAWN	[illegible]	[illegible]
		CHECKED		
		DRAFTING		
		DESIGN		
HARDNESS		MATERIALS		
HEAT TREAT SPEC		PROJECT		
		COST		
		FACTORY		
SURFACE COATING		RELEASE		DATE
MFG SPEC		EXPERIMENTAL		
		PRELIM PROD.		
		PRODUCTION		
MAKE FROM		PROD. CODE		

Hamilton Standard
WINDSOR LOCKS, CONNECTICUT • U.S.A.

YAW CHANNEL-HEADING COMMAND LOOP

CODE IDENT NO.	SIZE	
73030	C	SK52204
CONTRACT NO.		
SCALE: ~	WEIGHT: LB	SHEET

3-30220-002

NOW 62-0873-D

FPC-1

REVISIONS			
SYM	DESCRIPTION	DATE	APPROVAL

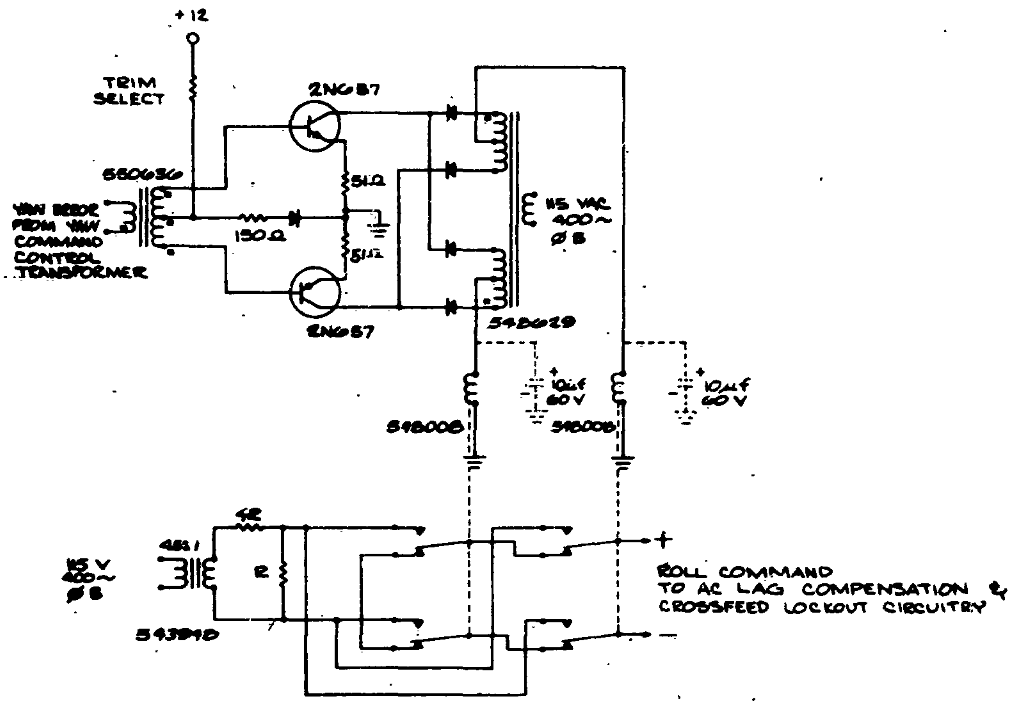
+12
TRIM SELECT
2N657
550636
YAW ERROR FROM YAW COMMAND CONTROL TRANSFORMER
150Ω
51Ω
51Ω
2N657
115 VAC 400~ ØB
548029
10µf 60V
10µf 60V
548008
548008
4Ω
48:1
115 V 400~ ØB
R
543940
+
−
ROLL COMMAND TO AC LAG COMPENSATION & CROSSFEED LOCKOUT CIRCUITRY

SK52203

1- ALL DIODES ARE IN695
NOTES:

UNLESS OTHERWISE SPECIFIED:

		APPROVALS		DATE
MATERIAL	~	DRAWN	B. [illegible]	7-10-63
		CHECKED		
		DRAFTING		
		DESIGN		
HARDNESS	~	MATERIALS		
HEAT TREAT SPEC	~	PROJECT		
		COST		
		FACTORY		
SURFACE COATING	~	RELEASE		DATE
MFG SPEC	~	EXPERIMENTAL		
		PRELIM PROD.		
		PRODUCTION		
MAKE FROM	~	PROD. CODE		

NEXT ASSY | USED ON
APPLICATION

HAMILTON STANDARD
DIVISION OF UNITED AIRCRAFT CORPORATION
WINDSOR LOCKS, CONNECTICUT, U.S.A.

ROLL COMMAND
GENERATOR

CODE IDENT NO. 73030
SIZE C
SK52203
CONTRACT NO.
SCALE: NONE
WEIGHT: LB
SHEET

3-30220-002

NOW 62-0873-0 FPC-1

When the Yaw-Roll Crossfeed signal is greater than 2V - AC (equiv. 10°) the Roll Command Generator feeds out ± 5.15 V AC signal (equiv. 25° roll), the size depending on the sense of the heading error at all other times the Roll Command Generator output is grounded.

3.3.7.1.8 Crossfeed Lockout Circuitry (Ref. SK 52205)

This network handles three inputs: Yaw-Roll Crossfeed, Pitch-Roll Crossfeed, and Drift Velocity Control. The Yaw-Roll Crossfeed is used when the Heading Command Loop is operated but is switched out during the transition to hover, to prevent a large roll angle command from appearing while the vehicle is transitioning. In its place, the Pitch-Roll Crossfeed is applied to prevent vehicle tilt during the tail end of the transition. When in hover, the pilot may select to use the Drift Velocity Control by depressing the DRIFT CONTROL momentary switch. When he starts the transition to cruise, the Drift-Velocity Control will automatically switch out and only the Pitch-Roll Crossfeed will remain. When the vehicle accelerates past 50 knots, the Pitch-Roll Crossfeed will switch out and the Yaw-Roll Crossfeed will be activated. This is summarized in the following:

TABLE 9

Crossfeed Lockout

Velocity Command	Forward Speed	Yaw-Roll Crossfeed	Pitch-Roll Crossfeed	Drift Control
V_c	50 Knots	In	Out	Out
V_c	50 Knots	Out	Out	Out
V_h	50 Knots	Out	In	Out
V_h	50 Knots	Out	In	Out
V_h	Hover	Out	In	Available

REVISIONS			
SYM	DESCRIPTION	DATE	APPROVAL

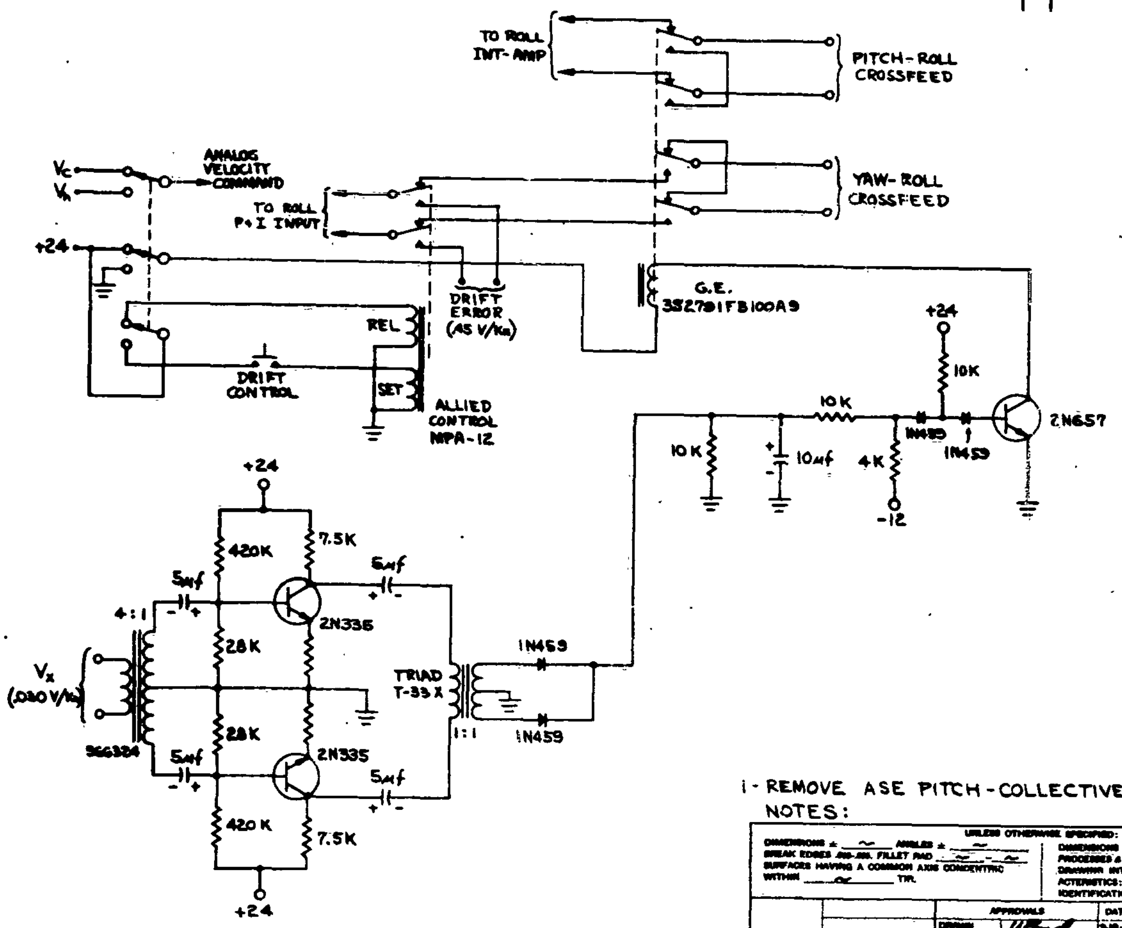
TO ROLL INT-AMP
PITCH-ROLL CROSSFEED
YAW-ROLL CROSSFEED
V_c
V_h
ANALOG VELOCITY COMMAND
TO ROLL P+I INPUT
+24
DRIFT ERROR (.45 V/Kn)
G.E. 3S2791F8100A9
REL
SET
DRIFT CONTROL
ALLIED CONTROL MPA-12
+24
10K
2N657
10K
1N459
1N459
10K
10μf
4K
-12
+24
420K
7.5K
5μf
5μf
4:1
2N335
V_x (.030 V/Kn)
28K
28K
TRIAD T-33X
1:1
1N459
1N459
566324
5μf
2N335
5μf
420K
7.5K
+24

SK52205

1 - REMOVE ASE PITCH-COLLECTIVE CROSSFEED

NOTES:

UNLESS OTHERWISE SPECIFIED:

DIMENSIONS ± ~ ANGLES ± ~
BREAK EDGES .005-.015 FILLET RAD ~ - ~
SURFACES HAVING A COMMON AXIS CONCENTRIC
WITHIN ~ TIR.

DIMENSIONS SHOWN ARE AFTER PLATING & SIMILAR PROCESSES & BEFORE PAINTING. THREADS PER MIL-S-7742. DRAWING INTERPRETATION PER HS1300. SURFACE CHARACTERISTICS: MIL-STD-10 PER HS1000. △MARK PART IDENTIFICATION: MIL-STD-130 PER HS000.

NEXT ASSY	USED ON
APPLICATION	

		APPROVALS		DATE
MATERIAL		DRAWN	WBond	3-18-63
		CHECKED		
		DRAFTING		
		DESIGN		
HARDNESS		MATERIALS		
HEAT TREAT SPEC		PROJECT		
		COST		
		FACTORY		
SURFACE COATING		RELEASE		DATE
MFG SPEC		EXPERIMENTAL		
		PRELIM PROD.		
		PRODUCTION		
MAKE FROM		PROD. CODE		

HAMILTON STANDARD
DIVISION OF UNITED AIRCRAFT CORPORATION
WINDSOR LOCKS, CONNECTICUT, U.S.A.

CROSSFEED LOCKOUT CIRCUITRY

CODE IDENT NO. 73030
SIZE C
SK52205
CONTRACT NO.
SCALE: ~
WEIGHT: LB
SHEET

3-30220-002

FPC-1

3.4 Digital System Design

3.4.1 Introduction

The design of the digital portion of the Flight Path Controller involved studies and simulations leading to the requirements of the system computer, design of the digital interface equipment, and the formulation of the computer program. The computer studies covered the feasibility of using channelized system or a central processor and whether the existing coupler functions should be digitalized or not. Simulation of the navigation section of the computer was directed toward establishing the computer speed, word length, and the type of integration approximation necessary to maintain the system accuracy. The digital interface equipment was designed for 17 real time inputs to the computer, 12 manual initial condition inputs, and 28 real time computer outputs consisting of 15 data words plus eight discrete commands. While the programming of the system equations is an essential task in itself, it also provides detail information as to the computer memory size and calculation speed required.

3.4.2 Design Conclusions

The results of the digital simulation conducted on the system indicate that a high speed, parallel word digital computer will be required to solve the system equations with a reasonable accuracy. By reasonable accuracy, it is meant that the computer contribution to the system position and velocity errors will be in the order of .5 nautical mile and .5 knot, respectively, after one hour of flight. To achieve this accuracy a computer having the following basic characteristics is required.

1. Word Length - 30 bits

2. Memory

   a) Program - 3000 words
   b) Data - 1000 words

3. Typical Operation Time

   a) Addition - less than 24 μsec.
   b) Multiplication - less than 150 μsec.

It is felt that a computer with this basic capability is within the present state-of-the-art.

The word length requirement is based on the computer round-off error experienced by the simulation on the IBM 7090. A 30 bit word (29bits + sign) will result in a one hour position error of approximately 1000 feet due to round-off.

The remainder of the computer error will then be a dynamic type which depends on the iteration time and the computer approximations used. While extensive dynamic simulations were not performed, the existing results indicate that a high order integration approximation such as fourth order Runge-Kutta is required to hold the dynamic errors to a reasonable value. By using fourth order Runge-Kutta and an iteration time of .2 second the combined round-off and dynamic errors should not exceed .5 nautical mile in one hour.

The computer speed requirement and the memory size is based on the length and complexity of the computer program. In order to accomplish all the system functions and maintain a .2 second iteration time in the Navigation Loop, the above operation times are required. This is particularly true of the multiply time, since half of the present calculation time is expended on multiply operations. The present computer program consists of approximately 2500 instructions and 700 data locations which results in the memory size requirement.

An investigation of the advantages and disadvantages of using a channelized digital system as opposed to a central processing unit resulted in the selection of the central processor on the basis of quantity of hardware. The amount of circuitry involved in channelizing the entire system to yield the same system accuracy was unreasonably large while the central processor essentially provides a built-in time sharing capability.

In designing the digital interface equipment, simplicity of the computer input and output capability was achieved. The computer need only have a one-word input channel and a one-word output channel to handle all system data and control functions. This approach was taken so that input-output capability would not restrict the choice of computer.

3.4.3 Coupler Trade-Off Study and Centralized VS Channelized Study.

A study was made on the feasibility of performing the ASE coupler functions digitally. Two approaches to this are possible; one being through the use of the central digital computer, whose main function is to perform the inertial guidance computations, and the other being with a channelized computer whose sole purpose will be to perform the coupler functions. In an effort to provide an adequate comparison of the two methods, a single coupler channel will be chosen and discussed. In actuality, there are three such coupler channels, the pitch, roll and collective. The most complex of these are the pitch and roll and for this study, the pitch channel has been chosen to illustrate the comparison.

3.4.3.1 Centralized Computer

The more straightforward approach to the implementation is with the central computer. It has the capability of performing a large number of mathematical operations and logical decisions and thus requires only the proper programming, assuming digital inputs are avaiable in the correct form, to implement the coupler functions. The central computer approach will therefore be discussed first.

The three main inputs to the pitch coupler channel are (1) longitudinal acceleration from an accelerometer, (2) velocity from AN/APN-130 Doppler navigation set and (3) cable angle with respect to the horizon measured by sonar detecting-ranging set AN/AQS-10. The first of these, the accelerometer, must be a type that permits digital readout. The inertial guidance accelerometers are of such a type (pulse torqued) and they are already read periodically by the central computer. It would be a relatively simple matter in the central computer approach to use the accelerometer signals also for the coupler functions. Since the coupler requires acceleration only for short term compensation, the accuracy available will be considerably greater than required and will allow for reasonable simplification.

The AN/APN-130 doppler velocity sensor produces a pulse train whose frequency is proportional to velocity. The inertial guidance system requires the use of doppler velocity and the necessary counters and gating circuitry are already available to convert the pulse trains to usable binary information.

It is again a simple matter to use this same information in the coupler computations.

The sonar detecting-ranging set AN/AQS-10 normally delivers a synchro signal whose magnitude represents the position of the sonar cable with respect to the horizon. This synchro output can be used to rotate a similar shaft device which will, in turn, position a shaft encoder. The encoder will provide a direct reading in binary of the existing cable angle.

In the doppler mode, the velocity signal obtained from the AN/APN-130 must be compared to a desired velocity which is dialed in by the pilot. This device might be a shaft encoder whose shaft would be attached to a circular dial and whose output would provide a binary (or gray code) indication of angular position. The hover trim control which allows the pilot to control pitch drift rate up to ± 6 kts would be a shaft encoder of the same type. Finally, the cable angle control which allows the pilot to control roll drift up to ± 3° would also be a shaft encoder.

To best illustrate the techniques by which the central computer would proceed through a typical cycle of the pitch coupler channel, a simplified program has been compiled. Each step in this program represents an operation and may be made up of several actual computer steps.

1. Read accelerometer and store
2. Read doppler velocity and store
3. Read desired drift velocity and store
4. Read cable angle error signal and store
5. Read cable angle control and store
6. Read hover trim control and store
7. Read mode. If doppler, continue. If cable angle, jump to 26
8. Modify 2 with appropriate conversion factors
9. Modify 3 with appropriate conversion factors
10. Subtract 2 from 3
11. If 10 is greater than 15 kts., let 10 be zero
12. Multiply 10 by Δt
13. Add 12 to 10
14. Modify 1 with appropriate conversion factors
15. Average 14 in with last 10 seconds of accel. info
16. Add 15 to 13
17. Modify 6 with appropriate conversion factors
18. Subtract 17 from 16
19. Read out 18 to hover indicator

20. If 18 is greater than Vmax., use Vmax
21. If 18 represents a change of greater than ΔV over the previous value, use ΔV
22. Read 21 out to D/A converter
23. Subtract 18 from VT
24. Divide 23 by K and generate the number of pulses indicated by the quotient to stick trim valve
25. Stop, go to 1
26. Modify 4 with appropriate conversion factors
27. Modify 5 with appropriate conversion factors
28. Add 4 to 5
29. Multiply 28 by Δt
30. Add 29 and 28
31. Modify 1 with appropriate conversion factors
32. Average 31 in with last 10 secs. of accel. info
33. Add 32 to 30 ΔV
34. Refer to 33 as 18 and jump to 19

3.4.3.2 Channelized Computer

The channelized approach requires a separate circuit for each function much the same as an analog device. This is commonly done digitally by a special purpose device such as a digital differential analyzer or incremental computer. Such functions as addition, subtraction and integration are possible with such a computer but the device is severely limited when it comes to data storage, logic decision or complex function generation. Unfortunately, these last three operations are all required in this application as can be seen from the sample program shown previously.

In addition some of the sensor inputs must be modified to allow use with a channelized computer. Unless the central computer is programmed to provide the channelized coupler with the accelerometer and doppler signals, they too must be sensed and modified with addition circuitry. It, therefore, becomes quickly apparent that the channelized approach for the complete coupler impementation will be quite large and expensive and to make a channelized digital approach feasible at all, a compromise must be made. A possible compromise would be to allow only the input comparisons to be performed digitally (such as actual minus desired velocity, actual minus desired altitude, etc.); the difference would then be converted to analog and the remainder of the functions performed with analog circuitry. Little can be gained by doing this, however, unless an extremely accurate difference is required.

From the above discussion, the following trade offs are apparent. The channelized approach allows a separate computation of all coupler functions with little or no reliance on the control computer. It requires a separate circuit for each computation, however, and some operations such as scaling and conversion will require special storage devices of reasonable complexity. The central computer, on the other hand, will offer flexibility for all computations and logic decisions which are required. Many inputs are already available and require no extra circuitry to obtain. Conversely, additional program memory is required and, even more important, additional program time. With a large number of computations already being handled within limited time, the additional requirements of the coupler functions would seem undesirable.

3.4.3.3 Conclusion

As a result of the previous discussion, it is therefore, recommended that if a choice must be made between using a digital channelized coupler and a central computer implemented coupler, the central computer approach is definitely more desirable. If, in addition, a choice must be made between continued use of the present analog coupler or conversion to the central computer implementation, it would be wise to remain with the analog approach. The central computer is presently burdened with an increasingly large computational load and any method of reducing or at least limiting this would be worthwhile.

3.4.4 Digital Simulation

3.4.4.1 Introduction

Basic difficulty arising from the use of a digital computer for the purpose of strapped down inertial navigation arises from the fact that the primary output of the system is a direct result of integration; but integration is performed in a digital computer by successively summing discrete quantities which may or may not be weighted in some manner and can thus only estimate the actual value of an integral. In general, the higher the order of integration and the smaller the sampling time (Δt) used, the closer the value of the integral can be approximated. Of course, since the raw data inputs to the computer are operated on in real time, there is only a finite amount of time available for calculations and a definite lower limit is established for the integration interval. Physical considerations of the probable dynamic inputs for an actual flight set limits on the integration time (interval) and this in turn restricts the choice of integration technique. Estimates of this sort tend to fix the basic computer speed. Similarly a decision relating to the speed of the machine can place restrictions on the sampling time and integration scheme. To further compound the problem, decimal fractions can only be represented in binary form to a certain accuracy with a given number of bit positions. The uncertainty associated with a result gets larger as the number of operations performed to achieve this result increases and/or as the quantities involved in the calculation increase in absolute value.

In general if the order of integration is increased or the sampling time decreased, the system will be capable of following higher order dynamic inputs. But the basic machine speed may also have to be increased due to the larger number of operations per unit time, and the word length may have to be longer to maintain the same accuracy. Taking the other case a lower order of integration or longer sampling time does not require as high a machine speed but may require the same number of bit positions and will not be as satisfactory on following the higher order dynamic inputs.

Consideration of all these interrelations and trade-offs are best considered by simulating certain aspects of a flight with a digital computer and writing the program with easily changeable parameters directly related to those variables discussed above. In this way, the speed, word length, and integration techniques can be chosen for the actual flight computer.

3.4.4.2 Description of Earth Model

Most children are at some educational level told that the earth is shaped like a ball, but their senses tell them that it cannot be perfectly smooth. As their knowledge increases they learn that the earth's surface features are very small when compared with its dimensions and also, that the earth more closely approximates the geometric shape of an ellipsoid of revolution than a sphere. Becoming more and more sophisticated attempts are made to make better and better mathematical models to describe the shape of the earth. However, to choose a model that must apply everywhere and not just in some predesignated locality the ellipsoid of revolution appears to be the most reasonable. Therefore, the model used in the actual flight system will be based on this geometrical shape and have an appropriate gravitational field model associated with it. However, since the purpose of this simulation is to spell out computer errors and limitations, it would seem that the most accurate inputs possible that are compatible with a specific model and also that the most tractable model, within reason, should be used during the simulation; hence, the model chosen for this effort is a spherical earth. To be specific, for the purposes of the simulation the earth is postulated to be as follows:

1. its geometrical shape is a sphere whose radius is 20,895,118 feet

2. its mass is homogeneously distributed and produces a gravitational acceleration of 32.000000 ft/sec^2 at the earth's surface

3. it rotates upon an axis passing through its center at a rate of 7.292115 X 10^{-5} r/sec

4. that the common definitions of east, west, north, south, latitude, longitude, up and down hold

Furthermore it is assumed that all of the navigation runs will be made on the earth's surface, thus eliminating the possibility of a positive feedback situation arising due to a $\left(\frac{G}{R^2}\right)$ type gravitational attraction model in the position tracking loop.

Having chosen an earth model for the simulation, the appropriate inputs for a desired situation are then generated. Next the computer results must be compared with what the inputs indicate should happen. Since computer errors enter into the calculations throughout the program a direct comparison of end results is not the most rewarding; hence, the computer program was separated into three parts: (1) the direction cosine computation, (2) the base motion isolation and (3) the position tracking loop -- so that the errors contributed by each of these separate sections could be separately evaluated. The first two sections can be analyzed using the same inputs; however, the third portion, the position tracking loop, required either separate inputs or a physical interpretation of what the errors represented and knowledge of the results due to these errors. Inasmuch as the response in terms of the position is an important phase of the system's operation and the deviation of the response of this digital approximation to the response of its analog counterpart is desirable information, the choice was made to use the erroneous outputs of the base motion isolation as inputs for the position tracking loop; thus automatically having a physical acceleration profile with realistic errors superimposed. This necessitates a knowledge of the response of the analog system to various error profiles which is accomplished by the generation of the transfer function to which the position tracking loop corresponds. This transform comes directly from an elementary servo mechanism analysis of the position tracking loop, as shown in the diagram of the basic navigation system (Reference Figure 3). Operation on the input profile with the transfer function and comparison of this result with the computer printouts then yield the error contributed by the position tracking loop.

For the computer simulation the basic navigation system as outlined in Section 3.1.4, was programmed. The proposed method of servo restrained loop for the final system was not programmed because it was thought unnecessary to achieve the established goals and because it would have been too time consuming to check out the entire program.

3.4.4.3 Inherent Computer Errors

In general there are two types of errors inherent in a digital computer when it is used in a real time system. These errors are functions of the word length (number of bits per word) and the cycle time (iteration time) of the computer. The first of these errors is generally referred to as either a round off error or a number truncation error. The second error is a dynamic or computer approximation type error which results from the discrete (noncontinuous) operation of the computer.

The round off or number truncation error arises from the fact that words in the computer are limited to a finite bit length and, therefore, have a definite granularity. For example, if we wanted to represent distance up to 1,000 feet in a 10 bit machine, the granularity of the least significant bit would approximately 1 foot. If the machine has a round off capability, the distance will have an uncertainty of ± .5 foot. If the number is truncated (least significant part ignored), the distance will have an uncertainty of -0 to +1.0 foot. In general, the truncation type of error exists in a digital machine. This error becomes important when an iteration process such as an integration approximation is used. The uncertainty of each increment consists statistically of a bias which is one-half of the value of the value of the least significant bit (LSB) and an associated RMS error. The error resulting from N iterations is $E = N\ (.5)\ (L.SB) + \sqrt{N}\ \sigma$.

This error can be reduced by increasing the word length of the computer or by reducing the number of iterations of the calculation.

The dynamic error in a digital computer is a function of the order of the input signal, the order of the computer approximation of the process being simulated and the cycle time (Δt of an iteration) of the computer. In the case of integration, the higher the order of the computer approximation the smaller the dynamic error becomes; also, as the computer cycle time is reduced the approximation approaches continuous integration and the dynamic error again decreases. It is, therefore, desirable to have as high an order of approximation and as small a cycle time as possible to reduce the dynamic error.

The ideal solution to computer errors would be to have a machine with infinite word length and infinite speed which would make both the round-off and dynamic errors negligible. Since this is an idealization, the final computer error is generally a compromise between round off error and dynamic error.

3.4.4.4 Discussion of Simulation

The simulation of the basic navigation system was done on an IBM 7090 general purpose digital computer. For the various simulation runs, analytic inputs were generated. From the analytic inputs certain quantities, e.g., the direction cosines between the inertial and present position axes, inertial position, etc., were calculated by engineering personnel and compared with computer results at different times during each run. From plots of the errors (differences between hand calculated and machine calculated results) it was possible to construct error models which accounted for systematic errors in the computer. Figure 41 compares the actual errors and those predicted by the model of the input errors; discrepancies between the two plots are caused by round off effects in the position tracking loop (PTL), linear approximations of the input errors, and due to the inaccuracy of the hypotheses upon which the loop's transfer function was derived.

In general it was found that the E and N axes were much more sensitive with respect to errors than the U axis. This is attributed to the fact that the rotation of the earth results in a changing acceleration along the E and N axes for normal ranges of latitude. This acceleration change results in a position error due to any time lag in the position tracking loop. The corresponding numerical position integrations along the E and N axes do not approximate as closely as the U axis an analog integration.

ACTUAL AND PREDICTED VALUES OF POSITION ERROR IN U VERSUS TIME

Figure 41

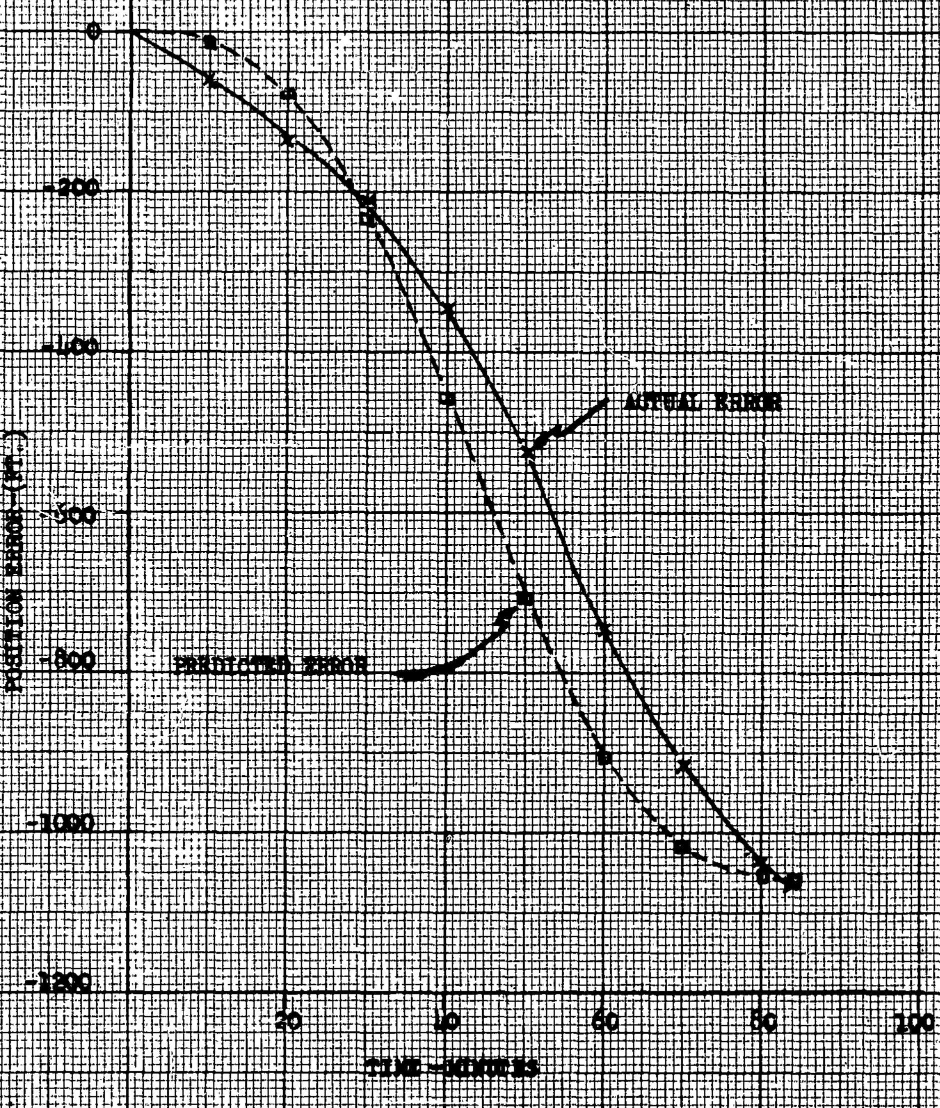

NO. 340 -20 DIETZGEN GRAPH PAPER
20 X 20 PER INCH
EUGENE DIETZGEN CO.
MADE IN U. S. A.

Figures 42, 43 and 44 show the error plots of longitude, latitude, and radius from the center of the earth, respectively, (as calculated by the computer) versus elapsed time for the situation in which the system was motionless with respect to the earth.

The changes made in the simulation that account for the various longitude errors, as shown in Figure 42, are:

Run 1: A relatively large iteration time (10 seconds) in the PTL accounts for the large oscillation.

Run 2: The oscillation in this run (and in Runs 3 and 4) is due to time lags introduced in the digital implementation of the system; however, for this run (and Runs 3 and 4) the PTL iteration time is reduced to one second, thus resulting in a much smaller over-all lag than in Run 1.

Run 3: The amplitude of oscillation shown for this run has been reduced by a better choice of the direction cosine computation (DCC) and base motion isolation (BMI) iteration time.

Run 4: This is a repeat of Run 3 on a Philco 2000 general purpose computer which has eight more binary bits of accuracy than the IBM 7090; thus, the comparison of Runs 3 and 4 gives an indication of the effects of round off errors.

The differences in end points of the various runs can be explained as a combination of round off and input lag errors.

The latitude plots are shown in Figure 43 and are described below:

Run 1: The large oscillation in this run is ascribed, as was longitude, to the large incrementing time in the PTL.

Run 2: The oscillation was greatly reduced by reducing the PTL iteration interval.

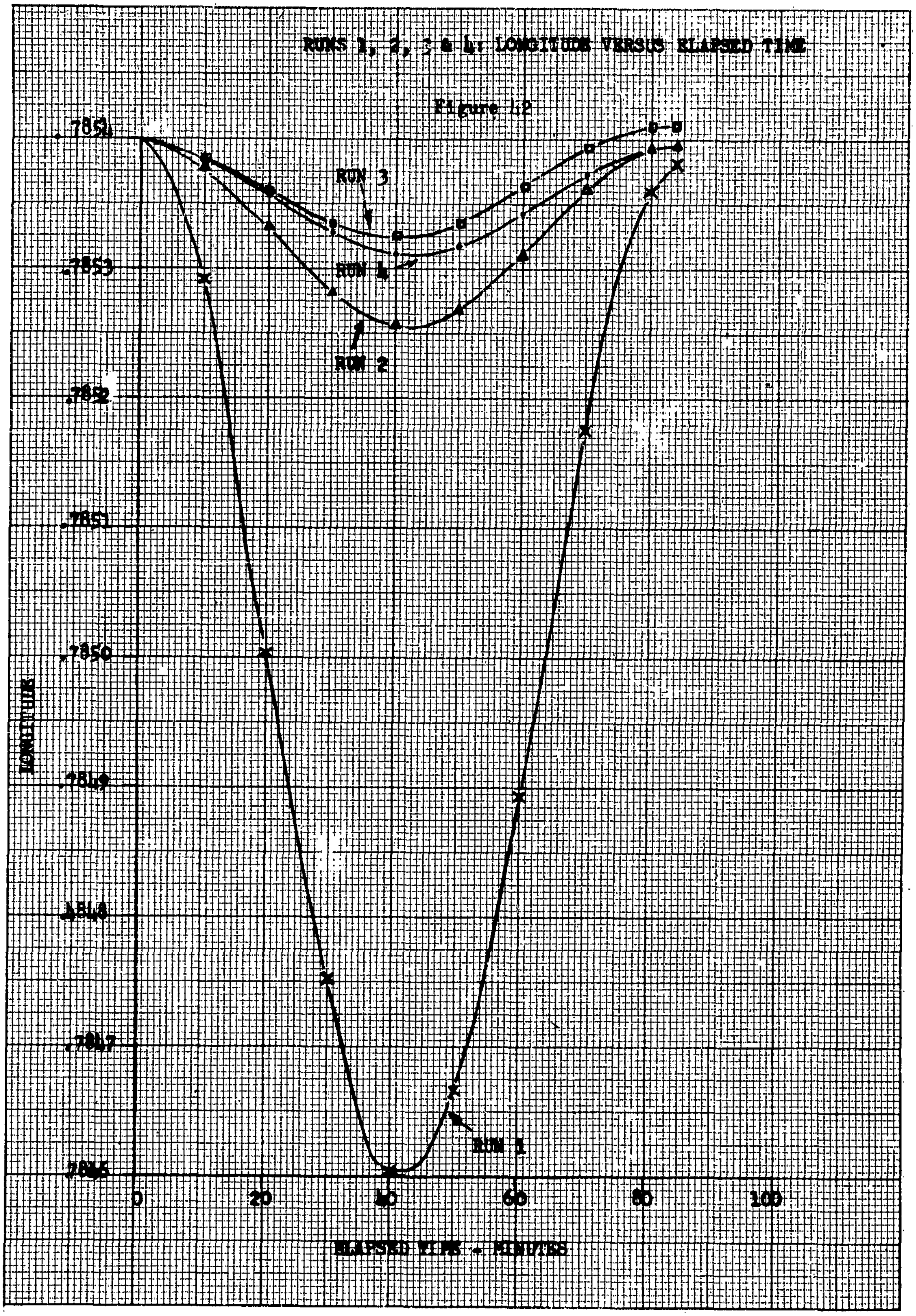

RUNS 1, 2, 3 & 4: LONGITUDE VERSUS ELAPSED TIME

Figure 42

NO. 340 -20 DIETZGEN GRAPH PAPER
20X20 PER INCH

EUGENE DIETZGEN CO.
MADE IN U. S. A.

LATITUDE VERSUS ELAPSED TIME

Figure 43

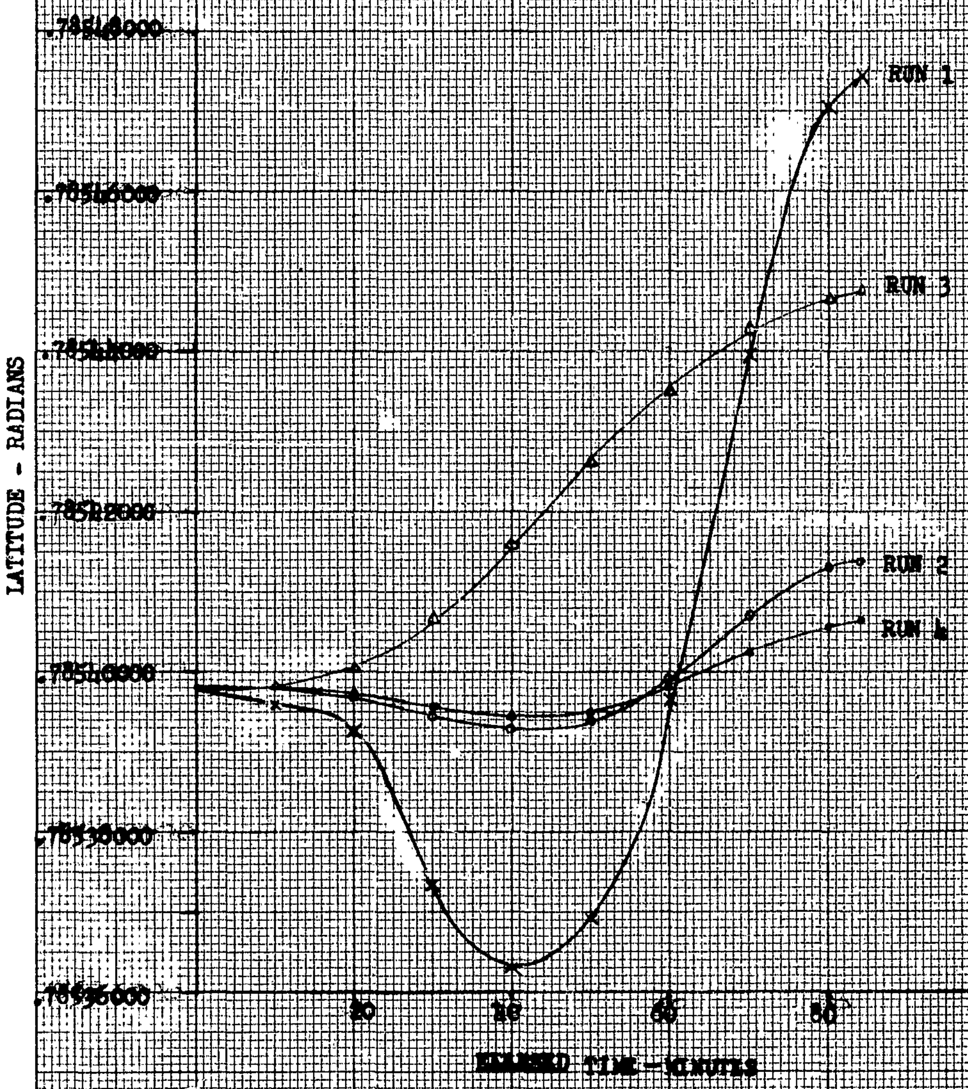

EUGENE DIETZGEN CO.
MADE IN U. S. A.

NO. 340 -20 DIETZGEN GRAPH PAPER
20X20 PER INCH

Run 3: The change of the DCC and BMI incrementing time, noted in the discussion of longitude errors above, has had two notable effects on the plot of latitude. First, the oscillation, which for Runs 1 and 2 was due primarily to a term proportional to cosine (kt), is now constituted mostly of a term proportional to sin (kt); secondly, the slope error has increased from Run 2 to Run 3. Both of these occurences are accounted for by the increased error due to round off in the DCC operation corresponding to the decreased incrementing time of the DCC and BMI.

Run 4: This run dramatically indicates the round off effects mentioned in the discussion above of Run 3; the curve is almost completely a result of time lag errors.

The radius plots, as shown in Figure 44, follow directly from the latitude plots because the variations in U were small as compared with the E and N errors, i.e., the sine of latitude equals the quotient of U divided by ρ (the radius); hence, the plots of radius can be related to the latitude plots, though in a nonlinear fashion.

The final portion of the simulation was a series of runs which compared the errors in the direction cosine computations (DCC) for different numerical integration techniques, viz., rectangular, modified Euler, and fourth order Runge-Kutta. Each run was performed both on the IBM 7090 and the Philco 2000 for a comparison of round off errors. Also for this series of runs a much higher angular rate was used than that used in Runs 1 through 4. The resultant errors indicated from the fourth order Runge-Kutta method were almost 1/100 of the errors generated by the rectangular technique (after 84 minutes of running time). The modified Euler errors fell between these, but no comparison is given because it is reasonably certain that this method could be programmed in a manner which would eliminate a major portion of the error observed.

RUNS 1, 2, 3 & 4 RADIUS ERROR VERSUS ELAPSED TIME

Figure 14

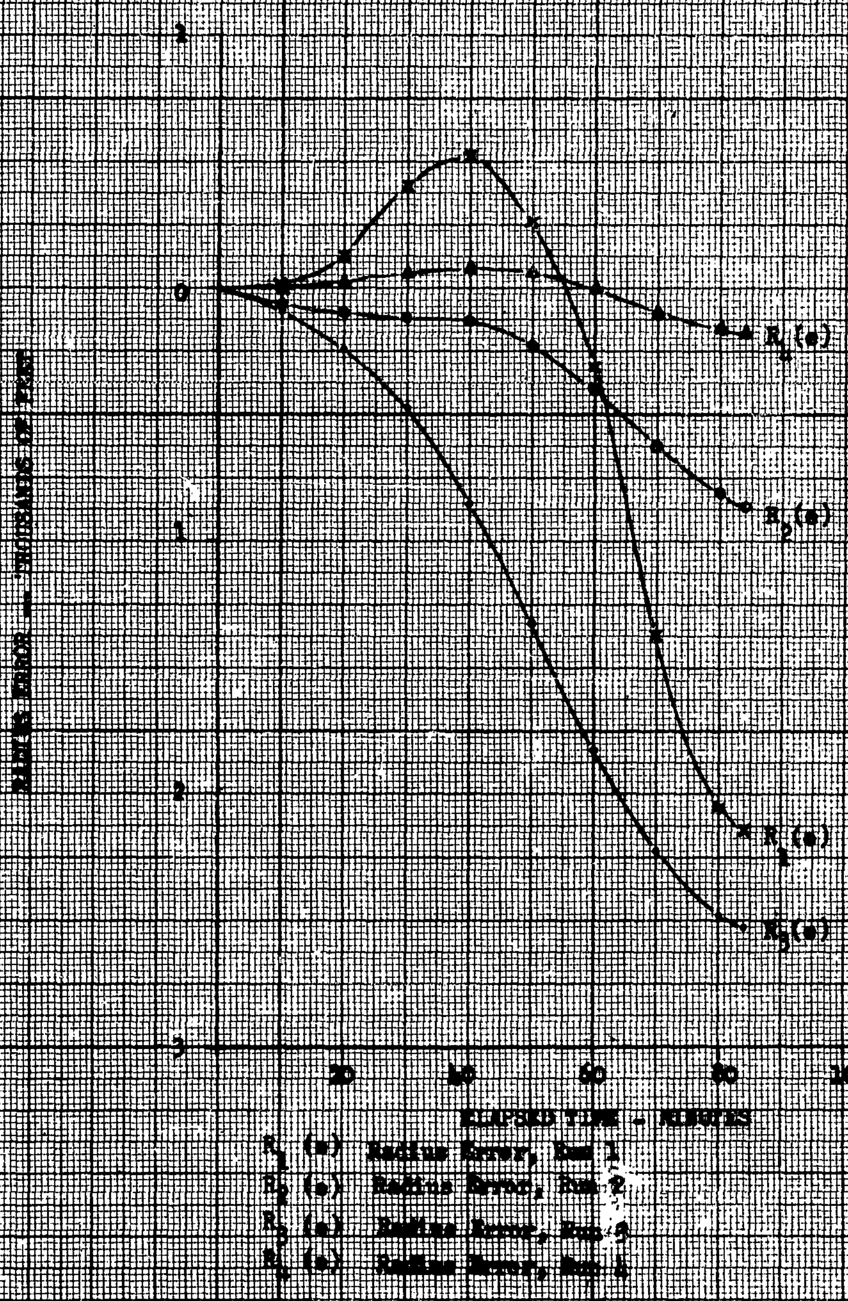

EUGENE DIETZGEN CO.
MADE IN U.S.A.

NO. 340R-M DIETZGEN GRAPH PAPER
MILLIMETER

3.4.4.5 Summary Knowledge Gained From the Simulation

From information gained via this simulation the following changes should yield sufficient accuracy from the computer to perform the required tasks.

1. Let the PTL incrementing time be the same as in the BMI and equal to two-tenths of a second.
2. Use a word length of 29 bits or greater.
3. Use 4th order Runge-Kutta as the integration technique.

The effects of changes (1) and (2) above, are:

- (a) Change (1) is the same type of change as was made from Run 1 to Run 2.
- (b) Change (2) is the same type of change as was made from Run 3 to Run 4.

These changes are improvements of Run 3 results which affect these results in the manner indicated above.

The fourth order Runge-Kutta integration technique is recommended as assurance of following non-linear inputs to a much better degree than rectangular or modified Euler.

3.4.5 Specification for A Digital Computer

This specification defines the requirements of a digital computer which is required to solve the navigation equations involved in a stabilized helicopter flight.

3.4.5.1 Performance

3.4.5.1.1 Type

The computer must be designed for real time control. It must be a general purpose, whole number, stored program device capable of high speed operation.

3.4.5.1.2 Number System

True binary with internal "ones" or "twos" complement operation is required.

3.4.5.1.3 Data Word Length

30 bits per word including sign. Fixed point binary.

3.4.5.1.4 Method of Data Processing

Parallel arithmetic operations, internal word transfer and input-output transfer.

3.4.5.1.5 Operation Times (Typical)

Add and Subtract less than 24 µsec.
Multiply less than 150 µsec.
Divide less than 200 µsec.

3.4.5.1.6 Control

Stored program modifiable by an indexing cycle.

3.4.5.1.7 Desired Instructions

Standard instruction repetoire with the following exceptions:

3.4.5.1.7.1 Sample Switch xx where xx shall specify availability of input information originated by pilot. If an "on" state is sensed, the computer will transfer to a read-in subroutine.

3.4.5.1.7.2 Read external xx where xx shall specify source of input information (buffer, code wheel, etc.).

3.4.5.1.8 Method of Internal Storage

Parallel input-output coincident current magnetic core memory or equivalent.

3.4.5.1.9 Memory Capacity

4096 words, 30 bits per word.

3.4.5.2 Inputs

The computer program shall be loaded into the memory via punched tape with automatic correct load verification.

Data tape inputs shall be read by the computer upon initiation by the pilot prior to a mission.

Manual data shall be inserted into the computer from an external buffer register of 30 bits.

Periodic data shall enter the computer sequentually in parallel through an interface package to be supplied by HSED.

The computer shall generate a discrete command to the interface after each read-in to establish the proper synchronization.

3.4.5.3 Outputs

Periodic outputs shall be transferred sequentually in parallel to a set of output buffer registers of 30 bits.

Identification line under control of the program shall be used to properly route the output information to its destination.

3.4.5.4 Status Panel

There shall be performance indicators, alarm lights, failure indicators and status indicators controlled by navigational results.

3.4.5.5 Mechanical Requirements

Size shall be limited by the space available, 5' high, 2' wide, 2' deep maximum. Weight shall be 500 lbs. maximum.

3.4.5.6 Electrical Requirements

Power will be supplied by the helicopter's available power 400 cps ± 20 cps, 3 Ø 115/200V. 500 watts maximum.

The regulation shall be ± 10%.

3.4.5.7 Environmental Condition

The equipment shall be capable of operating in a temperature range 0°F to 125°F.

The equipment shall be capable of withstanding normal vibration conditions encountered in helicopter flights. Shock Mounting is permitted.

3.4.6 Computer Input - Output Design

3.4.6.1 Input Data Insertion

There are 17 quantities which must be fed into the computer during each cycle. They are (in order):

1. Pitch Gyro
2. Roll Gyro
3. Yaw Gyro
4. X Accelerometer
5. Y Accelerometer
6. Z Accelerometer
7. Doppler #1
8. Doppler #2
9. Doppler #3
10. Doppler #4
11. True Airspeed
12. Cruise Velocity
13. Range (to new Dunk Point)
14. Bearing (to new Dunk Point)
15. E - W Position Fix
16. N - S Position Fix
17. Mode - Option

The first 10 quantities are obtained by counting a pulse train over a given period of time. The resulting words represent new information each cycle and are used periodically in the navigation computations. Quantities 11 - 17 change infrequently, although they are read every cycle to determine if any change has occurred.

The read in sequence is performed at a particular time during each cycle, each word being read in turn into the computer memory until the 17th has been received. The program then proceeds through the regular computations, using the input information from the memory when desired.

In addition to the 17 periodic inputs, there is a separate manual input console which is used to load 12 initial conditions at the start of each mission. These inputs are loaded one at a time in a given order so that no identification is required. Once the inputs have been loaded, the console is no longer required and the program does not return to that read-in subroutine. The 12 inital conditions are as follows:

1. η_H - True Helicopter heading aboard ship (DEG).
2. V_S - Ships velocity (knots).
3. η_S - True ships heading (DEG).
4. λ_S - Ships latitude. (DEG)
5. L_S - Ships Longitude (DEG).
6. R_D - Range between dunks (N.M.).
7. λ_G - Grid latitude (DEG).
8. L_G - Grid longitude (DEG).
9. E_D - Datum Point (N.M.).
10. N_D - Datum Point (N.M.).
11. δ - Arbitrary distance (range-yards).
12. γ - Arbitrary Angle (DEG.)

The design of the input equipment has proceeded under the assumption that the central digital computer possesses at least a 21 bit parallel input word capability. The read-in sequence will proceed as follows: When the input information is ready, an "information ready" signal will be sent to the computer. At a particular point in the program, the computer will observe this signal and, if it is in the affirmative state, then read the contents of the input register. After the information has been stored, the computer will send out an "information stored" signal which will be used to place the next input word into the computer input register. The order of the inputs will identify the information and thus no identification words will be required to accompany the data into the computer.

3.4.6.2 Pulse Torque Amplifier Interface

The six pulse torque amplifier counter-buffers are shown in Drawing B of SK 52212. They are used to obtain a binary count from the pulse trains eminating from the three gyro (pitch, roll and yaw) and the three accelerometer (X, Y and Z) pulse torque amplifiers. Assuming that the cycle time of the computer (the time between read in cycles) will be in the order of 200 ms, and that the pulse torquing rate will be 100 KC, it can be seen that a maximum count of (100,000) x (.2) = 20,000 can result. This requires a binary word of 15 bits, which can represent up to 32,767. A 15 bit binary counter has been designed therefore for each of the 6 pulse trains. At the completion of the

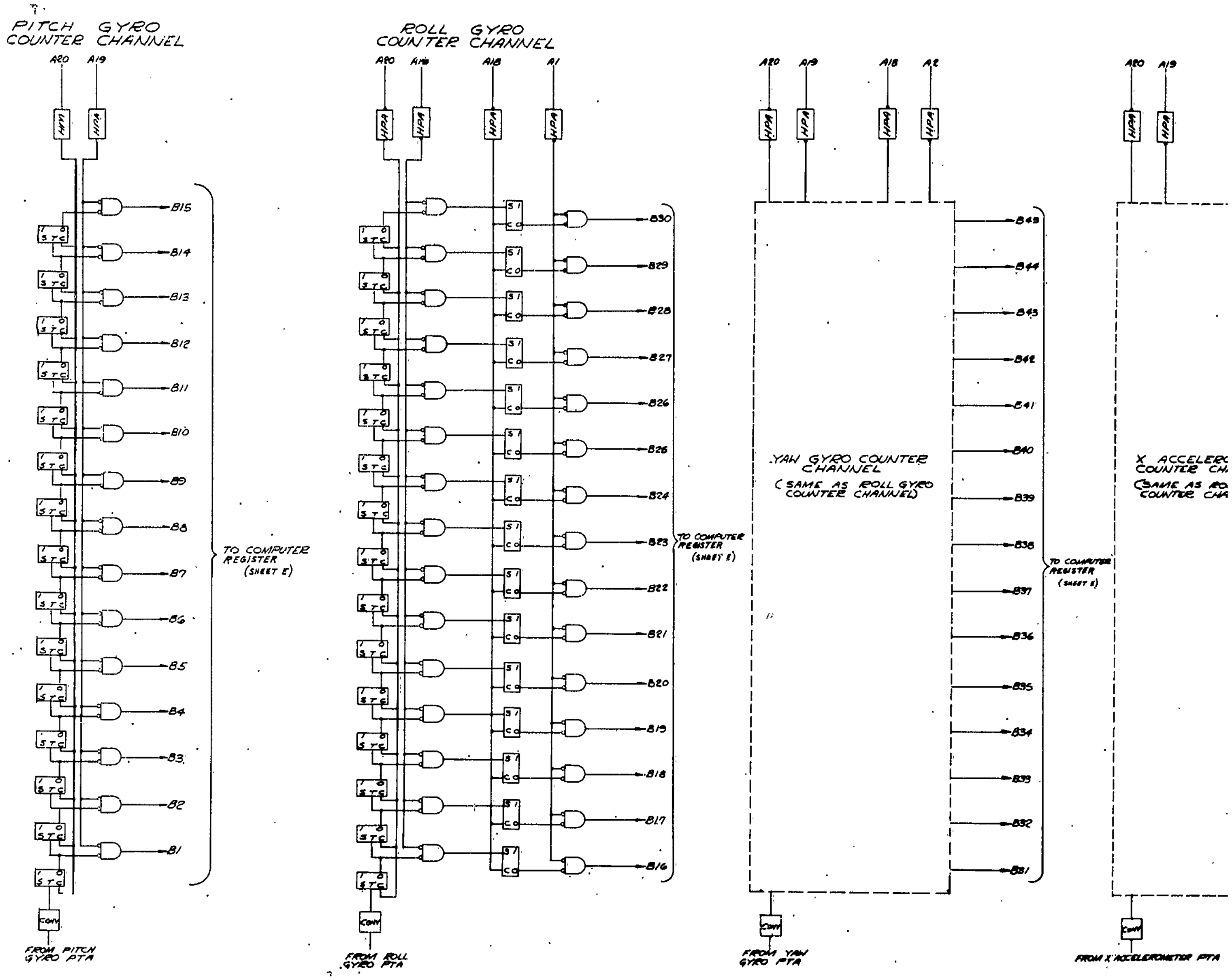
PITCH GYRO COUNTER CHANNEL
A20
A19
HPA
HPA
STC
B15
B14
B13
B12
B11
B10
B9
B8
B7
B6
B5
B4
B3
B2
B1
TO COMPUTER REGISTER (SHEET E)
CONV
FROM PITCH GYRO PTA
ROLL GYRO COUNTER CHANNEL
A20
A19
A18
A1
HPA
S 1
C 0
B30
B29
B28
B27
B26
B25
B24
B23
B22
B21
B20
B19
B18
B17
B16
TO COMPUTER REGISTER (SHEET E)
CONV
FROM ROLL GYRO PTA
A20
A19
A18
A2
YAW GYRO COUNTER CHANNEL
(SAME AS ROLL GYRO COUNTER CHANNEL)
B45
B44
B43
B42
B41
B40
B39
B38
B37
B36
B35
B34
B33
B32
B31
TO COMPUTER REGISTER (SHEET E)
CONV
FROM YAW GYRO PTA
A20
A19
X ACCELER
COUNTER CH
(SAME AS RO
COUNTER CHA
CONV
FROM X ACCELEROMETER PTA

1

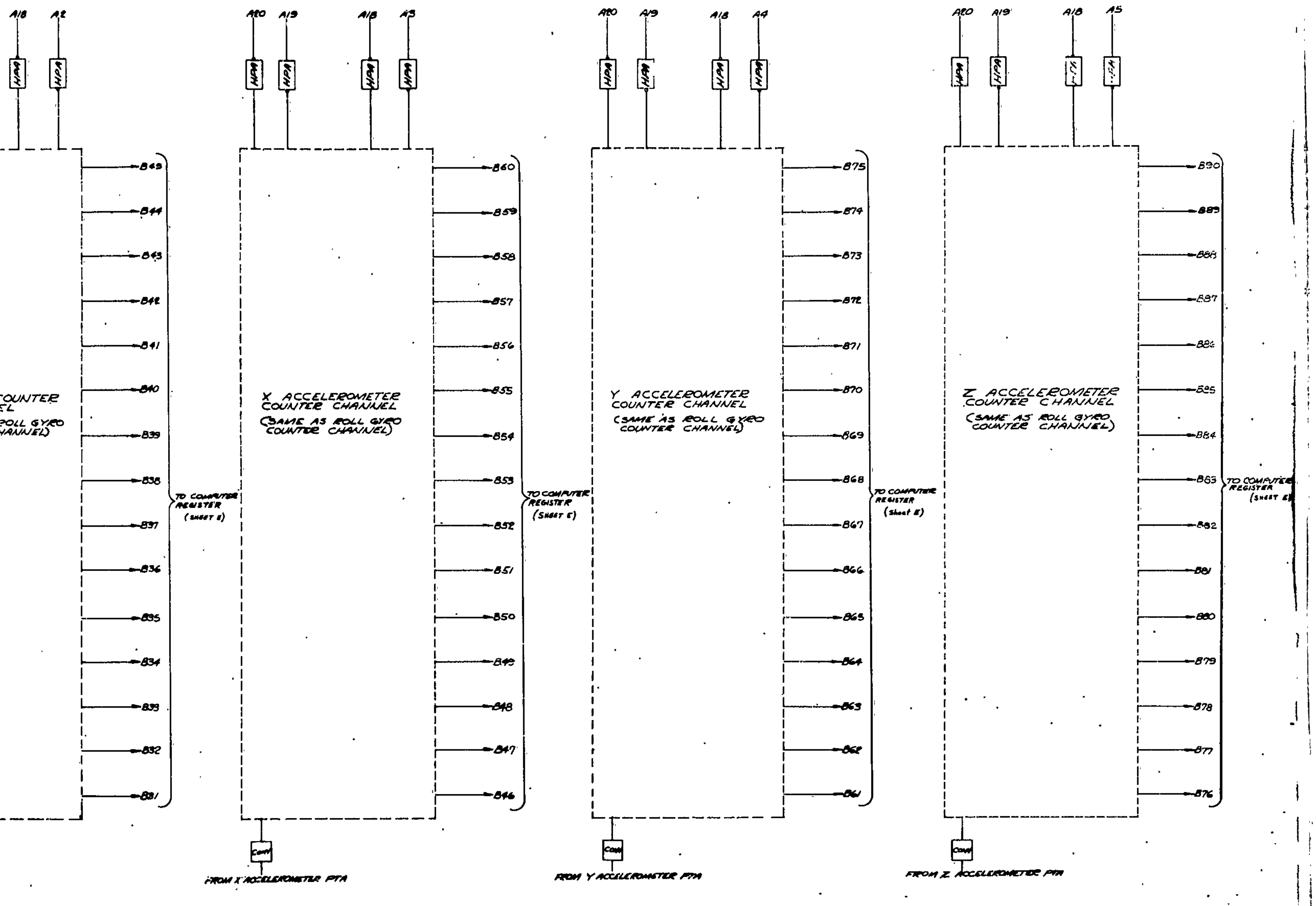

A18
A2
HPA
HPA
COUNTER
EL
ROLL GYRO
HANNEL)
B45
B44
B43
B42
B41
B40
B39
B38
B37
B36
B35
B34
B33
B32
B31
TO COMPUTER REGISTER (SHEET E)
A20
A19
A18
A3
HPA
HPA
HPA
HPA
X ACCELEROMETER COUNTER CHANNEL
(SAME AS ROLL GYRO COUNTER CHANNEL)
B60
B59
B58
B57
B56
B55
B54
B53
B52
B51
B50
B49
B48
B47
B46
TO COMPUTER REGISTER (SHEET E)
CONV
FROM X ACCELEROMETER PTA
A20
A19
A18
A4
HPA
HPA
HPA
HPA
Y ACCELEROMETER COUNTER CHANNEL
(SAME AS ROLL GYRO COUNTER CHANNEL)
B75
B74
B73
B72
B71
B70
B69
B68
B67
B66
B65
B64
B63
B62
B61
TO COMPUTER REGISTER (Sheet E)
CONV
FROM Y ACCELEROMETER PTA
A20
A19
A18
A5
HPA
HPA
HPA
HPA
Z ACCELEROMETER COUNTER CHANNEL
(SAME AS ROLL GYRO COUNTER CHANNEL)
B90
B89
B88
B87
B86
B85
B84
B83
B82
B81
B80
B79
B78
B77
B76
TO COMPUTER REGISTER (SHEET E)
CONV
FROM Z ACCELEROMETER PTA

1 — LETTERING OF INPUT LINE INDICATES SHEET WHERE INPUT ORIGINATES (E.G., A1 MEANS "FROM SHEET A, OUTPUT 1")

NOTES:

UNLESS OTHERWISE SPECIFIED:

NEXT ASSY | USED ON

APPLICATION

MATERIAL

HARDNESS

HEAT TREAT

SPEC

SURFACE COATING

MFG SPEC

MAKE FROM

APPROVALS | DATE

DRAWN

CHECKED

Hamilton Standard

WINDSOR LOCKS, CONNECTICUT • U.S.A.

PULSE TORQUE
AMPLIFIER INTERFACE
LOGIC DIAGRAM

CODE IDENT NO. 73030

SIZE

SK52212

SCALE: NONE

WEIGHT: LB

SHEET B

FPC-1

2

200 ms. counting period, a pulse is applied to A19 of each channel and the contents of the counters at that time are gated down into a storage register. The gating pulse is timed so that no torquing pulses will be arriving at the counter input and thus no counts are gained or lost during any cycle. Immediately after the contents are gated from the counters, a reset pulse is applied to A20, clearing the counters to zero and preparing them for the first pulse of the next cycle.

The word from the pitch gyro counter (B1 - B15) is gated directly into the computer input register shown in Drawing E of SK 52212. This can be done since it is the first word to be read by the computer and need not be temporarily stored in a separate buffer. All other readouts are stored in an adjoining buffer and held until the "information stored" signal from the computer commands their gate down into the computer input register.

3.4.6.3 Doppler Interface

The pulses arriving from the doppler unit, see Drawing C of SK 52212, are separated into two channels, one for positive and one for negative velocity. To gain a usable count, it becomes necessary to obtain the difference between the sum of the pulses in the positive channel and the sum of the pulses in the negative channel over a given period of time. This is accomplished through the use of an up-down counter with ± zero correction logic. The frequency of the two channels varies over a range of 0 - 3000 cps. With a cycle time of 200 ms., this provides a maximum count (one channel zero cps and the other 3000 cps) of 600. A 10 bit counter will represent up to 1023 in binary and will be used in this application. Since pulses cannot exist in both the positive and negative channel simultaneously, the two channels are combined and fed into the input of the counter. A detector F/F senses whether the input pulse is a positive (up count) pulse or a negative (down count) pulse and controls the count gates accordingly. If the total number of pulses is positive at the end of a count cycle, the number ($\overline{A-J}$) is gated from the counter into the buffer to await read-in by the computer. If the number is negative, it will be represented in the counter as a "ones complement" and will therefore be gated out of the opposite side (A-J) in order to obtain the true form.

REVISIONS				
	SYM	DESCRIPTION	DATE	APPROVAL

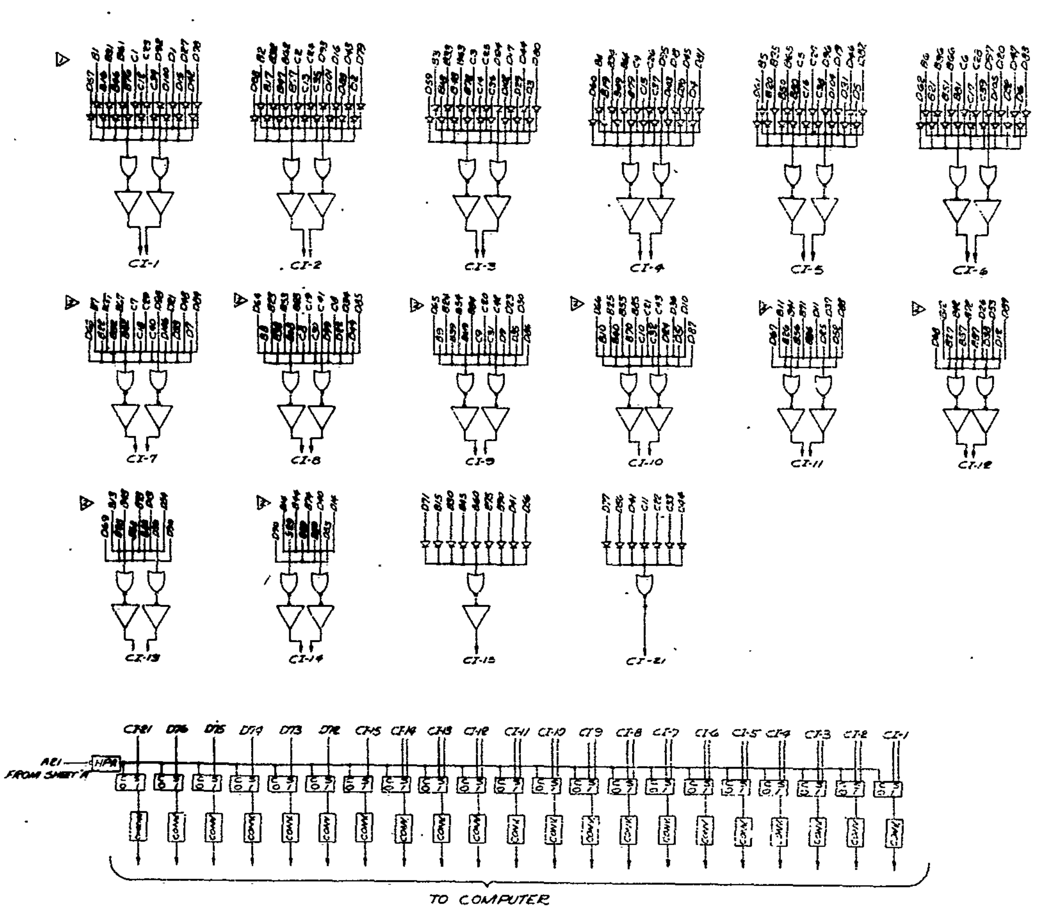
CI-1
CI-2
CI-3
CI-4
CI-5
CI-6
CI-7
CI-8
CI-9
CI-10
CI-11
CI-12
CI-13
CI-14
CI-15
CI-21
CI-21
D76
D75
D74
D73
D72
CI-15
CI-14
CI-13
CI-12
CI-11
CI-10
CI-9
CI-8
CI-7
CI-6
CI-5
CI-4
CI-3
CI-2
CI-1
AE1
FROM SHEET A
HPA
C S
O 1
CONV
TO COMPUTER

SK52212

NOTES:

1. DIODE INPUT LETTERING INDICATES ORIGIN OF INPUT (E.G. B1 MEANS "FROM SHEET B, OUTPUT 1")

2. EACH INPUT LINE CONTAINS ONE DIODE.

UNLESS OTHERWISE SPECIFIED:
DIMENSIONS ± ~ ANGLES ± ~
BREAK EDGES .005-.015 FILLET RAD. ~
SURFACES HAVING A COMMON AXIS CONCENTRIC WITHIN ~ TIR. CLEANING, PRESERVATION AND HANDLING PER HS1980-C __ P __
DIMENSIONS SHOWN ARE AFTER PLATING & SIMILAR PROCESSES & BEFORE PAINTING. THREADS PER MIL-S-7742. DRAWING INTERPRETATION PER HS1380. SURFACE CHARACTERISTICS, MIL-STD-10 PER HS1082. ▲ MARK PART IDENTIFICATION: MIL-STD-130 PER HS323.

NEXT ASSY	USED ON
APPLICATION	

		APPROVALS		DATE
MATERIAL		DRAWN	[illegible]	3-[illegible]
		CHECKED	[illegible]	3-[illegible]
		DRAFTING		
		DESIGN		
HARDNESS		MATERIALS		
HEAT TREAT SPEC		PROJECT		
		CUST		
		FACTORY		
SURFACE COATING		RELEASE		DATE
MFG SPEC		EXPERIMENTAL		
		PRELIM PROD		
		PRODUCTION		
MAKE FROM		PROD CODE		

Hamilton Standard
WINDSOR LOCKS, CONNECTICUT • U.S.A.

COMPUTER INPUT REGISTER LOGIC DIAGRAM

CODE IDENT NO. 73030
CONTRACT NO. [illegible]
SIZE D
SK52212
SCALE: NONE
WEIGHT: LB
SHEET E

FPC-1

1

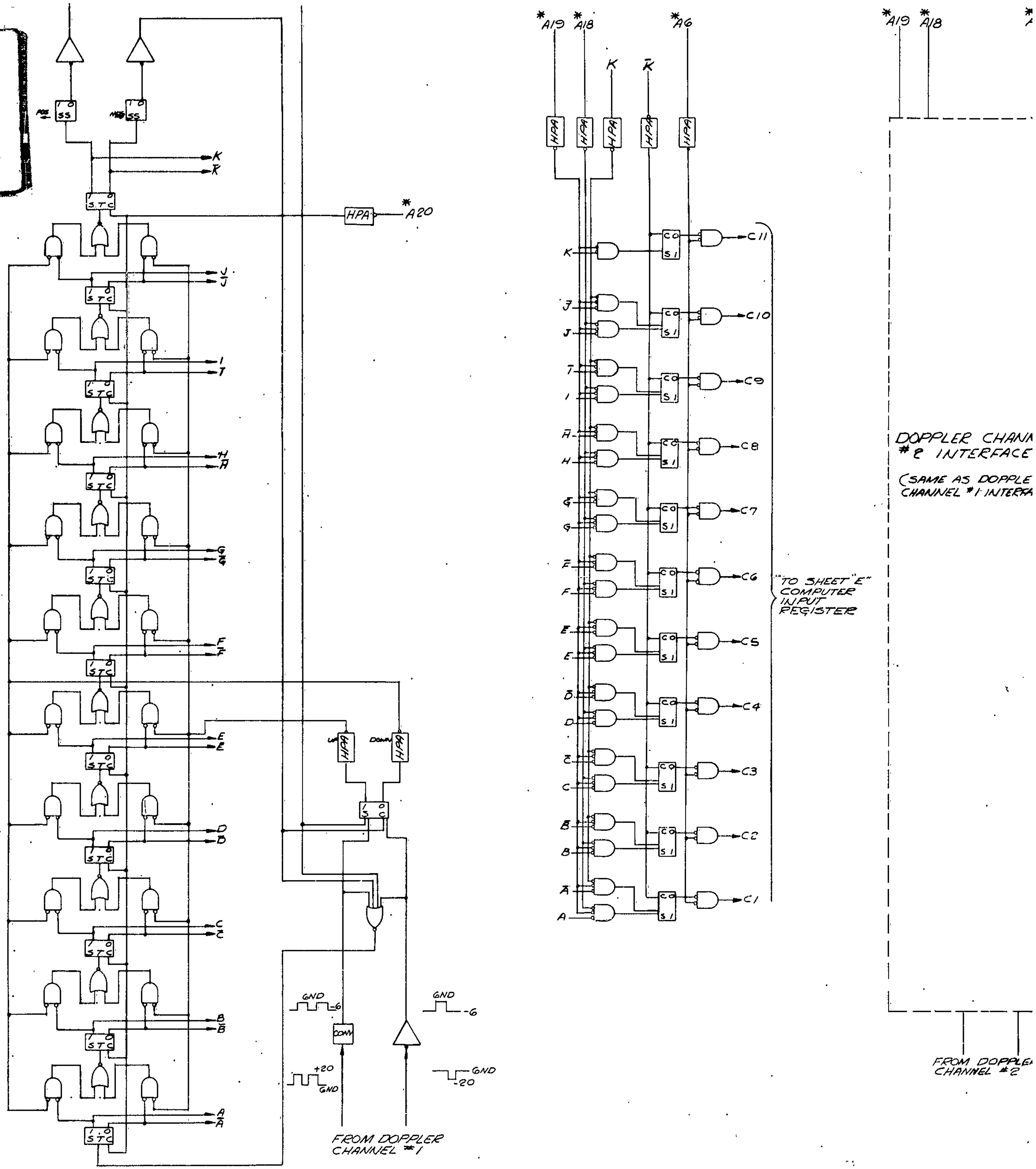

POS
NEG
SS
STC
K
K̄
J
J̄
I
Ī
H
H̄
G
Ḡ
F
F̄
E
Ē
D
D̄
C
C̄
B
B̄
A
Ā
HPA
*A20
UP
DOWN
HPA
CONV
GND
-6
+20
GND
-20
FROM DOPPLER CHANNEL #1
*A19
*A18
*A6
C11
C10
C9
C8
C7
C6
C5
C4
C3
C2
C1
"TO SHEET "E" COMPUTER INPUT REGISTER
DOPPLER CHANN
#2 INTERFACE
(SAME AS DOPPLE
CHANNEL #1 INTERFA
FROM DOPPLE
CHANNEL #2

DOPPLER CHANNEL #1 INTERFACE

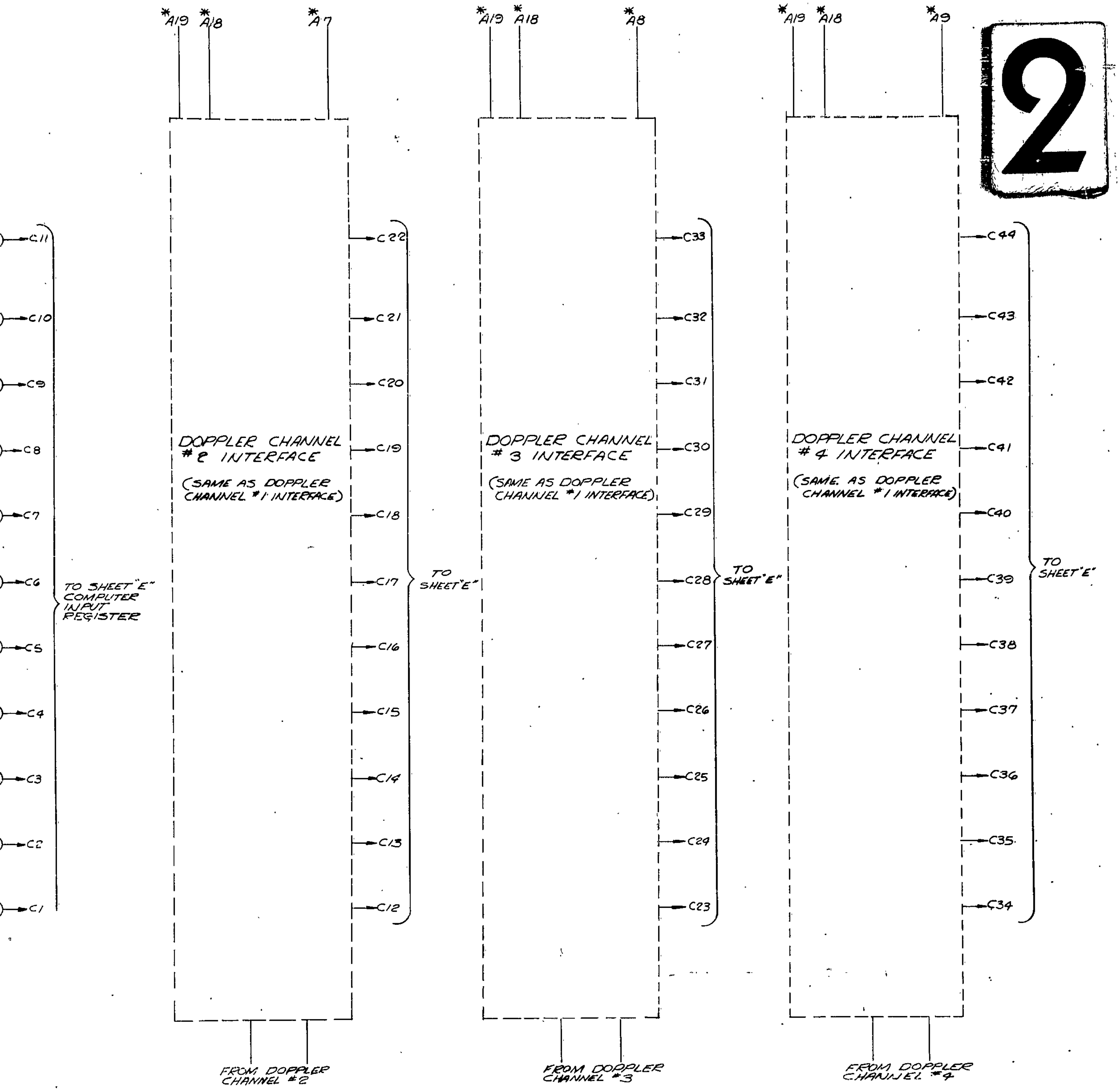

2
*A19
*A18
*A7
*A19
*A18
*A8
*A19
*A18
*A9
C11
C10
C9
C8
C7
C6
C5
C4
C3
C2
C1
TO SHEET "E" COMPUTER INPUT REGISTER
DOPPLER CHANNEL #2 INTERFACE
(SAME AS DOPPLER CHANNEL #1 INTERFACE)
C22
C21
C20
C19
C18
C17
C16
C15
C14
C13
C12
TO SHEET "E"
FROM DOPPLER CHANNEL #2
DOPPLER CHANNEL #3 INTERFACE
(SAME AS DOPPLER CHANNEL #1 INTERFACE)
C33
C32
C31
C30
C29
C28
C27
C26
C25
C24
C23
TO SHEET "E"
FROM DOPPLER CHANNEL #3
DOPPLER CHANNEL #4 INTERFACE
(SAME AS DOPPLER CHANNEL #1 INTERFACE)
C44
C43
C42
C41
C40
C39
C38
C37
C36
C35
C34
TO SHEET "E"
FROM DOPPLER CHANNEL #4

1- ONLY INPUTS WITH * INDICATE ORIGIN OF INPUTS (E.G. *A15 COMES FROM SHEET A, OUTPUT IF E)
NOTES:

UNLESS OTHERWISE SPECIFIED:
DIMENSIONS ± ____ ANGLES ± ____
BREAK EDGES .005-.015. FILLET RAD ____
SURFACES HAVING A COMMON AXIS CONCENTRIC WITHIN ____ TIR. CLEANING, PRESERVATION AND HANDLING PER HS1500-C ___ P ___
DIMENSIONS SHOWN ARE AFTER PLATING & SIMILAR PROCESSES & BEFORE PAINTING. THREADS PER MIL-S-7742. DRAWING INTERPRETATION PER HS1360. SURFACE CHARACTERISTICS: MIL-STD-10 PER HS1082. △ MARK PART IDENTIFICATION: MIL-STD-130 PER HS333.

NEXT ASSY	USED ON		
APPLICATION			

		APPROVALS		DATE
MATERIAL		DRAWN	D. E[illegible]	3-7-[illegible]
		CHECKED	[illegible]	[illegible]
		DRAFTING		
		DESIGN		
HARDNESS		MATERIALS		
HEAT TREAT		PROJECT		
SPEC		COST		
		FACTORY		
SURFACE COATING		RELEASE		DATE
		EXPERIMENTAL		
MFG		PRELIM PROD.		

Hamilton Standard
WINDSOR LOCKS, CONNECTICUT • U.S.A.

DOPPLER INTERFACE LOGIC DIAGRAM

CODE IDENT NO. 73030
CONTRACT NO.
SIZE
SK52212

If the count should change polarity during a cycle, a problem of ± zero will result. If, say, the count passes from + 1 to + 0 and then negative, the next count will be - 0 which is represented in the counter by all ones. This condition is sensed by the logic circuitry and a count is subtracted at this point to give - 1. A transition from the minus to plus polarity generates the opposite, the addition of a pulse, and therefore always maintains the correct count with no limitation on the number of polarity changes per cycle.

The four doppler channels shown in Drawing C fo SK 52212 are identical in design, each containing an 11 bit counter (10 bits and sign) and an associated 11 bit buffer to store the count until computer read-in.

3.4.6.4 Manual Inputs Interface

As shown on Drawing D of SK 52212, there are 5 manual input sources which are thumbwheels with binary coded decimal outputs. Four of these inputs are on the pilot's control panel (range, bearing, EW position fix, and NS position fix) and can be used at any time during the mission while the fifth is located on the control console (initial conditions) and is used only at the start of a mission. Each of the thumbwheel inputs must be converted from BCD to binary before insertion into the computer. To do this, a serial BCD to binary converter, also shown in Figure D, has been designed. Since conversion time is not an important factor, the converter has been designed with simplicity and economy in mind. Whenever an input is dialed into one of the 5 thumbwheel encoders, an insert button corresponding to that thumbwheel must be pushed. This sets one of 5 F/F's, storing the identification of that input, and also triggers a monostable whose output reads the BCD thumbwheel contents into a BCD register-counter. This register is a 24 bit BCD down counter and is accompanied by an adjoining 20 bit binary up counter. Six BCD digits can accomodate a count up to 999,999 while to accomplish this magnitude in binary, 20 bits (1,048,575) will be required. Immediately after the BCD quantity has been gated into the counter register, a square wave clock is gated into both inputs (the input to the binary counter operates on the opposite phase and thus lags by 180°) and the BCD counter begins to count down while the binary counter counts up. A detector constantly monitors the MSD

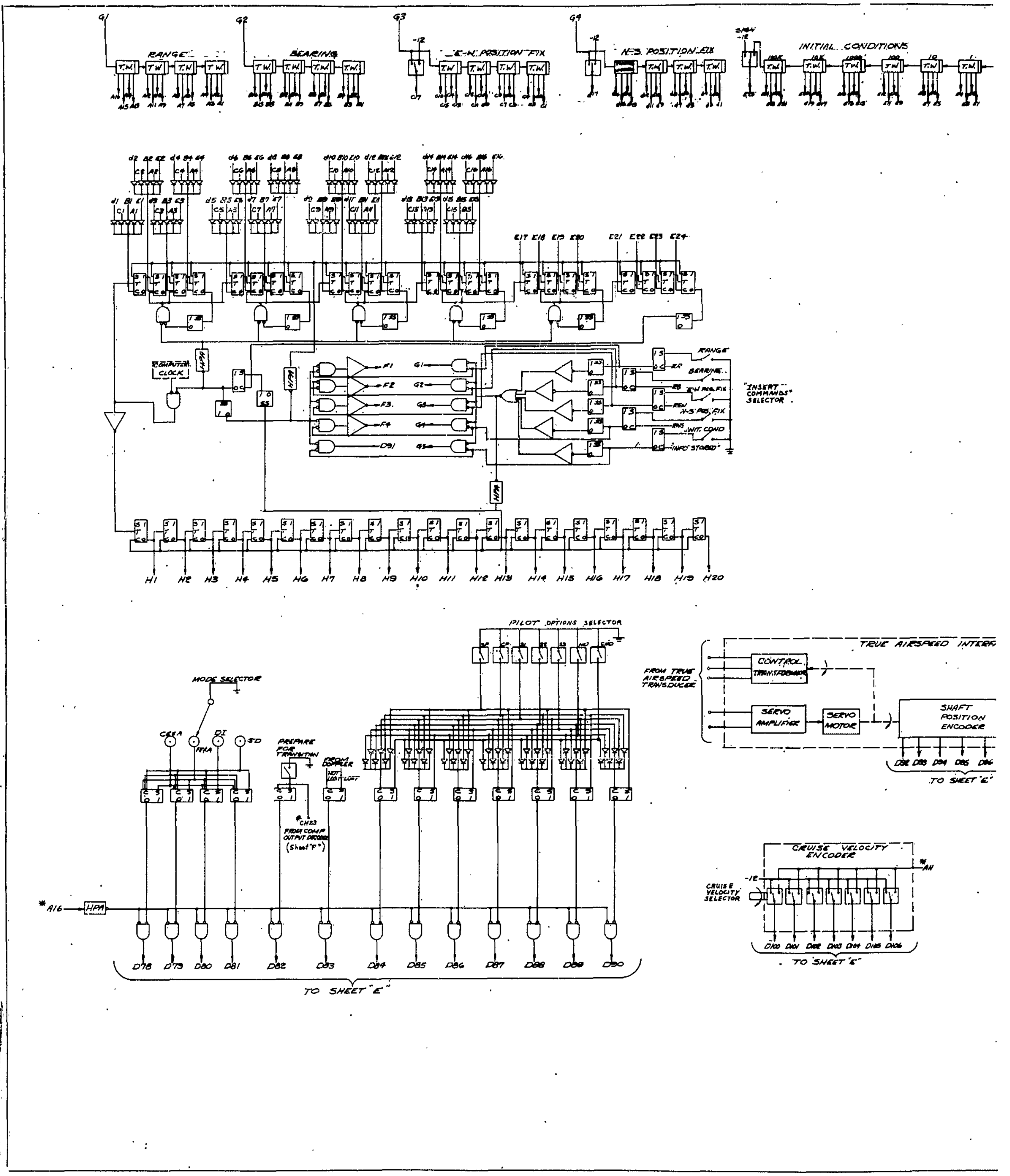
G1
RANGE
T.W.
G2
BEARING
G3
-12
E-W POSITION FIX
C7
G4
N-S POSITION FIX
-12
INITIAL CONDITIONS
100K
10K
1000
100
10
1
d2 B2 E2
d4 B4 E4
C2 A2
C4 A4
d6 B6 E6
d8 B8 E8
C6 A6
C8 A8
d10 B10 E10
d12 B12 E12
C10 A10
C12 A12
d14 B14 E14
d16 B16 E16
C14 A14
C16 A16
d1 B1 E1
C1 A1
d3 B3 E3
C3 A3
d5 B5 E5
C5 A5
d7 B7 E7
C7 A7
d9 B9 E9
C9 A9
d11 B11 E11
C11 A11
d13 B13 E13
C13 A13
d15 B15 E15
C15 A15
E17 E18 E19 E20
E21 E22 E23 E24
COMPUTER CLOCK
HPA
F1
F2
F3
F4
D91
G1
G2
G3
G4
G5
RANGE
ER
BEARING
EB
E-W POS. FIX
EEN
N-S POS. FIX
ENS
INIT. COND
"INFO STORED"
"INSERT COMMANDS" SELECTOR
H1
H2
H3
H4
H5
H6
H7
H8
H9
H10
H11
H12
H13
H14
H15
H16
H17
H18
H19
H20
PILOT OPTIONS SELECTOR
SP
CP
S1
S2
S3
NO
GND
MODE SELECTOR
CEEA
FEEA
DI
SD
PREPARE FOR TRANSITION
FROM DOPPLER
NOT LOST LOFT
*CH23
FROM COMP OUTPUT DECODER
(Sheet "F")
*A16
HPA
D78
D79
D80
D81
D82
D83
D84
D85
D86
D87
D88
D89
D90
TO SHEET "E"
TRUE AIRSPEED INTERF
FROM TRUE AIRSPEED TRANSDUCER
CONTROL TRANSFORMER
SERVO AMPLIFIER
SERVO MOTOR
SHAFT POSITION ENCODER
D92 D93 D94 D95 D96
TO SHEET "E"
CRUISE VELOCITY ENCODER
*AH
-12
CRUISE VELOCITY SELECTOR
D100 D101 D102 D103 D104 D105 D106
TO SHEET "E"

1

2

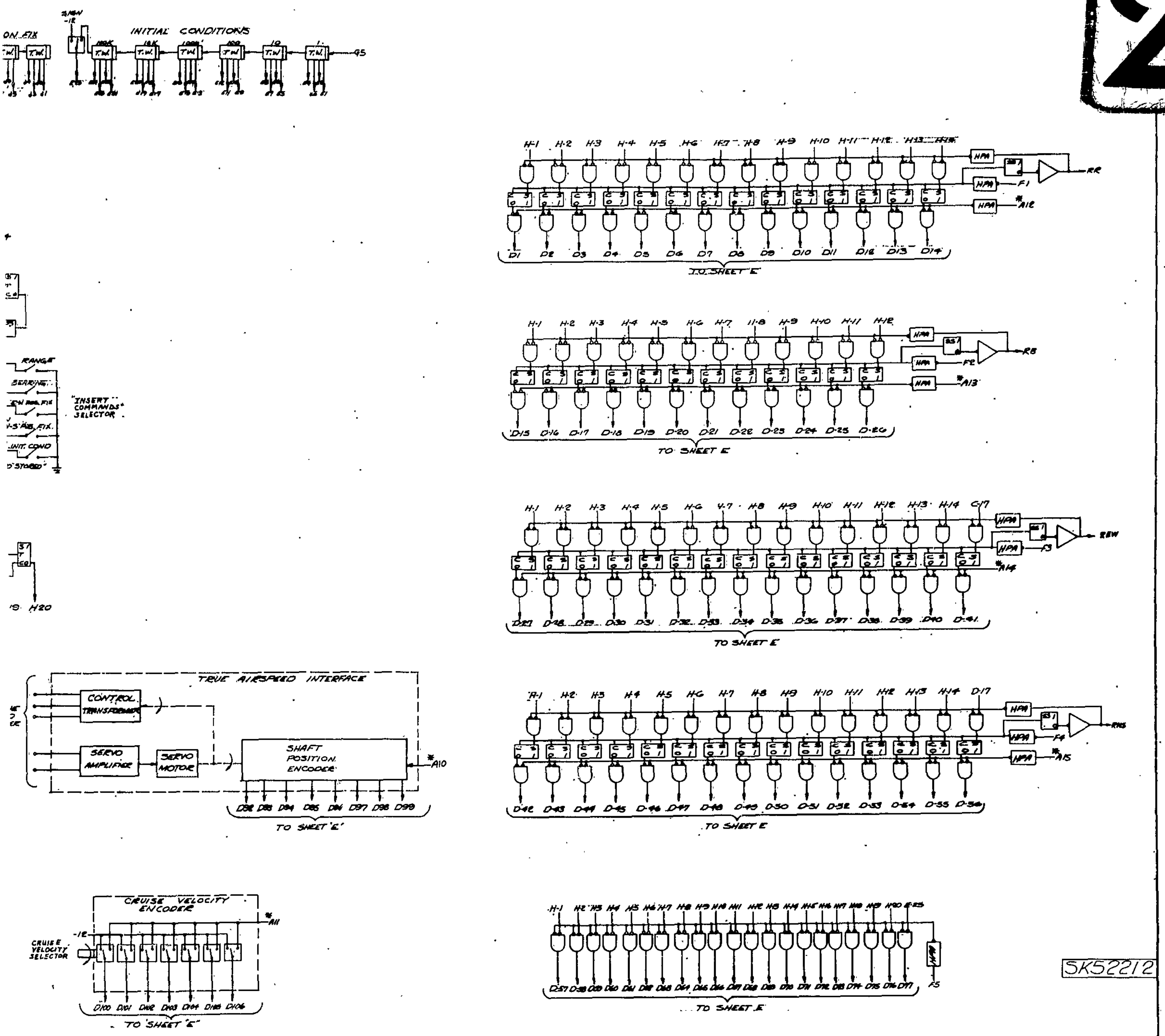

ON FIX
T.W.
SIGN -12
INITIAL CONDITIONS
100K
10K
1000
100
10
1
45
H-1 H-2 H-3 H-4 H-5 H-6 H-7 H-8 H-9 H-10 H-11 H-12 H-13
HPA
F1
RR
*A12
D1 D2 D3 D4 D5 D6 D7 D8 D9 D10 D11 D12 D13 D14
TO SHEET E
H-1 H-2 H-3 H-4 H-5 H-6 H-7 H-8 H-9 H-10 H-11 H-12
F2
RB
*A13
D-15 D-16 D-17 D-18 D-19 D-20 D-21 D-22 D-23 D-24 D-25 D-26
TO SHEET E
RANGE
BEARING
"INSERT COMMANDS" SELECTOR
INIT. COND
"STORED"
H-1 H-2 H-3 H-4 H-5 H-6 H-7 H-8 H-9 H-10 H-11 H-12 H-13 H-14 C-17
F3
REW
*A14
D-27 D-28 D-29 D-30 D-31 D-32 D-33 D-34 D-35 D-36 D-37 D-38 D-39 D-40 D-41
TO SHEET E
H20
TRUE AIRSPEED INTERFACE
CONTROL TRANSFORMER
SERVO AMPLIFIER
SERVO MOTOR
SHAFT POSITION ENCODER
*A10
D92 D93 D94 D95 D96 D97 D98 D99
TO SHEET 'E'
H-1 H-2 H-3 H-4 H-5 H-6 H-7 H-8 H-9 H-10 H-11 H-12 H-13 H-14 D-17
F4
RHS
*A15
D-42 D-43 D-44 D-45 D-46 D-47 D-48 D-49 D-50 D-51 D-52 D-53 D-54 D-55 D-56
TO SHEET E
CRUISE VELOCITY ENCODER
*A11
-12
CRUISE VELOCITY SELECTOR
D100 D101 D102 D103 D104 D105 D106
TO SHEET 'E'
H-1 H2 H3 H4 H5 H6 H7 H8 H9 H10 H11 H12 H13 H14 H15 H16 H17 H18 H19 H20 E-R5
F5
D-57 D-58 D-59 D-60 D61 D62 D63 D64 D65 D66 D67 D68 D69 D70 D71 D72 D73 D74 D75 D76 D77
TO SHEET E

SK52212

1— ONLY INPUTS MARKED WITH * INDICATES ORIGIN OF INPUTS (E.G., *A13 MEANS "FROM SHEET A, OUTPUT 13").

NOTES:

UNLESS OTHERWISE SPECIFIED:
DIMENSIONS ± ______ ANGLES ± ______
BREAK EDGES .005-.025, FILLET RAD ______
SURFACES HAVING A COMMON AXIS CONCENTRIC WITHIN ______ TIR. CLEANING, PRESERVATION AND HANDLING PER HS1550 C __ P __
DIMENSIONS SHOWN ARE AFTER PLATING & SIMILAR PROCESSES & BEFORE PAINTING. THREADS PER MIL-S-7742. DRAWING INTERPRETATION PER HS1380. SURFACE CHARACTERISTICS: MIL-STD-10 PER HS1082. △ MARK PART IDENTIFICATION: MIL-STD-130 PER HS333.

NEXT ASSY | USED ON
APPLICATION

MATERIAL
HARDNESS
HEAT TREAT SPEC
SURFACE COATING
MFG SPEC
MAKE FROM

APPROVALS | DATE
DRAWN
CHECKED
DRAFTING
DESIGN
MATERIALS
PROJECT
COST
FACTORY

RELEASE | DATE
EXPERIMENTAL
PRELIM PROD.
PRODUCTION
PROD CODE

Hamilton Standard
WINDSOR LOCKS, CONNECTICUT • U.S.A.

MANUAL INPUTS INTERFACE LOGIC DIAGRAM

CODE IDENT NO. 73030
SIZE
SK52212
CONTRACT NO.
SCALE: NONE
WEIGHT LB
SHEET D

FPC-1

of the BCD counter and when the couter goes through zero and reaches "all ones", the clock is switched off. The resulting binary number contained by the binary counter is then gated to one of 5 buffer registers, depending on the identification F/F states. It should be noted that the conversion time for a maximum magnitude number of 999,999 with a clock frequency of 200 KC is only 5 seconds, only a little longer than it takes for the operator to push the insert button.

The range, bearing, EW and NS position fix binary quantities are each gated into a separate buffer register, shown in Drawing D of SK 52212 and stored there for read-in during each cycle. Any change in contents will occur almost instantaneously during gate down from the converter. Since the computer reads the register each cycle, read in repetition will prevent any error from occurring due to number changeover during sampling. The initial conditions are gated from the binary counter directly into the computer input register. This can be done since no other inputs are occurring at that time and since the quantities are inserted one at a time by the operator.

Another set of manual inputs make up the Mode-Option word. This word is a 13 bit discrete character in which each bit represents a certain condition. Bits one through four represent the Mode commands - Coarse Erection and Alignment, Fine Erection and Alignment, Doppler Inertial, and Self Damping, respectively. Bit 5 represents doppler lost - not lost and bit 6 indicates the pilot's desire to "prepare for transition". Bits 7 through 13 account for the 7 pilot options which can be chosen during the mission. The resulting 13 bit word is read during every cycle and tested to determine if any change has occurred. The 13 bit register used to store this word has been designed so that when one switch of the mode or option group is actuated, all F/F's are reset except for the one concerned, which is set. This allows for an almost instantaneous change to the new states and prevents ambiguities which result from word changes occuring during periodic read in.

Two other quantities, True Airspeed and Cruise Velocity are shown in Drawing D of SK 52212. Cruise velocity is commanded by a rotary switch whose shaft is also attached to a potentiometer, used for analog display. During each read in cycle, a voltage interrogate pulse (All) is applied to the switch and the contents read directly into the computer input register. True airspeed is measured by an existing shaft position which is digitized by a binary shaft encoder. The shaft encoder is read during each cycle by interrogate pulse A10 and the resulting 8 bit word also fed directly to the computer input register.

3.4.6.5 Computer Input Register

The computer input register, shown in Drawing E of SK 52812 contains 20 bits plus sign. This is designed to accept the largest input available from any source which in this case happens to be the 20 bit plus sign initial condition word. The inputs into each F/F vary from a maximum of 18 at CI - 1 to a minimum of 1 at D76. Since each F/F can "or" 3-4 separate inputs into either the set or clear side and a gate can handle 10 "or" inputs, the method shown was selected to provide the large number of inputs to one point. Since only 9 diodes of a possible 10, and 2 inputs of a possible 4 have been used, room for expansion up to 40 inputs remains possible. Only 7 of the inputs are accompanied by a sign and therefore CI 21, the sign bit location, contains a 7 diode "or" gate. The outputs of the 21 bit register are fed through level converters which change the logic levels used in the input-output equipment to those of the central digital computer.

3.4.6.6 Computer Input Control

The computer input control shown in Drawing A of SK 52212 is the central control area for all input operations. Two operating states are possible; the initial condition mode IC and all others, $\overline{IC}$. In the IC mode, the initial condition word is entered via the thumbwheel and the "insert" button is pushed. The BCD to binary conversion is performed and, upon its completion, a binary word is gated into the computer input register. This same gating pulse D91 is fed to the set side of the "information ready" F/F, telling the computer that data is waiting to be read in. After the computer has read and stored the word, an "information stored" pulse is sent back to the input control by the computer. This pulse resets the computer input register with A21 and also clears the "info ready" F/F. The cycle again repeats itself with the next initial condition insertion.

REVISIONS			
SYM	DESCRIPTION	DATE	APPROVAL

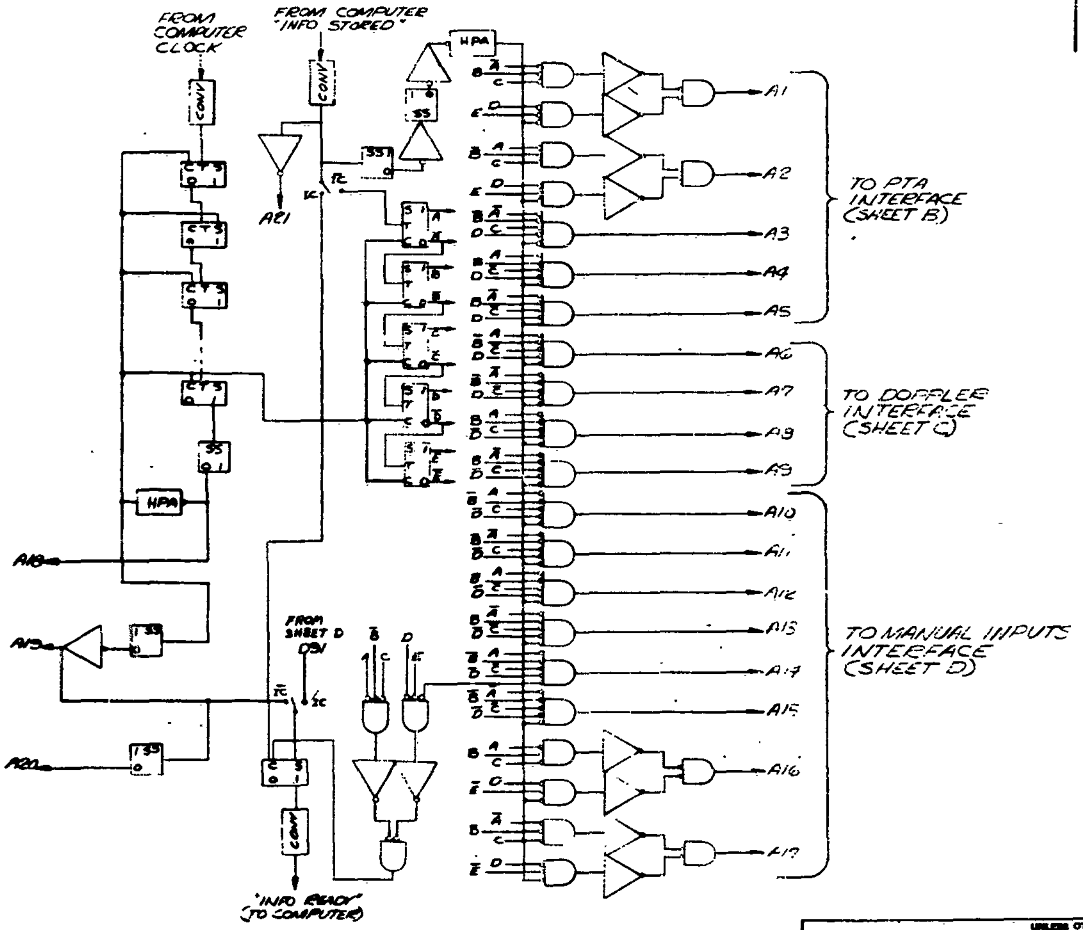
FROM COMPUTER CLOCK
CONV
CTS
CTS
CTS
CTS
SS
HPA
A18
1SS
A19
1SS
A20
FROM COMPUTER "INFO STORED"
CONV
A21
SST
TC
1C
HPA
SS
FROM SHEET D DSI
TC
1C
CONV
"INFO READY" (TO COMPUTER)
A1
A2
A3
A4
A5
A6
A7
A8
A9
A10
A11
A12
A13
A14
A15
A16
A17
TO PTA INTERFACE (SHEET B)
TO DOPPLER INTERFACE (SHEET C)
TO MANUAL INPUTS INTERFACE (SHEET D)

SK52212

UNLESS OTHERWISE SPECIFIED:

DIMENSIONS ± ________ ANGLES ± ________
BREAK EDGES .005-.015. FILLET RAD ________-________
SURFACES HAVING A COMMON AXIS CONCENTRIC
WITHIN ____________ TIR.

DIMENSIONS SHOWN ARE AFTER PLATING & SIMILAR PROCESSES & BEFORE PAINTING. THREADS PER MIL-S-7742. DRAWING INTERPRETATION PER HS1300. SURFACE CHARACTERISTICS: MIL-STD-10 PER HS1002. △ MARK PART IDENTIFICATION: MIL-STD-130 PER HS1003.

NEXT ASSY	USED ON
APPLICATION	

		APPROVALS		DATE
MATERIAL		DRAWN	D. E. Bynum	3-7-63
		CHECKED	L. Veholi	3-14-63
		DRAFTING		
		DESIGN		
HARDNESS		MATERIALS		
HEAT TREAT SPEC		PROJECT		
		COST		
		FACTORY		
SURFACE COATING		RELEASE		DATE
MFG SPEC		EXPERIMENTAL		
		PRELIM PROD.		
		PRODUCTION		
MAKE FROM		PROD. CODE		

HAMILTON STANDARD
DIVISION OF UNITED AIRCRAFT CORPORATION
WINDSOR LOCKS, CONNECTICUT, U.S.A.

COMPUTER
INPUT CONTROL
LOGIC DIAGRAM

CODE IDENT NO. 73030
CONTRACT NO. NONR-62-0E3-0
SIZE C
SK52212
SCALE: NONE
WEIGHT: LB
SHEET A THRU F
FPC-1

NOTICE TO ALL PERSONS RECEIVING THIS DRAWING
THIS DOCUMENT IS THE PROPERTY OF UNITED AIRCRAFT CORPORATION AND IS DELIVERED ON THE EXPRESS CONDITION THAT IT IS NOT TO BE DISCLOSED, REPRODUCED IN WHOLE OR IN PART, OR USED FOR MANUFACTURE FOR ANYONE OTHER THAN UNITED AIRCRAFT CORPORATION WITHOUT ITS WRITTEN CONSENT, AND THAT NO RIGHT IS GRANTED TO DISCLOSE OR SO USE ANY INFORMATION CONTAINED IN SAID DOCUMENT. THIS RESTRICTION DOES NOT LIMIT THE RIGHT TO USE INFORMATION OBTAINED FROM ANOTHER SOURCE.

In the normal operating mode $\overline{IC}$, pulses from the computer clock are counted down until a frequency equal to the cycle frequency is obtained. This provides a single pulse per computer cycle and is used to provide the proper gyro, accelerometer and doppler counting period.

During each cycle, A18 is first generated, resetting the gyro, accelerometer and doppler buffer registers. A19 then gates the counter contents into the buffer and A21 resets the counter before the next pulse arrives. A19 also gates the pitch gyro word directly to the computer input register and sets the info ready F/F, telling the computer to begin the read-in cycle whenever convenient. After the computer reads in this first word, the returning "info stored" pulse advances a 5 stage counter to position 1 and a delayed pulse enables A1. This gates the roll gyro word into the computer input register and the cycle repeats itself. At the completion of the 17th read in, the "info stored" pulse enables A17 which resets the "info ready" F/F and terminates the read-in. The 5 stage counter is reset by the next cycle pulse and the count begins anew at position 0.

3.4.6.7 Output Data Transmission

There are 15 separate data words and eight discretes which must be fed out of the computer. These are either displayed, converted to analog and used for control purposes, or used to turn on or off various functions within the system. The 15 data words are as follows:

1. λ_D - Latitude
2. γ - Longitude
3. V_x^{EF} - Longitudinal Velocity
4. V_y^{EF} - Lateral Velocity
5. V_z^{EF} - Vertical Velocity
6. V_n^{EF} - N - S Velocity
7. V_e^{EF} - E - W Velocity
8. θ - Pitch
9. ϕ - Roll
10. D_T - Range to Dunk Point
11. D_H - Bearing to Dunk Point
12. H - Bearing to Next Fixed Point
13. H_1 - Bearing to Next Fixed Point
14. H_2 - Bearing to Next Fixed Point
15. R - Range to Next Dunk Point

The eight discretes are as follows:

1. (ON) Turn
2. (OFF) Turn
3. (ON) Dunk Point
4. (OFF) Dunk Point
5. (ON) Final Dunk Point
6. (ON) Engage Transition to Hover
7. (ON) Prepare for Takeoff
8. (OFF) Prepare for Transition

A sequence has been assumed for all readouts from the digital computer and the design of the output section has been based on this. At the beginning of a readout cycle, an identification word will be placed on the ID output lines. The word will be decoded immediately by a 23 gate matrix and the resulting output used to select a routing path for the particular word being identified. The output data word will then be placed on the output lines (if data is to be read out) and a reset pulse will be generated by the computer which will reset a register at the selected destination. A read pulse generated by the computer will then gate the data word to the register and the cycle will be completed. If a discrete signal is to be read-out, the read pulse will only be used to provide the enabling signal after identification by the ID output has occurred.

3.4.6.8 Computer Output Interface

The computer output interface, w shown on Drawing F of SK 52212, provides a systematic readout of the 28 output lines of the computer. Five of the 28 lines are used as an identification word. This word is decoded into 23 separate outputs (CH-1 to CH-23) and the resulting level used to route an output to a desired location or to provide a discrete pulse to an on - off device. The 5 bit ID word can uniquely identify up to 31 outputs and therefore allows room for expansion in the future. Each of the 5 ID lines is fed through an input converter which transforms the logic levels of the computer to those of the output interface. Twenty three of the output lines are for the transfer of data. At the present time, only seven output data words are routed to a particular location and stored. These are all 10 bits or below and therefore only these lines are

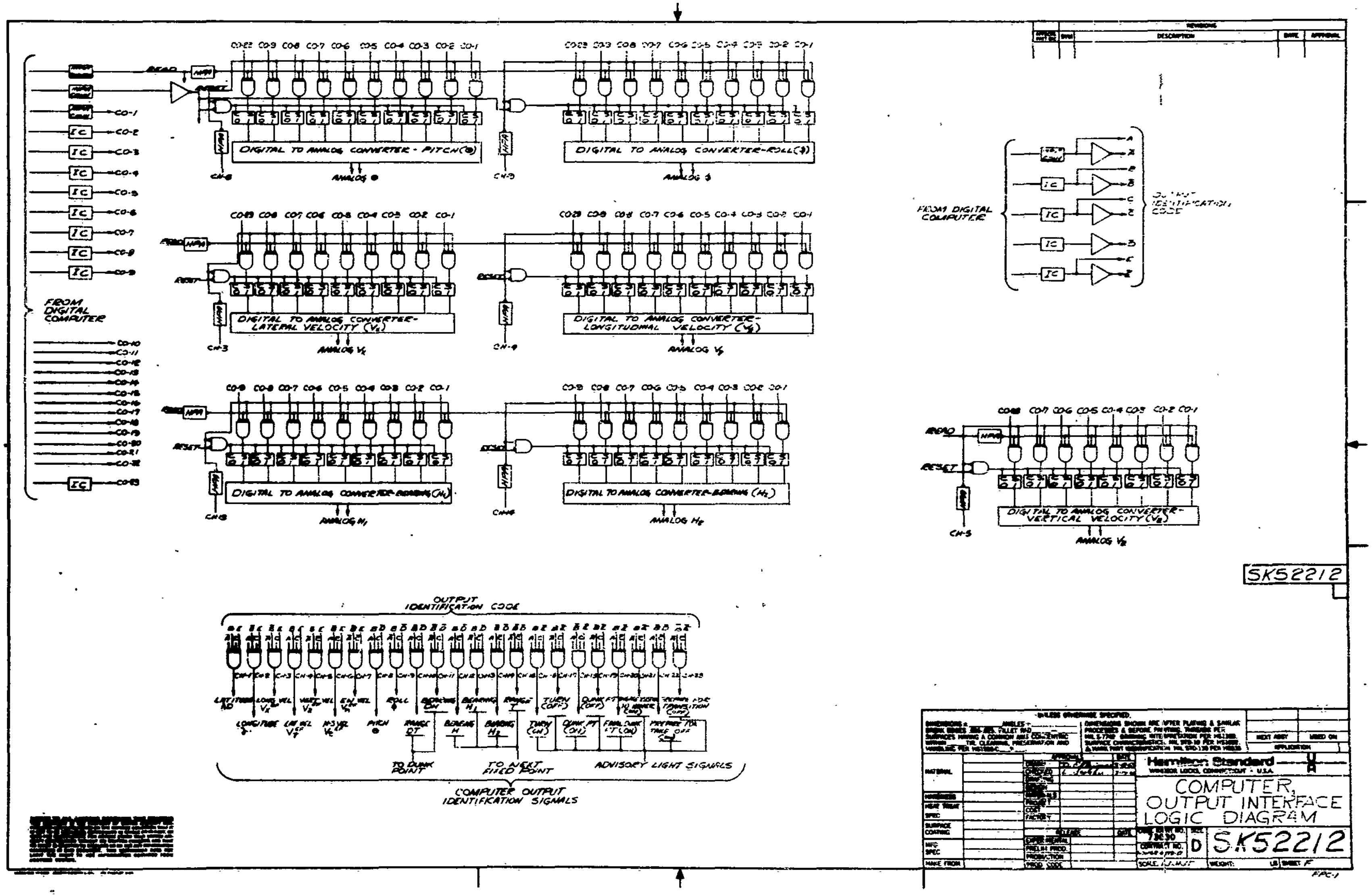
FROM DIGITAL COMPUTER
READ
RESET
CO-1
CO-2
CO-3
CO-4
CO-5
CO-6
CO-7
CO-8
CO-9
CO-10
CO-11
CO-12
CO-13
CO-14
CO-15
CO-16
CO-17
CO-18
CO-19
CO-20
CO-21
CO-22
CO-23
IC
DIGITAL TO ANALOG CONVERTER - PITCH (θ)
ANALOG θ
CH-8
DIGITAL TO ANALOG CONVERTER - ROLL (ϕ)
ANALOG ϕ
CH-9
DIGITAL TO ANALOG CONVERTER - LATERAL VELOCITY (Vx)
ANALOG Vx
CH-3
DIGITAL TO ANALOG CONVERTER - LONGITUDINAL VELOCITY (Vy)
ANALOG Vy
CH-4
DIGITAL TO ANALOG CONVERTER - BEARING (H1)
ANALOG H1
CH-13
DIGITAL TO ANALOG CONVERTER - BEARING (H2)
ANALOG H2
CH-14
DIGITAL TO ANALOG CONVERTER - VERTICAL VELOCITY (Vz)
ANALOG Vz
CH-5
FROM DIGITAL COMPUTER
OUTPUT IDENTIFICATION CODE
A
B
C
D
E
OUTPUT IDENTIFICATION CODE
LATITUDE
LONGITUDE
LONG VEL
LAT VEL
VERT VEL
N-S VEL
E-W VEL
PITCH θ
ROLL ϕ
RANGE DT
BEARING DN
BEARING H
BEARING H1
BEARING H2
RANGE I
TURN (ON)
TURN (OFF)
DUNK PT (ON)
DUNK PT (OFF)
FINAL DUNK PT (ON)
PREPARE FOR TAKE OFF (ON)
PREPARE FOR TRANSITION (OFF)
TO DUNK POINT
TO NEXT FIXED POINT
ADVISORY LIGHT SIGNALS
COMPUTER OUTPUT IDENTIFICATION SIGNALS
SK52212
UNLESS OTHERWISE SPECIFIED
Hamilton Standard
WINDSOR LOCKS, CONNECTICUT · U.S.A.
COMPUTER, OUTPUT INTERFACE LOGIC DIAGRAM
73030
D
SK52212
SCALE
WEIGHT
SHEET
FPC-1

modified by input converters. Shown in Figure F are seven digital to analog converters which are presently used for control purposes within the system. The ID decode gates identify one of the seven D/A registers and two lines, READ and RESET, are used to gate the data to that selected register. The D/A converter output is always present and will change from one level to another immediately upon arrival of an information change.

Future expansion of the readout requirements will likely include the display of several quantities with bit magnitudes utilizing all 23 output data lines. If decimal display is desired, a binary to BCD converter will also be required along with numerous F/F registers to store the information. Further studies will isolate these quantities and no attempt has been made for their inclusion at the present time.

3.4.7 Computer Program

3.4.7.1 Introduction

The purpose of this report is to present a computer program which performs the necessary computations and computer logic, related to inertial navigation and flight path control, and to supply the appropriate command signals, thereby, controlling the helicopter flight over a specified course.

The computer program consists of two general areas, which are 1) navigational computations and 2) flight path computations. In order to maintain a sufficient degree of accuracy the base motion isolation and position tracking loop calculations will be performed every cycle. The remaining navigational computations and flight path computations will be performed every other cycle, on an alternating basis (see Figure 45). This method is employed to reduce the cycle time requirements. Preliminary calculations, based on practical computer speeds, indicate a necessity of a cycle time of approximately 150 ms. A reduction in cycle time can be obtained by dividing the computations into additional branches. However, practical considerations fix the minimum level at approximately 100 ms.

3.4.7.2 Navigational Computations (Reference Figure 45)

The navigational computations are based on utilization of a strapped-down initial navigational system and consists of four modes of operation, which are as follows:

1. Course Erection and Alignment (CE & A) Mode.
2. Fine Erection and Alignment (FE & A) Mode.
3. Doppler-Inertial (D-I) Mode.
4. Self-Damped (S-D) Mode.

The selection of a particular mode is accomplished by the pilot through use of the mode selector switch.

Inasmuch as the helicopter will only be in the CE & A Mode while on board ship (or on a land base), the flight path computations will not be required during this mode. Therefore, a cycling action can be established with the CE & A Mode calculations being performed every cycle. This procedure results in a continuous updating of the initial direction cosines, for the base motion isolation computations, and insures the effective utilization of all output signals from the accelerometers and gyros. In addition, it theoretically allows the helicopter to remain in the CE & A Mode indefinitely. However, because of a limited computer word length, a maximum time limit will be realized before the acceleration summation overflows the computer word, resulting in erroneous data. For a practical word size, a time limit of approximately 3 minutes will be realized. Hence, the pilot should not remain in the CE & A mode for a period exceeding 3 minutes.

For the remaining modes, the flight path computations are required. Therefore, as stated in paragraph 3.4.7.1, the computations will be performed on an alternating basis. The inertial present position quantities will be updated every cycle by performing the base motion isolation and position tracking loop computations. Inasmuch as the remaining navigational computations are primarily concerned with the conversion of present position information and the outputting of information that does not require fast updating, they will be performed every other cycle. While the navigational computations are being performed, the mode selector switch will be tested. The appropriate branching

FLIGHT PATH CONTROLLER

BLOCK DIAGRAM - COMPUTER PROGRAM

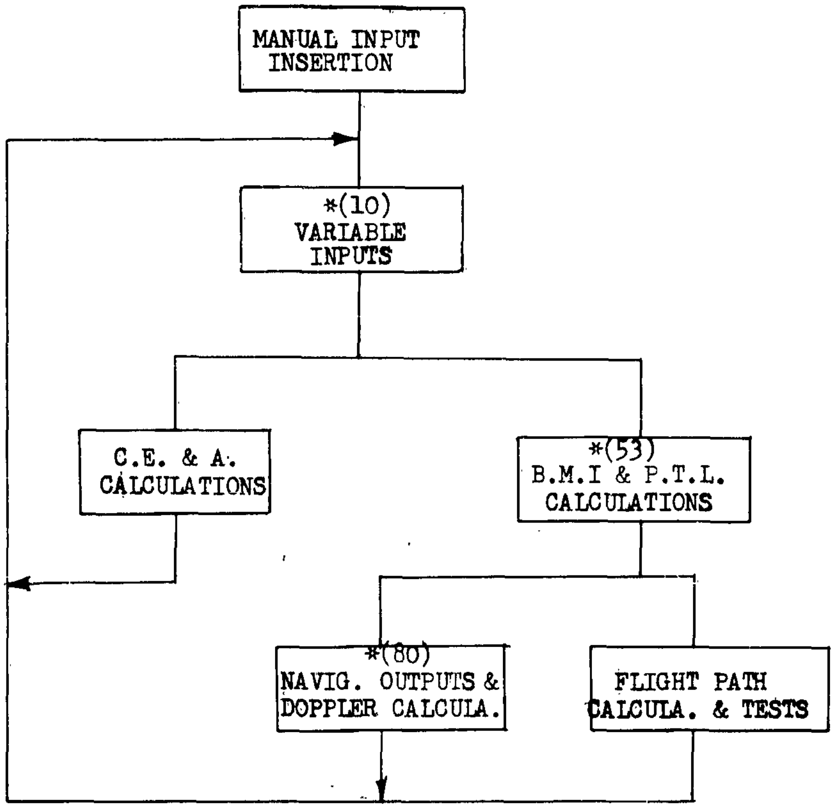
MANUAL INPUT INSERTION
*(10) VARIABLE INPUTS
C.E. & A. CALCULATIONS
*(53) B.M.I & P.T.L. CALCULATIONS
*(80) NAVIG. OUTPUTS & DOPPLER CALCULA.
FLIGHT PATH CALCULA. & TESTS

*Approximate maximum execution time based on the following:

108 ms for MPY and DVP instructions
24 ms for all other instructions
12 ms additional for indexed instructions

FIGURE 45

will be performed, allowing the program to obtain the appropriate quantities for the respective mode.

When the program is in the FE & A or D-I Mode, the application of the doppler velocities will be required. The doppler velocities will be averaged before they are utilized to modify the base motion isolation and position tracking loop quantities. The 30 most recent values for each velocity component will be retained and the 25 most recent values will be utilized in averaging process. This process eliminates utilization of the first 5 values, which may be erroneous. The 25 most recent values for each present position velocity component (in earth fixed coordinates) will also be averaged. The averaged quantities will be utilized to perform the computations pertaining to doppler resolution. The averaging process will not begin until 30 consecutive values have been obtained for the doppler velocities. This process insures that the doppler velocities will be obtained over approximately a 5 second interval before they are averaged. If the doppler signal has been lost, the process will be initialized and 30 new values, for each doppler velocity component, will have to be obtained before the averaging process will resume. The process will remain in the initialized state as long as the doppler signal is lost.

The following methods have been employed to perform the various functions encountered in the navigational computations. The sine, cosine, arcsine and arctangent functions are obtained by means of their series expansions. However, to limit the execution time to a specific value, only ten terms of the series expansion have been employed. It is felt that sufficient convergence will have resulted by the tenth term. The Newton-Rhapson approximation has been utilized for the square root functions. Here again, ten terms have been utilized in the computations. To perform the integrations required by the base motion isolation and position tracking loop computations, the Runge-Kutta approximation has been employed. For programming illustration, a fourth order approximation has been utilized for the base motion isolation computations and a first order approximation has been utilized for the position tracking loop. The finalized cycle time and computer performance will dictate the requirement of first or fourth order approximation for either or both integration procedures. The remaining computations are routine arithmetic functions and thus do not present any programming difficulties.

3.4.7.3 Flight Path Computations

The flight pattern is composed of eight phases as illustrated in Figure 45. For the flight to the first dunk point, the flight path will be composed of phases one, two, three, four, five and six, in that order. For the flight from dunk point to dunk point, the flight path will be composed of phases seven, eight, four, five and six in that order. A description of each phase is as follows:

Phase 1 - Home on dunk point. The bearing angle will be tested. When the angle is less than or equal to an arbitrary small angle, the program will enter the next phase.

Phase 2 - Home on dunk point and track to a distance g (equal to .7 of range from present position to dunk point) from dunk point. During this phase, the instantaneous wind components will be summed and the range to g will be tested. When the range is less than or equal to an arbitrary distance, the next phase will be entered. At the conclusion of phase two, the initial average wind components and the flight path (transition points) to the dunk point will be computed.

Phase 3 - Home on and track to first transition point (e_s, η_s). During this phase, the instantaneous wind components will be summed and the range to the transition point will be tested. When the range is less than or equal to an arbitrary small distance, the next phase will be entered.

Phase 4 (Flying to first dunk point) - Home on and track to second transition point (e_T, n_T). The range to the transition point will be tested. When the range is less than or equal to an arbitrary small distance, the next phase will be entered.

Phase 4a (Flying from dunk point to dunk point) - Home on and track to second transition point (e_T, n_T). The instantaneous wind components will be summed and the range to the transition point will be tested. When the range is

I Flight To First Dunk Point

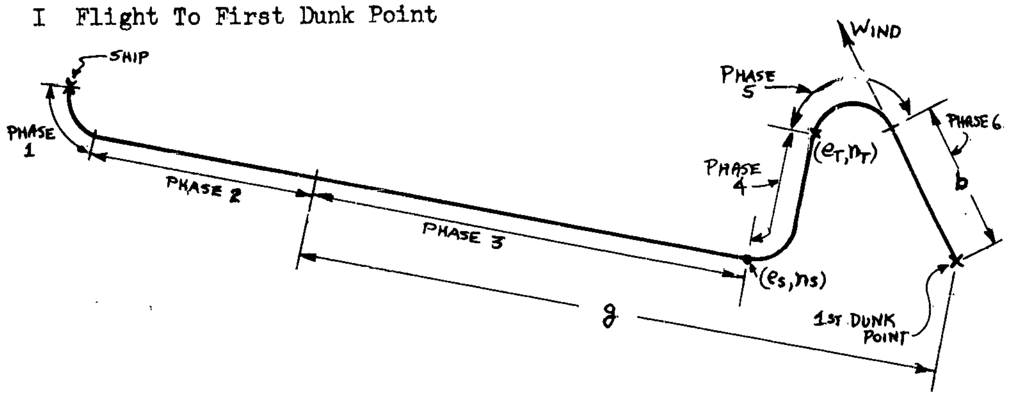
SHIP
PHASE 1
PHASE 2
PHASE 3
PHASE 4
PHASE 5
WIND
PHASE 6
(e_T, n_T)
b
(e_s, n_s)
g
1ST DUNK POINT

II Dunk Point To Dunk Point Flight

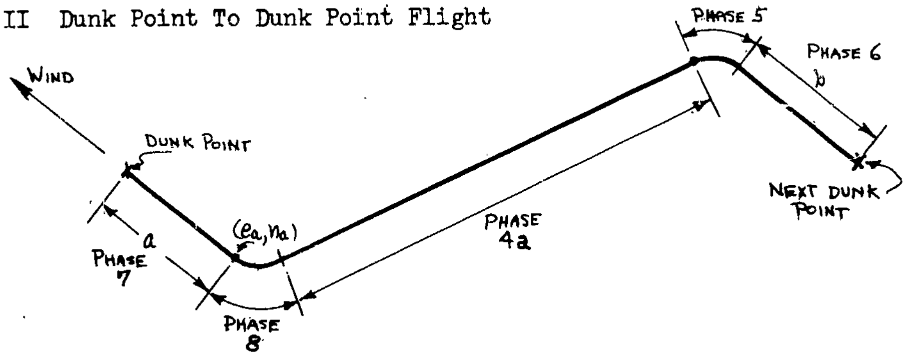
WIND
DUNK POINT
PHASE 5
PHASE 6
b
NEXT DUNK POINT
PHASE 4a
(e_a, n_a)
a
PHASE 7
PHASE 8

III Pattern Deviation From Cruise Mode

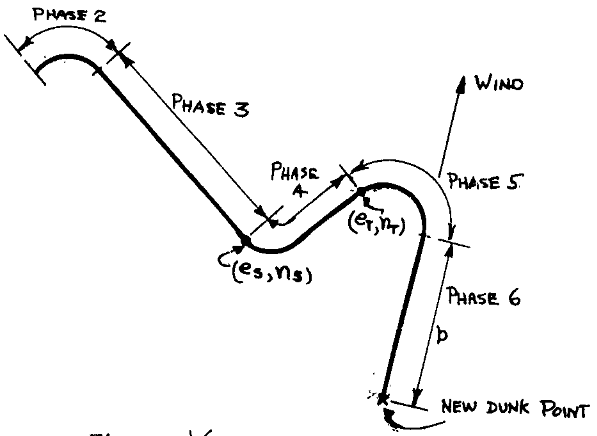
PHASE 2
PHASE 3
WIND
PHASE 4
PHASE 5
(e_T, n_T)
(e_s, n_s)
PHASE 6
b
NEW DUNK POINT

Figure 46
Flight Path Phases

less than or equal to an arbitrary small distance, the next phase will be entered.

Phase 5 - Home on dunk point and track to a distance b (transition distance) from the dunk point. The range to b will be tested. When the range is less than or equal to an arbitrary small distance, the next phase is entered. At the conclusion of phase 5, the pilot will be advised to engage the transition to hover command.

Phase 6 - Home on and track to dunk point. The range to the dunk point will be tested. When the range is less than or equal to an arbitrary small distance, the hover mode will be entered. At the conclusion of phase 6, the helicopter should be in a hover position.

Phase 7 - Home on and track to first transition point (e_a, n_a). The range to the transition point will be tested. When the range is less than or equal to an arbitrary small distance, the next phase will be entered.

Phase 8 - Home on second transition point (e_T, n_T). The bearing angle to the transition point will be tested. When the angle is less than or equal to an arbitrary small angle, the next phase will be entered.

During the execution of the flight pattern, the range and bearing to the next dunk point and the next fixed point will be outputed. When the helicopter encounters a turn maneuver, a turn indicator will be turned on and will remain on throughout the turn. When the helicopter enters a hover position, the ASE commands and the range and bearing to the next fixed point will not be outputed. While in the hover position, the "prepare for transition" switch will be tested. When this switch is turned on, the flight path (transition points) to the next dunk point will be computed and the pilot will be advised to prepare for takeoff. The program will then enter phase 7.

The pilot may deviate from the prescribed pattern by executing one of the pilot option switches. No action will be taken on the pilot option switches during the transition regions (phases 6 and 7) or until the initial wind components have been obtained (after phase 2). If the pilot exercises an option when the helicopter is in a hover position, the flight to the new point will be treated as a dunk point to dunk point flight with the new point as the next dunk point. If the pilot exercises an option when the helicopter is in a cruise mode, the flight to the new point will be treated as a flight to the first dunk point with an elimination of phase one and a modification of phase two. The modification will result in phase two becoming a home on dunk point (the new point) type of phase with a test of the bearing angle being conducted. The options available to the pilot are as follows:

a. He may compute a new pattern based on a new datum point and then fly to that point.

b. He may fly to a new point and 1) return to the pattern, 2) compute a new pattern with this point as the datum point, 3) compute a new pattern with a new point as the datum point or 4) fly to another new point.

c. He may skip one, two or three dunk points, as many times as feasible, within any pattern.

The new point selected by the pilot must be at least 5000 yards from his present position. If an incorrect point is selected while the helicopter is in a hover position, an impossible flight path (overlapping turn circles) may be required. For this case, the program will reject the selected point and continue to fly the prescribed pattern. If an incorrect point is selected while the helicopter is in the cruise mode, the flight path to the point will be computed. However, the helicopter may be required to make a 180° turn and fly to the transition point, thus encountering the transiton point at the incorrect angle or home on an impossible transition point, causing the helicopter to continue flying a circular pattern.

The first dunk point of the pattern will be stored in the computer twice (points A & B). This will insure that the prescribed pattern is executed. If the flight to the first dunk point (point A) results in the accumulation of an appreciable position error, causing the helicopter to miss the first dunk point by an appreciable amount, the next dunk point selected, after insertion of a position fix, will be the first dunk point (point B) and the pattern will continue from there. If no appreciable position error has been accumulated, the first dunk point (point B) will be rejected and the pattern will continue with the second dunk point.

If an impossible flight path, due to position errors, is obtained during the dunk point to dunk point computations, the dunk point will be rejected and the subsequent dunk points will be chosen. The pattern will continue from this point.

3.4.7.4 Program Outline

A generalized program outline is contained below. To supplement this outline, a generalized flow diagram has been prepared and is contained in Figure 47. The intent of this outline is to give the reader an over-all picture of the program flow during the various phases of flight. Thus, specific detail regarding the computations and the testing and branching instructions has been avoided.

The following outline is a generalized description of the computer program:

1. Read manual inputs - A read cycle will be established to read the manual inputs. After insertion of the sixteenth input, the program will halt. The program resumes with depression of the start switch.

2. Initialize - Initialization is composed of three areas as follows:

    a. The initial conditions for Coarse Erection & Alignment mode are computed.

    b. The initial conditions for starting the program are established.

    c. The initial conditions preceeding the dunk pattern computations are established.

3. Compute and store dunk pattern - After computation of the dunk pattern, a test is made to determine whether the pattern was computed in a cruise mode or hover mode. If computed in a cruise mode, program continues. If computed in a hover mode, program branches to step 23.

4. Read and store inputs.

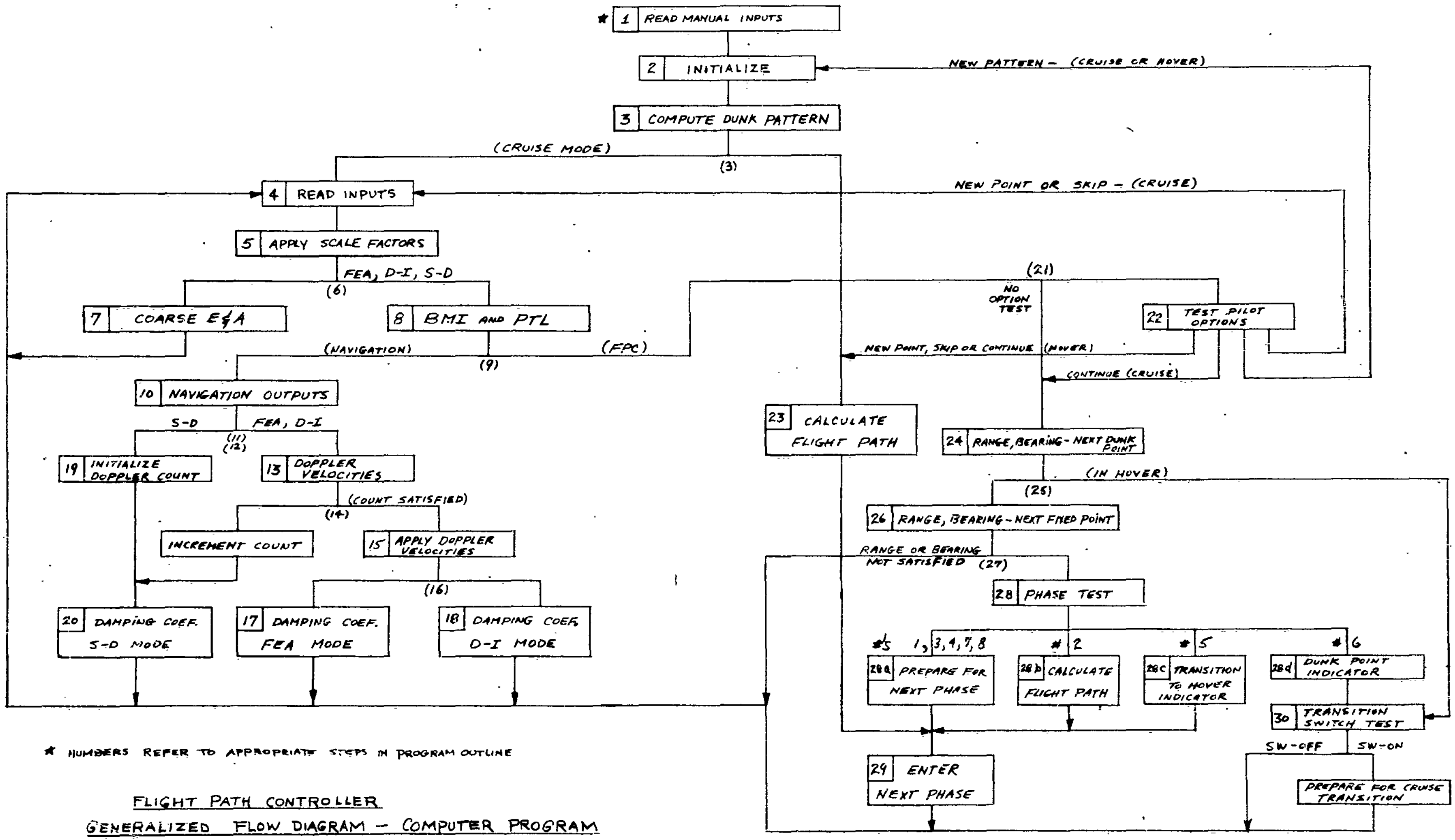
1 READ MANUAL INPUTS
2 INITIALIZE
3 COMPUTE DUNK PATTERN
(CRUISE MODE)
(3)
NEW PATTERN - (CRUISE OR HOVER)
4 READ INPUTS
NEW POINT OR SKIP - (CRUISE)
5 APPLY SCALE FACTORS
FEA, D-I, S-D
(6)
7 COARSE E&A
8 BMI AND PTL
(NAVIGATION)
(9)
(FPC)
(21)
NO OPTION TEST
22 TEST PILOT OPTIONS
NEW POINT, SKIP OR CONTINUE (HOVER)
CONTINUE (CRUISE)
10 NAVIGATION OUTPUTS
S-D
FEA, D-I
(11) (12)
19 INITIALIZE DOPPLER COUNT
13 DOPPLER VELOCITIES
(COUNT SATISFIED)
(14)
INCREMENT COUNT
15 APPLY DOPPLER VELOCITIES
(16)
20 DAMPING COEF. S-D MODE
17 DAMPING COEF. FEA MODE
18 DAMPING COEF. D-I MODE
23 CALCULATE FLIGHT PATH
24 RANGE, BEARING - NEXT DUNK POINT
(IN HOVER)
(25)
26 RANGE, BEARING - NEXT FIXED POINT
RANGE OR BEARING NOT SATISFIED
(27)
28 PHASE TEST
#5 1, 3, 4, 7, 8
# 2
# 5
# 6
28a PREPARE FOR NEXT PHASE
28b CALCULATE FLIGHT PATH
28c TRANSITION TO HOVER INDICATOR
28d DUNK POINT INDICATOR
30 TRANSITION SWITCH TEST
SW-OFF
SW-ON
PREPARE FOR CRUISE TRANSITION
29 ENTER NEXT PHASE

★ NUMBERS REFER TO APPROPRIATE STEPS IN PROGRAM OUTLINE

FLIGHT PATH CONTROLLER
GENERALIZED FLOW DIAGRAM - COMPUTER PROGRAM

FIGURE 47

5. The scale factors and bias terms are applied to the accelerometer and gyro inputs.

6. The mode selector switch is tested. If the switch is in the CE & A mode, program continues, otherwise the program branches to step 8.

7. The CE & A calculations are performed. When the calculations have been completed, the program branches back to step 4.

8. The Base Motion Isolation (BMI) and Position Tracking Loop (PTL) calculations are performed.

9. A test is performed. If navigation output calculations are desired, program continues. If flight path calculations are desired, program branches to step 21.

10. The navigation output calculations are performed.

11. The mode selector switch is tested. If the switch is in the Self Damping mode, the program branches to step 19, otherwise it continues.

12. The lost doppler switch is tested. If the doppler signal has been lost the program branches to step 19 otherwise it continues.

13. The doppler velocities are computed and stored in sequential storage locations. The 30 recent velocities are retained.

14. A test is performed - If 30 consecutive doppler velocities have been obtained, the program continues. Otherwise, the count is incremented and the program branches to step 20.

15. The 25 recent doppler velocities are averaged and the doppler resolution computations are performed.

16. The mode selector switch is tested. If the switch is in the Fine Erection and Alignment (FE & A) mode, the program continues. If the switch is in the Doppler Inertial (D-I) mode, the program branches to step 18.

17. The damping coefficients for the FE & A mode are obtained and the program branches back to step 4.

18. The damping coefficients for the D-I mode are obtained and the program branches back to step 4.

19. The doppler count is initialized.

20. The damping coefficients for the S-D mode are obtained and the program branches back to step 4.

21. A test is performed - If a test of the pilot option switch is desired, the program continues. If no test is desired, the program branches to step 24.

22. The pilot option switch is tested. The available options and appropriate branches are as follows:

    a. Compute new pattern (executed in a cruise or hover mode) - The appropriate datum point is selected and the program branches back to step 20.

    b. Skip points or select new point (executed in a cruise mode). - The appropriate pattern modifications are performed and the program branches back to step 4.

    c. Continue, no option selected (executed in a cruise mode) - The program branches to step 24.

    d. Skip points, select new point or continue (executed in a hover mode) - The appropriate pattern modifications are performed and the program continues.

23. The flight path (based on the craft being in a hover mode) to the next dunk point is calculated. The program then branches to step 29.

24. The range and bearing to the next dunk point are computed and outputed.

25. A test is performed. If the craft is in a hover mode, the program branches to step 30. If in a cruise mode, the program continues.

26. The range and bearing to the next transition point and the ASE commands are computed and outputed.

27. The range (or bearing) is tested. If the range (or bearing) is less than or equal to δ (or γ), the program continues. If it is greater than δ (or γ), the program branches back to step 4.

28. A phase test is performed. (Reference Figure 46) The appropriate branches are as follows:

    a. If the program is in phase 1, 3, 4, 7 or 8, preparations for the next phase are performed and the program branches to step 29.

    b. If the program is in phase 2, the flight path (based on the craft being in a cruise mode) to the next dunk point is calculated. The program prepares for the next phase and branches to step 29.

    c. If the program is in phase 5, the "engage transition to hover" indicator is turned on. The program prepares for the next phase and branches to step 29.

    d. If the program is phase 6, a dunk point indication is given and the program branches to step 30.

29. The program enters the next phase and branches back to step 4.

30. The "prepare for transition" switch is tested. If the switch is off, the program branches back to step 4. If the switch is on, the program prepares for a transition to cruise and branches back to step 4.

3.4.7.5 Flow Diagram

A detailed flow diagram for the computer program is combined in Drawing SK 52223 and a list of program control variables appears in Table 10. The box numbers referred to are those contained in the navigational loop block diagram, Drawing SK 52200. This flow diagram gives a detailed description of the actual computer program, therefore, it contains all the appropriate testing, branching

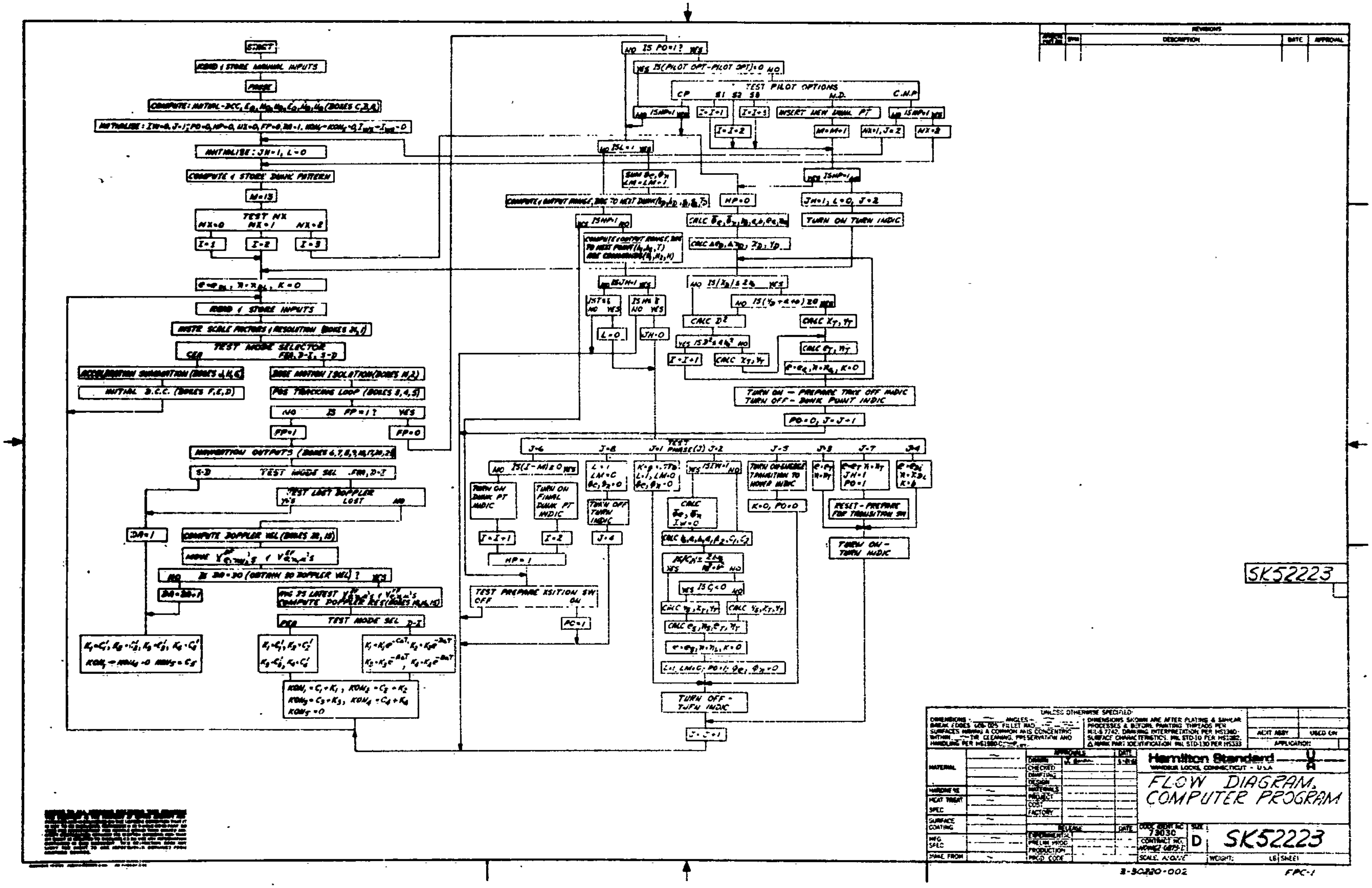
START
READ & STORE MANUAL INPUTS
PAUSE
COMPUTE: INITIAL-DCC, Eθ, Nθ, Uθ, Cθ, Nθ, Uθ (BOXES C,B,A)
INITIALISE: IW=0, J=1, PO=0, HP=0, UI=0, FP=0, DA=1, KON1=KON5=0, IWS=IWS=0
INITIALISE: JH=1, L=0
COMPUTE & STORE DUNK PATTERN
M=13
TEST NX
NX=0
NX=1
NX=2
I=1
I=2
I=3
θ=θDL, Π=ΠDL, K=0
READ & STORE INPUTS
WRITE SCALE FACTORS & RESOLUTION (BOXES 31, 1)
TEST MODE SELECTOR
CER
FBR, D-I, S-D
ACCELERATION SUMMATION (BOXES J, H, G)
INITIAL D.C.C. (BOXES F,E,D)
BASE MOTION ISOLATION (BOXES N,2)
POS TRACKING LOOP (BOXES 3,4,5)
NO
IS FP=1?
YES
FP=1
FP=0
NAVIGATION OUTPUTS (BOXES 6,7,8,9,10,17,20,21)
S-D
TEST MODE SEL
FBR, D-I
TEST LAST DOPPLER
YES
LOST
NO
DA=1
COMPUTE DOPPLER VEL (BOXES 22, 18)
MOVE V's & V's
NO
IS DA=30 (OBTAIN 30 DOPPLER VEL)?
YES
DA=DA+1
MOVE 25 LATEST V's & V's
COMPUTE DOPPLER RES (BOXES 14,16,15)
CER
TEST MODE SEL
D-I
K1=C1', K2=C2', K3=C3', K4=C4'
KON1=KON4=0, KON5=C5
K1=C1', K2=C2'
K3=C3', K4=C4'
K1=K1e^-C1T, K2=K2e^-C2T
K3=K3e^-C3T, K4=K4e^-C4T
KON1=C1+K1, KON2=C2+K2
KON3=C3+K3, KON4=C4+K4
KON5=0
NO
IS PO=1?
YES
YES
IS (PILOT OPT-PILOT OPT)=0
NO
TEST PILOT OPTIONS
CP
S1
S2
S8
N.D.
C.N.P
NO
IS HP=1
YES
I=I+1
I=I+2
I=I+3
INSERT NEW DUNK PT
NO
IS HP=1
YES
M=M+1
NX=1, J=2
NX=2
NO
IS L=1
YES
SUM θc, θπ
LM=LM+1
COMPUTE & OUTPUT RANGE, BRG TO NEXT DUNK (RD, AD, T)
YES
IS HP=1
NO
COMPUTE & OUTPUT RANGE, BRG TO NEXT POINT (R, A, T)
AND COMMANDS (H1, H2, H)
NO
IS JH=1
YES
IS T≤L
NO
YES
IS H≤
NO
YES
L=0
JH=0
YES
IS HP=1
NO
HP=0
CALC θc, θπ, ...
CALC Δθ, ΔΠ, XD, YD
NO
IS |XD|≤2
YES
NO
IS (YD+4.40)≥0
YES
CALC D²
YES
IS D²≤4
NO
I=I+1
CALC XT, YT
CALC XT, YT
CALC θT, ΠT
θ=θ, Π=Π, K=0
JH=1, L=0, J=2
TURN ON TURN INDIC
TURN ON – PREPARE TAKE OFF INDIC
TURN OFF – DUNK POINT INDIC
PO=0, J=J+1
TEST PHASE (J)
J=6
J=8
J=1
J=2
J=5
J=3
J=7
J=4
NO
IS (I–M)≥0
YES
TURN ON DUNK PT INDIC
TURN ON FINAL DUNK PT INDIC
I=I+1
I=2
HP=1
L=1
LM=C
θc, θπ=0
TURN OFF TURN INDIC
J=4
K=0, ...
L=1, LM=0
θc, θπ=0
YES
IS IW=1
NO
CALC θc, θπ
IW=0
CALC ...
YES
NO
YES
IS C<0
NO
CALC ..., XT, YT
CALC ..., XT, YT
CALC θS, ΠS, θT, ΠT
θ=θS, Π=ΠS, K=0
L=1, LM=C, PO=1, θc, θπ=0
TURN ON EMERGE TRANSITION TO HOVER INDIC
K=0, PO=0
θ=θT
Π=ΠT
θ=θT, Π=ΠT
JH=1
PO=1
θ=θDL
Π=ΠDL
K=6
RESET – PREPARE FOR TRANSITION SW
TURN ON – TURN INDIC
TEST PREPARE XSITION SW
OFF
ON
PC=1
TURN OFF – TURN INDIC
J=J+1
SK52223
REVISIONS
DESCRIPTION
DATE
APPROVAL
UNLESS OTHERWISE SPECIFIED
DIMENSIONS
ANGLES
BREAK EDGES .005-.025 FILLET RAD
SURFACES HAVING A COMMON AXIS CONCENTRIC WITHIN TIR CLEANING, PRESERVATION AND HANDLING PER HS1900
DIMENSIONS SHOWN ARE AFTER PLATING & SIMILAR PROCESSES & BEFORE PAINTING THREADS PER MIL-S-7742. DRAWING INTERPRETATION PER HS1380. SURFACE CHARACTERISTICS MIL STD-10 PER HS1382. MARK PART IDENTIFICATION MIL STD-130 PER HS333
NEXT ASSY
USED ON
APPLICATION
MATERIAL
HARDNESS
HEAT TREAT SPEC
SURFACE COATING
MFG SPEC
MAKE FROM
APPROVALS
DATE
DRAWN
CHECKED
DRAFTING
DESIGN
MATERIALS
PROJECT
COST
FACTORY
RELEASE
EXPERIMENTAL
PRELIM PROD
PRODUCTION
PROD CODE
Hamilton Standard
WINDSOR LOCKS, CONNECTICUT · U.S.A.
FLOW DIAGRAM, COMPUTER PROGRAM
CODE IDENT NO 73030
CONTRACT NO.
SIZE D
SK52223
SCALE NONE
WEIGHT
LB
SHEET
3-50220-002
FPC-1

and initializing conditions. To perform the appropriate tests and to execute the appropriate branches, various control variables have been utilized and are contained in the "Program Control Variables" preceeding Drawing SK 52223. Inasmuch as the specific coding format for the program will be dictated by the particular choice of computer, a detailed computer program has not been included in the report. However, preliminary programs have been written, utilizing the symbolic programming language for the IBM 7090 computer. From these preliminary programs, it appears that the final program will contain approximately 3000 instructions and approximately 1000 data storage locations. In programming the arithmetic computations, fixed-point arithmetic programming is being utilized in preference to floating-point arithmetic programming, because of the faster computer speeds attainable with the fixed-point method.

TABLE 10

PROGRAM CONTROL VARIABLES

I. Computer Generator

Variable	State	Function
J	= 1	In Phase one of Flight Path
	= 2	In Phase two of Flight Path
	= 3	In Phase three of Flight Path
	= 4	In Phase four of Flight Path
	= 5	In Phase five of Flight Path
	= 6	In Phase six of Flight Path
	= 7	In Phase seven of Flight Path
	= 8	In Phase eight of Flight Path
IW	= 0	Computation of initial wind components not desired
	= 1	Computation of initial wind components desired
PO	= 0	Testing of Pilot Options not desired
	= 1	Testing of Pilot Options desired
HP	= 0	Craft in Cruise mode
	= 1	Craft in Hover mode

Table 10 (Cont'd.)

Variable	State	Function
JH	= 0	Test on Range Magnitude desired
	= 1	Test on Bearing Magnitude desired
	= 0	Summation of Instantaneous wind components not desired
	= 1	Summation of Instantaneous wind components desired
NX	= 0	Initial Dunk Pattern Computed
	= 1	New Dunk Pattern Computed - In cruise mode
	= 2	New Dunk Pattern Computed - In hover mode
FP	= 0	Navigation output Calculations desired
	= 1	Flight Path calculations desired.
I		Dunk Point Index
M		Total No. of Dunk Points
LM		Total No. of Instantaneous Wind Components summed
DA		No. of Doppler Velocities obtained. (When DA = 30, averaging of Doppler Velocities begins).

II. Inputed

The following functions will be contained in a test word, which will be altered (if so desired) every cycle. Testing of appropriate function is accomplished by testing appropriate portion of test word. Initiation of a particular function is indicated by a "1" in the respective bit.

Mode Selector (Only one bit will contain a "1" at a given time)

CE & A mode	Bit 1
FE & A mode	Bit 2
D-I mode	Bit 3
S-D mode	Bit 4

Lost Doppler Switch Bit 5
"0" Bit - Doppler Signal Present
"1" Bit - Doppler Signal Lost

Prepare for Transition Switch Bit 6
"0" Bit - Switch Off
"1" Bit - Switch On

Pilot Option Switch (Only one bit will contain a "1" at a given time)

Continue	(C.P.)	Bit 7
Skip one dunk point	(S1)	Bit 8
Skip two dunk points	(S2)	Bit 9
Skip three dunk points	(S3)	Bit 10
Select new dunk point	(N.D.)	Bit 11
Compute new pattern	(C.N.P.)	Bit 12

3.4.7.6 It must be borne in mind that this program is of a preliminary nature. A certain degree of modification will undoubtedly be required before the program can be finalized. In addition, changes in the flight path control requirements will certainly require programming changes. Finally, changes will be required to fit the program to the actual computer utilized. Although this particular program has not been run on a computer, it is felt that with appropriate change to the input-output instructions and any necessary modifications, meaningful results can be obtained.

3.5 General Systems Design

3.5.1 Introduction

The detail design in several general areas was performed including an error analysis, an analysis of GFE equipment, a power supply design, a sensor trade off study and the electronics package design.

The error analysis defines the position error of the navigation system during the first hour of flight and during each hour of pure inertial navigation.

The analysis of Government Furnish Equipment (GFE) describes the equipment required by the FPC and their potential interface.

The FPC power supply is described including the power requirements and a list of commercial and integral power supplies required for the flight test.

A study is included outlining the feasibility and practicality of using the strapped down sensors for stabilization purposes. The electronics equipment console design is described and design layouts are included.

3.5.2 Conclusions

The position errors in the Flight Path Control navigation are generally caused by the following:

a. Inertial instruments--gyros, accelerometers
b. Pulse torque amplifier electronics
c. Incorrect erection and alignment
d. Digital computer errors

An analysis of the errors indicates that a 7.5 nautical mile (root sum square) error in position during the first hour of flight from a moving base will be accumulated. There will be a 6.2 nautical mile (RSS) error during each hour of flight in a pure inertial navigation mode. These errors result primarily from the gyro drift rate shift. It was assumed that the tactical operating environment prevented periodic calibation of the gyros. The gyro drift rate shift will be portionally compensated during fine erection and alignment by the doppler velocity signal resulting in a reduction of the error. As a comparison an inertial platform will have a similar position error when periodic calibration is impractical.

Assuming that the flight test will be performed using a SH-3A, the government furnished equipment shall be on AN.APN130, Doppler Radar, a True Airspeed Transducer, an AN/APN117 Radar Altimeter, a Barometric Altimeter and several Co-pilot Display Instruments. The FPC power supply will require the following voltages:

a. 100 VDC
b. 33 VDC
c. 24 VDC
d. 12 VDC
e. + 6 VDC
f. - 12 VDC
g. - 6 VDC
h. 26, 400 cps, 3 ∅

It will consist of three commercial D. C. supplies, two HSED D. C. supplies and the 400 cps A. C. supply.

The utilization of the inertial navigation sensors to provide stability augmentation signals will result in a cost reduction of approximately $3,000 over a system which incorporates separate inertial sensors and stability augmentation sensors.

A series of standard electronic modules are being used in the HSED supplied equipment. These modules are physically large which has necessitated a large electronics package. The electronics package has been divided into six consoles and a pilots control panel. The combined weight of these assemblies is 550 pounds.

3.5.3 Error Analysis

A detailed error analysis of the system was performed to assist in establishing component specifications and to predict the over-all system errors during various modes of operation. The sources of error in the strapped-down inertial navigational system proposed by HS may be divided into five categories.

1. Construction errors such as mechanical alignment.
2. Errors in knowledge of precise geodetic information.
3. Errors in mechanization - instrument errors.
4. False information errors -- gravity, erection, alignment.
5. Errors in data handling - computer errors.

3.5.3.1 Construction Errors and Geodetic Information Errors

In general these errors are quite small and will be neglected. HS proposes a mechanical alignment method by use of which appropriate corrections are applied to the alignment of accelerometer and gyros. The resulting position error is negligible.

The ellipsoidal model represented by R_E,R_P ,E, and the gravity correction functions F (U, P) and H (U, P) give a satisfactory account of the variation of the gravity vector over the surface of the Earth so that the resulting position and velocity errors may be neglected.

3.5.3.2 Instrument Errors

The major error contributors of the system are the gyro, accelerometers and pulse torque amplifiers.

3.5.3.2.1 Gyro Errors

The linearity of scale factor, threshold and drift rate are the contributing factors to gyro errors. Linearity errors are negligibly small because HS utilizes the gyros in a null seeking loop in which the pulse torque amplifier is continuously torquing the pendulous element to a null position. Threshold errors are also negligible with the state-of-the-art gyros.

Drift errors are a very serious problem in the strapped down inertial navigational system which is required to provide navigational information over extended periods of time.

Drift is caused by erroneous torques acting about the output axis and causing the spin axis to process according to the equation

$$\omega_o = \frac{T}{H} = \frac{T}{I\omega_s} = \frac{T}{K^2 m\omega_s} = \frac{T}{\left(\frac{120f}{P}\right)(mK^2)}$$

where ω_D drift rate
I = MK^2 - moment in inertia about the spin axis
R = radius of gyration about the spin axis
f = frequency of the power supply to the motor
P = number of poles of the rotor, usually 2 or 4
T = torque
H = angular momentum

From the above equation of drift, one concludes that angular momentum "H" must be high in order that drift be minimized.

To increase H, eigher I or W_s or both must be increased. "I" is made large by utilizing high density material for the rotor and by building the gyro motor inside-out so that K becomes large. W_s varies from 12,000 to 24,000 rpm.

The erroneous torques which cause constant drift originate from many sources as shown below:

A. Non acceleration sensitive

1. Elastic
2. Viscous Coupling
3. Magnetic
4. Non-orthogonality of suspension axis

B. Acceleration Sensitive

1. Mass unbalance
2. Compliances or deflection
3. Temperature
4. Fluid torque

The erroneous torques which cause random drift originate from the following sources:

1. Friction
2. Gimbal balance instability
3. Instability in elastic coupling - hysteresis
4. Suspension fluid

3.5.3.2.2 Accelerometer Errors

Resolution, scale factor stability, threshold bias stability and cross coupling are the major causes of accelerometer errors.

Resolution errors are negligible because HS is using accelerometer with electromagnetic pick-off which have, theoretically, infinite resolution.

Pick-off scale factor cause acceleration errors proportional to the input acceleration.

Threshold errors appear as constant acceleration errors but are effective at all times during system operation.

Cross coupling errors and vibropendulous errors are very similar. The instantaneous cross coupling errors may be largely due to the mechanism of pulse torquing employed. Effectively the accelerometer will swing around the null point with a frequency of 1 KC.

All of the above influences are minimized by the accelerometer designer. HSED has designed a control to regulate temperature to within satisfactory limits, .1°F.

3.5.3.2.3 Pulse Torquing Amplifier - PTA Errors

The PTA errors are primarily caused by granularity, torquer scale factor stability, non equivalency of positive and negative pulses and servo errors.

There is one pure integration in the PTA loop and consequently step inputs result in no steady state errors. For ramp inputs the resulting servo error is proportional to the input and inversely proportional to the loop gain. This servo error is very small with the existing high loop gain of the PTA.

The pulse granularity error exists because the PTA does not have infinite resolution. The PTA output will only change in incremental steps controlled by the system clock. Hence for small input increments no output torque is indicated.

The torque generated by the PTA is given by

$$T = K_t K_{pc} (p-n) + K_t (p+n) \left(\frac{K_{pp} - K_{pn}}{2} \right)$$

where K_t Instrument Torquer Scale Factor
K_{pc} PTA Scale Factor
K_{pp} Magnitude of Positive Current Pulses
K_{pn} Magnitude of Negative Current Pulses

It can be seen that PTA average output current instability (variations in K_{pc}) manifest itself as an error source, The inequivalency of K_{pp} and K_{pn} result in a bias term being present in the torque output from the PTA. This inequivalency at present is manifested as an instrument bias error. These two PTA errors, scalefactor instability and bias, will be added to instrument errors.

3.5.3.2.4 Erection and Alignment Errors

The desired erection in the strapped-down system considered is a vertical reference within 20 seconds of arc from the true vertical. The 20 seconds of arc contributes to position error by coupling a portion of the g vector to the input of the Schuler loop. This results in 9 position error as a function of flight time. Before the system is erected to the desired vertical, it must go through a coarse and then a fine erection phase. During this time a large velocity and position errors are accumulated. Coarse erection (5 minutes) brings the system to within 2° from the true vertical. During the fine erection the 2° error is reduced to 20 seconds of arc. The accumulated position error at the end of fine alignment will contribute to the system error.

The desired alignment in this application is a north reference within 7 milliradians from true North. Coarse alignment brings the system to within 1° from North and fine alignment will decrease the 1° error to 7 milliradians. The accumulated position error due to coarse and fine alignment will contribute to the system error.

3.5.3.3 Position Error Equation

The list of position error equations following, will be used for error computations. There are two equations derived for each error source. One is Schuler tuned and the other, non-Schuler. The criteria as to which of the two equations will be used depends on the time involved. Generally the non-Schuler will be used when time is small. (See Figure below)

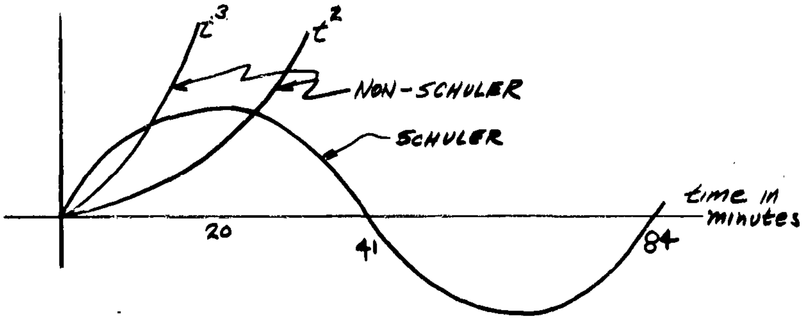

For large periods of time, the RMS value of the Schuler equation will be used.

3.5.3.3.1 Error Equations

Gyro Drift

$$\Delta x = \frac{1}{6} g \omega_d t^3$$ (Non-Schuler Tuned)

$$\Delta x = \omega_d R t - \omega_d R \sqrt{\frac{R}{g}} \sin \sqrt{\frac{g}{R}}\, t$$ (Schuler-Tuned)

Accelerometer

$$\Delta x = \frac{1}{2} \Delta a t^2$$

$$\Delta x = \Delta A \cdot \frac{R}{g} \left(1 - \cos \sqrt{g/R}\, t\right)$$

Erection

$$\Delta x = \frac{1}{2} g \Delta \theta t^2$$

$$\Delta x = R \Delta \theta \cos \sqrt{g/R}\, t$$

Alignment

$$\Delta x = \frac{1}{3} g \Delta H t^3$$

$$\Delta x = \left[\Delta H \sqrt{R/g} \left(R \omega_e \cos \lambda + V_{gf}\right) \sin \sqrt{g/R}\, t\right]$$

3.5.3.4 Position Error for One Hour Flight

The position error during one hour of flight will be computed based on the RMS value of the Schuler equations.

3.5.3.4.1 Assumptions

The following assumptions are made to arrive at a typical error value.

a. The accelerometer error coefficient can be calculated from an assumed average input acceleration of 2×10^{-3}g acting constant for one hour.

b. The accelerometer PTA error coefficient can be calculated from the strapped down analysis and an acceleration of 2×10^{-3}g. In addition, the impulse term will be assumed equal to zero in this calculation.

c. The gyro effective drift rate is constant for one hour and equals to .1°/hour.

d. The gyro PTA error coefficient can be calculated from the strapped down analysis and from an assumed average turning rate of 2°/sec. for one hour. In addition, the impulse term will be taken as equal to zero contribution in this calculation.

e. The vehicle velocity is negligible compared to the Earth's velocity.

f. The helicopter has a Latitude = 0 so that $RW_e \cos\lambda = 900$ N. M./hour.

g. The Schuler equations can be adequately represented as follows:

Accelerometer: - - $\Delta x_a = \sqrt{3/2}\; R/g\, \Delta A$

Gyro: — — — - $\Delta x_g = \omega_D R t$

Erection: — — — $\Delta x_e = .707\, R \Delta\theta$

Alignment: — — $\Delta x_a = .707\, \Delta H \sqrt{R/g}\, (R\omega_e \cos\lambda + V_{yf})$

where

$R = 3.5 \times 10^3$ N. M.

$g = 6.7 \times 10^4$ N. M./hr.^{2}

$W_e = 15°$/hour

h. The PTA imperfections will be converted to equivalent accelerometer and gyro errors.

3.5.3.4.2 Position Error Calculation

The position error will be computed as follows:

$$\Delta x = A_{acc} + A_{PTA} + \omega_{DG} + \omega_{PTA} + \theta + H$$

where Δx = Position Error
A_{cc} = Error caused by accelerometer
A_{PTA} = Error caused by accelerometer PTA
ω_{DG} = Error caused by gyro drift
ω_{PTA} = Error caused by gyro PTA
θ = Error caused by Erection
H = Error caused by alignment

a. Accelerometer contribution

$$A_{acc} = 1.21(R/g)\Delta A_{acc} = (1.21)(.052\ hr^2)(3.12 \times 10^{-5}\ g)(4.15 \times 10^{8}\ ft/hr^2)$$
$$= 830 \text{ feet} = \boxed{.134 \text{ N.M.}}$$

b. Accelerometer PTA contribution

$$A_{PTA} = 1.21\,(R/g)\,\Delta A_{PTA} = (1.21)(.052\ hr^2)(7.7 \times 10^{-8}\ g)(4.15 \times 10^{8}\ ft/hr^2)$$
$$\equiv \boxed{.0003 \text{ NM}}$$

c. Gyro Drift Contribution

$$\omega_{DG} = \omega_D R t \doteq (1.73 \times 10^{-3}\ R/h)(3.45 \times 10^{3} \text{ N.M.})(1 \text{ hour})$$
$$= \boxed{6.1 \text{ N.M.}}$$

d. Gyro PTA Contribution

$$\omega_{PTA} = \Delta\omega_{PTA} R t = (1.24 \times 10^{-4}\ R/h)(3.45 \times 10^{3} \text{ N.M.})(1 \text{ hour})$$
$$= \boxed{.43 \text{ N.M.}}$$

e. Erection Contribution

$$\theta = .707 R \Delta\theta = (.707)(3.45 \times 10^{3} \text{ N.M.})(10^{-4} \text{ RAD.})$$
$$= \boxed{.25 \text{ N.M.}}$$

f. Alignment Contribution

$$H = .707\,\Delta H \sqrt{R/g}\,(R\omega_e \cos\lambda + V_{gf}) = (.707)(7 \times 10^{-3})(.227)(900)$$
$$= \boxed{1.01 \text{ N.M}} \text{ at } \lambda = 0 \text{ (EQUATOR)}$$

The resultant position error is the arithemetic sum.

$$\Delta x = \Delta\chi_{acc} + \Delta\chi_{acc_{PTA}} + \Delta\chi_{g} + \Delta\chi_{g_{PTA}} + \Delta\chi_{e} + \Delta\chi_{a}$$

$$= (.134) + (.0003) + (6.1) + (.43) + (.25) + (1.01)$$

$$= \boxed{7.92\ N.M}\ \text{during one hour flight}$$

Some of the error sources have a probability of occurrence associated with them. Taking the root sum square of the errors:

$$\Delta\chi_{rss} = \sqrt{(A_{acc})^2 + (A_{PTA})^2 + (\omega_{DG})^2 + (\omega_{PTA})^2 + (\theta)^2 + (H)^2}$$

$$= \sqrt{.0188 + 0 + 37.1 + .182 + .063 + 1.21}$$

$$= \sqrt{38.57} = \boxed{6.2\ N.M.}\ \text{root-sum-square error}$$

The root sum square error indicates clearly that the gyro drift rate is the major error source.

3.5.3.5 Position error during the first hour of flight.

3.5.3.5.1 General

This section sums the position error during the first hour of flight which includes erection and alignment. This period of 60 minutes is divided into 3 phases of operation and the error accumulated during each phase is computed. The CEP of the system starts as soon as the helicopter takes off. Coarse erection and alignment errors, therefore, will not be added to the CEP error.

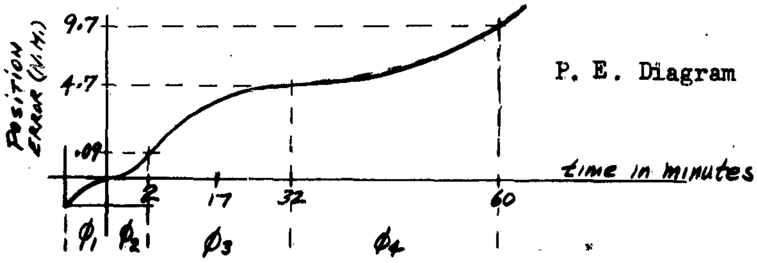

P. E. Diagram

ϕ_1 = Error build up due to error in ship's velocity during coarse alignment.

ϕ_2 = Error build up due to misalignment ± 1°, erection of 1 minute of arc and undamped gyro drift errors W_d = .2°/h.

$$\phi_3 = \begin{cases} \text{Error is damped by the 2\% doppler input} \\ W_d = .1^\circ/h, \text{ erection} = 20'' \text{ arc, alignment} = 7 \times 10^{-3} \text{ radians} \end{cases}$$

ϕ_4 - error is due to undamped gyro drift error W_d = .2°/h

The period of time from the instant power is turned on-coarse alignment begins - up to 65 minutes later is divided into 4 phases of operation.

Phase one, begins at t = -5 minutes and ends at t = 0. Thus, 5 minutes are allowed for coarse erection and alignment for accuracies of ±1° heading and 1 minute of arc vertical error. Error builds up due to ship's velocity error but will not be included in the system error. System performance error begins to accumulate at t = 0.

Phase two, begins at t = 0 and ends at t = 2 minutes. At t = 0 the helicopter takes off, climbs and levels off. At t = 3 it will be located approximately within 1 N. M. from the point of takeoff. The error builds up due to misalignment and miserection.

Phase three, begins at t = 2 and ends at t = 32 minutes. This is the period of fine alignment using doppler. At t = 32 minutes the system will be aligned to 7 milliradians and erected to 20 seconds of arc. The error during phase three is due to gyro, accelerometer, miserection, misalignment, and doppler radar.

Phase four, begins at t = 32 and ends at t = 60 minutes. During this period the system is operating in pure inertial mode. The P. E. diagram indicates position error vs. time for four phases. The error during ϕ 1 will not be included in the circular error probability (CEP) calculation. The one hour period will consist of phases two, three and four.

3.5.3.5.2 Phase Two (Ø 2) error

The gyro drift rate, misalignment and miserection errors are considered. All other sources of error are neglected during this period of only 3 minutes. The values of the significant parameters are:

$\Delta\theta$ = 1 minute arc = 2.9×10^{-4} radians = 1 N. M.

ΔH = 1° system is slewed to helicopter's compass

t = 3 minutes

$\bar{v}$ = 30 knots = 66 ft/sec. = 9×10^{-3} radians/hour

x = 1.5 N. M. during 3 minutes

ω_d = .2°/h = 3.3×10^{-3} radian/hour

ω_e = .26 R/hour at the equator

g = 32 ft/sec^2 = 6.7×10^4 N. M./hr^2

The non-Schuler equations will be used since the time involved is only 3 minutes.

$$\Delta x = \frac{1}{2} g \Delta\theta t^2 + \frac{1}{6} g \Delta H t^3 (\omega_e \cos\lambda + \bar{v}/R) + \frac{1}{6} g \omega_d t^3$$

$$= \frac{6.7 \times 10^4 \times 3 \times 10^{-4}}{2 \times (30)^2} + \frac{6.7 \times 10^4 \times .016 \times .26}{6 \times (30)^3} + \frac{6.7 \times 10^4 \times 3.3 \times 10^{-3}}{6 \times (30)^3}$$

$$\cong .013 + .007 + .0007 \cong \boxed{.021 \text{ N.M.}}$$

3.5.3.5.3 Phase Three (Ø 3) Error

During Ø 3 a perfect doppler will reduce erection and alignment errors to 20" of arc and 7 milliradians respectively. Hence the phase three error will be a function

$$\Delta x_{\phi_3} = f(\Delta\theta, \Delta H, \omega_d, \Delta a_{acc}, \Delta D_{doppler})$$

of gyrodrift rate, miserection, misalignment, accelerometer errors and doppler errors. Significant parameters are listed on the following page.

$\Delta\theta$ = 20" arc = 9.8 x 10^{-5} radians

ΔH = 7 x 10^{-3} radians

ω_d = .1°/h = 1.73 x 10^{-3} radians/hour including gyro PTA effect

Δa = 6 x 10^{-6}g including accelerometer PTA effect

$\bar{v}$ = 100 knots = 220 ft/sec.

For $\Delta\theta$ and ΔH the Schuler equations (RMS) will be used.

For ω_d and Δa non-Schuler equations will be used.

$$\Delta x = .707\,R\Delta\theta + .707\sqrt{\frac{R}{g}}(R\omega_e + \bar{v})\Delta H + \frac{1}{6}g\omega_d t^3 + \frac{1}{2}\Delta a t^2$$

$$= .707 \times 3.5 \times 10^3 \times 10^{-4} + .707 \times .227 \times 10^3 \times 7 \times 10^{-3} + 1.11 \times 10^4 \times 1.73 \times 10^{-3} + \frac{.402}{2 \times 4}$$

$$= .246 + 1.11 + 2.45 + .051 = \boxed{3.85\ N.M.}$$

So far, we have assumed a perfect doppler. Doppler errors will be introduced and will be converted to equivalent miserection and misalignment effective during Ø 3. Assume a 2% doppler, then doppler velocity error during Ø 3

$$\Delta D_{Dopp.} = .02\,\bar{v} = \boxed{2\ N.M.}$$

$\Delta\theta_d$ = .5 (hour) ΔD_d for doppler error frequencies of 10 radians per hour (Worst case) and τ = 6 minutes erection system time constant -- settling time = 5τ = 30 minutes = fine erection time

$\Delta\theta_d$ = .5 x 2 = 1 N. M. x2.9 x 10^{-4} radians/N. M.
= 2.9 x 10^{-4} rad.

ΔH_d = 1 hour ΔD_d
= 2 N. M. x 2.9 x 10^{-4} radians/N. M. = 5.8 x 10^{-4} radians

Substituting $\Delta\theta_d$ and ΔH_d into the RMS Schuler expressions:

$$\Delta \chi_{dopp.} = .707 R \Delta \theta_d + .707 \sqrt{R/g}\,(R\omega_e + \bar{v})\,\Delta H_d$$

$$= .738 + .092 = \boxed{.83\ N.M.}$$

Adding $\Delta\chi$ and $\Delta\chi_{DOPP}$ to get the total error during Ø 3.

$$\Delta\chi_{\phi_3} = 3.85 + .83 = \boxed{4.68\ N.M.}$$

3.5.3.5.4 Phase Four (Ø 4) Error

Phase four is an inertial phase, erection and alignment errors will not be included since the RMS value was used in computing their effect during phase three. During phase three only the time varying drift rate was used $W_d = .1°/h$. The reason being that a third order erection alignment system eliminates the constant drift effect. During phase four, however, doppler is not used and the effective drift includes the constant portion.

$$\Delta\chi = \frac{1}{6} g \omega_d t^3 + \frac{1}{2} \Delta a t^2$$

$$\Delta\chi = \frac{6.7 \times 10^4 \times 3.3 \times 10^{-3}}{6 \times 8} + \frac{6.7 \times 10^4 \times 6 \times 10^{-6}}{2 \times 4}$$

$$= 4.89 + .051 = \boxed{4.94\ N.M.}$$

3.5.3.5.5 Total Error Summation

Adding all the error during Ø 2, Ø 3, and Ø 4 arithmetically the position error is

$$\Delta\chi = \Delta\chi_{\phi_2} + \Delta\chi_{\phi_3} + \Delta\chi_{\phi_4}$$

$$= .088 + 4.68 + 4.94$$

= 9.71 N. M. during the first hour of flight

Determining the root-sum-square error

$$\Delta\chi = \sqrt{(1.17)_a^2 + (.261)_e^2 + (7.35)_g^2 + (1.02)_{acc.}^2 + (.77)_{dopp.}^2}$$

$$\cong \sqrt{56.1} = \boxed{7.5\ N.M}$$

3.5.4 Government Furnished Equipment (GFE)

This section offers a brief description of the equipment to be furnished by the Navy that is essential to the operation of the Flight Path Control. Existing equipment on the SH-3A is planned for use during the flight test phase.

3.5.4.1 Doppler Radar Navigation Set, AN/APN-130

The main function of the doppler radar in this system is to provide long-term correction to the inertial navigation system. This is described in greater detail in previous paragraphs. The velocity outputs of the standard APN-130 set are normally analog voltages. These are not needed since a digital output is required to enter the computer. Thus, the APN-130 set is modified to by-pass the 3A2 Modulator Module and the 3A6 Velocity Computer Module and to use the outputs of the four 3A1 Converter Modules directly. These outputs, which are + 20 volt and -20 volt pulse trains, are fed directly to the digital doppler interface. This interface, described in greater detail in section 3.4.6.3, obtains a net count of pulses from each doppler channel and presents to the computer four binary numbers. Each binary number represents the velocity of the helicopter in the direction of one of the four doppler beams.

The land sea bias, which previously was added to the velocity components in the 3A6 Velocity computer, now corrects the velocity components through use of a scale factor in the digital computer program.

3.5.4.2 True Airspeed Transducer

The True Airspeed Transducer is comprised of a transducer and a synchrotel transmitter. The unit mechanically computes true airspeed using pitot pressure, static pressure, and bulb temperature. This true airspeed is sent to the digital computer where it is used in the computation of the wind velocity.

3.5.4.3 Radar Altimeter (APN 117)

The radar altimeter supplies a signal to the basic ASE. This portion of the ASE has not been modified and hence the radar altimeter Flight Path Control Interface is exactly the same as the existing interface in the SH-3A helicopter.

3.5.4.4 Barometric Altimeter

The barometric altimeter supplies a signal to the basic ASE which has not been modified in this area. As in the radar altimeter no modification of the barometric altimeter is required.

3.5.4.5 Display Instruments

It is necessary, during the test flight, to be able to view certain important parameters coming from the digital computer. Some of these parameters may be displayed on the following existing co-pilot instruments: Bearing Distance Heading Indicator (BDHI), True Course and Distance Repeater (TCDR), Ground Speed and Drift Angle Indicator (GSDA), and Vertical Gyro Indicator (VGI). For the remaining parameters, it will be necessary to install non-GFE displays. These non-GFE displays and all computer-display interfaces are described in a Hamilton Standard proposal which proposes to supply this equipment for a later phase of this program.

3.5.4.5.1 BDHI

This instrument will be used to display the range and bearing to the "next dunk point." The range is in nautical miles and the bearing is in degrees. The BDHI requires a three-phase voltage to drive the bearing pointer and each of the digits of the range counter.

3.5.4.5.2 TCDR Indicator

This instrument will display the "next fix point" bearing in degrees. It also requires a 3-phase voltage to drive the bearing pointer.

3.5.4.5.3 GSDA Indicator

This instrument displays the ground speed and drift angle of the helicopter. It receives the drift velocity and the heading velocity in the form of single phase voltages and resolves these components into the ground speed and drift angle.

3.5.4.5.4 Vertical Gyro Indicator

The VGI will display the helicopter pitch and roll attitudes. The inputs to this instrument are two sets of 3 phase voltages, one for pitch and one for roll.

3.5.5 Flight Path Control Power Supply

The FPC System is intended to be operated from the SH-3A 115V, 400 CPS primary supply. This supply is regulated in accordance with MIL STD 704. The FPC power supply is designed such that it can draw power from 1, 2 or 3 phases of the aircraft power to minimize unbalances.

3.5.5.1 Requirements

The individual power requirements for the equipment operating from the supply described herein are listed in Table 11. The regulation percentages indicate the allowable variance in voltage for input variations of ± 10%, load variations as indicated and temperature change from 0°F to +125°F. The temperature requirement is the strictest of the three variations. For example, to maintain a voltage within 1% over the temperature range typically requires a supply that will regulate to 0.05% at room temperature.

The total power requirements are outlined in Table 12. The currents listed for each voltage are the total estimated required power and are not the total capacity of the supply. The current indicated for the +12V and -12V supplies include about 1 amp each to supply the +6V and -6V regulators.

3.5.5.2 System Block Diagram

The power supply system chosen for the Flight Test Model FPC is shown in Figure 48. It consists of three commercial supplies feeding two HSD built regulators, two HSD D. C. supplies, one feeding a 0.01% regulator in a temperature controlled environment, and the 3 Ø supply. It is intended that the final design will contain all HSD built supplies.

There are two considerations that led to the inclusion of the commercial supplies; time and the uncertainty of the required power. In order to minimize weight and size in the final design, the actual power required must be known. At this time we have only estimates of current needed. It is conceivable that the estimates may be in error up to a factor of 2. That is, the actual power may be as little as 1/2 or as much as twice the estimated power.

Individual Power Requirements

Table 11

Equipment	Volts	Amps	Power	Regulation	Ripple
Countdown Circuitry	+12	.45	5.4w	±1% 25% to F. L.	50mv P-P
	-12	.1	1.2w	" "	"
Pulse Torque Servo Amplifier	+100V	.5	50 w	.01% 15-90% F. L.	1mv rms.
	+33V	.18	6 w	±2% 25% to F. L.	50mv P-P
	+24V	.34	8.2w	±1% "	"
	+12V	.45	5.4w	" "	"
	- 6V	.1	.6w	" "	"
	+ 6V	.1	.6w	" "	"
Interface Equipment	+24V	1.1	26 w	" "	"
	+12V	.9	10.8w	" "	"
	+6V	.25	1.5w	" "	"
	-6V	.25	1.5w	" "	"
	-12V	14.	168 w	" "	"
+6V Regulator	+12V	1.	12 w	2% "	"
-6V Regulator	-12V	1.	12 w	2% "	"
Gyro Wheel Motors	26V		15 va	1% "	3 ∅, 400 ~

Total Power Required

Table 12

Voltage	Current	Regulation
Volts	Amps	Per Cent
+100V DC	0.5 A	0.01%
+33V DC	0.18A	±2%
+24V DC	1.42A	±1%
+12V DC	2.8A	±1%
-12V DC	15.1A	±1%
+6V DC	0.25A	±1%
-6V DC	0.35A	±1%
26V, 400∼,3 ∅	15 VA	±1%

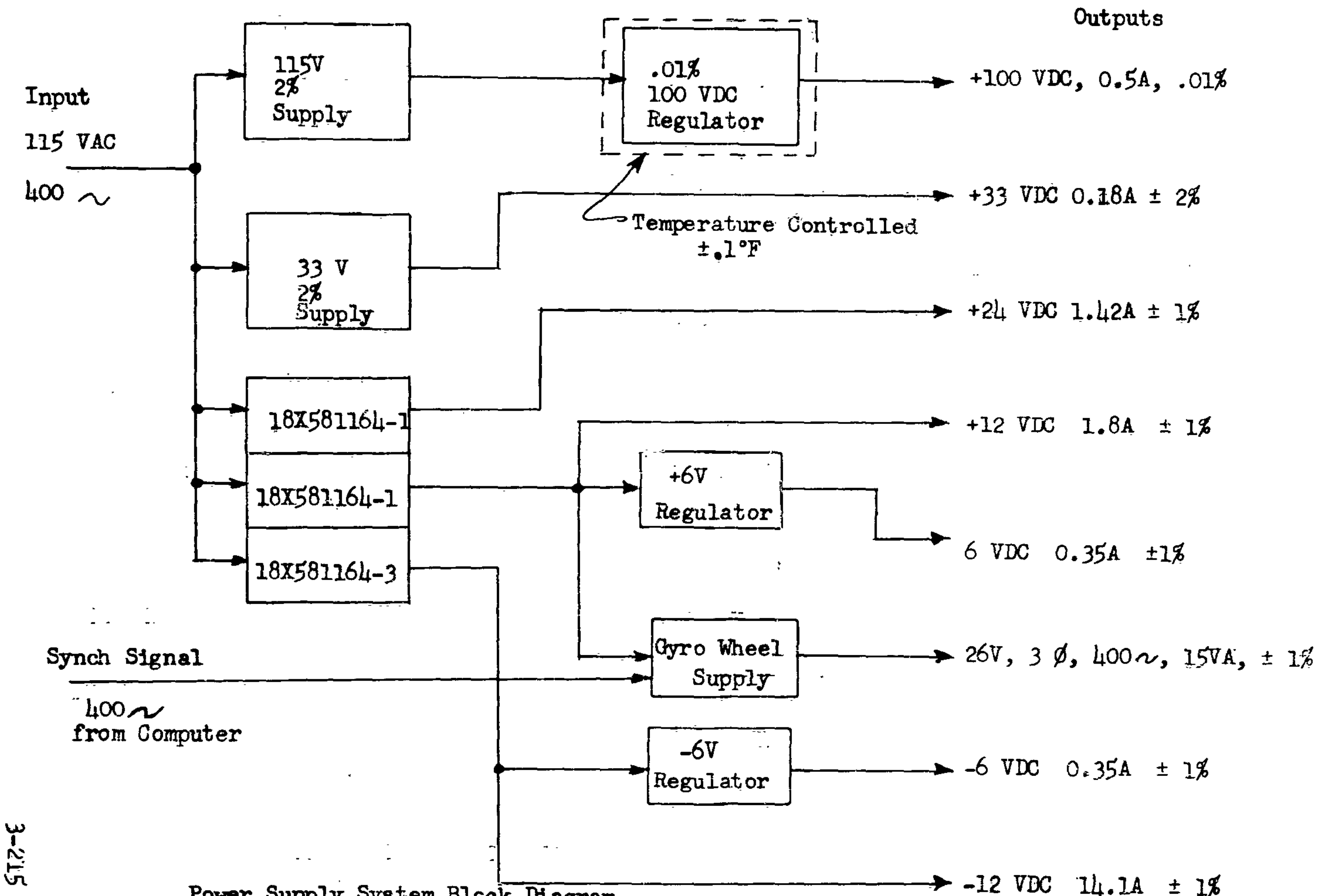
Input
115 VAC
400 ~
115V
2%
Supply
33 V
2%
Supply
18X581164-1
18X581164-1
18X581164-3
Synch Signal
400~
from Computer
.01%
100 VDC
Regulator
Temperature Controlled
±.1°F
+6V
Regulator
Gyro Wheel
Supply
-6V
Regulator
Outputs
+100 VDC, 0.5A, .01%
+33 VDC 0.18A ± 2%
+24 VDC 1.42A ± 1%
+12 VDC 1.8A ± 1%
6 VDC 0.35A ±1%
26V, 3 Ø, 400~, 15VA, ± 1%
-6 VDC 0.35A ± 1%
-12 VDC 14.1A ± 1%

Power Supply System Block Diagram
Figure 48

In the lower current ranges, the number, size and total weight of components will not vary significantly due to changes in required power. However, as an example: a high current supply designed for an estimated 15 amps would have to be designed for at least 30 amps plus a safety factor, and it may only have to supply an actual 7.5 amps. In the higher current ranges, such a variation would cause significant weight and size penalties. It is for these reasons that we decided to use wide range, high capacity commercial supplies and hold off on the design of the higher current supplies until the actual values of current are known.

The commercial supplies selected are specified in Table 13. The HSD designed circuits are shown on SK52199. These circuits will be fabricated by HSED and contained in one 5" high module in a standard 19" "relay" rack panel.

3.5.6 Cost Reduction Trade Off Study

3.5.6.1 Purpose

The purpose of this study is to determine the feasibility and practicality of using the Inertial Navigation System sensors to replace the existing ASE accelerometers, gyros and tilt table.

3.5.6.2 Existing SH-3A ASE

In the present system there are two accelerometers, two vertical gyros, a tilt table and a yaw rate gyro. The accelerometers are used as a source of negative feedback in the ASE coupler; there is a pitch and a roll accelerometer. The two vertical gyros are used to operate the pilot's and co-pilot's V.G.I., (Vertical Gyro Indicator). The output of either gyro is used in the ASE for attitude position and attitude derived rate signals. The yaw rate gyro is used in the ASE for rate damping. The tilt table is used to inject a test input into the ASE.

3.5.6.3 Flight Path Control Sensor Replacements

The two accelerometers can be replaced by two of the accelerometers in the Strapped-Down Inertial System.

Power Supply AC-DC
Table 13

18 X Number	Mfr's. Number	Voltage	Current
18X581164-1	TP 24-20	23-25 VDC	0-2A
" 2	2(TP 12-25)	11-13 V	0-5A
" 3	LE 106 Mod.	0-12 V	0-16A

a. Line Regulation: 0.05% maximum or 8 mv maximum for input variations of 105-125 VAC.
b. Load Regulation: 0.05% maximum or 8 mv maximum for 0 to full load
c. Ripple + Noise: 0.5 mv RMS maximum
d. Temperature Coefficient: 0.015% 1°C maximum
e. A.C. input 105-125 VAC 400 cps
f. Operating Temperature 0- 50°C ambient
g. Size and Weight:

Model	Maximum Size			Maximum Weight	
	H	W	D		
TP 24-20	4"	5"	7"	9 lbs.	
2(TP12-25)	4"	10"	7"	18 lbs.	
LE106 Mod.	5¼"	19"	16½"	75 lbs.	

h. Items 1 and 2 may be purchased from AC DC electronics Inc, 2979 No. Ontario St. Burbank, California
Item 3 from Lambda Electronics Corp., 515 Broad Hollow Road, Huntington, L. I., New York

i. Item 3 will be modified to provide 16 amps at 12 volts from its normal rating of 0-18V, 0-15A by the manufacturer.

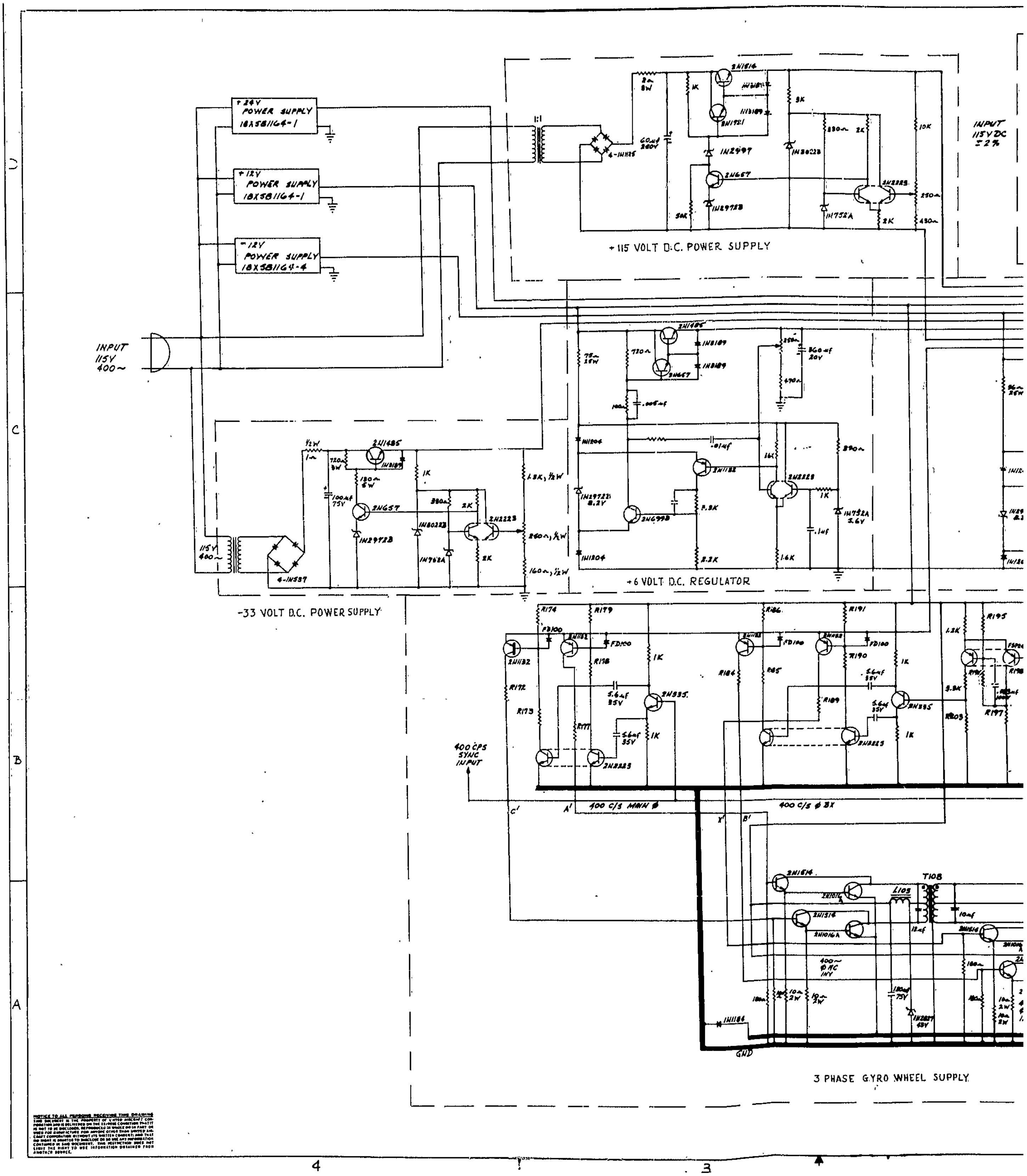
D
C
B
A
4
3
+24V POWER SUPPLY 18X58II64-1
+12V POWER SUPPLY 18X58II64-1
-12V POWER SUPPLY 18X58II64-4
INPUT 115V 400~
1:1
4-1N1125
2Ω 8W
60μf 250V
1K
2N1614
1N3189
2N1721
1N2997
2N657
1N2972B
5K
3K
1N3022B
330Ω
2K
10K
1N752A
2N2223
250Ω
2K
450Ω
INPUT 115VDC ±2%
+115 VOLT D.C. POWER SUPPLY
2N1485
1N3189
720Ω
2N657
75Ω 25W
250Ω
360μf 20V
470Ω
100Ω
.005μf
1N1204
.01μf
1K
390Ω
2N1132
2N2223
1N2972B 8.2V
2N699B
3.3K
1K
1N752A 5.6V
.1μf
2.2K
1.6K
1N1204
+6 VOLT D.C. REGULATOR
56Ω 25W
½W 1Ω
2N1485
720Ω 3W
1N3189
130Ω 5W
1K
100μf 75V
2N657
1N2972B
330Ω
2K
1N3022B
1N752A
2N2223
2K
1.3K, ½W
260Ω, ½W
160Ω, ½W
115V 400~
4-1N537
-33 VOLT D.C. POWER SUPPLY
R174
R179
FD100
2N1132
2N1132
FD100
R178
1K
R172
R173
R177
5.6μf 35V
2N335
5.6μf 35V
1K
2N2223
R186
R191
2N1132
FD100
2N1132
FD100
R190
1K
R184
R185
5.6μf 35V
R189
5.6μf 35V
2N335
2N2223
1K
R195
1.2K
3.3K
R203
R197
400 CPS SYNC INPUT
C'
A'
400 C/S MAIN ϕ
400 C/S ϕ 3X
X'
B'
2N1614
2N1016A
T108
L105
2N1514
2N1016A
10μf
12μf
2N1514
2N1016A
100Ω
400~ ϕ AC INV
100Ω
10Ω 2W
10Ω 2W
180μf 75V
1N2827 43V
100Ω
10Ω 2W
10Ω 2W
1N1184
GND
3 PHASE GYRO WHEEL SUPPLY

NOTICE TO ALL PERSONS RECEIVING THIS DRAWING
THIS DOCUMENT IS THE PROPERTY OF UNITED AIRCRAFT CORPORATION AND IS DELIVERED ON THE EXPRESS CONDITION THAT IT IS NOT TO BE DISCLOSED, REPRODUCED IN WHOLE OR IN PART OR USED FOR MANUFACTURE FOR ANYONE OTHER THAN UNITED AIRCRAFT CORPORATION WITHOUT ITS WRITTEN CONSENT; AND THAT NO RIGHT IS GRANTED TO DISCLOSE OR SO USE ANY INFORMATION CONTAINED IN SAID DOCUMENT. THIS RESTRICTION DOES NOT LIMIT THE RIGHT TO USE INFORMATION OBTAINED FROM ANOTHER SOURCE.

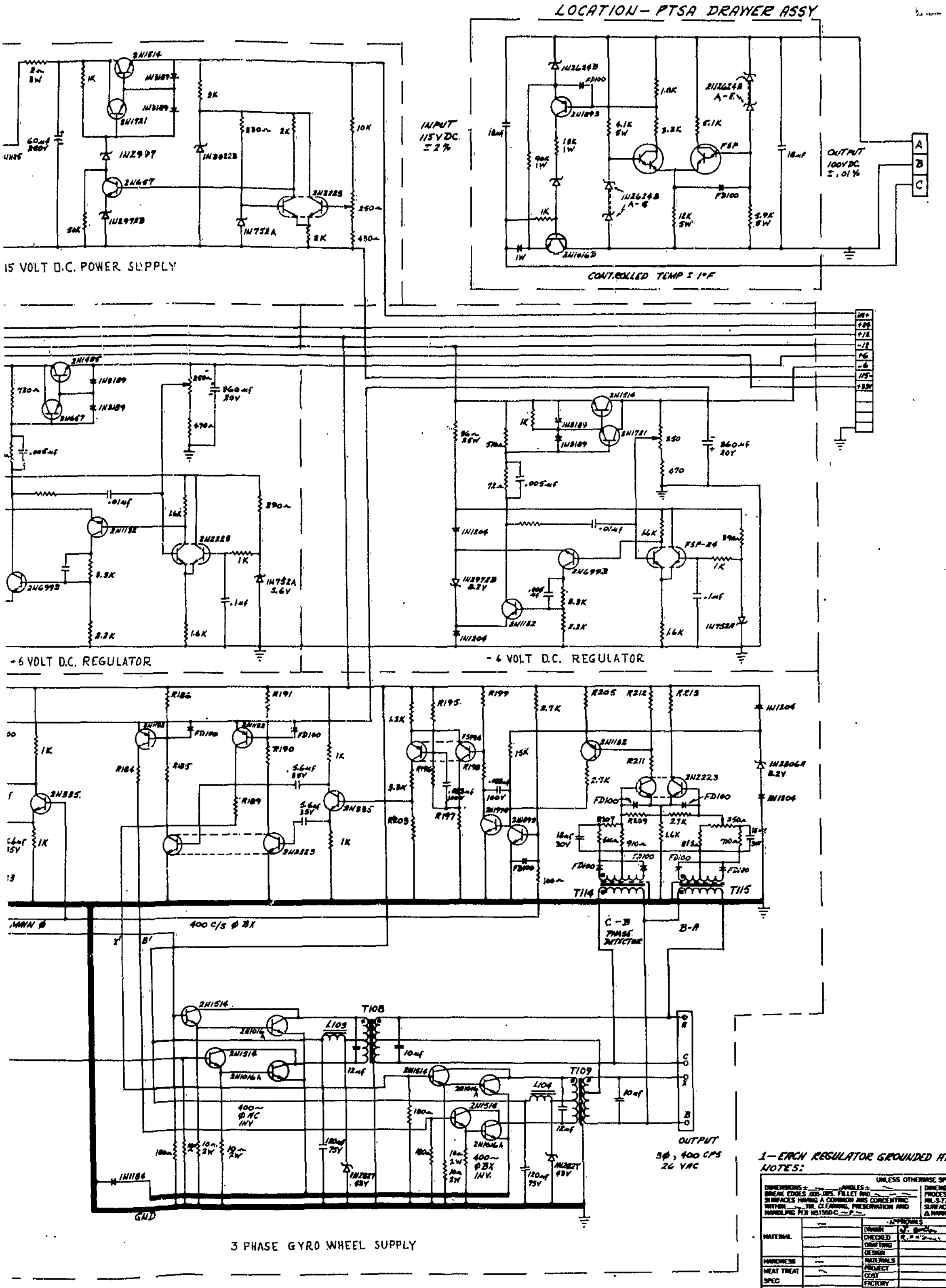
LOCATION – PTSA DRAWER ASSY
INPUT 115 V DC ± 2%
OUTPUT 100 V DC ± .01%
A
B
C
CONTROLLED TEMP ± 1°F
1N2624B
2N1893
2N1016D
FSP
FD100
15 VOLT D.C. POWER SUPPLY
2N1514
2N1721
1N2997
2N697
1N2973B
1N3022B
1N752A
2N2223
+6 VOLT D.C. REGULATOR
– 6 VOLT D.C. REGULATOR
2N1485
2N657
2N1132
2N699B
1N1204
1N2973B
FSP-24
2N1132
1N752A
R184
R185
R186
R189
R190
R191
R195
R196
R197
R198
R199
R203
R205
R207
R209
R211
R212
R213
2N335
2N2223
FD100
1N3806A 8.2V
1N1204
T114
T115
400 c/s φ 3X
MAIN φ
C-B PHASE DETECTOR
B-A
T108
T109
L103
L104
2N1514
2N1016A
400~ φAC INV
400~ φBX INV.
1N2827 43V
1N1186
GND
OUTPUT 3φ, 400 CPS 26 VAC
3 PHASE GYRO WHEEL SUPPLY

2

SK52199

1—EACH REGULATOR GROUNDED AT ONE POINT

NOTES:

UNLESS OTHERWISE SPECIFIED: DIMENSIONS ± — ANGLES ± — BREAK EDGES .005-.015. FILLET RAD — — — SURFACES HAVING A COMMON AXIS CONCENTRIC WITHIN — TIR. CLEANING, PRESERVATION AND HANDLING PER HS1560-C —P—			DIMENSIONS SHOWN ARE AFTER PLATING & SIMILAR PROCESSES & BEFORE PAINTING. THREADS PER MIL-S-7742. DRAWING INTERPRETATION PER HS1380. SURFACE CHARACTERISTICS: MIL-STD-10 PER HS1082. △ MARK PART IDENTIFICATION: MIL-STD-130 PER HS333.			NEXT ASSY	USED ON
						APPLICATION	
MATERIAL	—	APPROVALS		DATE	Hamilton Standard WINDSOR LOCKS, CONNECTICUT • U.S.A.		
		DRAWN	J. [illegible]	1/7/63			
		CHECKED	R. P. H. [illegible]		SANE / FPC POWER SUPPLY		
		DRAFTING					
		DESIGN					
HARDNESS	—	MATERIALS					
HEAT TREAT SPEC	—	PROJECT					
		COST					
		FACTORY					
SURFACE COATING	—	RELEASE		DATE	CODE IDENT NO 73030	SIZE J	SK52199
MFG SPEC	—	EXPERIMENTAL			CONTRACT NO. [illegible]		
		PRELIM PROD					
		PRODUCTION					
MAKE FROM	—	PROD CODE			SCALE: NONE	WEIGHT: LB	SHEET

UDW62-0873-D 1 3-30220-002 FPC-1

The current waveform which is feeding back a restraining force, in the accelerometer, can be filtered to DC and modulated at 400 cycles per second and used in the ASE.

The pitch and roll can be generated by performing a digital to analog conversion on the digital outputs of the system for roll, pitch and yaw rate signals, the inertial gyro PTA current waveform can be filtered. The output of the filters would be DC which can be modulated to a 400 cycle signal and fed into the ASE in place of the yaw rate gyro and derived rate signals.

In order to incorporate a gravity component correction for the accelerometers, an out-of-phase signal to cancel the output of the accelerometer D to A converters can be generated as a function of aircraft attitude. These signals can be obtained from the D to A converters which are used to generate the pitch and roll angle. These angle signals are a linear approximation of the gravity signal and will be only 3% in error at a 30° displacement.

In the existing ASE there is a tilt table which can be replaced by a test function to be built into the flight control system. This function test will replace the existing ASE pre-flight test with an augmented version. It will still be necessary to retain one of the vertical gyros for a "back up" on the proposed system. Since there is no redundancy on the yaw rate gyro and the two accelerometers in the present ASE system, the proposed use of the Inertial Navigation System sensor should not appreciably reduce the system reliability. However, the yaw rate gyro will be retained for basic ASE reliability.

3.5.6.4 Cost Summary

The proposed utilization of the navigation system components will result in a reduction in cost of sensors with no sacrifice in system performance over a system which contains both inertial sensors and stabilization sensors. The cost trade-off is shown below:

Present System		Proposed System	
2 accelerometers	$1,300	2 D/A Converters	$500
1 vertical gyro	1,800		
1 tilt table	300		
Total	$3,400	Total	$500

The cost of the modulator circuits are negligible as is the derived rate network cost. Therefore, a cost reduction of $2,900 per FPC system can be achieved when the inertial instruments are used for stability augmentation.

3.5.7 Electronics Packaging

3.5.7.1 Detail Design (Reference 18X590802, 18X590810, 18X590815)

Due to the weight and the volume of control, computer, display, and power supply electronics required for the system, the electronics package is designed into small groups for versatility and for optimum weight distribution. Separate cabinets were therefore designed for the power supplies and controls and for the sensor and computer input interfaces.

These two cabinets are nearly identical and are made from "Bud Imlock" standard extrusions and connectors which are riveted together to form a strong rigid framework capable of absorbing the stresses and deflections within specifications without depending upon the skin for support. Shelves made from strucutral angles add to the rigidity of the cabinet and provide a sliding surface for each drawer. The mounting feet are an integral part of this structure and are capable of withstanding the shock crash loading without rupture. Four 3/8" mounting studs are to be used to mount each cabinet to the airframe structure. Each of the two cabinets occupies slightly over five cubic feet and together they weigh around 550 pounds.

3.5.7.2 Pulse Torque Amplifier Circuitry

Several critical electronic components in the sensor amplifier are anticipated to require as rigid a temperature control as does the inertial package itself 0.1°F. The balance of the pulse-torque amplifier circuit must be held to ±5°F.

To achieve this temperature control, a drawer of one of the cabinets will be insulated and enclosed. This drawer, known as the "oven", will be maintained at 140° ± 5°F and will exude its thermal flux to the ambient surrounding the cabinet and to the airframe.

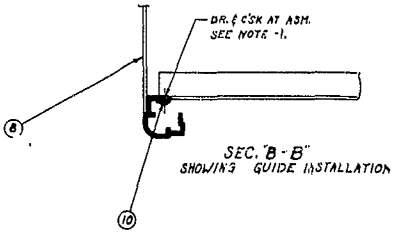
DR. & C'SK AT ASM.
SEE NOTE -1.
⑧
⑩

SEC. "B-B"
SHOWING GUIDE INSTALLATION

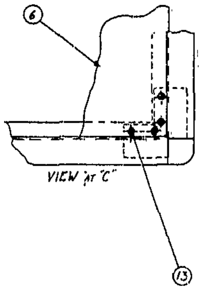

VIEW AT "C"

PT.NO.	CUT SIZE
3	28.45 LG.
4	19 1/16 LG.
5	17.8 LG.
6	19.5 × 16.5
7	28.66 × 16.25
8	28.66 × 19.05
9	16.35 LG.

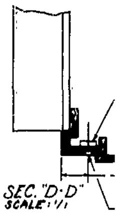

SEC. "D-D"
SCALE: 1/1

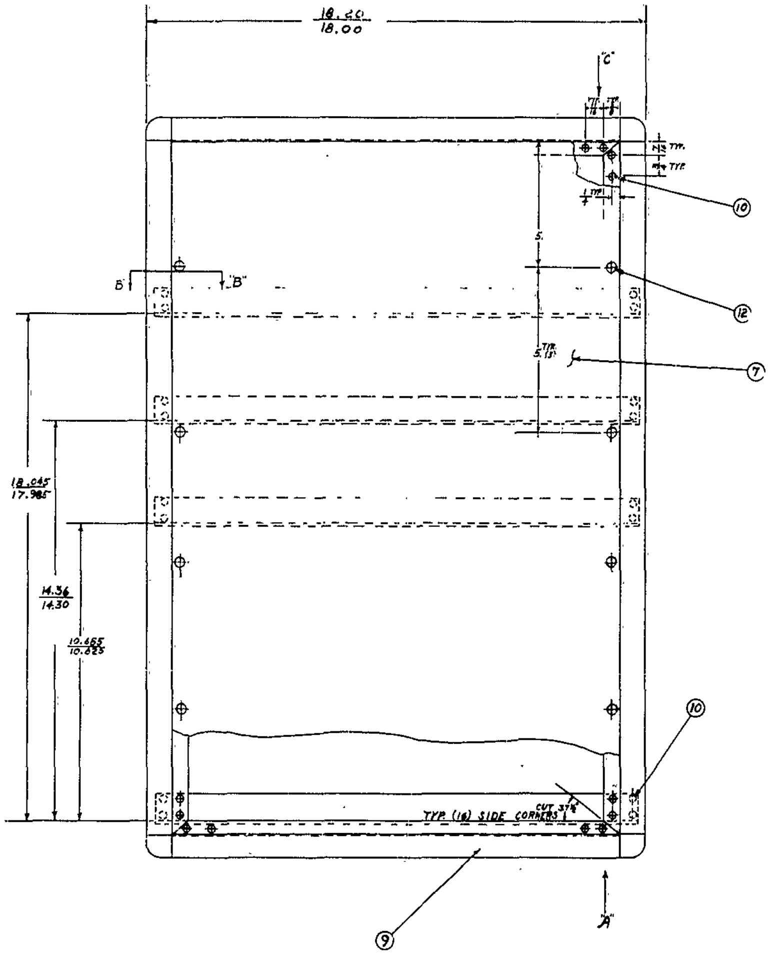
18.20
18.00
"C"
TYP.
TYP.
TYP.
⑩
5.
5.13 TYP.
⑫
⑦
B
"B"
18.045
17.985
14.36
14.30
10.465
10.625
⑩
CUT .375
TYP (16) SIDE CORNERS
⑨
"A"

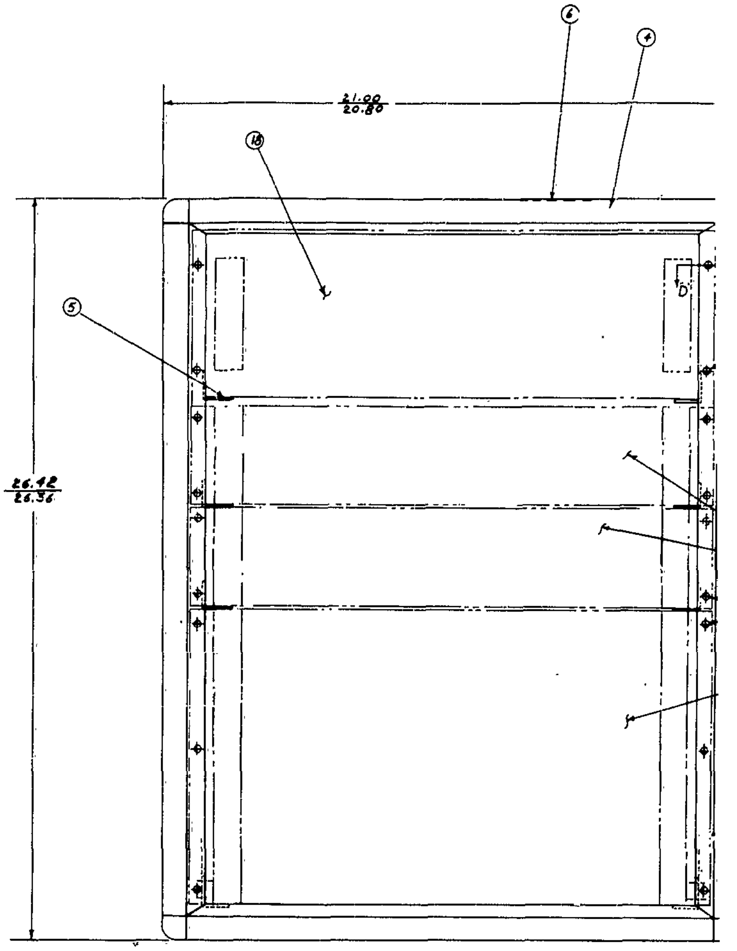
⑥
④
21.00
20.80
⑱
⑤
"D"
26.42
26.36

NOTES:

1. HORIZONTAL UPPER SURFACE PAIRS OF SHELVES PT-6 TO BE CO-PLANAR WITHIN .030".
2. FINISH PER

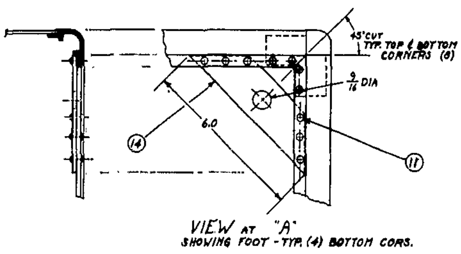
45° CUT
TYP. TOP & BOTTOM CORNERS (8)
9/16 DIA
6.0
⑭
⑪

VIEW AT "A"
SHOWING FOOT - TYP. (4) BOTTOM CORS.

1

PT. NO.	CUT SIZE
3	28.45 LG.
4	19 1/16 LG.
5	17.5 LG.
6	19.5 × 16.5
7	28.66 × 16.85
8	28.66 × 19.05
9	16.35 LG.

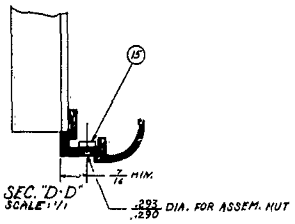

SEC. "D-D"
SCALE: 1/1

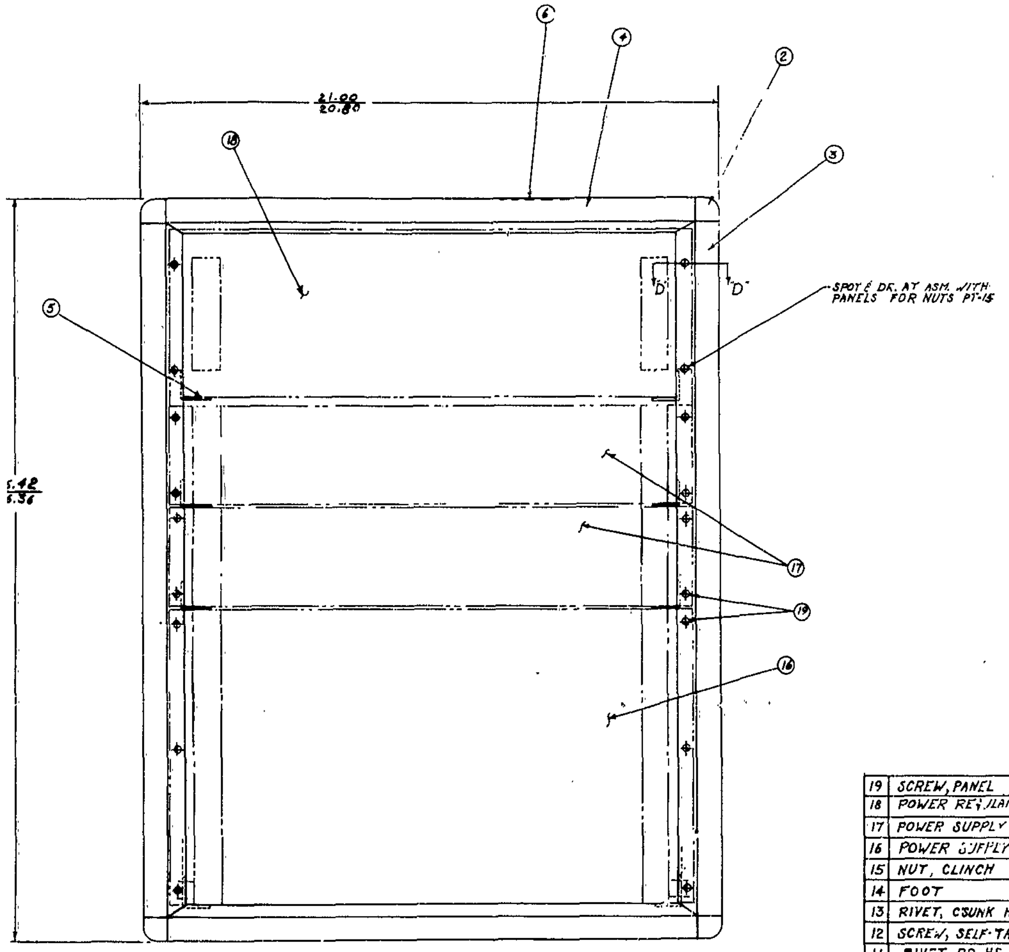

2

NOTES:
1. HORIZONTAL UPPER SURFACE PAIRS OF SHELVES PT-5 TO BE CO-PLANAR WITHIN .030".
2. FINISH PER

PT. NO.	NAME	QTY.	DESCRIPTION
19	SCREW, PANEL	18	#8-32 × 3/4 LG, WASHER HD., AN525-832 12
18	POWER REGULATOR	1	18X 590813
17	POWER SUPPLY	2	LE-101, LAMBDA ELECTRONICS
16	POWER SUPPLY	1	LE-104, LAMBDA ELECTRONICS, HUNTINGTON, L.I., N.Y.
15	NUT, CLINCH	18	PEM NUT TYPE [illegible], PENN [illegible] & MFG CORP
14	FOOT	4	3/4 STK × 2.1/4 DIA. AA-[illegible]
13	RIVET, C'SUNK HD.	16	1/8 DIA. ALUM. × 1/2 LG.
12	SCREW, SELF-TAP	24	#6 × 7/16 LG., AN504 C6R5
11	RIVET, RD. HD.	24	1/8 DIA. ALUM. × 7/16 LG.
10	RIVET, C'SUNK HD.	112	1/8 DIA. ALUM. × 7/16 LG.
9	EXTERNAL EXTRUS.	4	CAT. # BI-2004, BUD IMLOCK
8	BACK COVER	1	.040" THK. ALUM. SHEET
7	SIDE COVER	2	.040" THK. ALUM. SHEET
6	TOP COVER	1	.040 THK. ALUM. SHEET
5	SHELF ANGLE	8	CAT. # BI-2044, BUD IMLOCK
4	EXTERNAL EXTRUS.	4	CAT. # BI-2004, BUD IMLOCK
3	HEAVY DUTY EXTRUS.	4	CAT. # BI-2034, BUD IMLOCK
2	CORNER CONNECTOR	8	CAT. # BI-1001, BUD IMLOCK, BUD RADIO, INC.
1	ASSEMBLY	X	

LIST OF PARTS

UNLESS OTHERWISE SPECIFIED:
DIMENSIONS ± ______, ANGLES ± ______
BREAK EDGES .005-.005, FILLET RAD ______
SURFACES HAVING A COMMON AXIS CONCENTRIC WITHIN ______ TIR.

DIMENSIONS SHOWN ARE AFTER PLATING & SIMILAR PROCESSES & BEFORE PAINTING. THREADS PER MIL-S-7742. DRAWING INTERPRETATION PER HS 1300. SURFACE CHARACTERISTICS: MIL-STD-10 PER HS 1002. & MARK PART IDENTIFICATION: MIL-STD-130 PER HS 333

NEXT ASSY	USED ON
APPLICATION	

		APPROVALS		DATE
MATERIAL		DRAWN	R.J.L.	7/24/63
		CHECKED		
		DRAFTING		
		DESIGN		
HARDNESS		MATERIALS		
HEAT TREAT SPEC.		PROJECT		
		COST		
		FACTORY		
SURFACE COATING		RELEASE		DATE
		EXPERIMENTAL		
MFG. SPEC.		PRELIM PROD.		
		PRODUCTION		
MADE FROM		PROD. CODE		

HAMILTON STANDARD
DIVISION OF UNITED AIRCRAFT CORPORATION
WINDSOR LOCKS, CONNECTICUT, U.S.A

INPUT-OUTPUT
CONSOLE "A"

CODE IDENT NO. 73030
SIZE
18X 590802
CONTRACT NO. NOW 62-0827D
SCALE: 1/2, 1/1
WEIGHT: EST 350 LB
SHEET 1/

FPC-1

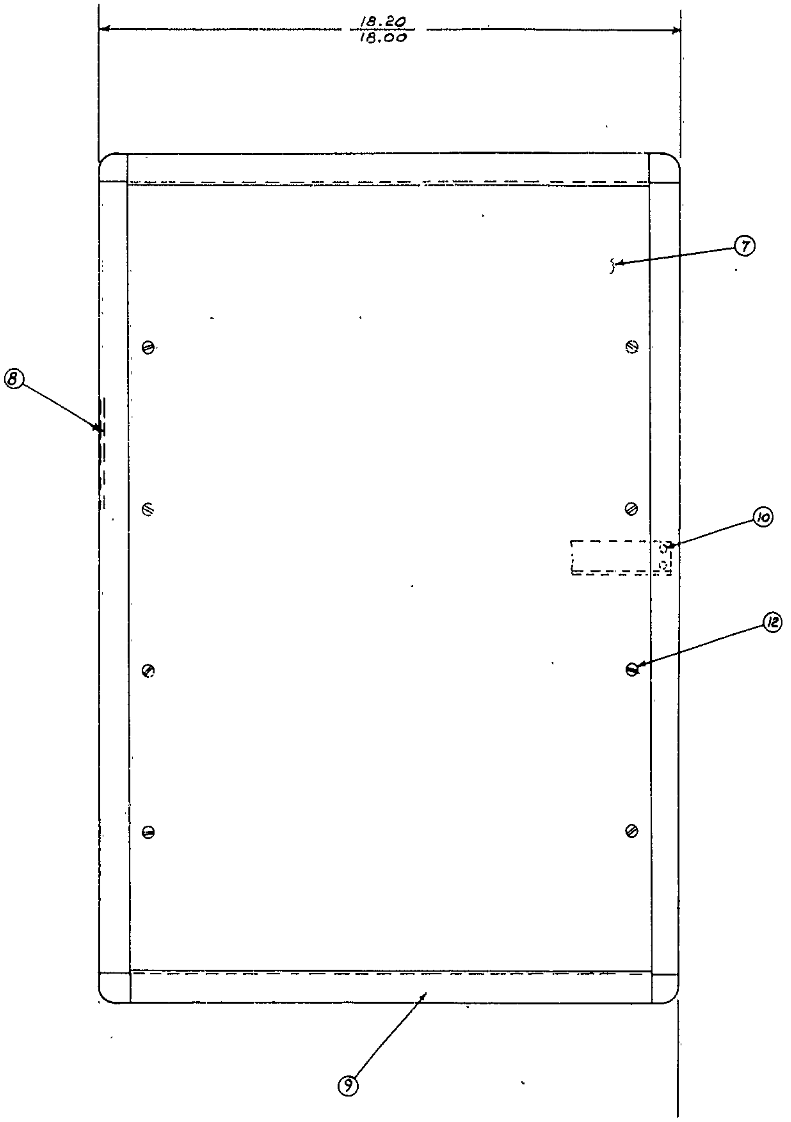
18.20
18.00
⑦
⑧
⑩
⑫
⑨

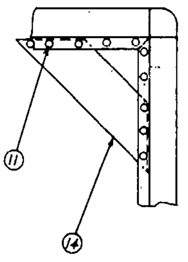

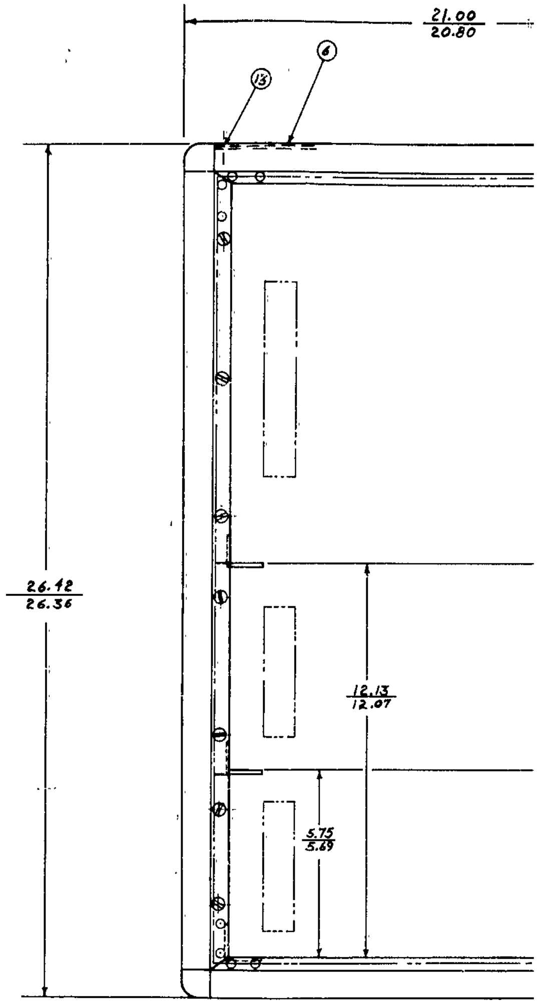
21.00
20.80
⑬
⑥
26.42
26.36
12.13
12.07
5.75
5.69

NOTES:
1. CONSTRUCT (FABRICATE) CABINET
2. FINISH PER

1

2

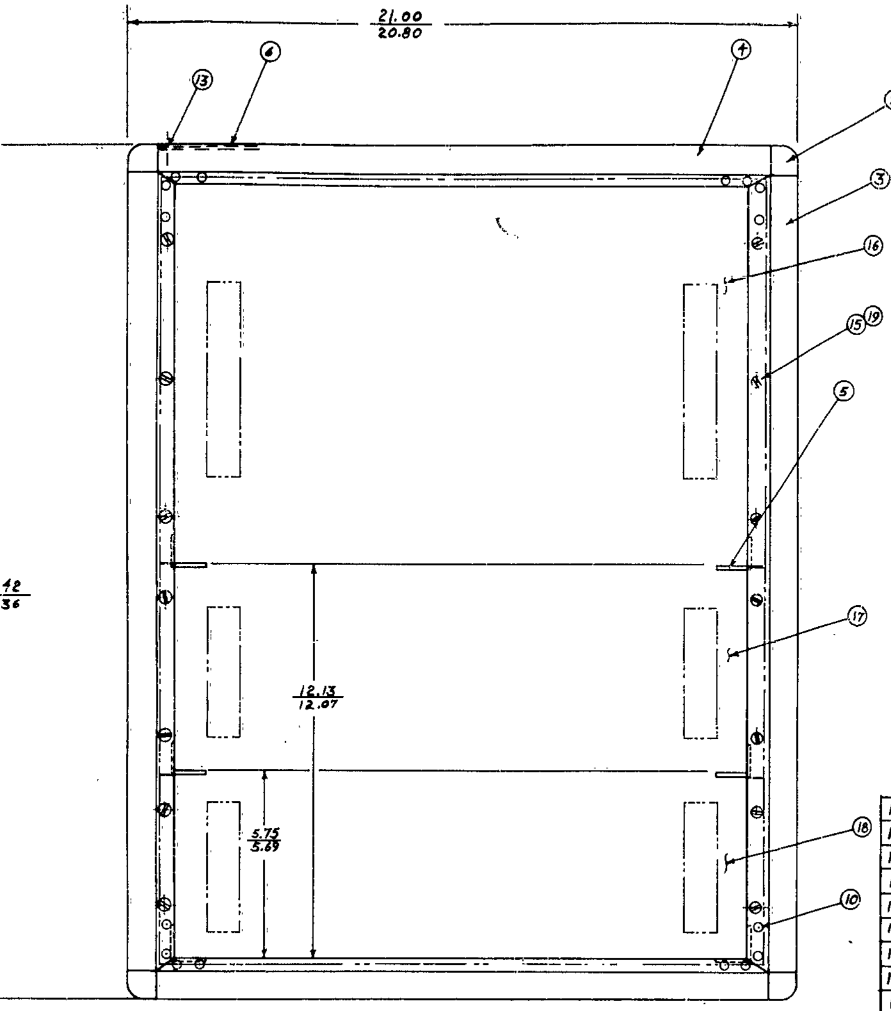

NOTES:
1. CONSTRUCT (FABRICATE) CABINET PER 18X590802.
2. FINISH PER

PC NO.	NAME	QTY	DESCRIPTION
19	SCREW, PANEL	14	#8-32 × 3/4 LG, WASHER HD, AN525-832-12
18	P.T.S.A. OVEN	1	18X590811
17	ANALOG OUTPUT	1	18X590812
16	CONTROL PANEL	1	18X590814
15	NUT, CLINCH	18	PEM NUT, TYPE FE-832, PENN. ENGRG. & MFG. CO.
14	FOOT	4	3/8 STK. × 2." WD., AA6061
13	RIVET, C'SK. HD.	16	1/8 DIA. AL. × 1/2 LG
12	SCREW, SELF-TAP	24	#6 × 5/16 LG., AN504C6R5
11	RIVET, RD. HD.	24	1/8 DIA. ALUM. × 5/16 LG.
10	RIVET, C'SK. HD.	104	1/8 DIA. ALUM. × 7/16 LG
9	EXTERNAL EXTRUSION	4	CAT. # BI-2004, BUD
8	BACK COVER	1	.040" THK. AL. SHT.
7	SIDE COVER	2	.040" THK. ALUM. SHT.
6	TOP COVER	1	.040" THK. ALUM. SHT.
5	SHELF ANGLE	6	CAT. # BI-2044, BUD
4	EXTERNAL EXTRUSION	4	CAT. # BI-2004, BUD
3	HVY. DUTY EXTRUSION	4	CAT. # BI-2034, BUD
2	CORNER CONNECTOR	8	CAT. # BI-1001, BUD IMLOCK, BUD RADIO, INC.
1	ASSEMBLY		

LIST OF PARTS

UNLESS OTHERWISE SPECIFIED:
DIMENSIONS ± ______ ANGLES ± ______
BREAK EDGES .005-.025, FILLET RAD ______-______
SURFACES HAVING A COMMON AXIS CONCENTRIC WITHIN ______ TIR.
DIMENSIONS SHOWN ARE AFTER PLATING & SIMILAR PROCESSES & BEFORE PAINTING. THREADS PER MIL-S-7742. DRAWING INTERPRETATION PER HS 1360. SURFACE CHARACTERISTICS: MIL-STD-10 PER HS 1002. & MARK PART IDENTIFICATION: MIL-STD-130 PER HS 333.

NEXT ASSY	USED ON
APPLICATION	

MATERIAL
HARDNESS
HEAT TREAT SPEC
SURFACE COATING
MFG SPEC
MAKE FROM

APPROVALS		DATE
DRAWN	R. L.	3-27-6
CHECKED		
DRAFTING		
DESIGN		
MATERIALS		
PROJECT		
COST		
FACTORY		

RELEASE		DATE
EXPERIMENTAL		
PRELIM PROD.		
PRODUCTION		
PROD. CODE		

HAMILTON STANDARD
DIVISION OF UNITED AIRCRAFT CORPORATION
WINDSOR LOCKS, CONNECTICUT, U.S.A.

INPUT - OUTPUT
CONSOLE "B"

CODE IDENT NO. 73030
CONTRACT NO. NOW 62-0873 D
SIZE
18X590810
SCALE: 1/2
WEIGHT: LB
SHEET

FPC-1

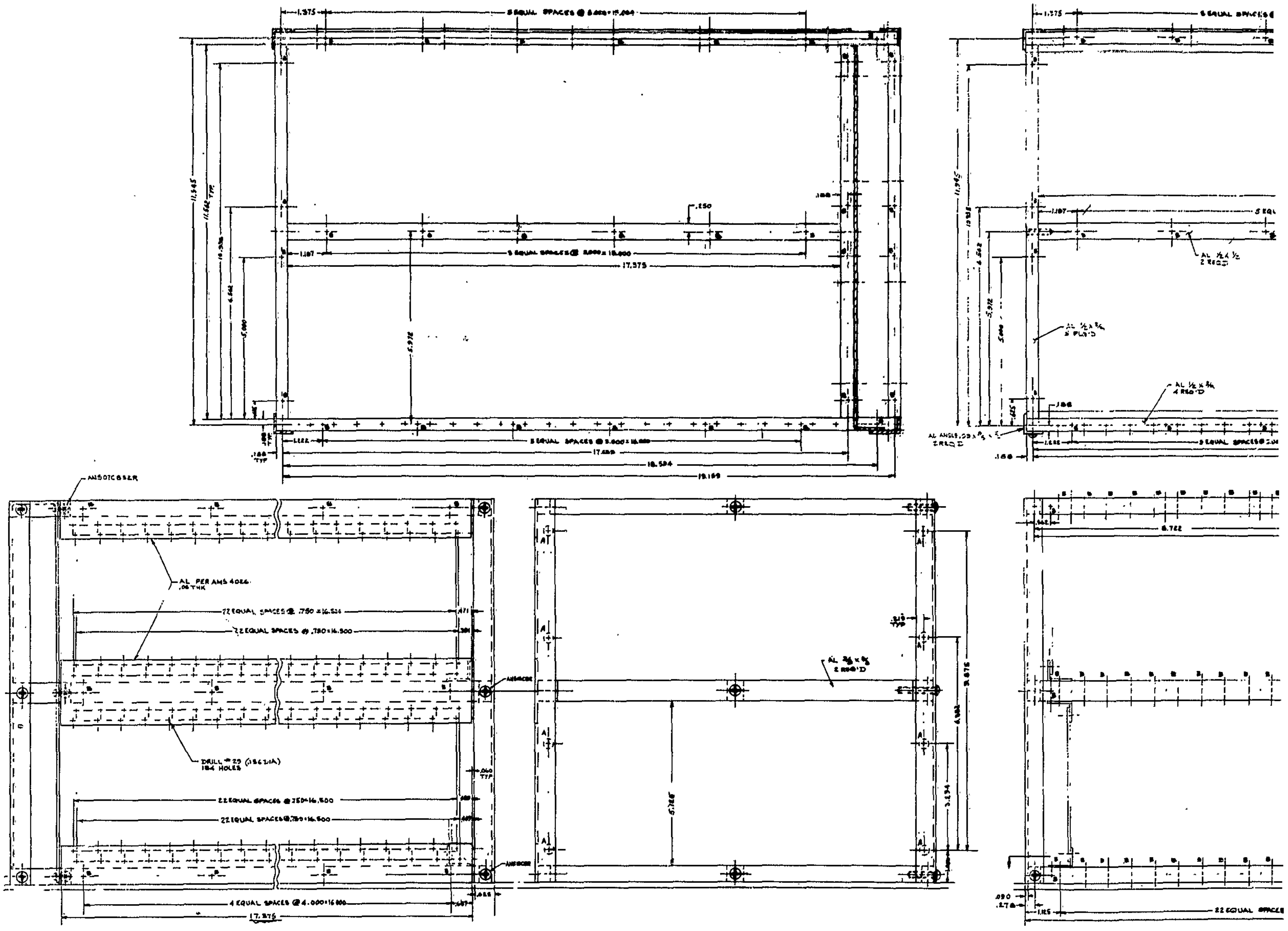
1.375
5 EQUAL SPACES @ 3.000=15.000
11.545
11.562 TYP
.250
.188
1.187
5 EQUAL SPACES @ 3.000=15.000
17.375
5.912
5.000
.188 TYP
5 EQUAL SPACES @ 3.000=15.000
17.489
18.594
19.189
AL ½ x ½
2 REQ'D
AL ½ x ¾
5 PLS'D
AL ½ x ¾
4 REQ'D
AL ANGLE
2 REQ'D
.188
.625
MS07C832R
AL PER AMS 4026
.06 THK
22 EQUAL SPACES @ .750=16.500
DRILL #29 (.136 DIA)
184 HOLES
.040 TYP
4 EQUAL SPACES @ 4.000=16.000
17.375
AL ⅜ x ⅝
2 REQ'D
9.875
6.562
3.234
5.188
.090
.278
6.722
22 EQUAL SPACES

1

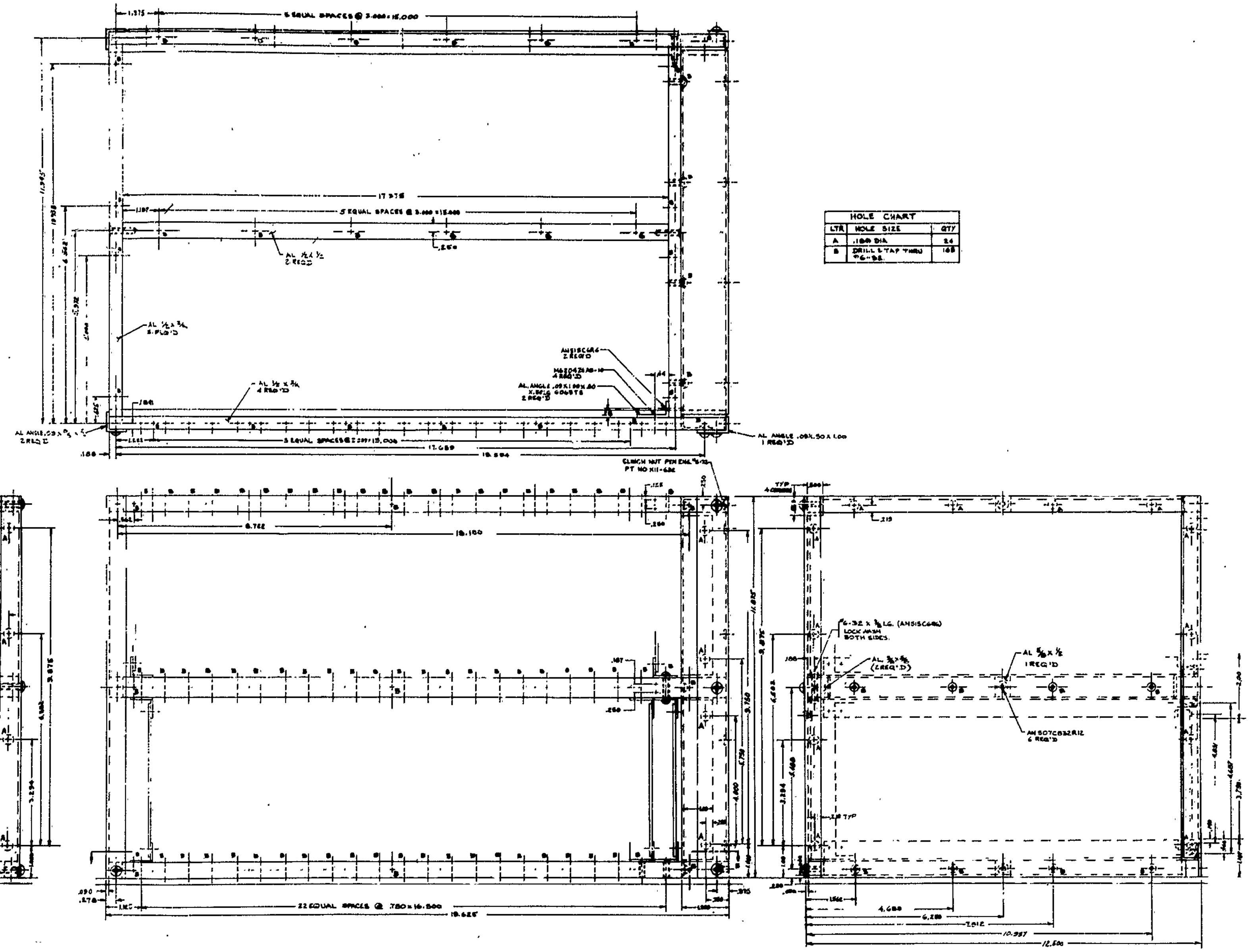
5 EQUAL SPACES @ 3.000=15.000
1.375
17.375
1.187
5 EQUAL SPACES @ 3.000=15.000
.250
AL ½ x ½
2 REQ'D
AL ½ x ¾
5 REQ'D
AL ½ x ¾
4 REQ'D
AN515C6R6
2 REQ'D
AL ANGLE .09 X 1.00 X .50
2 REQ'D
AL ANGLE .09 X .50 X 1.00
1 REQ'D
.188
5 EQUAL SPACES @ 3.000=15.000
17.689
19.594
11.945
CLINCH NUT PEN ENG. #6-32
PT NO KII-632
8.762
18.100
.187
.250
22 EQUAL SPACES @ .750=16.500
19.625
.125
.250
6-32 x ⅜ LG. (AN515C6R6)
LOCK WASH
BOTH SIDES.
AL ⅜ x ⅜
(2 REQ'D)
AL ⅝ x ½
1 REQ'D
AN507C632R12
6 REQ'D
.219
TYP
1.562
4.680
6.250
7.812
10.937
12.500
A
B

HOLE CHART		
LTR	HOLE SIZE	QTY
A	.189 DIA	24
B	DRILL & TAP THRU #6-32	168

2

UNLESS OTHERWISE SPECIFIED:

NEXT ASSY | USED ON

APPLICATION

APPROVALS | DATE

HAMILTON STANDARD

DIVISION OF UNITED AIRCRAFT CORPORATION

WINDSOR LOCKS, CONNECTICUT, U.S.A.

FRAME ASSY
LOGIC MODULE

18X590815

SCALE

SHEET

A single "on-off" type thermoswitch will actuate a heater to maintain this temperature range. At the maximum operating ambient temperature within the cabin (100°F) a thermal balance is maintained between the "oven" components and the ambient, with the heater never being required. At the low ambient operating temperature (40°F), the heater will be "on" nearly constantly in maintaining the desired temperature.

Secured to the oven will be six constant-temperature blocks containing the critical circuit elements. Each block, representing a specific sensor, will be temperature controlled by a bridge circuit to ± 0.1°F, which will offer proportional heater control from "off" to the full heater power of ten watts. These components will be held at 145°F.

3.5.7.3 Digital Logic

Four separate racks are required to house the digital logic, each weighing around seventy pounds and occupying 1.8 cubic feet. The small size of these racks will facilitate their placement within the vehicle.

Each rack is constructed to withstand the vibration and shock loads required. It has a light-weight structure into which are stacked 46 "mother-boards". These boards add to the rigidity of the assembly, since they are in sliding contact with each other. Since each "mother-board" has a capacity of ten 2" x 2" flip-flop boards, the total capacity of each rack is 460 flip-flops. Each mother-board fits into an electrical connector and is screwed securely into place. A dust cover encloses the entire rack.

3.5.7.4 Pilots Control Panel (Reference 18X590801)

A preliminary pilots panel layout has been included to show the basic FPC controls. This panel will be constructed as a breadboard, and will not contain lighting, nor etched lettering. The panel layout may be revised at a later date to insure compatibility with the SH-3A cockpit layout.

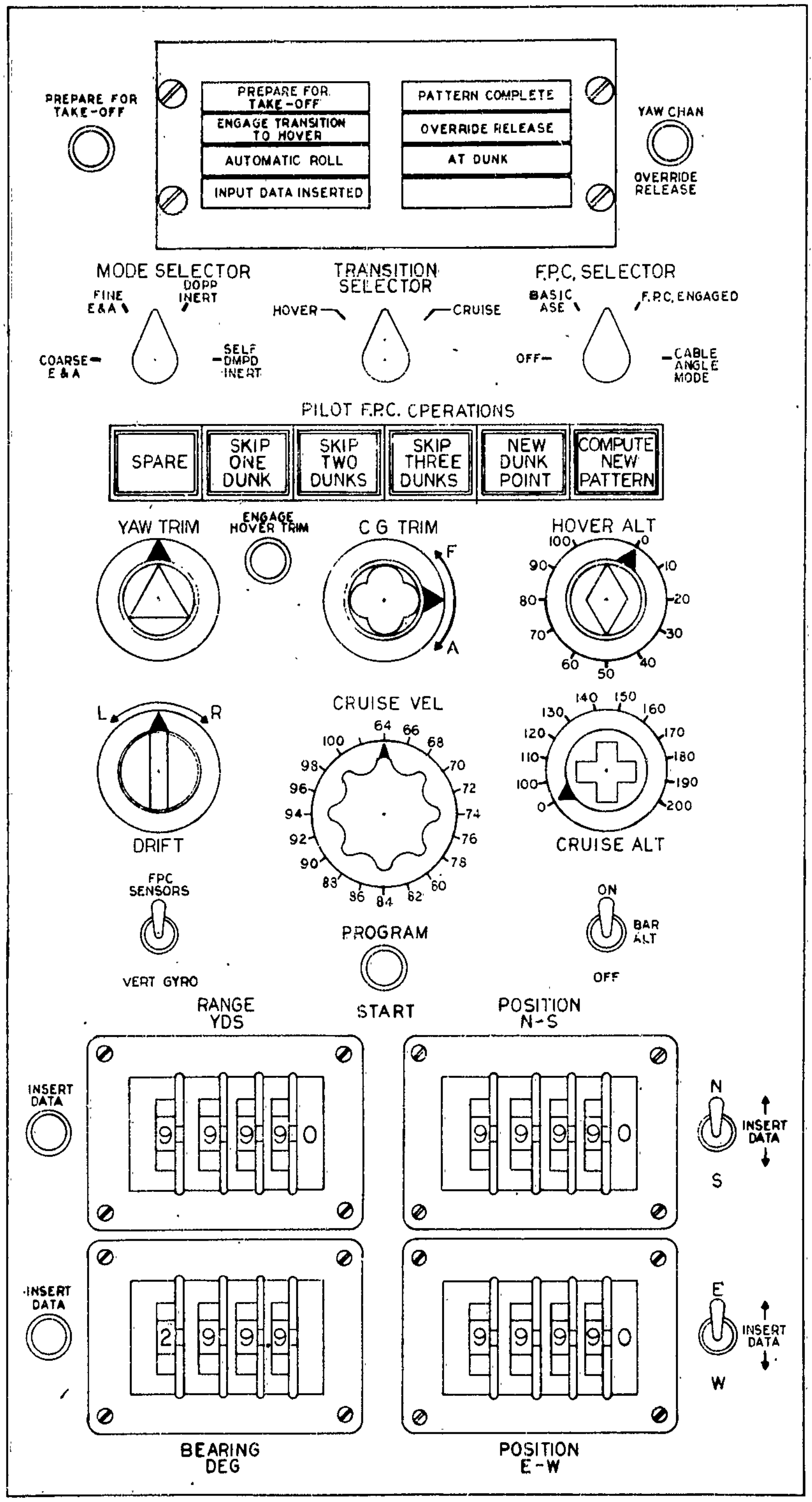
PREPARE FOR TAKE-OFF
PREPARE FOR TAKE-OFF
ENGAGE TRANSITION TO HOVER
AUTOMATIC ROLL
INPUT DATA INSERTED
PATTERN COMPLETE
OVERRIDE RELEASE
AT DUNK
YAW CHAN
OVERRIDE RELEASE
MODE SELECTOR
FINE E&A
DOPP INERT
COARSE E&A
SELF DMPD INERT
TRANSITION SELECTOR
HOVER
CRUISE
F.P.C. SELECTOR
BASIC ASE
F.P.C. ENGAGED
OFF
CABLE ANGLE MODE
PILOT F.P.C. OPERATIONS
SPARE
SKIP ONE DUNK
SKIP TWO DUNKS
SKIP THREE DUNKS
NEW DUNK POINT
COMPUTE NEW PATTERN
YAW TRIM
ENGAGE HOVER TRIM
C G TRIM
F
A
HOVER ALT
100 0 10 20 30 40 50 60 70 80 90
L
R
DRIFT
CRUISE VEL
64 66 68 70 72 74 76 78 80 82 84 86 88 90 92 94 96 98 100
CRUISE ALT
130 140 150 160 170 180 190 200 0 100 110 120
FPC SENSORS
VERT GYRO
PROGRAM
START
ON
BAR ALT
OFF
RANGE YDS
POSITION N-S
INSERT DATA
9 9 9 9 0
9 9 9 9 0
N
S
INSERT DATA
INSERT DATA
2 9 9 9
9 9 9 9 0
E
W
INSERT DATA
BEARING DEG
POSITION E-W

PRELIMINARY
PILOT CONTROL PANEL
18X590801

4.0 LIST OF CONFERENCES

The following is a list of meetings and conferences held during the design program:

1. Naval Aviation Facility at Indianapolis, Indiana
   August 6, 1962
   Mr. Richard Wisehart (NAFI)
   Mr. Arpad Ostheimer (HSED)
   The purpose of this meeting was to explore further the erection and alignment problems encountered on an aircraft carrier.

2. Naval Air Development Center, Johnsville, Pa.
   August 20, 1962
   Lt. Cmdr. J. Waldron (NADC)
   Mr. R. Bell (NADC)
   Mr. A. Allen (NADC)
   Mr. G. Davis (NADC)
   The purpose of this meeting was to obtain information on ASW tactics and discuss erection and alignment techniques on a moving base.

3. Naval Ordnance Test Station, China Lake, California
   September 13, 1962
   Mr. R. Cole (NOTS)
   Mr. R. Seely (NOTS)
   Mr. W. Roehrs (NOTS)
   Mr. D. Shefrin (HSED)
   The purpose of this visit was to discuss the erection and alignment of platform and strapped down systems.

4. Sikorsky Aircraft Division of U.A.C., Stratford, Conn.
   September 18, 1962
   Mr. R. Stutz (SA)
   Mr. L. Freeman (SA)
   Mr. J. Corso (SA)
   Mr. H. Monterose (HSED)
   The purpose of this meeting was to obtain information on the generation of a flight path based on Sikorsky's previous experience.

5. Bell Aerosystems Company, Buffalo, New York
September 19, 1962
Mr. F. Powell (Bell)
Mr. T. O'Brien (HSED)
Mr. D. Brown (HSED)
This visit was made to obtain data on aircraft carrier motion specifically the power spectral density in roll, pitch and translational accelerations.

6. Sikorsky Aircraft Division of U.A.C., Stratford, Conn.
September 21, 1962
Various personnel of Sikorsky Aircraft
Mr. H. Monterose
This trip was made to obtain data on existing navigational equipment on the SH-3A, specifically AN/APN130, AN/ASA13A, AN/ARN21B, AN/APN117 and the AQS/10.

7. Bureau of Naval Weapons, Washington, D.C.
October 8, 1962
Mr. G. Tsaparas (BuWeps)
Mr. R. Russ (HSED)
Mr. T. O'Brien (HSED)
This meeting was held to review progress to date on the FPC program.

8. Hamilton Standard Division, U.A.C., BroadBrook, Conn.
October 29 and 30, 1962
Mr. G. Tsaparas (BuWeps)
Mr. H. Welk (NADC)
HSED Project Engineering and Sales
A meeting was held to review progress to date on the FPC.

9. Naval Ordnance Test Station, China Lake, California
November 8, 1962
Mr. R. Cole (NOTS)
Mr. R. Seely (NOTS)
Mr. D. Brown (HSED)
This discussion was concerned with the overall erection and alignment of the FPC inertial system and the preliminary system block diagram was reviewed.

10. Sikorsky Aircraft Division, U.A.C., Stratford, Conn.
November 16, 1962
Mr. H. Oakes (SA)
Mr. T. Meeks (SA)
Mr. S. Opie (SA)
Mr. T. O'Brien (HSED)
Mr. A. Ostheimer (HSED)
The purpose of this visit was to obtain information on the SH-3A flight characteristics in order to initiate a suitable design of the autopilot.

11. Bureau of Naval Weapons, Washington, D. C.
November 19, 1962
Mr. C. Schaeffer (BuWeps)
Mr. T. O'Brien (HSED)
This conference was held to discuss the basic operational techniques and problems associated with the ASW problem.

12. Bureau of Naval Weapons, Washington, D. C.
December 11, 1962
Mr. G. Tsaparas
Mr. T. O'Brien (HSED)
Mr. J. Gorman (HSED)
This visit was made to appraise BuWeps of the latest progress on the FPC.

13. Sikorsky Aircraft Division of U.A.C., Stratford, Conn.
December 28, 1962
Mr. T. Meeks (SA)
Mr. T. O'Brien (HSED)
A proposed text of a work statement was reviewed for a subcontract to SA.

14. Bureau of Naval Weapons, Washington, D. C.
January 28, 1963
Mr. G. Tsaparas (BuWeps)
Mr. C. Brahm (HSED)
Mr. J. Bambling (HSED)
Mr. J. Shaubaugh (HSD Washington Office)
Mr. T. O'Brien (HSED)
This visit was made to review the progress to date and to discuss the future program content.

15. Sikorsky Aircraft Division, U.A.C., Stratford, Conn.
February 12, 1963
Mr. T. Meeks
Mr. T. O'Brien
This visit was made to discuss progress on the S.A. subcontract.

16. Sikorsky Aircraft Division, U.A.C., Stratford, Conn.
March 1, 1963
Mr. T. Meeks
Mr. T. O'Brien
This meeting was held to review the conclusions of the SA design study.

17. Bureau of Naval Weapons, Washington, D. C.
March 14, 1963
Mr. G. Tsaparas
Mr. J. Shaubaugh (HSD Washington Office)
Mr. T. O'Brien (HSED)
This meeting was held to discuss the program progress to date.

5.0 APPENDIX

5.1 Flight Path

5.1.1 Derivation of Flight Path Equations

Dunk Point - To - Dunk Point

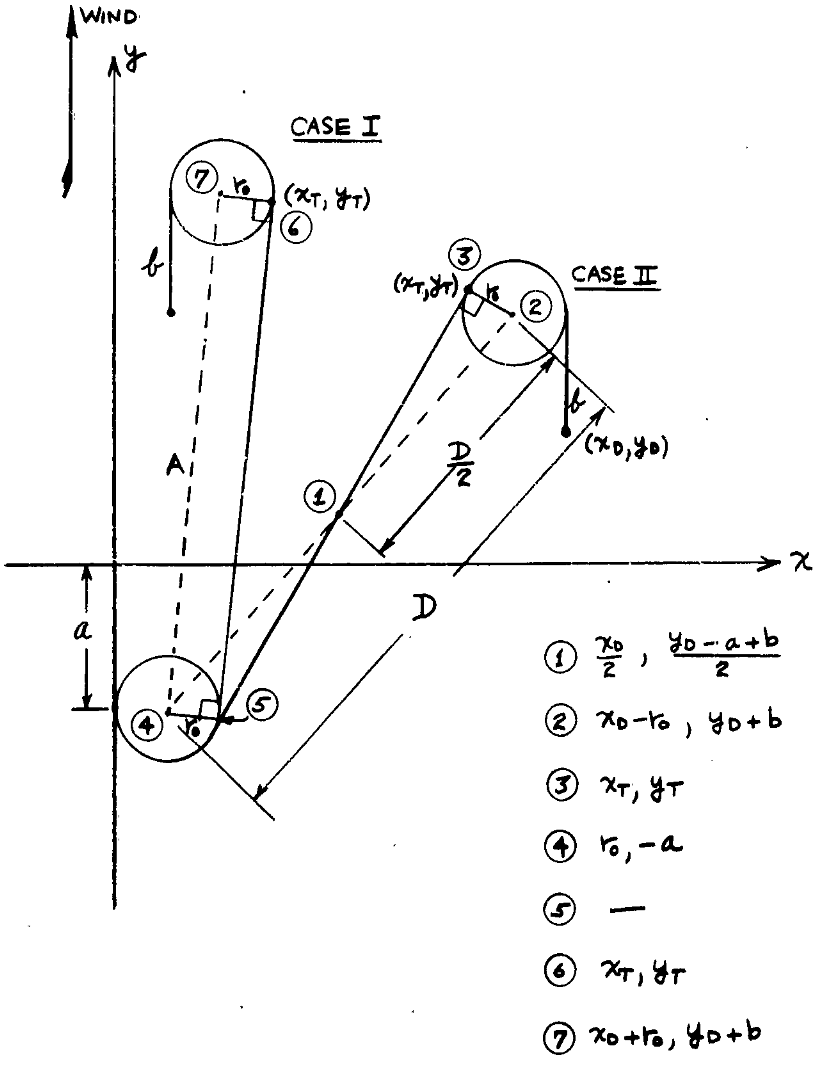
WIND
y
CASE I
⑦
r_0
(x_T, y_T)
⑥
b
A
③
(x_T, y_T)
r_0
②
CASE II
b
(x_D, y_D)
$\frac{D}{2}$
①
x
a
D
⑤
④
r_0

①	$\frac{x_D}{2}$, $\frac{y_D - a + b}{2}$
②	$x_D - r_0$, $y_D + b$
③	x_T, y_T
④	$r_0, -a$
⑤	—
⑥	x_T, y_T
⑦	$x_D + r_0, y_D + b$

CASE I

Finding (X_T, Y_T) reduces to solving the right triangle formed by the line of centers of the turn circles, the common tangent which crosses the line of centers at point 1, and the radius to the point of tangency (X_T, Y_T).

Points 1 and 2 and distances $\overline{1,2}$ and $\overline{2,3}$ are known; therefore point 3 may be located, and (X_T, Y_T) may be specified as in Sect. 3.3.5.2.

CASE II

Figure $\overline{4,5,6,7}$ is a rectangle; points 4 and 7 are known as well as the length of all four sides. The rectangle is solved for point 6 = (X_T, Y_T).

Base - To - First Dark Point

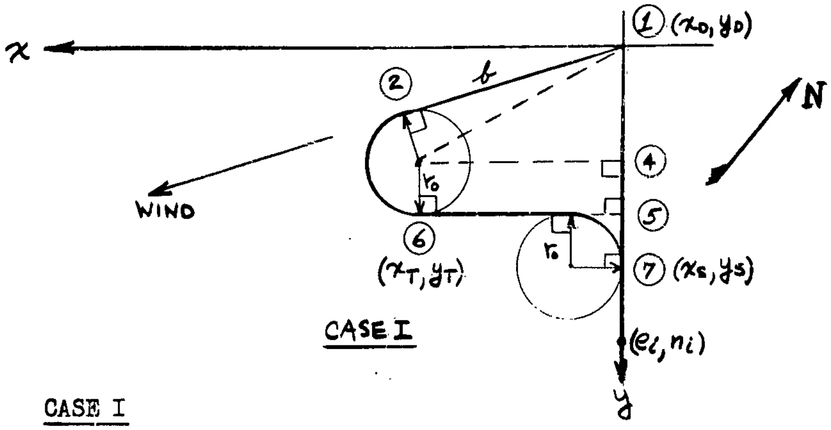

CASE I

The length of the sides of right triangle $\overline{1,2,3}$ are known, as well as the location of point 1. Point 2 is found from the distance, b, and the direction of the wind. The triangle is solved for the location of point 3. Figure $\overline{3,4,5,6}$ is a rectangle, hence finding a solution for point 3 leads directly to point 6 = (X_T, Y_T) and point 7 = (Xs, Ys).

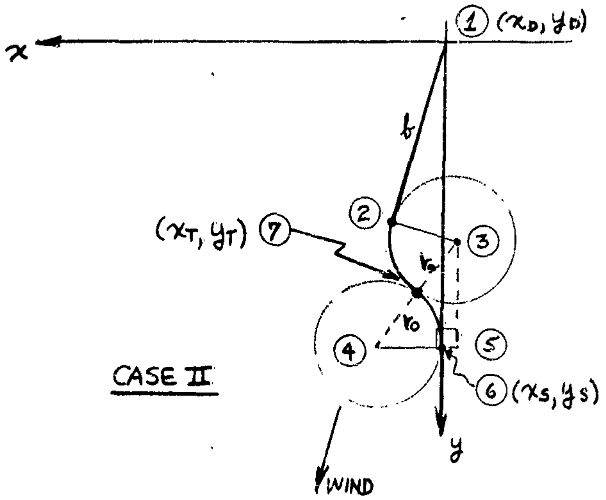

CASE II

As in case 1, the right triangle $\overline{1,2,3}$ is solved for point 3. From knowledge of the distance $\overline{3,4}$ and the X component of point 4, it is possible to solve the right triangle $\overline{3,4,5}$ for points 4 and 5, and this leads to a solution for point 6 = (Xs, Us). By averageing the X and Y components of points 3 and 4, point 7 = (X_T, Y_T) is determined.

5.1.2 Flight Path Errors

The following is a derivation of the flight path error expression, $\Delta \Phi_{max.}$, presented in Sec. 3.3.6.1.5

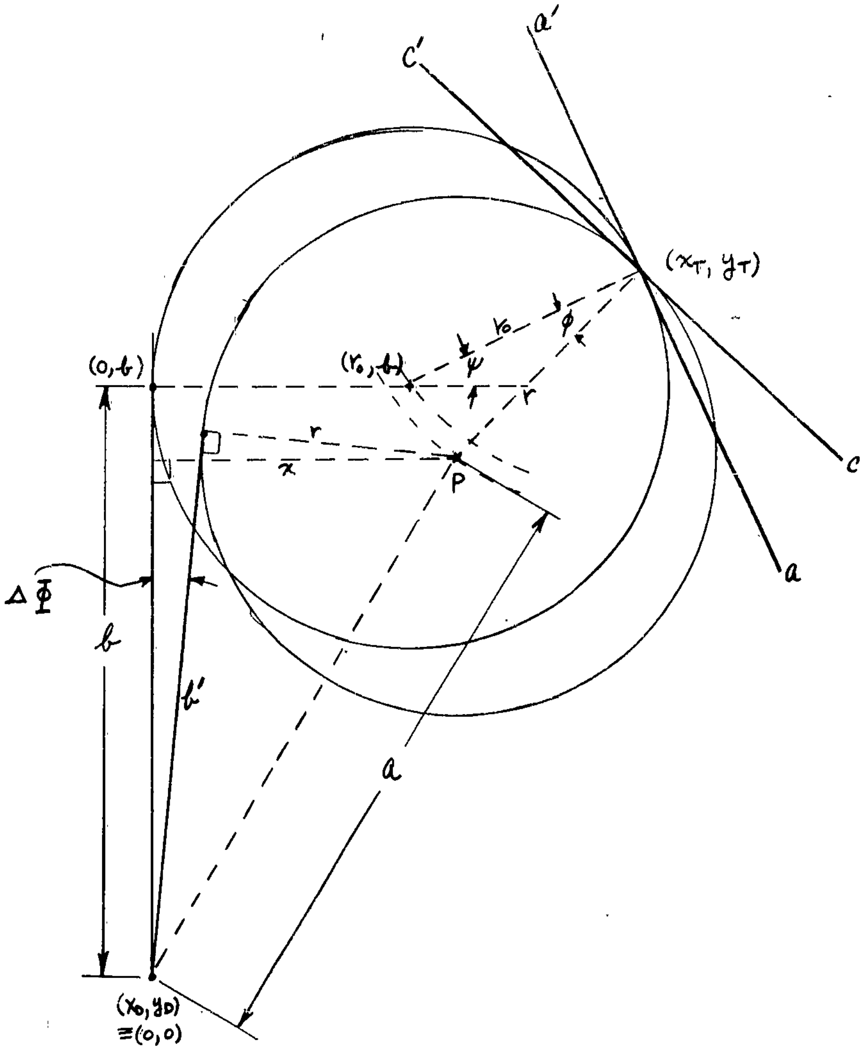
a'
c'
(x_T, y_T)
r_0
ψ
ϕ
(r_0, b)
$(0, b)$
r
r
x
P
c
a
$\Delta\Phi$
b
b'
a
(x_0, y_0)
$\equiv (0,0)$

$$\Delta\Phi = \sin^{-1}\left(\frac{x}{a}\right) - \sin^{-1}\left(\frac{r}{a}\right) = \sin^{-1}\left[\frac{x\sqrt{a^2-r^2} - r\sqrt{a^2-x^2}}{a^2}\right]$$

$$P = \underbrace{\left[r_0 - (r-r_0)\cos\psi + r\phi\sin\psi\right]}_{x}, \underbrace{\left[b - (r-r_0)\sin\psi - r\phi\cos\psi\right]}_{y}, \text{For Small}$$

SMALL VALUES OF ϕ.

Value of ϕ

$A^2 = X^2 + Y^2 = b^2 + ro^2 + (r-ro)^2 + (r\phi)^2 - 2\,(r-ro)(ro\cos\psi + b\sin\psi)$
$-2r\phi\,(b\cos\psi - r_0\sin\psi)$

For the case when ϕ is small we can eliminate all terms in ϕ^2, $(r-ro)^2$, and $(r-ro)\phi$. (Section 3.3.6.1.5 made the assumption that $r \rightarrow ro$ as ϕ o.)

Thus, $a^2 \approx b^2 + ro^2 - 2(r-ro)\,(r\cos\psi + b\sin\psi) - 2r\phi\,(b\cos\psi - ro\sin\psi)$
and, $X^2 \approx ro^2 - 2\,ro\,(r-ro)\cos\psi + 2\,r_0 r\psi\sin\psi$

Therefore,

$$\Delta\Phi = \sin^{-1}\left\{\frac{\left[r_0-(r-r_0)\cos\psi + r\phi\sin\psi\right]\left[-\sqrt{b^2-(r-r_0)^2-2(r-r_0)(r_0\cos\psi+b\sin\psi)-2r\phi(b\cos\psi-r_0\sin\psi)}\right] - r\sqrt{-b^2-2(r-r_0)b\sin\psi-2r\phi\, b\cos\psi}}{b^2+r_0^2-2(r-r_0)(r_0\cos\psi+b\sin\psi)-2r\phi(b\cos\psi-r_0\sin\psi)}\right\}$$

Under the assumption of section 3.3.6.1.5 to get the bounding value of $\Delta\Phi$ we let $r \rightarrow r_0$.

$$\Delta\Phi \rightarrow \sin^{-1}\left[\frac{r_0(1+\phi\sin\psi)\sqrt{b^2-2r_0\phi(b\cos\psi-r_0\sin\psi)} - r_0\sqrt{b^2-2r_0\phi b\cos\psi}}{b^2+r_0^2+2r_0\phi(b\cos\psi-r_0\sin\psi)}\right]$$

$$= \sin^{-1}\left[\frac{b r_0(1+\phi\sin\psi)\sqrt{1-2\phi\left(\frac{r_0}{b}\cos\psi-\frac{r_0^2}{b^2}\sin\psi\right)} - b r_0\sqrt{1-2\phi\frac{r_0}{b}\cos\psi}}{b^2+r_0^2\left[1+2\phi\left(\frac{b}{r_0}\cos\psi-\sin\psi\right)\right]}\right]$$

For the case when ϕ is small ($<15°$):

$$\Delta\Phi \approx \sin^{-1}\left[\frac{br_0\left[(1+\phi\sin\psi)\left(1-\phi\left\{\frac{r_0}{b}\cos\psi-\frac{r_0^2}{b^2}\sin\psi\right\}\right)-\left(1-\phi\frac{r_0}{b}\cos\psi\right)\right]}{b^2+r_0^2\left[1+2\phi\left(\frac{b}{r_0}\cos\psi-\sin\psi\right)\right]}\right]$$

$$\doteq \sin^{-1}\left[\frac{br_0\phi\sin\psi\left(1+\frac{r_0^2}{b^2}\right)}{b^2+r_0^2\left[1+2\phi\left(\frac{b}{r_0}\cos\psi-\sin\psi\right)\right]}\right]$$

This expression has a maximum value when $\sin\psi=1$, and

$$\Delta\Phi_{max} = \sin^{-1}\left[\frac{br_0\phi\left(1+\frac{r_0^2}{b^2}\right)}{b^2+r_0^2(1-2\phi)}\right] = \sin^{-1}\left(\phi\frac{r_0}{b}\right)$$

and for small values of ϕ:

$$\Delta\Phi_{max} \approx \phi\frac{r_0}{b}$$

5.2 List of References

1. MIT Instrumentation Lab. 1
   Analysis of an Inertial Navigational system, by Charles Broxmeyer, MIT R-241, August, 1959, Page 112.

2. MIT Instrumentation Lab.
   Compensation of a Digital Integrating Accelerometer, by Robert Haym, thesis. MIT R-T-209A, June, 1959. Page 112
   MIT Instrumentation Lab.
   Coordinate Frames in Inertial Navigation

3. MIT Instrumentation Lab.
   Effects of Quantization in Local Vertical Inertial System, by D. F. McAllister, thesis. MIT R-156, September, 1957. Page 46.

4. MIT Instrumentation Lab.
   Inertial Guidance, by W. Wrigley, R. Woodbury, and J. Havorka. AD 124260, January 28-31, 1957. Page 69.
   NASA TECH. NOTE

5. Investigation of the Errors of an Inertial Guidance System During Satellite re-entry, by J. S. White, TN-D 322, August, 1960. Page 42.

6. ARS JL, March, 1961. Pages 356-360.
   Alignment of an Inertial Autonavigator, by L. R. McMurray.

7. Control Eng., May, 1961. Pages 121-122.
   Autocompensation of Errors in Gyros and Accelerometers, by J. M. Slater.

8. SAE PREPRINT, October 3-9, 1959. Page 7.
   Doppler-Inertial Navigation for High Performance Aircraft, by L. S. Reel.

9. Ryan Reporter, February 27, 1960. Page 10.
   A Precision Navigational System - Doppler - Inertial, by Reel

10. AAS Preprint, January 16-18, 1961. Page 20
    Gimballess Inertial Navigation in Lunar or Planetary Guidance, by Don McAllister, 7th Annual Meeting, Dallas, Texas

11. ARS Preprint, October 9-15, 1961. Page 18
Guidance and Navigation Systems for Lunar Missions, by R. C. Hakes. ARS Space Flight Report to the Nation, New York, New York Preprint 2294-61

12. Inst. Aerosp. Sci. Preprint, January 22-24, 1962. Page 18
A Hybrid Strapped-Down Inertial Stellar Guidance System, by I. Citron. 30th Annual Meeting, New York, New York

13. ARS Preprint, November 17-21, 1958. Page 14
Inertial Guidance, by B. W. Hilburger, 13th Annual Meeting, New York, N. Y.

14. Electronics, V. 34, November 17, 1961. Pages 95-99
Missile and Space Electronics - Guidance and Control, by J. F. Mason and M. F. Wolff.

15. Flight, V. 73, May 16, 1958. Pages 659-665.
Navigation, Inertial, Doppler, Radio

16. Electromechanical Design, January, 1962. Pages 38-54.
Newtonian Navigation, Part 1, by J. M. Slater.

17. ARS JL, December 1959. Pages 946-957
Recent Progress in Inertial Guidance, by J. Hovorka, J. W. Hursh, E. J. Frey, et al.
Seven papers on recent aspects of inertial guidance.

18. Control Eng., August, 1960. Pages 86-92.
System Aspects - Inertial Navigation Design, by D. P. Sarett.

19. IRE Trans. on Aeron and Navigational Electronics, September, 1959. Pages 158-178.
Vector Principles of Inertial Navigation, by A. M. Schneider.

20. Instrument Construction, March 3, 1962.
British Scientific Instrument Research Association.
Printed and Published by Taylor and Francis, LTD.

21. Principles of Inertial Navigation, by C. F. Savant
McGraw-Hill Book Company, Inc., 1961

22. Gyroscopes: Theory and Design, by P. H. Savet, 1961

23. The Gyroscope Applied, by K. I. T. Richardson
The Phylosophical Library, New York, 1955.

24. U.S. Army Ballistic Missile Agency on the Mid-Course
Navigation AD 204698

25. U.S. Naval Ord. Test Station
Alignment of Moving Inertial Navigational Systems,
AD 234263.

26. NOTS TP 2279
Alignment of Moving Inertial Navigational System

27. Kaplan, W., Advanced Calculus, Chapter I - Vectors,
Cambridge, Addison - Wesley Press Inc., 1952

28. McClure, C. L. Theory of Inertial Guidance, Page 63,
Prentice-Hall, Inc., Englewood Cliffs, N.J. 1960

29. Kolk, W.R. Modern Flight Dynamics, Prentice Hall, 1960

30. Reference 28, Page 14

31. UAC Internal Correspondence (from Corporate Systems
Center) From: M. H. Ullock; To: File,
Date: June 6, 1962 and Memo from G. K. White to
T. E. O'Brien, Dated: September 6, 1962; Entitled:
"Determination of Initial Direction Cosine Matrix
for a Strap Down Inertial System"

32. Inertial Guidance by Draper, Wrigley, and Hovorka
Pergamon Press, 1960

33. Inertial Navigation by R. Parvin
D. VanNostrand Company, 1962

34. Synthesis of Optimum Control Systems by Change
McGraw-Hill Book Company, 1961

35. The Oceans by Sverdrup, Johnson and Fleming

36. Practical Methods for Observing and Forecasting Ocean Waves
U.S. Navy Hydrographic Office 1955
H. O. Publication No. 603

37. On the Motions of Ships in Confused Seas by M. St.Denis and W. J. Pierson
Transactions of the Society of Naval Architects and Marine Engineers, 1953

38. On the Stabilization of Roll by J. H. Chadwick
Transactions of the Society of Naval Architects and Marine Engineers, 1955

39. Ship Motions - Confidential Report #106-989-001
Bell Aerosystems Company

40. Ships Motion Instrumentation Programs - Confidential Report #60003-012
Bell Aerosystems Company, April 1959

41. NAVWEPS 01-230HLC-1 Flight Manual, Navy Model HSS-2 Helicopter; Section V

42. NAVWEPS 01-230HLC-2-9 Automatic Stabilization Equipment

43. Sikorsky Aircraft, SH-3A (HSS-2) Flight Path Program (Study HS PO #E689918E)

44. Selected semiconductor circuits Handbook 1960, Seymour Schwartz Ed. J. Wiley

45. Semiconductor Components Guide
2nd ed. G. E. Company

46. Motorola Zener Diode/Rectifier Handbook

47. A Report Covering the Derivation of Equation for Gyro Calibration
W. Burwell - 5-4-62 (HSED)

48. Mechanization and Calibration of a Strapped-Down Inertial Navigation System
A. Scoville and R. Furber, 11-14-61 (HSED)